FOR A CANDIDATE FOR THE DEGREES OF

B.D., M.Litt., M.Sc., or D.Phil.,

or for the Diploma in Law

The Secretary of Faculties writes to inform you that the following have been appointed your examiners:-

1. **Professor R. Guillery.**

2. **Professor Dr. M.W. Singer.**

Your thesis is being sent to them, and they will inform you in due course of the date of your examination. You are responsible for ensuring that any letter sent to you at your College (or Hall or Society) or at any other address which you may have is forwarded without delay, and you should at once acknowledge the receipt of any letter from your examiners. You are not expected to take the initiative in communicating with them.

If you do not hear from your examiners within a period of four weeks from the date of this communication you may, if you so wish, let the Secretary of Faculties know and he will get in touch with your examiners.

[Candidates who have resubmitted a thesis should allow their examiners a longer period, say up to eight weeks, before enquiring about the date for their oral examination. This is to allow both examiners time to re-read the thesis and decide whether a further oral examination is necessary.]

Initialed for the
Secretary of Faculties ..... NC

Date ...10.10.91.....

To ..Mr E.M. Kasper.....

KIGS: 2000:10.86

After the examination on 19/12/92:

A list of errata has been added to the book.

Maturation of projection neurons in the visual cortex of the rat

Ekkehard M. Kasper

St. John's College

Thesis submitted for the degree of Doctor of Philosophy at the

University of Oxford

October 1991

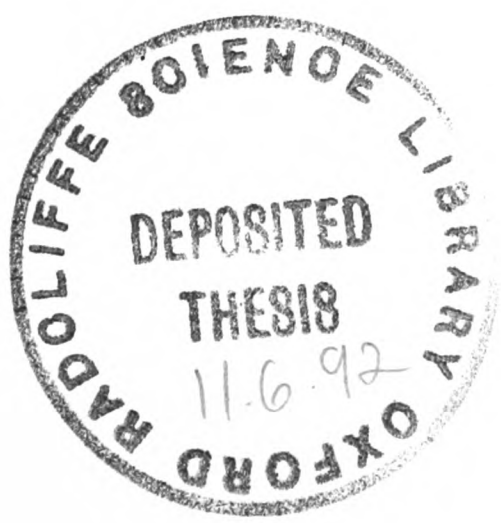

Acknowledgements

First of all I would like to thank the Rhodes Trust, without whom I would not have had the opportunity to spend three valuable years in Oxford. The most generous support I have received from them has enabled me to broaden my horizon in a way that will influence me throughout my life.

Secondly I would very much like to thank my "extended family" and all the friends who encouraged me to go, as well as those who have supported me during the time of my stay.

I am extremly grateful to my joint supervisors, Professor Colin Blakemore and Dr. Alan Larkman, whose excellent supervision has made this work possible. It was a great pleasure to work in Dr. Larkman's group throughout these last three very active years and I wish to express my deep gratidude to him for spending endless hours with me.

I should also like to thank Dr. J. Lübke, who has helped me to establish the technique for intracellular dye injection in fixed tissue and has contributed significantly to the success of the experiments done this way. The period of collaboration with him was one of the most enjoyable and most rewarding phases of my time of research in this laboratory.

I am especially indebted to Dr. E. Buhl, Dr. A. Hainsworth, and Dr. T.P.S. Powell for valuable comments on parts of the manuscript. Their careful suggestions were of great help. I would also like to thank Mr. L.Waters and Ms. A. Morgan from the photographic unit of this department for all the superb photographic work they have done for me.

Finally my thanks go to Familie Lübke, F.Sengpiel, A.Rau and G. Hillenbrand, whose enormous support during the later part of this thesis work kept me going.

Statement :

I was responsible for the design, the execution and the data analysis of all experiments presented in this thesis, except for those experiments described in Chapter 6, which I have carried out in collaboration with Dr. J. Lübke, who is a research worker in the Department of Human Anatomy, University of Oxford.

No part of this thesis has already been accepted or been submitted to this or any other university for the fullfilment of an academic degree.

Ekkehard Kasper

Ekkehard Matthias Kasper,

St John's College,

Oxford, October 9th, 1991

Abstract

Maturation of projection neurons in the visual cortex of the rat

Ekkehard M. Kasper

St. John's College, D.Phil Thesis, October 1991

A variety of *in vitro* brain slice preparations were employed to study the development of electrophysiological and morphological characteristics of pyramidal neurons from layer 5 of the rat visual cortex.

By combining conventional intracellular recording techniques with intracellular dye injection into neurons which were back-labelled from their respective target, it was possible to demonstrate a correlation between the intrinsic electrophysiological properties and the morphology of projection neurons. Superior colliculus projecting neurons fired action potentials in a burst-firing pattern whereas interhemispheric projecting neurons fired action potentials in a regular spiking pattern. Both groups differed also in the morphology of their dendritic arborizations.

A developmental study of the physiological properties of morphologically identified layer 5 neurons demonstrated that subthreshold properties and characteristic action potential parameters of these neurons change progressively during the early postnatal period. Membrane time constants and input resistances changed to lower values and action potentials became higher, faster and thus briefer. No burst-firing patterns were found in early developmental stages.

Using intracellular injection of Lucifer Yellow in fixed slices, it was then shown that superior colliculus (SC) projecting neurons and interhemispheric (CLH) projecting neurons differ significantly in their morphology already early in development. SC-nneurons have more basal dendrites which give rise to more branches and total tips than neurons projecting to the CLH.

Contents

3.4) Preparation of slices from fixed brains

-Photoconversion of single cells injected with LY

3.5) Procedures for back-labelling cortical projection neurons

3.5.1-Injections into the ipsilateral superior colliculus
3.5.2-Injections into the contralateral occipital cortex

Chapter 4: Projection neurons in layer 5 of the adult rat visual cortex : Correlations between single cell morphology and intrinsic electrophysiological properties in corticotectal and interhemispheric pyramidal neurons studied *in vitro*

4.1) Introduction

4.2) Materials and Methods

4.3) Results

4.3.1) Qualitative anatomical observations
a) SC-neurons
b) CLH-neurons

4.3.2) Quantitative electrophysiological results from SC and CLH neurons
a) General findings
b) Subthreshold properties
Membrane resting potential; -Membrane time constant --
Current/Voltage relations
c) Suprathreshold properties
Burst-firing patterns
Spike afterpotentials
Repetitive firing
d) Neurons with a twin apical dendrite

4.4) Discussion

4.4.1 Anatomy:

-Possible reasons for a sampling bias
-Subpopulations of pyramidal neurons in the infragranular layers
-Comparison of the laminar distribution of cortical projection neurons
-Dendritic morphology of single neurons

4.4.2 Physiology:

-Evaluation of subthreshold properties
-Suprathreshold properties

4.5.) Conclusions

Chapter 5: The development of intrinsic electro-physiological properties of pyramidal neurons from layer 5 of the rat visual cortex studied *in vitro*

5.1) Introduction

5.2) Materials and Methods

5.3) Results

5.3.1) General findings

5.3.2) Qualitative morphological observations

- Dye coupling between neurons from the developing visual cortex

5.3.3) Electrophysiological results

-Subthreshold properties
-Rectification phenomena
-AP-parameter
-AP-firing-pattern

Chapter 1:

Historical Introduction

The early days of neuroscience :

It is not easy to determine who actually first saw a neuron in the cerebral cortex as we might think of it today. It most probably was the microscopist Ehrenberg, who was aware of single neurons in cortex preparations from animals as well as from man, but he referred to them as "granules" or "globules" (1833, 1836) and did not publish any specifying illustrations. Shortly thereafter Valentin (1836) and Remak (1841) gave more elaborate descriptions of what they called nucleated "ganglion bodies" with Remak also mentioning what we know to be myelinated fibres which he felt were continuously arising from processes of the ganglion cells of the cortex. The morphological term "pyramidal" was subsequently introduced by von Kölliker (1849), who described cells from unstained material of deeper parts of the human cortex. He was also the first to affirm that nerve fibres were the continuation of nerve cell processes, although it was not yet possible to demonstrate it then. The definite statement was made several years later by Deiters (1865).

In those early years of cellular neuroanatomy Berlin (1858) was the first one to describe observations indicating that the cortex is organized in layers as well as the fact, that it is composed of different cell types which he called pyramidal, granular and fusiform, although he might have chosen these names with reference to von Kölliker (1852), who had used such descriptive terms as "triangular, round and spindle cells" as well as "pyramidal" cells for neurons in the cortex .

Cortical lamination :

The first systematic description of layering in the cortex was made by Meynert (1867-1872), who studied tissue of animals and man. He distinguished a common type of stratification that was five layered and was discernible in most parts of the human cortex. He described an outer "neuroglia layer" with only a few angular nerve cells, a second layer of small pyramidal cells , a third layer of large pyramidal cells, a fourth layer of multiform and granular cells and a fifth layer containing large but short pyramidal cells and deeper located spindle-shaped cells. His fifth layer thereby includes both our layers 5 and 6. Meynert was also in a position to detect what he called projection fibres and association fibres entering and leaving the cortex, clearly showing continuity with the processes (axons) arising from pyramidal cells.

The next important step ahead was the series of studies carried out by Lewis as well as Clarke, his collaborator, on the comparative structure of cortex in man, sheep and cat (1878). Lewis noted that the motor cortex was five layered, but concluded that fundamentally the cortex should be regarded as six layered. The idea of six layers as the basic pattern of cortical stratification became firmly established in the literature as a result of its adoption by the Vogts (O.Vogt, 1903; C.and O.Vogt, 1919) and their pupil Brodmann (1903, 1909, 1912), who believed that it showed the fundamental evolutionary as well as embryological scheme of cortical organization. Most of this work was done on Nissl stained material, although the subsequently adopted nomenclature relating to the fibre lamination emerged as a result of new methods for fibre staining, used by the German school (Mauss, 1908; Vogt and Vogt, 1919; Edinger, 1896; Flechsig, 1898) but also others (Campbell, 1905; Bechterew, 1894; Ramon y Cajal, 1909-1911). The myelin stains were naturally not suitable to add any information about cellular morphology.

Morphology of individual cell types :

It is important to mention that the variety of cell types was only recognisable as a result of the application of new methods such as the methylene blue (Ehrlich 1868) or the Golgi stain (Golgi 1873), which also brought to light the extent of ramification of individual cells. Golgi himself had applied the silver method to the cerebral cortex around 1883, when he described both pyramidal and nonpyramidal cells in some detail (1884, 1885, 1886, 1894). The most revolutionary observation he contributed thereby (according to Cajal 1954) was probably the fact that the processes of cells did not form anastomoses, but ended freely. He also distinguished for the first time clearly between axons and dendrites, a notion he took up from earlier work by Deiters. Other eminent studies on the cortex were done by Ramon y Cajal (1891,1894), Retzius (1893, 1896) and von Kölliker (1896).

The most important contribution to the field made by a single person is without any doubt the work of Ramon y Cajal. He classified cells as belonging to one of two basic categories named "pyramidal cells" and "cells with short axons" (1911) and recognised the similarity of all pyramidal cells of all layers. Nevertheless he also detected differences amongst them such as for example the considerable variation of the branching pattern of the dendritic tree depending on the layer in which the soma of observed cell was located in. The section on cortex in his final work about the nervous system ends thus: "One thing is certain: classification of the manner of connection between the innumerable centrifugal and centripetal, terminal and collateral branches emanating from thalamic, callosal and association fibres constitutes at present an overwhelming problem. In it many generations of future neurologists will put in their sagacity and their patience to the test".

Chapter 2:

General Introduction :

2.1 Structure and organisation of a sensory system: the development of pyramidal neurons in the visual cortex of the rat

Neurons of the neocortex can be assigned to various classes according to distinctive anatomical details (Golgi, 1909; Ramon y Cajal, 1911; for an extensive description see Peters and Jones, 1984). In recent years it has been shown that the same is possible with respect to electrophysiological features (e.g. Connors et al., 1982; Connors and Gutnick, 1984; McCormick et al., 1985; for reviews see Peters and Jones, 1984; Connors and Gutnick, 1990). Another way of grouping cells has emerged from investigations of the circuits in which cells are involved. Using various tracing techniques and employing lesion studies it has been be demonstrated that neocortical neurons project to a variety of targets. The following general principle emerged throughout the last two decades from studies on mammals: projections from the smaller supragranular cells located in the upper part of layers 2/3 tend to be intrahemispheric (cortico-cortical cells projecting ipsilaterally), whereas the axons of cells with somata located in layer 3 tend to be interhemispheric (cortico-cortical cells projecting contralaterally). However, no rigid size or sublaminar separation of the parent cells of these different projections could be found (for review see: Jones, 1984). In addition to these supragranular intracortical projections found in all mammals studied so far, only rodents seem to possess a significant number of callosally projecting cells in the infragranular layers (Wise and Jones, 1976; Dürsteler et al., 1979).

Neurons from the infragranular cortical layers project to a variety of targets, partly cortical, but mainly subcortical, such as the contralateral hemisphere, the superior colliculus, the pons, the spinal cord, the claustrum, the lateral geniculate nucleus. This has been shown for various species including the rat (e.g. Nauta and Bucher, 1954; Miller, 1986a, 1988b; Miller and Vogt, 1984b; Legg et al., 1989; the cat (e.g. Holländer, 1974; Gilbert and Kelly, 1975; Magalhaes-Castro et al., 1975; Katz, 1987); and some monkeys (e.g. Graham et al.,1979, Lund et al., 1975); for review see Swadlow, (1983); Jones, (1984).

Nevertheless it is still unclear whether those classes defined on the basis of neuronal morphology, electrophysiology or circuitry bear any functional significance. One of the greatest problems in studies of neurons from the mammalian central nervous system (and in particular cortex) is the large number of anatomical or physiological features which can be used to classify neurons as belonging to particular subclasses. Attempts have been made to correlate receptive field types such as simple and complex with different morphological cell types in the cat (Gilbert and Wiesel, 1979; Martin and Whitteridge, 1984). Other studies tried to correlate the orientation of dendritic fields of neurons within the cortex with visual patterns the animal has experienced under certain rearing conditions (Coleman et al., 1981). Nevertheless it is very difficult to assess the biological significance of such a finding and consequently of the subdivision.

One way to avoid epiphenomenal classification, not reflecting any biological functional implications, is to look for correlations between several characteristic features within a given population of neurons. This can be achieved by the combination of experimental techniques which allow the simultaneous investigation of several aspects of

neuronal form or function. This has been done to link questions concerning single cell morphology with questions concerning circuitry. Other studies have linked the investigation of physiological properties with simultaneous investigation of morphological aspects of the cells studied (e.g. Deschenes et al., 1979; Larkman and Mason, 1990).

Pyramidal cells are the predominant cell type in the six-layered rat visual cortex and account for up to 90% of the entire neuronal population in adult animals (Peters and Kara, 1985; Peters et al., 1987; Winfield et al., 1980). Using an interdisciplinary approach as mentioned above, it was demonstrated that pyramidal cells even within a given layer of neurons can show distinct morphological features which are correlated with their site of projection in rat (Schofield et al., 1987; Hallman et al., 1988; Hübener and Bolz, 1988) and also in cat (Katz, 1987).

From those studies it could be concluded that, for example, cells projecting to the superior colliculus are of the large type found in layer 5 and they all have an apical dendrite which ascends towards the pial surface and arborizes to form a terminal tuft in layer 1. In contrast, cells projecting to the contralateral hemisphere via the corpus callosum, which are also found in layer 5 of the rat cortex, are smaller in size and have an apical dendrite that tapers in most cases below the upper border of layer 2/3 or within one of those layers and does not form a terminal arborization in layer 1. Similar findings have been reported for other rodents (Klein et al., 1986; for hamster), the rat (Hübener and Bolz, 1988), the cat (Buhl and Singer, 1989) and monkeys (Lund et al., 1975; Valverde, 1985).

In addition to these obvious differences in neuronal morphology it has been

reported that pyramidal cells of the visual and somatosensory cortex of various species have different characteristic intrinsic electrophysiological properties (Connors et al., 1982; Staftstrom et al., 1985; McCormick et al., 1985; Connors and Prince, 1990; Larkman and Mason, 1990: Mason and Larkman, 1990). One striking difference was whether cells fired distinctive bursts of action potentials or steady trains in response to injected depolarizing suprathreshold current pulses (Connors et al., 1982; Schwindt at al., 1985; McCormick et al., 1985; Kriegstein et al., 1987; Mason and Larkman, 1990; Chagnac-Amitai et al., 1990).

In this thesis experimental results are presented which demonstrate that another step can be made in correlative studies, by combining retrograde labelling techniques with conventional electrophysiological techniques for intracellular recording and dye-injection. This combination allowed the investigation of pyramidal cells belonging to particular classes of cortical projection neurons and made it possible to examine simultaneously whether there is a correlation between the intrinsic electrophysiological properties, the individual neuronal morphology and the projection site.

2.2 The development of central neurons :

Several previous studies have attempted to describe the maturation of pyramidal cells using intracellular recording techniques for physiological changes (McCormick and Prince, 1987; Kriegstein et al., 1987) or staining methods for anatomical analysis (Juraska, 1982; Miller, 1981, 1984a, 1985, 1986, 1988; Petit et al., 1988). Nevertheless there is an important aspect that has largely been ignored in previous studies: neurons that are finally located in different cortical layers are generated at

different birthdates during cortical ontogenesis. The cells whose final destination is in the infragranular layers are generated and in place much earlier than the cells destined for the supragranular layers. Thus at any one time during the early postnatal period there are cells of various developmental stages present in the cortex, a situation that can confuse developmental studies. Because the process of laminar and cellular differentiation are so closely linked I shall first give a brief review of the period of corticogenesis.

2.3 The generation of the cerebral cortex :

The laminae of neurons in the mammalian cerebral cortex are derived from the cortical plate, a histological entity consisting of postmitotic neurons. This transient structure exists throughout the migration period of neurons in early differentiating stages at the beginning of corticogenesis (see Boulder Committee, 1970; Caviness, 1982; McConnell, 1988). The neurogenesis proper takes place in the so-called ventricular zone (Sauer, 1935; Fujita, 1963, 1964; Berry, 1974; Shimada and Langman, 1977), a pseudostratified epithelium that forms the walls of the cerebral vesicles at the very beginning of forebrain development. More recent evidence indicates that projection neurons and local circuit neurons are generated at the same time (Miller, 1985). Cohorts of postmitotic neurons leave the ventricular zone to migrate along guiding radial glial cells (Rakic, 1970; Butler and Caley, 1972; Sidman and Rakic, 1973; Caviness and Rakic, 1978; Rakic, 1988) towards the pial surface to stop their migration and thereby form the cortical plate (e.g. Hicks and D'Amato, 1968).

After the first "wave" of generated neurons is positioned within the cortical plate, the following "wave" of neurons will settle progressively more superficially

(closer to the pia). This creates an "inside out sequence" of positioning in which the earlier generated cells occupy the deeper layers of the emerging laminar structure and the later generated cells form the more superficially located layers (Angevine and Sidman, 1961, 1962; Berry et al., 1964). However, prior to the appearance of the cortical plate, a primordial plexiform layer or "preplate"is formed by a group of early generated neurons (Marin-Padilla, 1971, 1972). This is later split into the prospective cortical layer 1 and the subplate, probably including layer 6b in the rat (see Luskin and Shatz, 1985; Chun and Shatz, 1989; Bayer and Altman, 1991), this happening through the arrival of neurons forming the cortical plate. Therefore layers 2-5 and the upper half of layer 6 of the adult cerebral cortex are derived from the cortical plate, whereas layer 1 and the lower half of layer 6 are considered to be derivatives of the primordial plexiform layer.

This "inside-out sequence" of neurogenesis of cells settling in the cortical plate is typical for both projecting neurons and local interneurons (Miller, 1985) although the two classes of neurons are considered to be derived from separate progenitor cells (Price and Thurlow, 1988; Luskin et al., 1988).

The anatomical development of pyramidal cells from the rat cerebral cortex has been previously investigated in a number of studies using techniques for either the light microscope, the electron microscope or both (e.g. Ramon y Cajal, 1911; Eayrs and Goodhead, 1959; Berry and Rogers, 1965; Berry, 1974; Parnavelas and Lieberman, 1979; Miller, 1981; Miller and Peters, 1981; Juraska, 1982; Juraska and Fifkova, 1979a; Petit et al., 1988; see reviews by Jones, 1981; Miller, 1988b). Despite the ever increasing amount of data available concerning the anatomical maturation of single cells, the intrinsic physiological changes occurring throughout the same postnatal period have received comparatively little attention. This is most probably due to the great number of

technical difficulties the experimenter faces in such investigations. Therefore the bulk of available physiological observations is concerned with either extracellular single unit recording or evoked potentials in response to central or peripheral stimulation (Huttenlocher, 1967; Mathers et al., 1974; Verley and Axelrad, 1975; Verley, 1977; Schwob et al., 1984; see also Fregnac and Imbert, 1984) or cortical encephalography (Purpura, 1969; Snead and Stephens, 1983). *In vivo* studies have provided useful data, primarily on the development of synaptic potentials in these cells (Purpura et al., 1965; Purpura, 1969) but they were not successful in showing the developmental changes involved in the generation of action potentials. There are only two more recent studies on the topic employing intracellular recording techniques extensively *in vitro* (McCormick and Prince, 1987; Kriegstein et al., 1987). Both groups investigated the development of properties in neurons from the somatosensory cortex but neither of these studies differentiated between subsets of neurons: they pooled cells from all cortical layers rather than focusing on a particular subset of neurons. This approach suffers from two major disadvantages. First, data from cells at different maturational stages will be pooled at each time point. Second it ignores the differences that are known to exist between different types of neurons in different layers and even within the same layer (see e.g. Larkman and Mason, 1990; Mason and Larkman, 1990).\

I therefore wanted to describe developmental changes of neurons from within a single layer. I decided to limit the experiments for this study to the investigation of pyramidal cells from layer 5 of the **visual cortex** because those cells are generated relatively late in the gestation period - around embryonic day 16/17 (Berry et al., 1964; Berry, 1974; Brückner et al., 1974; Bayer and Altman, 1991) - and reach a distinguishable layer of destination at around p3 (see below). Because pyramidal cells start their main differentiation period only after having arrived in their correct laminar position, this provides the investigator with a situation in which a considerable part of

the maturation process can be studied postnatally.

To avoid pooling of cells in different stages of the maturation process it is necessary to record exclusively from cells in one particular layer. This is possible with a technique which combines electrophysiological as well as histological methods. The cell type and the laminar localization of the soma was confirmed by visualizing the cell from which recordings were taken. The simultaneous use of intracellularly injected tracers such as HRP or Biocytin makes it possible to obtain anatomical and electrophysiological data from the same neurons within a single experiment and yields further insight into neuronal function (See **Chapter 3**).

2.4 Using the slice technique :

Since the establishement of the *in vitro* slice technique it has been widely accepted as a valid tool for electrophysiological investigation (Lynch and Schubert, 1980; Schwartzkroin, 1981; Richards, 1981; Schurr et al., 1984). More recently, it has also been used for anatomical studies (e.g. Buhl and Lübke, 1989; Buhl and Singer, 1989; Burkhalter, 1989) or combined morphological-electrophysiological investigations (e.g. Larkman et al., 1988; Aghajanian and Rasmussen, 1989; Mason and Larkman, 1990). Nevertheless it should always be considered that the slice preparation creates an artificial situation in which a region of relatively intact tissue is bounded by two layers of damaged tissue. Therefore the structural and metabolic integrity of the slice might be altered (for a review see Reid et al.,1988), although intact cells appear to be healthy as can be judged by comparison with data collected from tissue *in vivo* (Bindman et al., 1988; Reid et al., 1988).

Within the last few years studies using the slice preparation have elucidated many of the developmental changes of intrinsic physiological properties of various principal neuronal cells (Llinas and Sugimori, 1979; Schwartzkroin, 1982; Schwartzkroin and Kunkel, 1982; Gardette et al., 1985; Walton and Fulton, 1986; Kriegstein et al., 1987; McCormick and Prince, 1987).

A study of **layer 5** neurons is of particular interest because these neurons project to a variety of targets including the superior colliculus (SC) and the contralateral hemisphere (CLH) in rat. At least two distinct morphological types, which are correlated with the projection target, have been identified for these cells (Klein et al., 1986; Hallman et al., 1988; Hübener and Bolz, 1988). Very recently it has been shown that pyramidal cells in layer 5 can be subdivided into two groups according to whether they display a burst-firing pattern or a regular spike-firing pattern, when depolarized to above threshold (Chagnac-Amitai et al., 1990; Mason and Larkman, 1990). The distinct response patterns are also correlated with a distinct morphological appearance. Therefore it would be interesting to ask the question whether cells with different firing patterns project to different targets and when this difference appears during development.

The aim of this investigation was to determine whether pyramidal neurons in layer 5 of the visual cortex of the albino rat that project to the same target area exhibit homogeneous electrophysiological properties and share common features of morphology. I also wanted to study the development of electrophysiological properties and morphology to see whether pyramidal cells follow a particular time table during maturation in which physiological changes are correlated with simultaneous structural changes.

Both intracellular recording and staining techniques were used in combination with a retrograde tracing technique to characterize the structure and morphology of identified pyramidal neurons in living brain slice preparations. In addition, a fixed slice preparation was employed to investigate the structure of projection neurons in the visual cortex at early developmental stages in postnatal corticogenesis.

Chapter 3:

Materials and Methods :

A variety of techniques were used for the work presented in this thesis which are centred around the ***in vitro*** slice preparation. Because a number of technical procedures were employed in each single experiment performed the main common procedures will be described in detail in this chapter, whereas specific methods or analysis techniques relevant to only one part of the study will be described in the appropriate individual chapters in more specific terms.

3.1 Nissl study of the development of the visual cortex :

In the experiments carried out for the investigation of the development of electro-physiological properties of pyramidal cells from the cerebral cortex (see **Chapter 5**) individual cells or cell layers could not be resolved in the living slice preparation at the time of the experiment. Therefore the location of layer 5 had to be established beforehand by measuring the distance of layer 5 cells from the pia. To this end a set of Nissl stained coronal sections was prepared from transcardially prefused animals of different postnatal ages. From each age group (p3, p6, p9, p12, p15, p18, p21 and adult i.e.around p49) two animals of the average litter size were anesthesized either with s.c. injection of sodium pentobarbitone (Sagatal, RMB 60mg/ml) if older than one week or via prolonged hypothermia, if younger than one week. Sufficient depth of anesthesia was assessed by ensuring that the animal did not show any response to pinching one of its extremities. They were then perfusion-fixed as follows. The animals

Figure **3.1:** Nissl-stained coronal sections of the visual cortex of the rat prepared from animals of various postnatal stages : a) **p3**; b) **p6** c) **p12**; d) **p15**; e) **p18**; f) **p21**

Each photograph shows the medial border of area 17 (towards area 18b) which is approximately indicated on each plate by a black arrow on the pial surface. White arrows indicate the depth at which impalements were attempted .

Note the following features in the plates shown:

a) No cortical layers can be distinguished at **p3**.

b) The superficial layers are not yet fully differentiated at **p6** as can be seen by the narrow band of high cell density close to the pia representnig the cortical plate.

c)-f) From the second postnatal week onwards **layer 5** can always be recognized as layer of a loosely packed neurons with relatively large somata.

Scale bare in f) =250μm and applies to all plates; wm= white matter

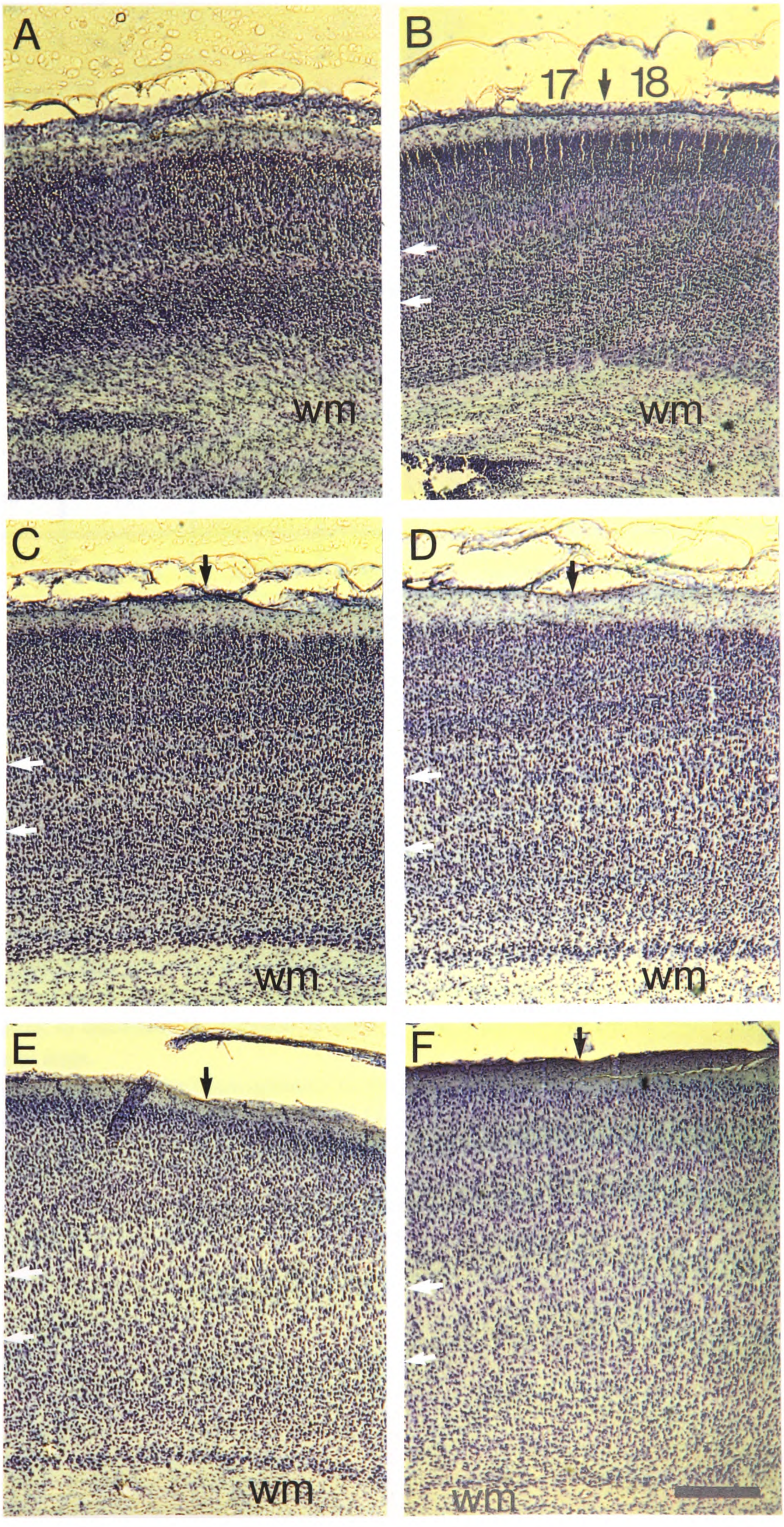
A
wm
B
17
18
wm
C
wm
D
wm
E
wm
F
wm

Table 3.1 Age-related changes in cortical thickness.

	AGE in postnatal days					
Method	P_6	P_9	P_{12}	P_{15}	P_{21}	Adult
Golgi *	290-500	400-700	550-850	650-1000	750-1100	850-1250
Nissl	≈400	≈500	≈700	≈800	≈900	≈1000
In vitro +	10u	13u	17u	20u	22u	26u

* from Miller 1981,88

\+ u=units as seen through a microscope equipped with an eyepiece with graticules; 1u=40μm

The distance between pial surface and the grey matter/white matter border was measured in living slices to determine the location of layer 5 with respect to the pia at each developmental stage.
Coronal slices were stained for Nissl-substance to study the developing cytoarchitecture and to delineate the borders between areas 17 and 18. The progressing differentiation of layer 5 could clearly be seen in these preparations and is illustrated in the plates of Figure 3.1.
Impalements were attempted in a living slice preparation by choosing a region equivalent to the values obtained from the Nissl study and to data from published litterature

were positioned on a foam-covered board ventral side up, the thorax opened and a butterfly syringe needle of the appropriate size inserted into the left ventricle. The vena subclavia dextra was cut open to serve as an outflow port. After an initial rinse with sterile phosphate buffered 0.9% saline (pH 7.4) each animal was sequentially perfused with several fixative solutions of different composition (see table below).

1. 4% paraformaldehyde in 0.1M phosphate buffered 0.9% saline
2. 10% paraformaldehyde in 0.1M phosphate buffered 0.9% saline (PBS)
3. 30% sucrose enriched10% paraformaldehyde in 0.1M PBS

After the final perfusate the animal was left for a few minutes to allow time for afterfixation. The fixed brain then was removed from the skull and stored for 48 hours in 30% sucrose-enriched 10% formalin in phosphate buffered 0.9% saline prior to sectioning on a freezing microtome. This time was required to achieve an even sucrose-infiltration within the tissue, which is important for smooth sectioning and cryoprotection of the tissue during the sectioning procedure. Brains were embedded in gelatine blocks for stabilization and then cut in 50µm sections on a conventional sledge-cryo-microtome (Leitz Kryostat 1400, Wetzlar). All sections taken from the occipital pole were mounted on gelatinized (subbed) slides and subsequently stained using a protocol for cresyl violet stain for Nissl substance (see appendix **1**). From those sections the depth of layer 5 cells was determined as the distance measured from the pia at various postnatal stages (see Table 3.1 and Figure 3.1). Results were compared to data from published litteratur on Golgi-material (Juraska and Fifkova, 1979; Miller 1981, 1984, 1988).

Table 3.2 Fixative amounts used for transcardial perfusion of animals of different postnatal stages.

	POSTNATAL AGE IN WEEKS			
	PNW 1	PNW 2	PNW 3	Adults
0.9% PBS	25	40	75	100
4% PFA	100	175	250	350
10% PFA	25	25	50	50
10% PFA + sucrose	50	50	100	100

The sequentially used fixatives are listed on the left side. The PNW number indicates the postnatal age of the perfused animal in weeks.

3.2 Preparation and maintenance of living slices :

Details of the technique for preparing and maintaining slices in an interface-type chamber configuration have been given previously (Larkman et al., 1988; Mason and Larkman, 1990; Larkman and Mason, 1990; Mason et al., 1990; Kasper et al., 1991). A brief discussion of the advantages and disadvantages of the slice preparation for combined morphological and electrophysiological studies is given in the appendix to Larkman and Mason (1990).

3.2.1 The slicing procedure :

Wistar rats of the approriate age groups were deeply anesthesized via inhalation of halothane (Fluothane, I.C.I) and decapitated. The brains were then rapidly removed from the skull and placed in ice-cold artificial cerebrospinal fluid (ACSF) at about 2°C for ca.3 min. The composition of the ACSF used throughout the preparation of slices and the subsequent electrophysiological recording was :

constituent	concentration in **mM**	amount in **gram/l**
NaCl	**125.00**	**7.305**
$NaHCO_3$	**26.00**	**2.184**
KCl	**2.30**	**0.171**
KH_2PO_4	**1.26**	**0.172**
$MgSO_4$	**1.00**	**0.246**
$CaCl_2$	**2.50**	**0.277**
Glucose	**10.00**	**1.802**

SLICE CHAMBER

A

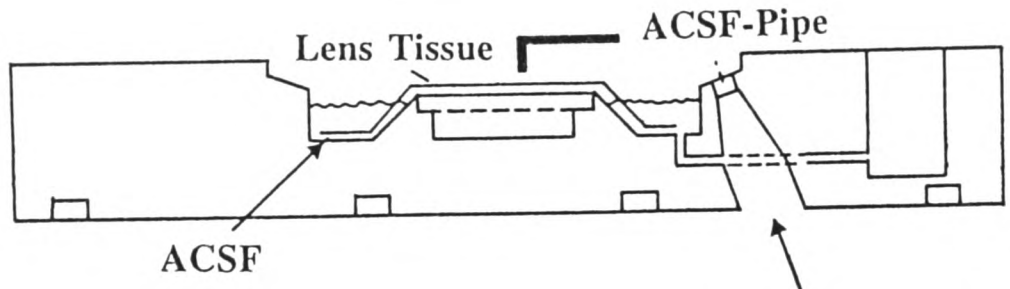

Equidistanced Holes for O_2/CO_2 Supply

B

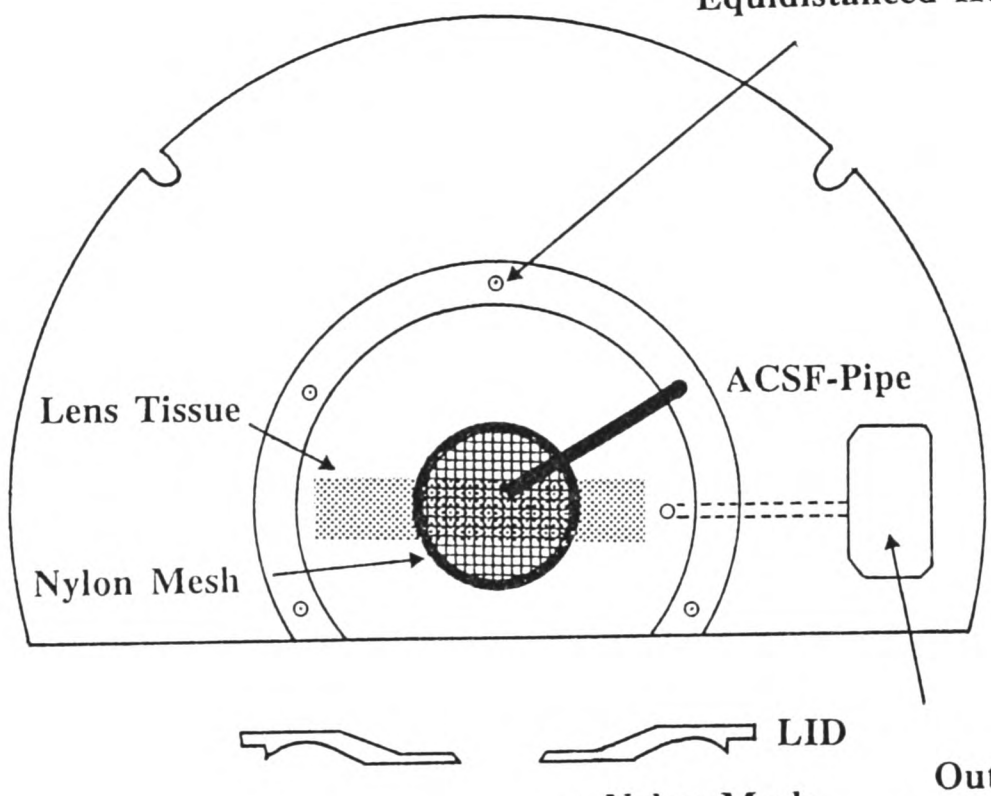

LID

Outlet Reservoir (Suction)

Nylon Mesh

C

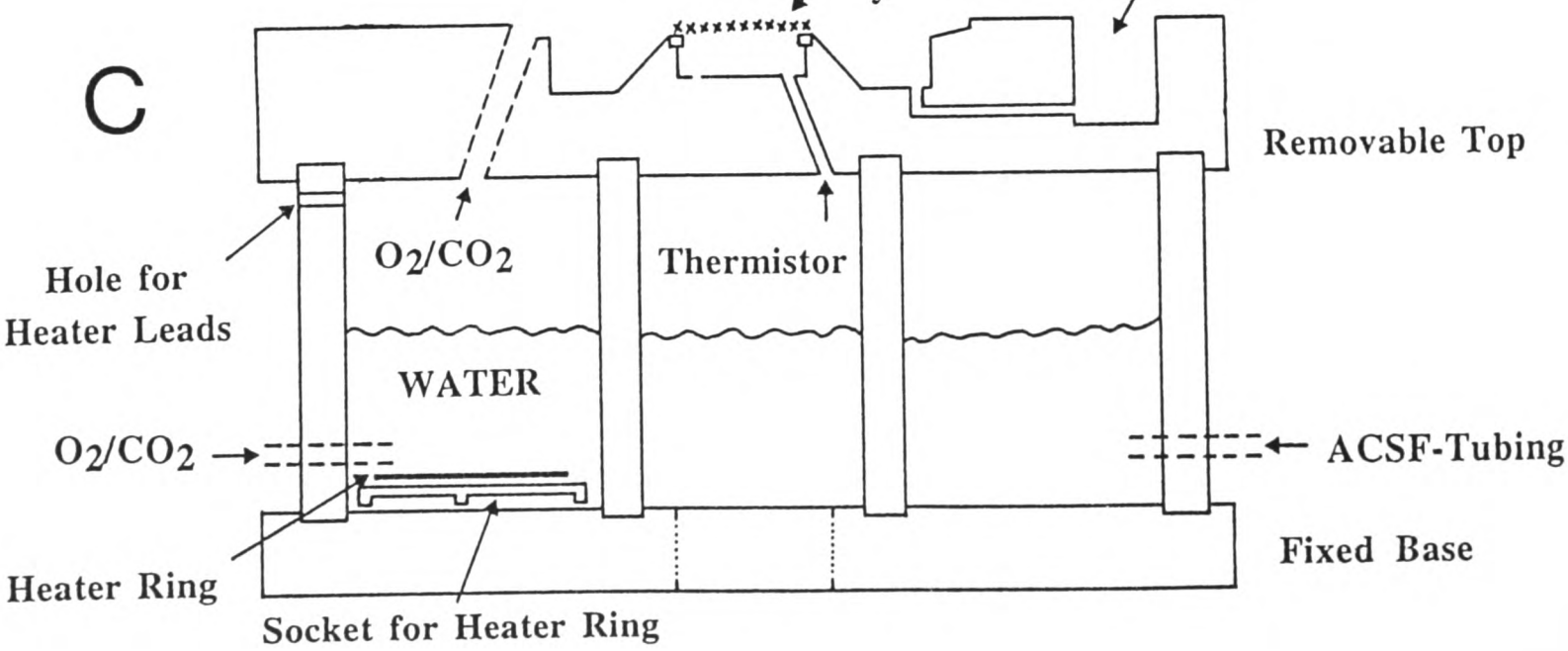

The pH-value was 7.4 at 35 °C when the solution was gassed with **95%** O_2 **/ 5%** CO_2. All subsequent steps were performed with the brain kept cold. Three or four coronal slices (400µm thick) were cut on a vibrating microtome (Campden Instruments Ltd.) from about 2mm anterior from the pole of the occipital cortex of the left hemisphere. The coronal slices were then trimmed with a razor blade to consist entirely of visual cortex as determined from published stereotactic and cytoarchitectonic studies (Zilles et al. 1984, 1985; Schober and Winkelmann, 1975; Peters and Kara, 1985). Each slice was then cut in half orthogonal to the pial surface to finally obtain two tissue pieces of about 1.5 mm width. The slices were transferred and maintained in an interface-type recording chamber where they sat on a wet lens tissue strip on top of a nylon mesh. For a detailed description of the chamber see opposite page.

The chamber was constantly supplied with humidified gas (95%O_2/5%CO_2) and throughout the whole experiment the chamber temperature was maintained at 35.0±0.5°C. The slices were constantly superfused at a rate of ≤1ml/min with warm (≈35°C) ACSF of the same composition as mentioned above. Slices remained in the chamber for at least two hours for recovery before impalements for intracellular recordings were attempted.

3.2.2 Electrophysiological recording :

After the initial two hour recovery period intracellular impalements were attempted by the advancement of the micropipette via a computer controlled microdrive with position display (Digitimer SCat-01).

Recording electrodes were filled with 2M $KMetSO_4$ (pH 7.4) and 1% Biocytin (Sigma). This electrolyte solution was used for intracellular recording with backfilled glass microelectrodes (WPI Instruments, o.d. 1.2mm, i.d. 0.69mm, standart-wall, inset filament) pulled on a horizontal puller (BB-CH Mechanex, Switzerland) and having a DC-resistance of 50-170 MΩ (measured in ACSF). Electrodes were positioned on the surface of the slice at the depth from the pia corresponding to layer 5 (from the Nissl study) using a calibrated eyepiece gratilule in an inverted microscope (Wild, Germany). The distance of layer 5 was determined previously according to the procedure mentioned above.

The recording micropipette was then advanced until a cell was impaled. Conventional bridge balance techniques were employed to allow current injection and voltage recording with a single micropipette (see Figure 3.3). Capacitance compensation was continuously monitored throughout the recording period. Signals from the micropipette amplifier (WPI model 701 or Axoprobe 1A) were amplified and then digitized (CED 1401, Cambridge Electronic Design Ltd.) to be stored on a computer (IBM PC AT). The recordings were subsequently measured using software from C.E.D. (Signal averaging system, version 3.3).

To ensure that an impaled cell still had all the major parts of its dendritic branches neuronal impalements were only accepted at a depth greater than 100µm and less than 250µm as defined with the position display of the microdrive used. After each recording procedure the slice was fixed by immresion in a mixture of 2% paraformaldehyde and 4% glutaraldehyde in 0.1 M PB (pH 7.4) and processed according to a modified protocol for the biocytin-reaction originally described by

Figure **3.3**: Simplified circuit diagram of the equipment showing the main features of the *single microelectrode current clamp* configuration.

A trigger device (Digitimer D4030), initiates a pulse sequence and triggers simultaneously all circuits involved in current injection, recording and display of the signal.

After a specified delay, the microelectrode receives a current injection signal via an external pulse generator (Digitimer DS2), whose command voltage-output is converted to the appropriate current pulse via a voltage/current converter within the amplifier (WPI Model 701 or Axoprobe 1A).

The microelectrode sends its signal to the head stage amplifier (represented by a FET) which in turn connects to a buffer-amplifier to drive the external micreoelectrode shield, thus minimizing signal distortions. The capacitance of the recorded signal can be adjusted via the capacitance compensation loop, to counteract stray capacitance. The output signal is then fed into an external homebuilt amplifier also equipped with bessel filters. This final signal is sent to the analog/digital converter (CED 1401) and subsequently recorded on a IBM AT computer for later analysis.

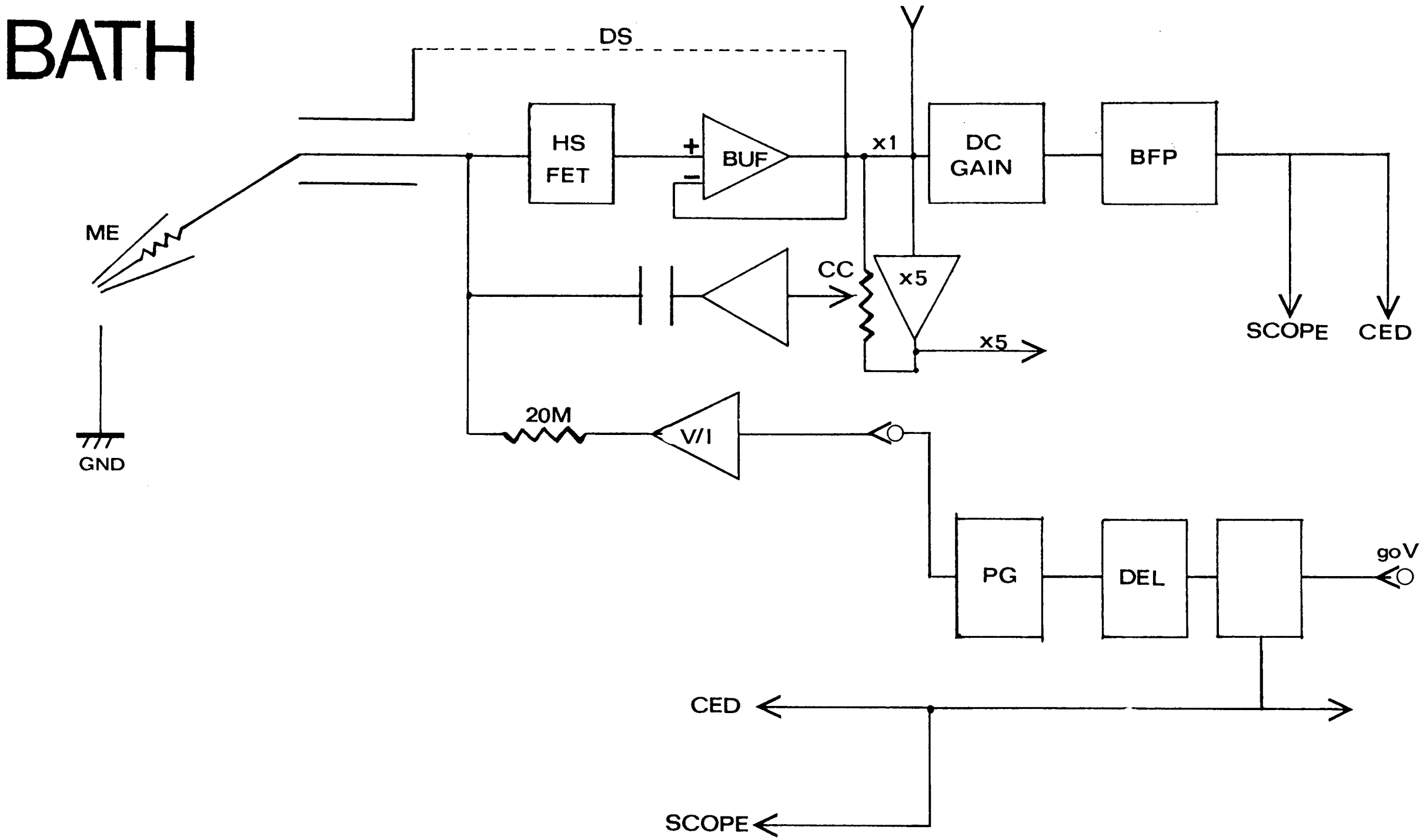
BATH
DS
HS
FET
+
−
BUF
x1
DC
GAIN
BFP
ME
CC
x5
x5
SCOPE
CED
20M
V/I
GND
PG
DEL
goV
CED
SCOPE

Figure **3.4**: A) Experimental set up as used for conventional recording techniques employing an interface-type slice chamber for electrophysiological studies of neurons in living brain slices. The slice chamber (3) is fixed on an air-table and can be observed via a stereoscope from above (2). The microelectrode and amplifier headstage are mounted onto a microdrive-stepper (SignifiCat) which in turn is positioned on a Leitz micromanipulator (1). A second micromanipulator (4) serves to position the tungsten stimulus electrode on the slice.

B) Close up view of the slice chamber (3). The microelectrode (1) and the stimulus electrode (4) are positioned on the same slice, indicated by a white arrow. The slice sits on top of a lens tissue, which itself is located on a nylon mesh.

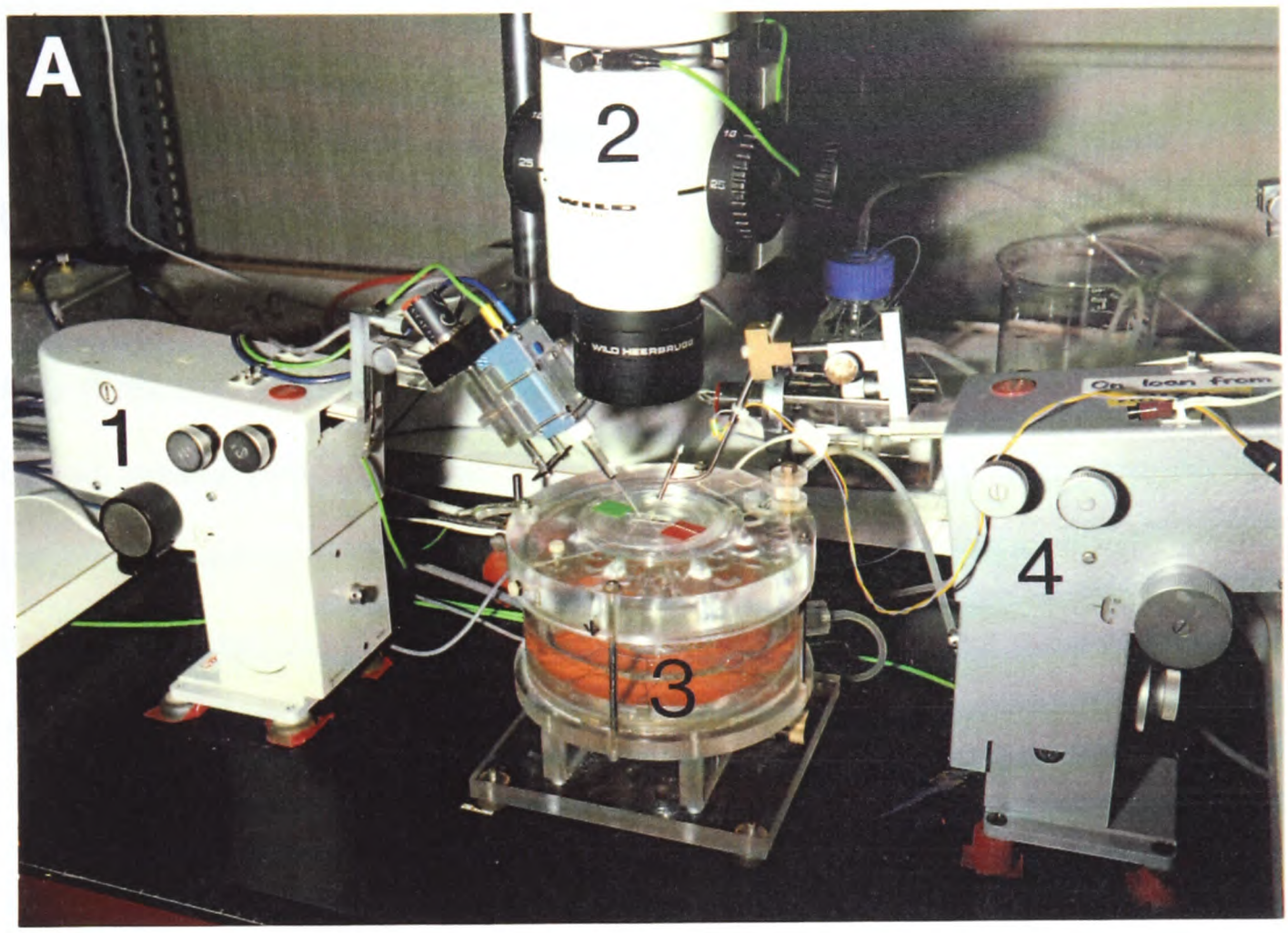
A
1
2
3
4
On loan from

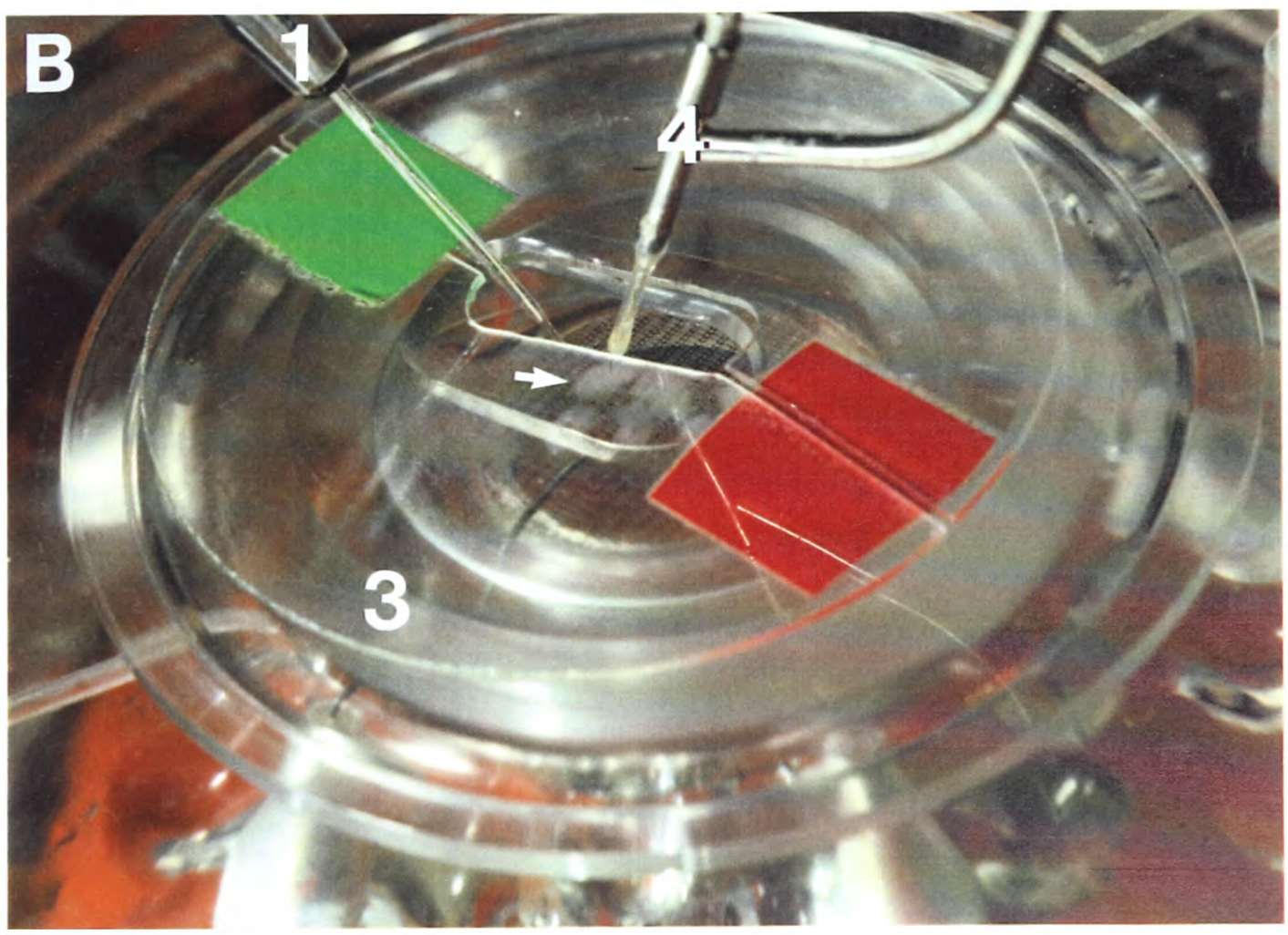
B
1
4
3

Horikawa and Armstrong (1988, see below) to get additional information about the location and morphology of the cell from which recordings were taken.

3.2.3 Histochemical protocol to visualize cells containing intracellularly injected biocytin :

Cells were filled with biocytin, which could be ejected from the electrode using 0.1nA to 0.5 nA current pulses of either polarity. It is therefore likely, that some biocytin was injected during the period of gathering the electrophysiological data. Additionally, after the recording protocol, long (250ms) negative current pulses of approx. 0.3 nA were applied at about 3Hz for at least 10 more minutes.

1. After each successful recording period from a single cell (in one of the electrophysiological experiments of the kind described in **Chapter 4**) the corresponding slice was immersion fixed in a solution of 2.5% glutaraldehyde and 1% paraformaldehyde in 0.1M phosphate buffer (PB) and stored in a specimen-jar at 4°C over night.

2. During next day's further processing, each single slice was glued down onto a layer of dental wax using an extremly thin film of cyanoacrylate-glue and mounted on the block of an vibrating microtome. Following this, each slice was re-immersed into buffer solution and resectioned into several sections of 60µm each on a vibrating microtome (Campden Instruments Ltd.). Thin sections were kept in a multiwellplate (Falcon Inc.) in PB.

3. Sections were incubated for 1 hour in the detergent Triton X-100 (Sigma, 1% in

0.1M PB)to permeabilize the cell membrane to facilitate the penetration of the HRP-complex needed later.

4. Sections were then incubated for 2 hours with avidin-horseradish peroxidase (Vector Lab.) diluted for a final concentration of 1:200 in 0.1 PB (Vector Lab.) with 0.5% permeabilizer (Triton X-100).

5. Sections were rinsed three times for 10 min. in PB to decrease the tissue concentration of unbound avidin- HRP which otherwise causes a high level of background staining.

6. Sections were incubated for 15 min in Hanker-Yates reagent (Sigma, 0.16g in 100ml 0.1M PB at 4C°.

7. To initialize the enzymatic visualization-reaction a few drops of 0.2% H_2O_2 were added and after a few minutes cells could be observed appearing slowly.

8. To stop the chromogenic reaction sections were rinsed 3 times with PB for 10 min..

9. To improve the contrast between reacted filled cells and the level of background staining sections were reacted with 1% OsO_4-solution for 15 minutes and subsequently rinsed twice for 10min. with PB.

10. Sections were dehydrated in an ascending ethanol series (50%, 70%, 90%, 3x100% and finally in absolute alcohol), before being embedded and coverslipped

in resin (E-mix resin, medium grade, Em-Scope Laboratories Ltd.).

3.3 Electrophysiological recording with simultaneous carboxyflourescein staining :

In further experiments, intracellular recordings were obtained from cells which had been prelabelled by incorporation of retrogradely transported fluorescent microspheres conjugated with rhodamine (Katz et al., 1984, 1987).

For these experiments I used an interface recording chamber mounted onto a crosstable attached to an epifluorescence compound microscope (Oxford Microinstruments, with Nikon optics and Nikon FAX photo attachment). (see Figure 3.5). In this way it was possible to change the relative position of both the chamber and the micromanipulator independently. To avoid condensation on the microscope objective lenses which were very close to the slice surface, the objectives in use were warmed up to about 35°C via steady DC-current flow from a low noise power supply (Farnell Electronics Ltd.) passed through a high resistance wire wrapped around the terminal part of the objectives. A part of the slice which contained a high proportion of backlabeled cells in layer 5 was then placed in the microscope-field as seen through a x10 LWD objective with a filter-block (Nikon G2A) appropriate for the emission-wavelength of excited rhodamine beads. Afterwards a carboxyfluorescein (CF) containing electrode (for details see below) was also placed in the same region of layer 5 using a second filter set (Nikon B2A). This also allowed me to see a faint picture of prelabelled cells because of an overlapping bandwith of the emission wavelength for

Figure **3.5**: A) Experimental set-up combining the interface-type slice chamber with an epifluorescent microscope to study neurons back-labelled by fluorescent microspheres in living brain slice preparations. The slice chamber (3), the microscope (1) and the manipulator (2) are placed on a heavy steel plate, which is supported by four rubber feet to dampen vibrations.

B) Close view of the slice chamber. The objective of the epifluorescence microscope (1) is heated by a high resistance wire, which is wrapped around its end. An external power supply delivers a DC-current to heat the objective lenses to ≈ 35°C to avoid condensation of moist air from the chamber. The recording microelectrode containing another fluorescent dye (2) is positioned with the aid of a Leitz micromanipulator. The focal illumination of one particular slice can be seen by the spot of green light which is appropriate for rhodamine excitation.

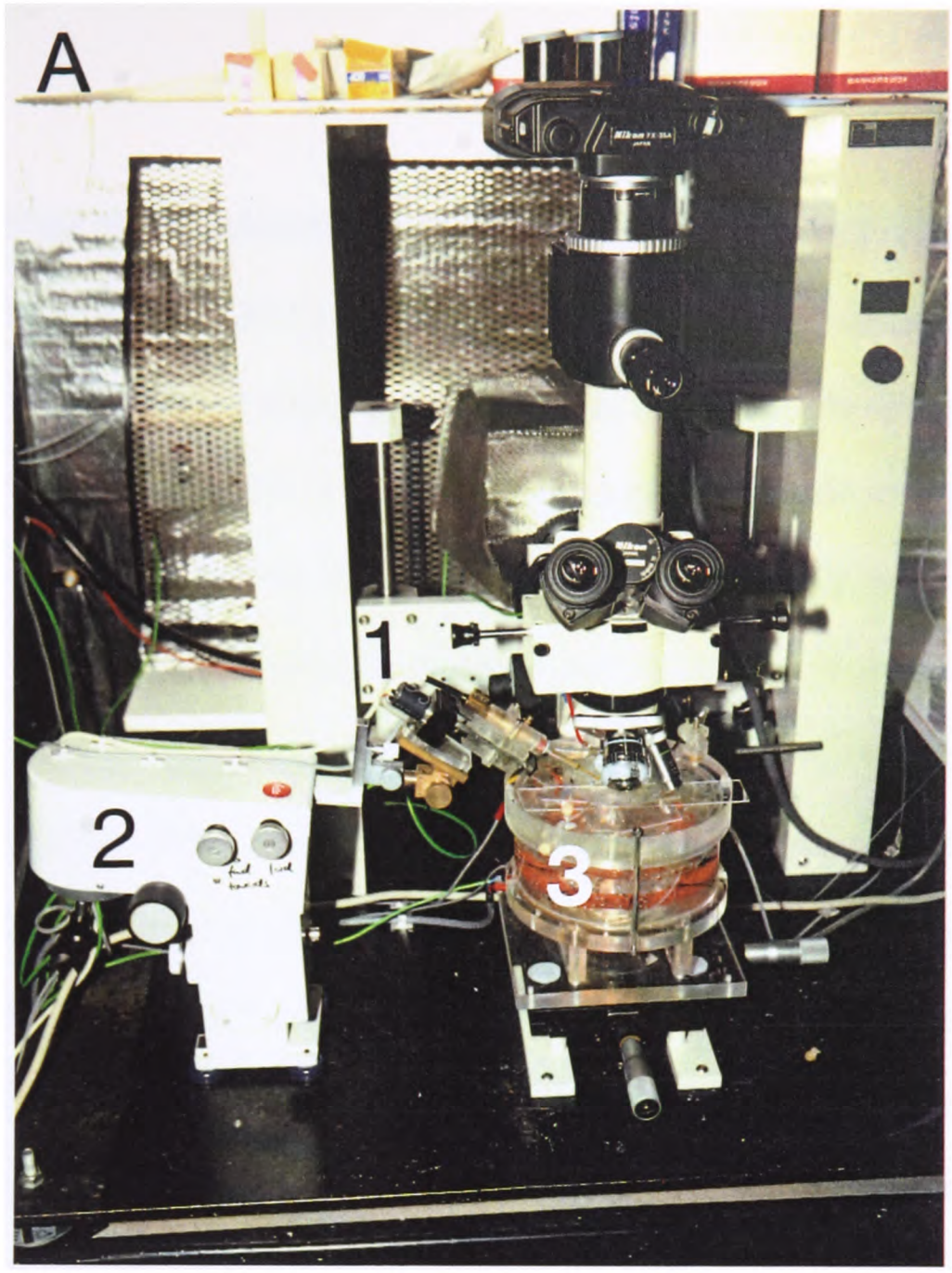
A
1
2
3

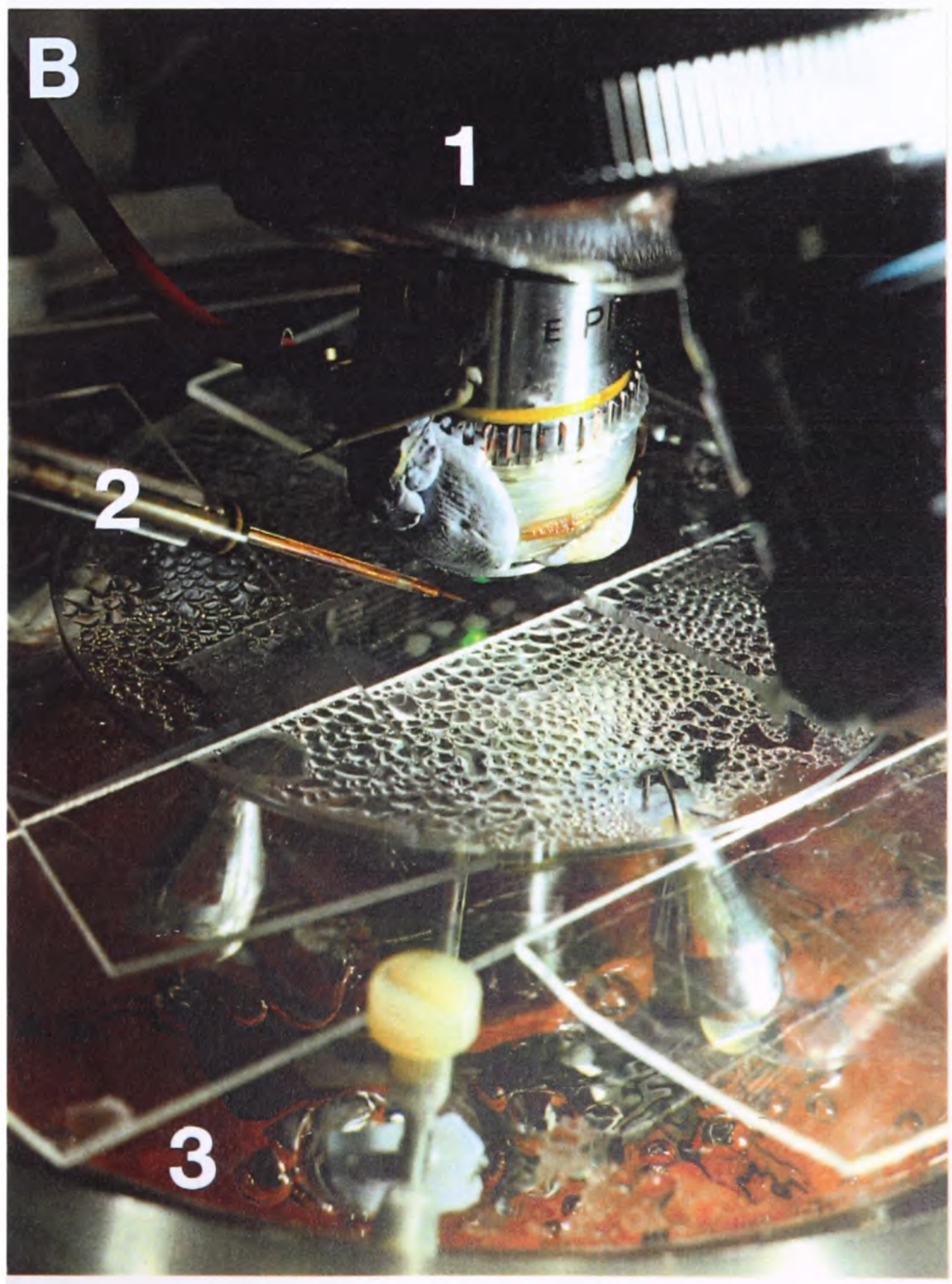
B
1
2
3

rhodamine and the B2A-filterblock specificity (see appendix **2**). I originally attempted visually-controlled impalements using a Leitz hand-guided micromanipulator for advancement of bent micropipettes under visual control (for bending technique: see appendix **3**). This procedure was surprisingly successful in achieving impalements of the in cells for which I aimed, but the electrophysiological recordings obtained this way were not of high enough quality, probably due to damage of the cell membrane. I therefore refrained from employing this particular technique any further. Subsequently intracellular impalements were attempted blindly via advancement of the micropipette through the slice using a stepping microdrive with position display as described previously (see above and Larkman et al., 1988). This technique yielded electrophysiological and morphological results of good quality. Again, neuronal impalements were accepted only at a depth greater than 100µm and less than 250µm to ensure that the impaled cell still had all the major parts of its dendritic branches. Only **after** the recording and filling procedure did I examine under fluorescence optics and higher magnification (x40 ELWD) whether the cell from which the recordings were made was properly filled and backlabelled with microspheres. This procedure was adopted because the cell's physiological properties suffered seriously if they were exposed to the light of excitation during the recording and filling period. This deterioration is most probably due due to intensive formation of free chemical radicals and subsequent oxidation of intracellular metabolites (Ross et al., 1977; Valenzeno and Pooler, 1978; Waggoner, 1979).

In experiments intended to visualize the entire dendritic arborization of such RH-prelabelled cells at the time when intracellular recordings were made, an electrolyte solution containing another fluorescent dye had to be used, which had to have an

excitation/emission bandwidth different from that of the rhodamine conjugated beads. I initially tried a 2% Lucifer Yellow (LY) solution in dH_20 or in 2M $KMetSO_4$ (Eastman Kodak) made from either the LY-dilithium salt or the more recently available LY-dipotassium salt, but in both cases the quality of the recordings was impeded by the LY. I later used a electrode filling solution containing **1.25** % carboxyflourescein in 2M $KMetSO_4$, which had the advantage of possessing approximately five times the fluorescent yield of Lucifer Yellow but the disadvantage of fading more quickly. Eventually the most satisfactory method was the use of the dye in its diacetate form (obtained from Sigma). This was prepared by adding 25 mg dye to 2 ml of a filtered 2M $KMetSO_4$ solution, heating it up in a water bath to about 75 °C and adding drops of 2M KOH to the solution (ca.**2µl**/mg dye) until the dye granules dissolved. The pH was subsequently re-adjusted to 7.4.

This electrolyte solution was suitable for successful intracellular recording with backfilled glass microelectrodes (WPI Instruments, o.d. 1.2mm, i.d. 0.69mm, standard-wall, inset filament) pulled on a horizontal puller (BB-CH Mechanex, Switzerland). Electrode -DC-resistance ranged from 55 to 125 MΩ (measured in ACSF).

3.4 Preparation of slices from fixed brains :

In some experiments I investigated the morphology of single cells via the injection of fluorescent dyes into prelabelled neurons in fixed slices prepared from the developing cerebral cortex.

For theses slices brains were used from animals, which were perfused transcardially as follows: Following the stereotaxic injection of tracer and a suitable recovery period (vide infra) the rats were reanaesthesized with a high dose of pentobarbitone sodium (Sagatal, RMB, 60mg/ml). The animal was then positioned on a foam-covered board ventral side up and the thorax opened. An incision was made in the right atrium to provide an outflow port and a butterfly-syringe needle was inserted into the left ventricle through which solutions were injected by pressure. To clear the blood vessels the animal firstly received a rinse with a solution of 0.9% NaCl in 0.1M phosphate buffer (PB) followed immediately by a solution of 4% paraformaldehyde (PFA) also made up in 0.1M PB. The amount of solutions used varied with the age of the animal perfused, (for details see Table 3.2).

After a 10min. postfixation period, the brains were removed from the skull and kept in the same fixative for at least two more hours. Coronal slices were then cut at 150µm thickness on a vibratome (Campden Instruments Ltd.). Sections not immediately used for intracellular injections were stored in 2% PFA in 0.1M PB at 4C°. A single slice was then transferred into a special slice chamber where it was held in position by a fenestrated millipore filter to prevent floating of the tissue (see Figure 3.6).

The slice chamber was then attached to the stage of an epifluorescence microscope (Oxford Microinstruments) equipped with x10 and x40 long working distance objectives (Nikon) and a part of the presumptive primary visual cortex brought into the viewing field. This way layer 5 neurons backlabelled from either the contralateral hemisphere or the ipsilateral superior colliculus could be visualized and impaled with micropipettes. For intracellular staining cells were injected via a steady negative DC-

Figure **3.6**: The experimental set up employing a brain slice chamber in combination with an epifluorescence microscope to study the morphology of back-labelled neurons in fixed slices. The slice chamber (2) and the microscope (1) and the microelectrode (indicated by an arrow) are shown in a close view. The epifluorescence objective is illuminating one immersed slice containing back-labelled cells. The slice is held in position by a fenestrated piece of filter paper which itself is stabilized with three pieces of a stainless steel rod. The microelectrode, containing Lucifer Yellow, is positioned on the surface of a slice with the aid of a Leitz micromanipulator and advanced with a computer controlled microdrive.

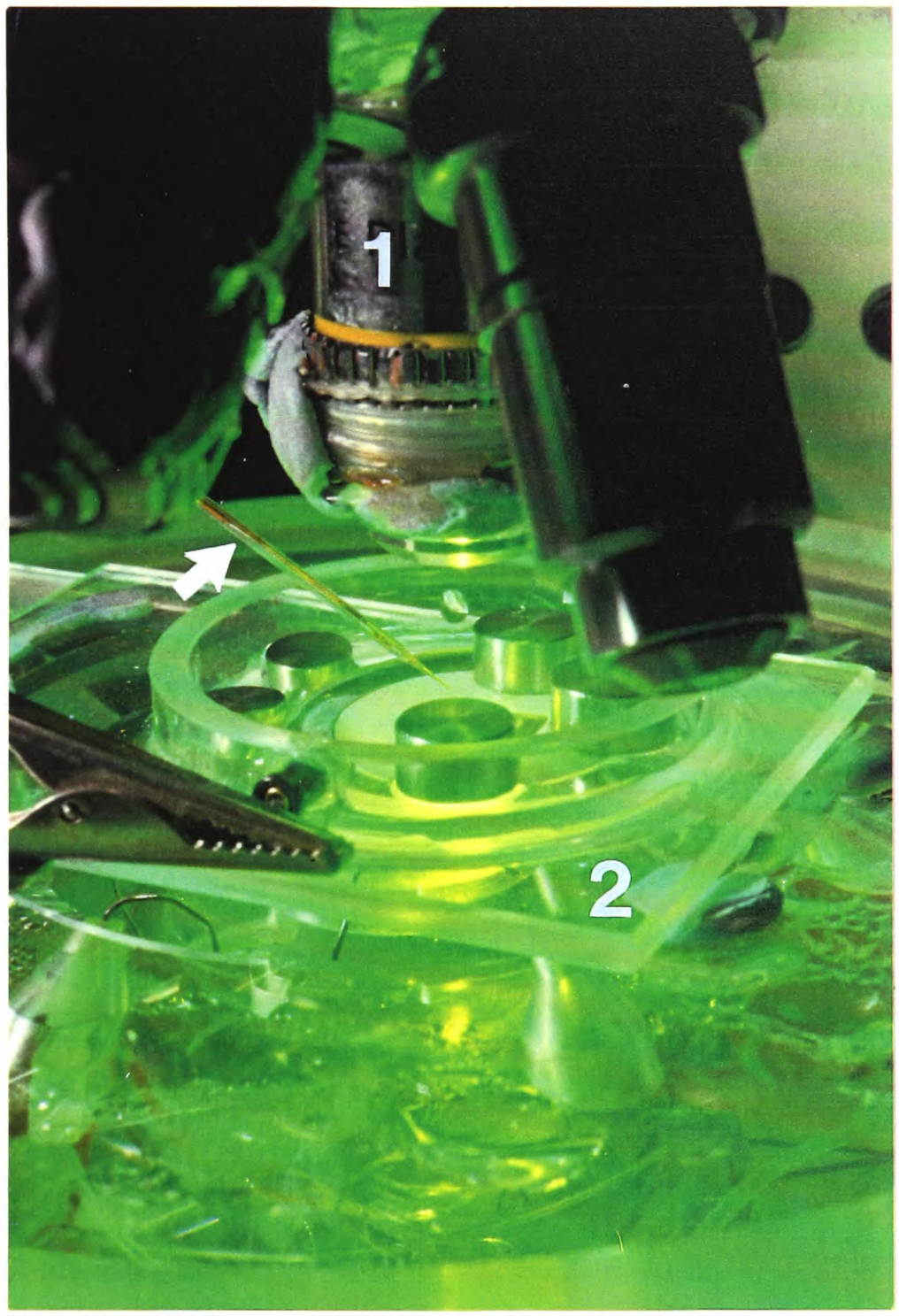
1
2

current of 0.5-4 nA using electrodes containing 5% Lucifer Yellow dissolved in distilled water. Electrodes pulled from a different glass were found to be superior for this work, probably because of their greater stiffness. Such borosilicate glass micropipettes (F.Hilgenberg, Germany) were pulled on the horizontal electrode puller (BB-CH, Geneva, Switzerland), had a tip diameter of 0.1-0.2 µm and a final DC-resistance ranging from 80-250 MΩ (measured in 0.1 M phosphate buffer). Impaled cells could be observed throughout the filling period and were subsequently photographed or photo-converted to a permanent preparation.

Photoconversion of single cells after injection with Lucifer Yellow:

In the experiments to investigate the morphology of immature prelabelled pyramidal neurons fixed slices were prepared form the early postnatal phase of cortical development. Cells were injected intracellularly with Lucifer Yellow (LY, see above) as the intracellularly visible marker (see Stewart, 1978, 1981; Tauchi and Masland, 1984; Buhl and Lübke, 1989).

There are several great advantages of LY which make it a powerful tool for the investigation of neuronal morphology: Firstly it is highly charged, which is advantageous for iontophoresis; secondly its low molecular weight (457.2 as dilithium salt and 521.6 as dipotassium salt) allows it to diffuse relatively quickly within the cell and its branches. It is therefore suitable for filling the cell with all its dendrites to the very tip, also including appendices like spines and growth-cones; thirdly it bleaches to a much lesser extent than any other fluorescent dye (e.g. carboxyfluorescein) suitable for intracellular injection and it can therefore even be used under long exposure to light of its excitation wavelength. The last property makes it one of the ideal tracers for a

photoconversion technique using diaminobenzidine (DAB) as a chromogen for the injected dye. The result is a permanently stable reaction product which can be used for light microscopy or even processed further for electron microscopy (Maranto, 1982; Buhl and Schlote, 1987; Buhl and Lübke, 1989; for review see Lübke, 1991). The protocol for processing the tissue was as follows.

After intracellular filling of single neurons with LY the brain slice was incubated for about 10min. in ice-cold 0.1 M phosphate buffer containing freshly dissolved DAB (Sigma, Grade II) at a concentration of 1.5mg/ml PB (Maranto, 1982; Buhl and Lübke 1989).The solution was filtered and 1mg/ml potassium-cyanide was added to reduce background staining caused by endogenenous peroxidase activity in the tissue. The pre-incubation period without illumination was needed to enable the DAB-solution to equilibrate within the slice. Fresh DAB-solution was placed into the chamber and the reaction was initialized by exposure of the cells to light appropriate to the LY-excitation bandwidth (Nikon filter-block B-2A and Osram 100W high pressure mercury bulb, see appendix **2**) using a medium power objective (Zeiss Neofluar x16 or Nikon Fluar 10x).

The photo-conversion was judged to be successful when an opaque brown reaction product had formed that could be observed under bright field illumination and the fluorescence of cells had faded completely. The conversion time varied between 20 min. and about one hour. Success was, in my experience, mainly dependent on the quality of the preceding filling process, but it is difficult to be definite because the underlying oxidation reaction is only poorly understood. After the photo-oxidation, slices were given three 10 min. rinses with 0.1M phosphate buffer and subsequently

mounted on gelatine subbed slides and air-dried for about 24 hours. Sections were then briefly (1-2 min.) immersed in 1% OsO_4 in 0.1M PB to improve the contrast between cell and background. Following this intensification reaction, sections were dehydrated in an ascending ethanol series, cleared in xylene and coverslipped in DPX .

These preparations were permanently stable and cells could be drawn like Golgi-stained material (see Figures in **Chapter 4**) under normal bright field illumination with the help of a camera lucida attachment to a suitable microscope (Nikon Optiphot or Leitz Dialux 20) under a final magnification of x1250. Any quantification subsequently carried out for a more detailed morphological description of the neuronal sample from the immature cortex was based on the drawings produced in such a way.

3.5 Procedures for back-labelling projection neurons :

3.5.1 Operations on adult animals :

Male Wistar albino rats of about 130 - 160 grams (aged about seven weeks) were deeply anaesthesized using a two phase and two component anesthesia of firstly Halothane (Fluothane, I.C.I.) followed by i.m. injections of hypnorm (0.3 ml/kg:; Jansen) and hypnovel (0.4 ml/kg; Roche). The breathing performance of each animal was carefully observed and if necessary improved via s.c. injections of atropine (0.1ml/kg; Veterinary Inc.). After shaving the dorsal aspect of the skull and disinfection of the bare skin with an antiseptic solution (Pevidine, BK Veterinary Products Ltd.) the animal was placed in a stereotaxic-frame (Narashige). A parasagittal longitudinal

animal was placed in a stereotaxic-frame (Narashige). A parasagittal longitudinal incision was made, the wound edges were covered with a gel of local anesthetic (Xylocaine 2%, Astra Pharmaceuticals Ltd.) and an operation retractor inserted to keep the wound wide open. Trepanation was performed by means of a dental drill at predetermined sites using stereotactic coordinates obtained from published literature (Zilles et al., 1984, 1985; Schober and Winkelmann, 1975; Paxinos and Watson, 1986) (see also Table in appendix **5**). After the craniotomy and a cut through the underlying dura mater, injections of 0.3µl - 1.0µl dispersed flourescent latex microspheres (diameter range 0.02µm-0.2µm, LumaFlour Inc.) suspended **1:4** in sterile 0.9% saline were made into either the superior colliculus (SC) or the primary visual cortex of the right hemisphere. In cases of SC-injections the ipsilateral occipital cortex was penetrated posterior to the area from which brain slices were prepared later. For the injection of the tracer solution a homebuilt pressurized air ejection device with inserted backfilled glass micropipettes (Clarke Biomedical Instruments, od 1.2mm, no inset filament) was used. About 2-3 minutes later the pipette was withdrawn from the injection site and the exposed brain surface covered with an absorbable piece of sterile gelatine sponge (Allen and Hanburys Ltd.). The skull opening was then closed with Horsley's sterile bone wax (Macarthys Ltd.), the wound sutured and finally covered and stabilized with tissue adhesive (Vet Bond, Animal Care Products/3M) which also helped to avoid infections. The total duration of each operation procedure was about 45 minutes.

To prevent hypothermia the animals were placed on a heating pad during the immediate postoperative period. To prevent dehydration and to improve recovery animals also received postoperative s.c. injections of warm 4% glucose-enriched

0.18% saline (Baxter Healthcare Ltd.). The rats treated this way survived well and behaved normally after about 6 hours, taking food and drinking water by then. After the operation animals were allowed to survive a time of at least two days for the retrograde transport of the injected tracer before slices were prepared from their brains.

3.5.2 Operation procedure for young and juvenile animals :

Wistar albino rats of both sexes at ages as early as postnatal day 3 (p3) were used for this set of experiments. At this postnatal age they have a total body weight of only 5 grams. This postnatal date was chosen for the operation procedure because it had previously been reported to be the earliest stage at which cortical cells can be labelled reliably by retrogradely transported tracers injected into either the superior colliculus (Thong and Dreher, 1986; Thong and Dreher 1987; Richburg and Kirby, 1989) or one of the hemispheres in living animals (Miller and Vogt, 1984; Miller, 1984). Because animals at that postnatal day are very small and there is no stereotaxic atlas available for the early phases in corticogenesis a different procedure was adopted.

The rats were deeply anaesthesized via inhalation of diethylether (BDH) and fixed with tape on an operation stage to remain in a stable position throughout the operation procedure.

a) Injections into the contralateral occipital cortex to identify corticocortical projection neurons :

A part of the occipital cortical surface located paramedian about 2mm lateral from

the sagittal suture and about half way between the lambdoid suture and the bregma point was exposed by trepanation and removal of the overlying dura mater. This occipital cortical area is later to become primary visual cortex (T.P.S. Powell, personal communication). In this region of the right hemisphere about 0.5µl tracer solution (Rhodamine-conjugated latex microspheres, LumaFluor Inc., dispersed 1:4 in 0.9% saline) was pressure injected into multiple sites from a sharp glass micropipette at a depth of 0.5mm-0.8mm, where interhemispheric axons are thought to terminate (Miller 1986). After 2-3 minutes, the pipette was withdrawn, the skull opening covered with a piece of absorbable gelatine sponge and then the excised bone flap repositioned to close the area injected.

During the postoperative recovery period the animals were placed on a heating pad at around 37°C to prevent hypothermia. After about 2 hours the animals behaved normally again and they were placed back with the litter in the original cage. After a survival time of several days animals were reanaesthesized (at p5 and p10 respectively) with 0.1ml i.p. injections of pentobarbitone (Sagatal RMB, 60mg/ml) and perfused transcardially as mentioned above to obtain tissue suitable for single cell injection in fixed slices.

b) Injection into the ipsilateral superior colliculus for identification of corticotectal projection neurons :

The mesencephalon was exposed from dorsal by taking off the squama occipitalis just posterior to the lambdoid suture carefully avoiding damage to the transverse sinus (See photographic illustration in appendix **5**). Tracer was then injected into the left superior colliculus (the ipsilateral side for slices subsequently prepared from the left

occipital cortex) at a depth of about 0.5-0.8mm which corresponds to the stratum griseum superficiale and the stratum opticum, where most corticotectal fibers terminate in rat and hamster (Thong and Dreher, 1987; Schofield, 1987; Ramirez et al., 1990). Subsequent steps were the same as those described above.

Chapter 4:

Projection-neurons in layer 5 of the adult rat visual cortex: Correlations between single-cell morphology and intrinsic electrophysiological properties in corticotectal and interhemispheric pyramidal neurons studied *in vitro:*

4.1 Introduction:

Pyramidal neurons in layer 5 of the visual cortex are involved in several specific projecion circuits, and show diversity in their dendritic morphology and intrinsic electrophysiological properties. The aim of this set of experiments was to determine whether pyramidal neurons projecting to a given target share common electro-physiological and morphological features.

Several anatomical studies have convincingly shown that, in some cortical regions, neurons projecting to a single target area share a common morphology (e.g. Deschenes et al., 1979; Katz, 1987; Hübener and Bolz, 1988). Very recently it was also shown by means of intracellular recording techniques that characteristic intrinsic physiological properties of neocortical pyramidal cells are correlated with a distinct morphology (Larkman and Mason, 1990; Mason and Larkman, 1990).

It was demonstrated that pyramidal neurons of layer 5 of the visual cortex, that fired action potentials in a burst, when stimulated by intracellularly injected currents, formed a morphologically homogeneous group of cells, all having a thick apical dendrite that arborized with a terminal tuft in layer 1. Furthermore the authors showed that regular spiking cells (also termed non-bursters) possessed an apical dendrite, which tapered as it ascended and did not show any arborization in layer one. The two types of cells also showed other differences in their intrinsic electrophysiological properties. Thick, burst-firing neurons had low input resistance values and short membrane time constants whereas neurons of the slender, regular-spiking type had high input resistance values and long membrane time constants. Thick, burst-firing neurons also showed more time-dependent rectification in response to injected current pulses than slender cells besides several other significantly different electrophysiological features (for the details the reader should refer to Mason and Larkman, 1990). These findings were essentially confirmed for neurons from primary visual and somatosensory cortex by Chagnac-Amitai et al. (1990) but are not fully consistent with results from secondary visual cortex (Lohmann et al., 1991) and the *in vivo* results from neurons in motor cortex by Pockberger (1991).

Other authors (Klein et al., 1986; Schofield et al., 1987; Hallman et al., 1988) have shown that cells of similar appearance to the thick neurons noted above projected to the superior colliculus, whereas callosally projecting cells did not have an apical dendrite reaching into layer 1. The morphological description (Hallman et al.,1988; Hübener and Bolz, 1988) of interhemispheric projection neurons resembled that of slender cells (Larkman and Mason, 1990; Larkman 1991a).

Although several research groups have been able to correlate either the intrinsic physiology with the individual neuronal morphology or the individual cell morphology with the respective projection target, it has not previously been shown directly that cells projecting to the same target area share similar physiological properties as well as common anatomical features e.g.that thick, burst-firing neurons project to the superior colliculus (SC) and slender regular spiking neurons project to the contralateral hemisphere (CLH), as might be suggested on the basis of previous findings. This correlation could most clearly be demonstrated with the use of combined experimental techniques, simultaneously investigating the dendritic morphology, the electro-physiological properties and the projection targets of individual cells. Such a study would also confirm (or otherwise) the findings of Larkman and Mason (1990), Mason and Larkman (1990) and Chagnac-Amitai et al. (1990).

In this study I have therefore combined a retrograde tracing technique with subsequent intracellular recording and simultaneous intracellular staining of individual prelabelled neurons located in layer 5 of the visual cortex.

4.2 Materials and Methods :

Neurons were back-labelled by incorporation of rhodamine-conjugated microspheres, after injection of tracer into either the SC or the CLH and its retrograde transport to the cell somata. (For details of the surgical procedure, for stereotaxic injection of rhodamine conjugated microspheres, details of the slice preparation, the use of an electrode filling solution containing the fluorescent tracer carboxyfluorescein (CF)

and the techniques employed for electrophysiological recording and the subsequent analysis (see **Chapter 3,** Materials and Methods).

Back-labelled neurons were impaled in living slices and their intrinsic electrophysiological properties characterized using electrodes containing CF. After a successful recording period they were also completely filled with CF and were photographed using a low power objective to reveal their morphology immediately after electrode withdrawal. The cell body of each injected neuron was subsequently examined for backlabelling using a higher power objective.

4.3 Results :

From 26 animals a total of 53 layer 5 pyramidal neurons were recorded in two series of prelabelling experiments. In one set of experiments corticotectal projection neurons were investigated, whereas in the other set of experiments interhemispheric projection neurons were studied. 14 cells were unequivocally prelabelled from the superior colliculus (SC) and 19 were unequivocally prelabelled from the contralateral hemisphere (CLH). In addition I recorded from 20 pyramidal neurons which were not backlabelled from either site of injection but were impaled while searching for backlabelled cells in the same slice preparations. A survey of the electrophysiological properties of all groups is compiled in the results section in Tables 4.1 and 4.2.

In the following sections I shall first describe the observations made concerning the morphology of individual cells before presenting the electrophysiological properties

Figure **4.1**: Coronal slices from the rat visual cortex which contained neurons back-labelled by injection of fluorescent microspheres into A) The **contralateral hemisphere** or B) the **superior colliculus.**

Both plates show the equivalent medial part of area 17 with the medial border between area 17 and 18b to the right side. Cortical laminae are indicated approximately on the right side of plate a.

a) Slices containing back-labelled CLH-neurons. A large number of labelled neurons is visible in layers 2/3 and in layer 5. Note the large number of back-labelled CLH-cells which was always present in the lower part of layers 2/3. Layer 4 and the upper portion of layer 5 can be recognized as a zone containing only a few back-labelled CLH-neurons.

b) Slices containing back-labelled SC-neurons. Note that all back-labelled neurons were exclusively located in layer 5 with a higher number of neurons found in the upper portion of the layer.

Scale bar in b =50μm and applies to both.

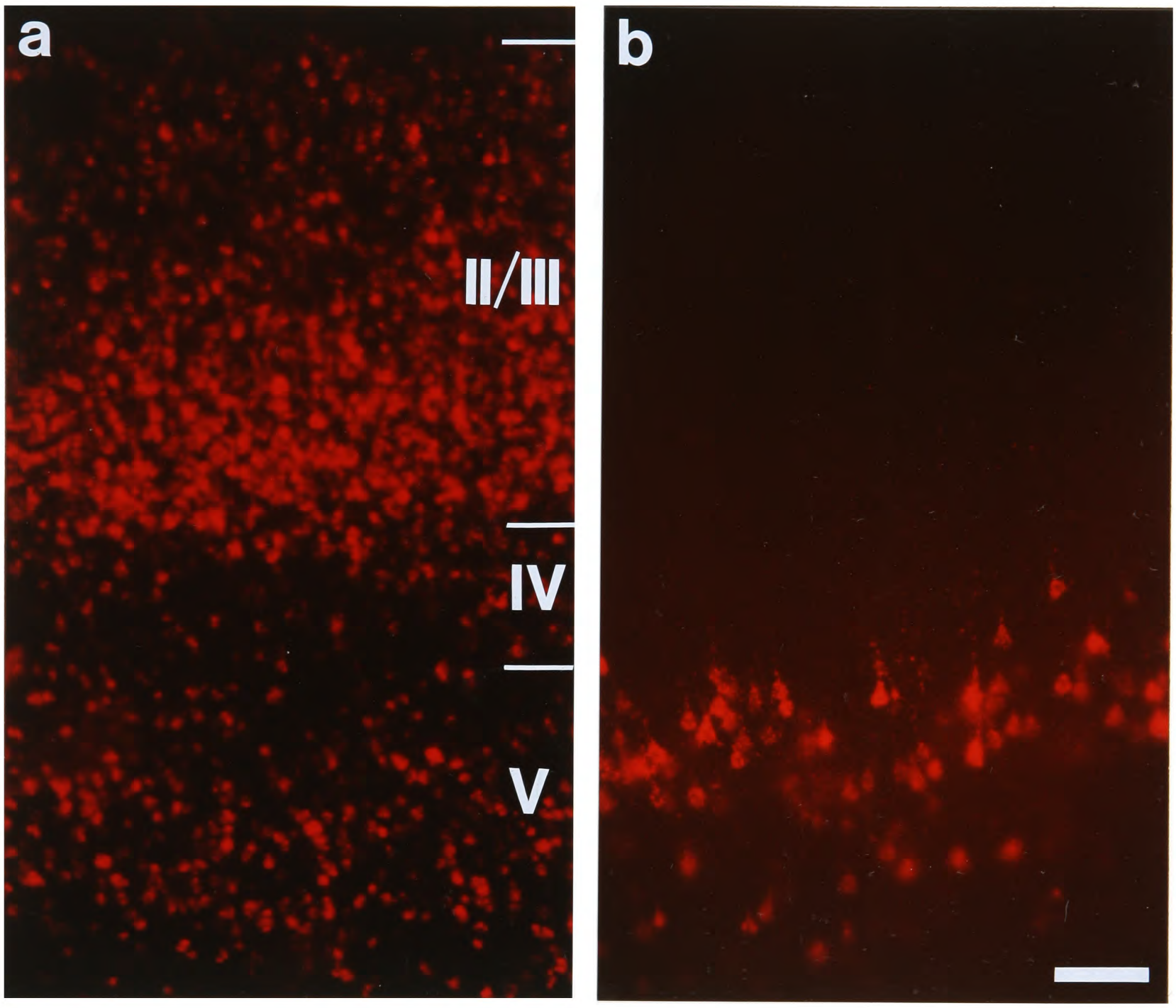
a
II/III
IV
V
b

of the back-labelled cells studied. In the following sections data comparing the two neuronal populations back-labelled from the SC or CLH are presented. For an abbreviated description I have termed neurons that were back-labelled from the superior colliculus **SC-neurons** and neurons that were back-labelled from the contralateral hemisphere **CLH-neurons**.

4.3.1 Qualitative anatomical observations :

a) General results from slice preparations containing cells backlabelled from the SC:

All the cells prelabelled via the injection into the ipsilateral SC were located in layer 5 of the visual cortex. This population of projection neurons formed an uninterrupted band of cells that extended from medial to lateral throughout the whole cortical visual area 17 and extended further laterally into area 18a and medially into area 18b (see Figure 4.1B).

A total of 14 back-labelled neurons was recorded from and simultaneously filled with CF. They all had a similar morphology showing the following characteristic features: a large elongated soma that was higher than wide (see Figure 4.2a,c), a thick apical dendrite that emerged gradually from the upper pole of the soma and ascended towards the pial surface to divide near the border of layers 2/3 and layer 1 to form an extensive arborization in layer 1 (see Figure 4.3 see also **Chapter 7**). All the backlabelled cells possessed between 3 and 7 basal stem dendrites which were

Figure **4.2**: Somata of layer 5 pyramidal neurons of the visual cortex which were back-labelled by injection of fluorescent microspheres into the superior colliculus and subsequently filled intracellularly with carboxyfluorescein (CF).
Plates show two representative neurons from the sample described in **Chapter 4**.

a) High power magnification of the cell body of a corticotectally projecting neuron filled with CF during the recording period.

b) Corresponding picture after the filter block was changed to the wavelenght appropriate for excitation of rhodamine fluorescence. The white arrow points to the neuron also shown in a). Rhodamine- conjugated microspheres could clearly be seen in the soma extending into the apical dendrite.

c) High power magnification of another soma of a corticotectally projecting neuron filled with CF during the recording period.

d) corresponding picture after the filter block was changed to the wavelength appropriate for rhodamine excitation. The white arrow points to the neuron also shown in c).

Scale bar in d =25μm and applies to all plates.

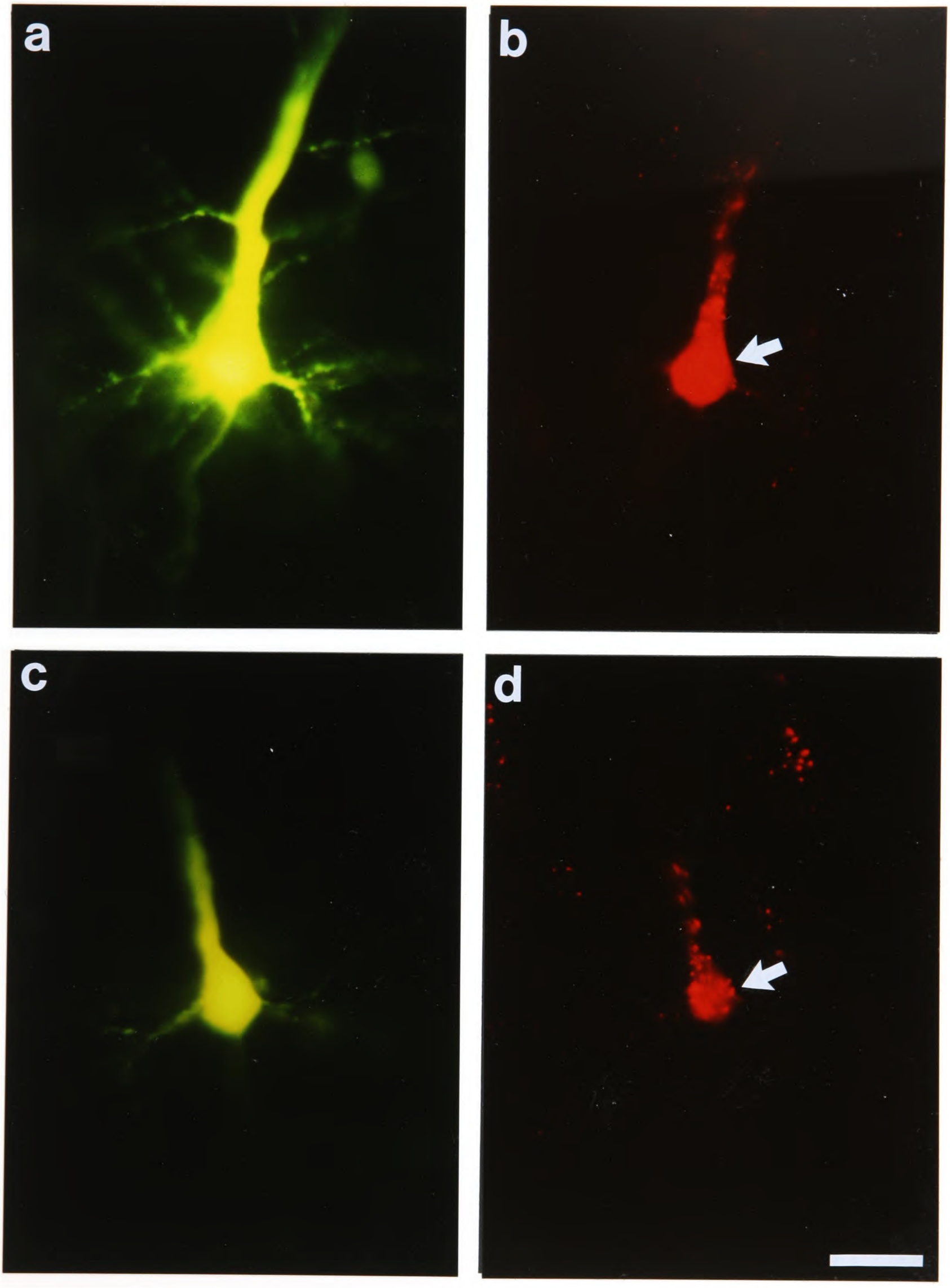
a
b
c
d

Figure **4.3**: Morphology of two layer 5 pyramidal neurons of the rat visual cortex which were back-labelled via tracer injection into the ipsilateral superior colliculus and subsequently filled intracellularly with carboxyfluorescein (CF) during the recording period.

Plates are photo-montages of two representative SC-neurons from the sample described in **Chapter 4,** whose physiological characteristics are shown in Figures 4.8A and 4.9. In both neurons the thick apical dendrite can be seen ascending towards the pial surface and forming a terminal arborization in layer 1.

Scale bar in b =50μm and applies to both plates.

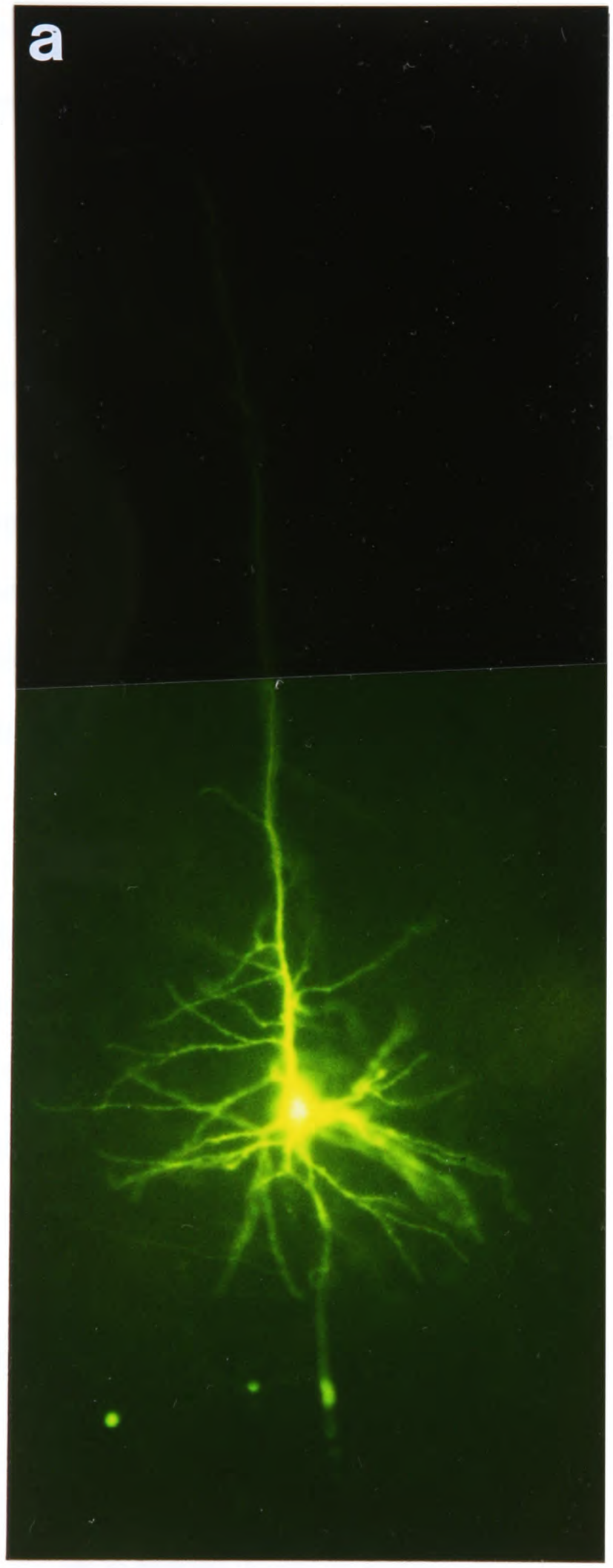
a

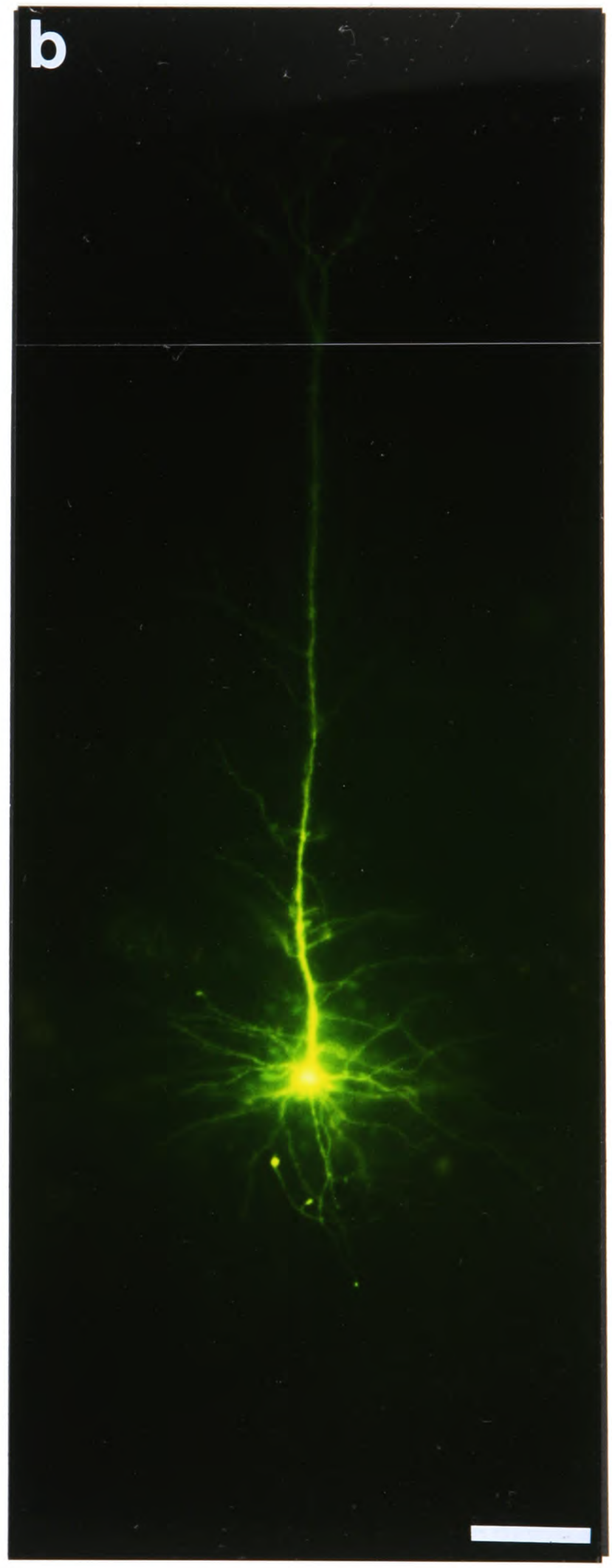
b

generally short, highly branched and extended radially into the vicinity of the cell body but showed no obvious preference in direction. In addition the thick apical trunk of these cells gave rise to a high number of oblique stem branches which were located predominantly near the soma.

Recordings and fills were also made from 10 non-backlabelled cells. One of those non- backlabelled cells had a thick ascending apical dendrite forming a terminal arbor in layer 1 and its dendritic skirt had the same pattern of structure as the SC-neurons. The other 9 non-back-labelled cells from which I recorded in these preparations differed substantially from the SC-backlabelled neurons in their morphological appearance, mainly because they did not possess a thick apical dendrite. Those neurons had only a thin apical dendrite, fewer basal stem dendrites (between 3 and 5) with less branches and therefore a slender appearance.

There were two more non-labelled cells of a different appaerance than the non-labelled cells of the slender type mentioned above. These two neurons (see Figure 4.6) had a thick apical dendrite which bifurcated approximately at the lower border of layers 2/3 and gave rise to two daugther trunks, each of which ascended further up through layers 2/3 to form an apical tuft in layer one.

b) General anatomical results from slice preparations containing cells prelabelled from the contralateral hemisphere :

In a second series of experiments (n=13) fluorescent microspheres were injected into area 17 of the right hemisphere and slices were prepared from the

Figure **4.4**: Somata of two layer 5 pyramidal neurons of the visual cortex which were back-labelled by injection of fluorescent microspheres into the contralateral hemisphere and subsequently filled intracellularly with carboxyfluorescein (CF) during the recording procedure.

Plates show the somata of two representative CLH-neurons from the sample described in **Chapter 4**.

a) High power magnification of the soma of an interhemispheric projecting neuron.

b) Corresponding picture after the filter block was changed to the wavelength appropriate for rhodamine excitation. The white arrow points at the neuron also shown in a). Rhodamine-conjugated microspheres can clearly be seen in the soma of this neuron, although the quality of the prints is lower than that of the respective slides.

c) High power magnification of the cell body of another interhemispheric projecting neuron filled with CF during the recording period.

d) Corresponding picture after the filter block was changed to the wavelength appropriate for rhodamine excitation. The white arrow points at the neuron also shown in c).

Scale bar in d =25μm and applies to all plates.

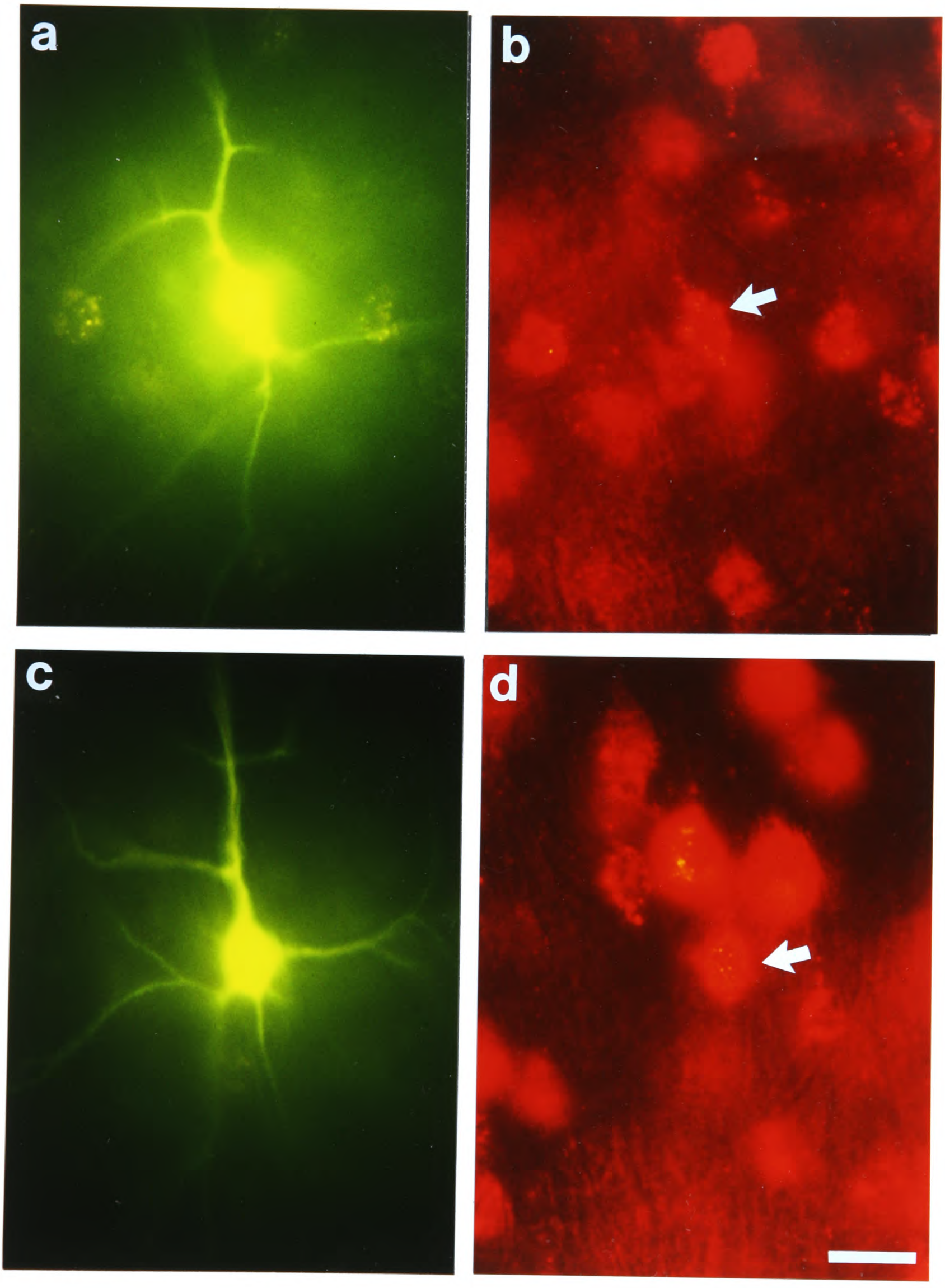
a
b
c
d

Figure **4.5**: Morphology of two layer 5 pyramidal neurons of the rat visual cortex which were back-labelled via tracer injection into the contralateral hemisphere and subsequently filled intracellularly with carboxyfluorescein (CF) during the recording period. Plates show two representative CLH-neurons from the sample described in **Chapter 4,** whose physiological characteristics are shown in Figures 4.8B and 4.10.

In both CLH-neurons the thin apical dendrite can be seen as it tapers and ends below the pial surface without forming a visible arborization in layer 1.

Scale bar in b =50μm and applies to both plates.

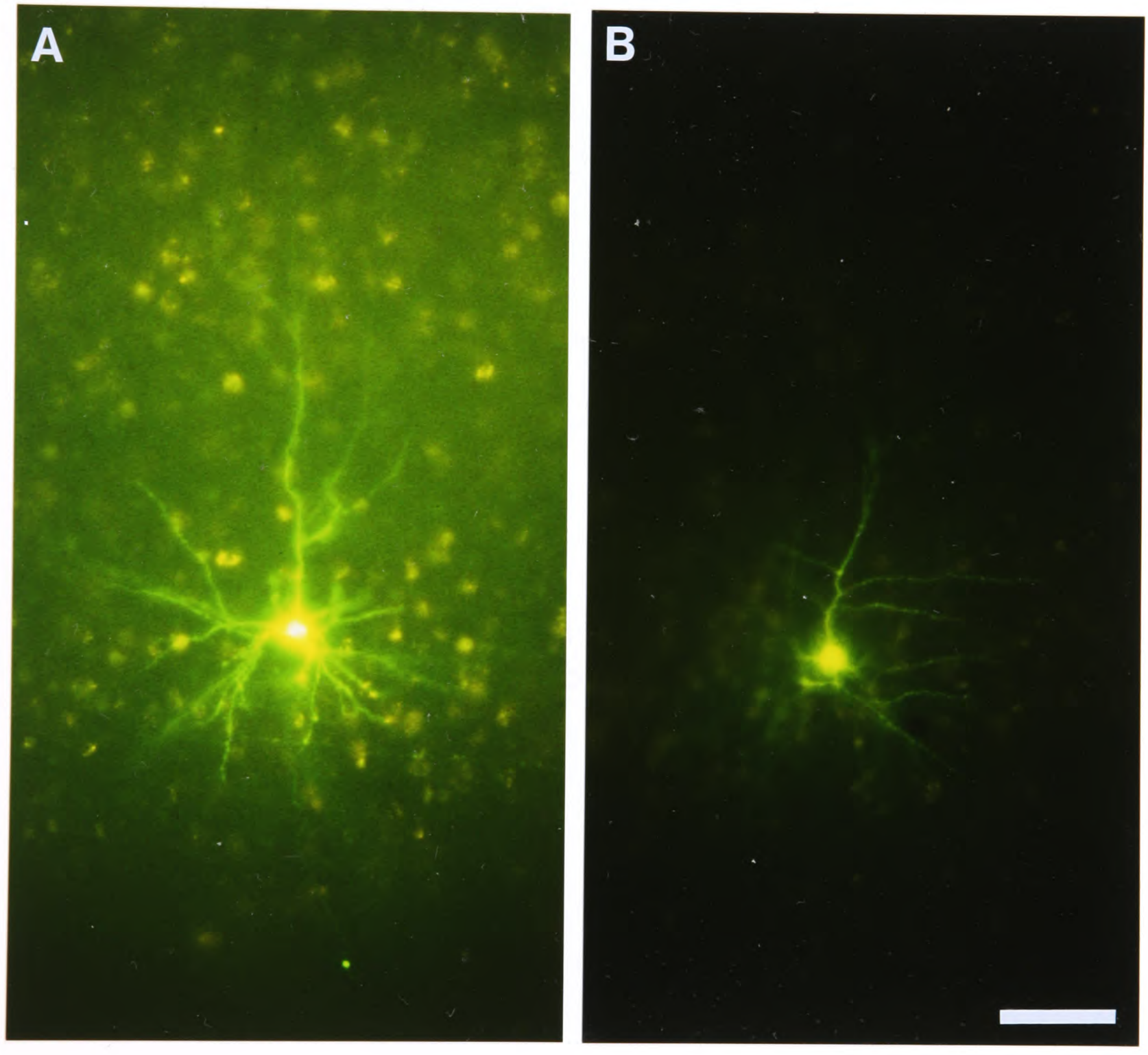
A
B

Figure **4.6**: Morphology of a cortical layer 5 pyramidal neuron with a twin apical dendrite filled intracellularly with carboxyfluorescein (CF) during the recording period. This neuron was not back-labelled in a slice containing back-labelled SC-neurons.
The plate shows a photo-montage of one of two such neurons from the sample described in **Chapter 4,** whose physiological characteristics are also shown in Figures 4.8C and 4.11.

Note that the apical dendrite bifurcates on its way towards the pial surface. Both apical dendrite daughter branches form an extensive terminal arborization in layer 1.
Scale bar =50μm.

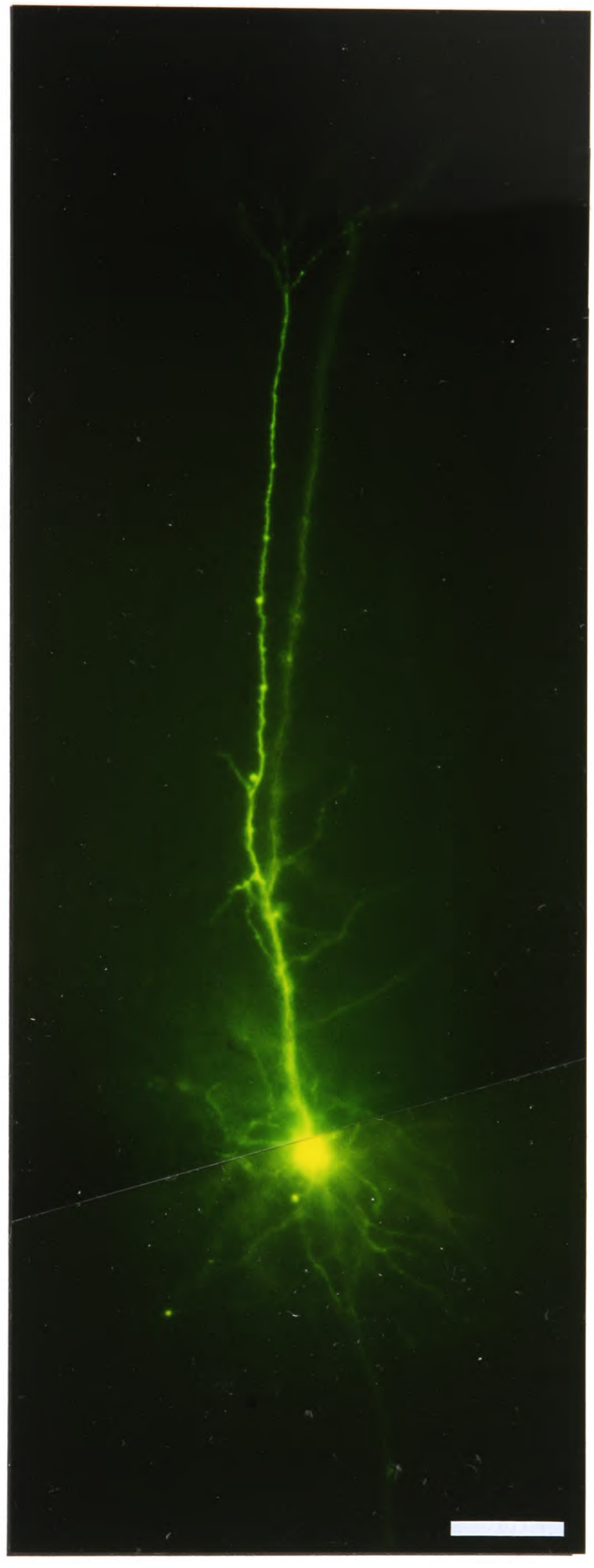

homotopic area of the contralateral cortical hemisphere. There, backlabelled cells were distributed from medial to lateral throughout the visual areae 17 and 18 and found in **all** layers except layer 1 (see Figure 4.1A). Towards and beyond the medial border of area 17 the number of prelabelled cells in the superficial layers increased substantially, whereas in more lateral directions the density of labelled cells decreased in the superficial layers 2/3, but rose again towards the borders of areas 17 and 18a. Layer 4 was always recognisable as a zone of sparse labelling.\

In the slice preparations with such backlabelled corticocortical projection neurons a total of 27 layer 5 pyramidal cells was recorded, of which 19 were backlabelled via the tracer injection and the remaining 8 were unlabelled.

All backlabelled interhemispheric projection neurons formed a group that was distinctly different from the SC-cells described above. Their morphology was of the slender type described by Larkman and Mason (1990) and could be characterized by the following features: a slender appearance, a small cell soma of about equal height and width and an apical dendrite that emerged abruptly from the upper part of the soma (see Figures 4.4a,c and 4.5). In some cases the cell body appeared to be "displaced" (see also Miller, 1988a; Bueno-Lopez et al., 1991). The trunk of the apical dendrite was relatively thin and tapered to a fine diameter as it ascended towards the pial surface to terminate in layers 2/3 without reaching the pial surface (see Figure 4.5). Not a single apical dendrite of any of these cells reached layer 1 or formed an arborization which extended visibly into layer 1. The basal dendritic skirt pattern was less uniform (compared to the group of SC-neurons) but consisted always of a few (between 3 and 5) basal stem dendrites, which showed only a few branch points. Those basal dendrites

seemed to be longer than those from SC-projecting neurons. Sometimes the basal dendrites did not extend uniformly in all directions but were biased towards one side of the soma. Oblique stem dendrites were present in all cells but occurred in relatively smaller numbers, compared to the cells backlabelled from the SC.

All but two of the 8 non-backlabelled neurons recorded from in these experiments with CLH tracer injections belonged morphologically to the slender class. The two remaining other neurons showed a morphology that fitted well into that of cells of the group backlabelled from the SC.

4.3.2 Intrinsic electrophysiological properties :

a) General findings :

All cells included in this sample were capable of firing multiple action potentials overshooting the zero potential if stimulated via intracellularly injected suprathreshold rectangular current pulses but did not fire action potentials spontaneously at the resting membrane potential.

b) Subthreshold properties :

Resting potential: The resting membrane potential ($\mathbf{V_m}$) did not differ between the two groups of backlabelled projection neurons with values of $\mathbf{Vm_{SC}} = 68.8 \pm 3.1$mV and $\mathbf{Vm_{CLH}} = 69.7 \pm 3.6$mV (see Table 4.1).

Membrane time constant: The membrane time constant (tau) was measured from the voltage decay (averaged) following a brief (0.5ms) current pulse (see Figure 4.7). A straight line was selectively fitted to a region of the semilog plot by least-squares linear regression and the region was chosen (by eye) to exclude the initial, faster decay which represents redistribution of charge over the neuron (Rall, 1969; see also **Chapter 3**: Materials and Methods for details). The membrane time constant, tau, of **SC**-neurons was significantly shorter than the time constant obtained from **CLH**-neurons ($p<0.01$) (see Table 4.1). In almost all layer 5 cells the voltage decay following a brief hyperpolarizing current pulse showed some time-dependent rectification phenomenon called "sag" (Connors et al., 1982). Thus the transient voltage decay became more rapid with later times than expected from a single exponential decay. This phenomenon was especially pronounced in **SC**-neurons. In most **SC**-neurons the voltage response following such a brief pulse also showed a transient overshoot with respect to the resting membrane potential. This was much less than during long pulses (used for the investigation of other I/V relations) and is not likely to affect the conclusions.

Current voltage relationship: To test the current/voltage relationship of single cells long ($t \geq 200$ms) current pulses of different amplitude and polarity were injected repeatedly through the microelectrode and the resulting voltage response averaged (see Figure 4.8). The input resistance ($\mathbf{R_{in}}$) was measured from the range negative to rest using values of a voltage deflection between –5mV to –10mV. The result of the measurements showed that **SC**-neurons had significantly lower R_{in} values than **CLH**-neurons ($p<0.01$) (see Table 4.1). Non-backlabelled regular-spiking neurons ($n=17$) had R_{in}-values, which were indistinguishable from **CLH**-neurons, whereas values of

Figure **4.7**: Membrane time constants of layer 5 projection neurons from the visual cortex. Semilogarithmic plots of the voltage decay following brief (0.5ms), hyperpolarizing current pulses injected into

A) a **SC**-neuron

B) a **CLH**-neuron.

Inset scale bars in A apply also to B. Zero value on the X-axis corresponds to the end of the injected current pulse. The dotted lines (from which time constants were taken) are least-squares fits to the straightest portion of the plots.

Membrane time constants from layer 5 pyramidal neurons projecting to the SC or CLH

A

SC-projecting and burst-firing neuron

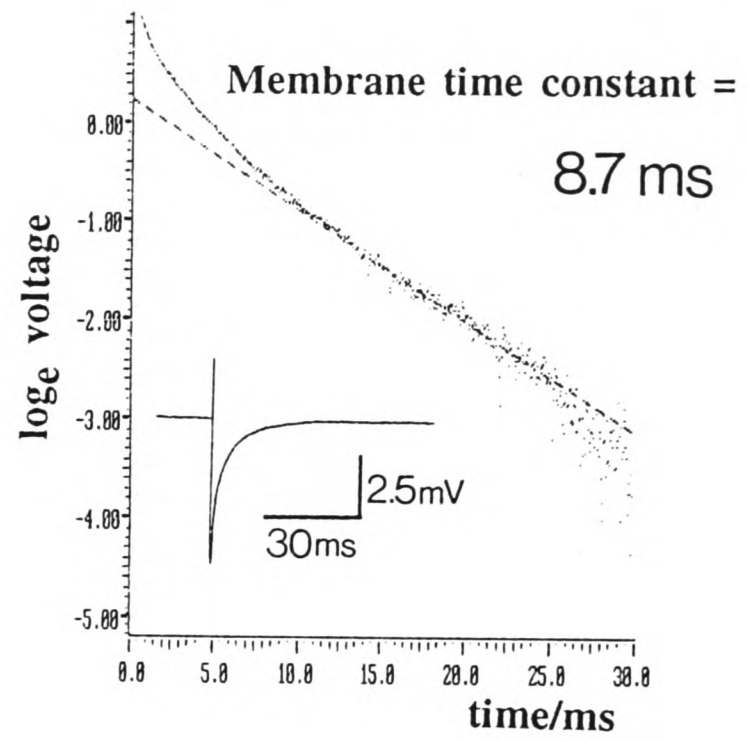

B

CLH-projecting and regular-spike-firing neuron

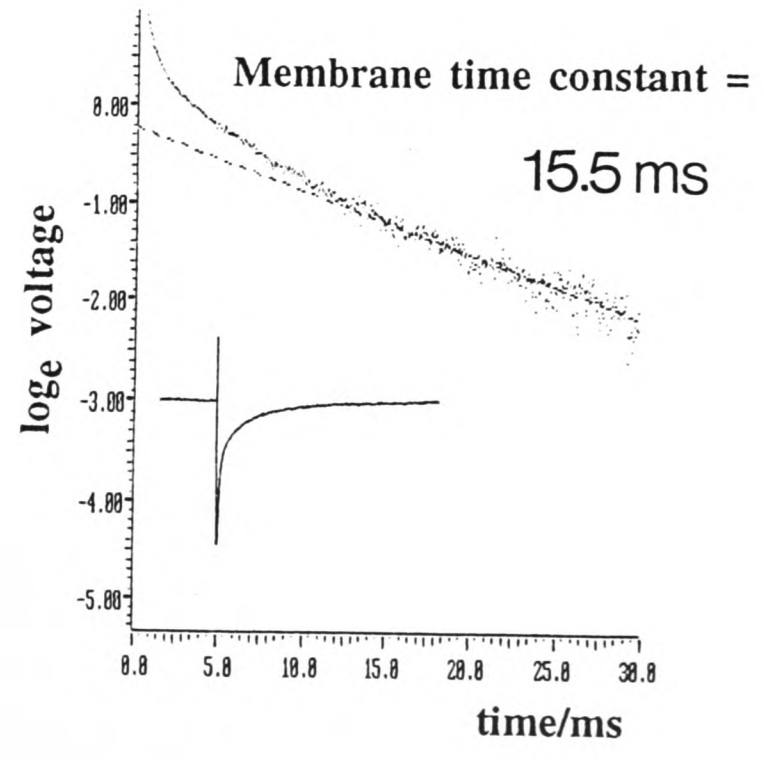

Figure **4.8**: Current voltage relationships of layer 5 projection neurons from the rat visual cortex. Voltage responses (*left side top traces*) to long (t=200ms) current pulses (*left side bottom traces*) injected into:

A) a **SC**-neuron

B) a **CLH**-neuron

C) a non-labelled **twin** apical dendrite neuron.

The voltage response was measured at its peak (hollow circles) and just before the end of the current pulses. Both voltage values were plotted for each pulse against the respective injected current amplitudes (*right side plots* in A, B, C).

Scale bars in Calso apply to A and B.

Current/voltage relations of layer 5 pyramidal neurons projecting to the SC or CLH

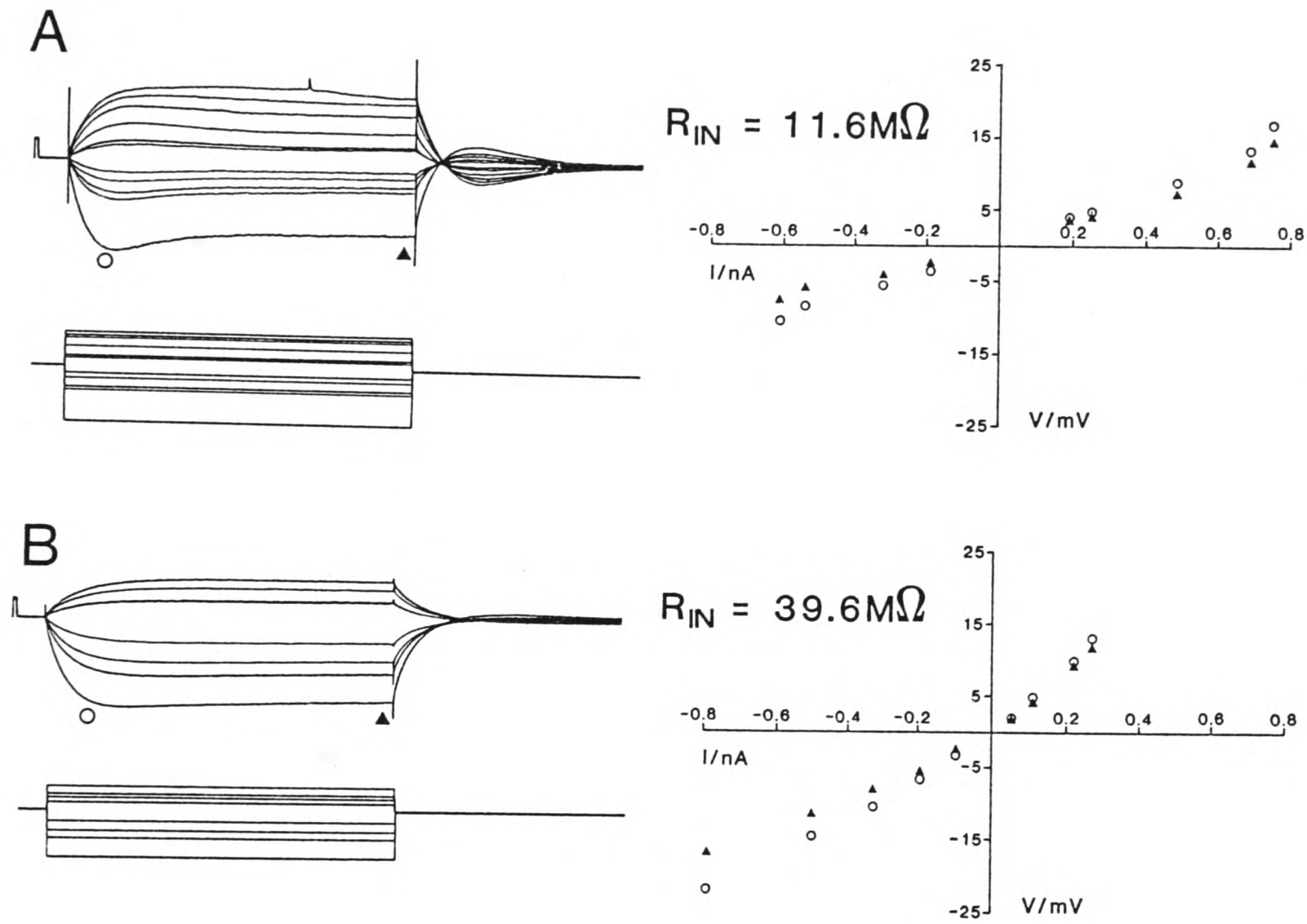

Table 4.1: Subthreshold membrane properties of back-labelled layer 5 projection neurons from the visual cortex.

	SC-Cells	CLH-Cells	non-labelled NB	non-labelled B
no. of cells	10	13	11	3
$-V_m$/mV	68.6 ± 3.1	69.7 ± 3.6	69.8 ± 4.3	67.9
R_{in}/MΩ	14.3 ± 4.6 +	33.7 ± 11.2	35.7 ± 15.7	18.9
time constant/ ms	9.1 ± 3.1 +	16.9 ± 4.7	17.8 ± 3.2	12.1

Data in this and subsequent tables are given as mean values ± SD (where possible).Statistical differences (student's t-test) between SC-neurons and CLH-neurons are indicated as follows:

+ = $p \leq 0.01$; □ = $p \leq 0.05$; ▲ = $p \leq 0.1$

non-backlabelled burst-firing neurons (n=3) fell into the **SC**-neuron range (see Table 4.1). During such long current pulses of both polarities the membrane potential of **SC**-neurons and **CLH**-neurons tended to "sag" back towards the resting membrane potential. Although I did not quantify this in the present study, it appeared that the sag was more pronounced in cells from the group of **SC**-neurons compared to the group of **CLH**-neurons or non-backlabelled neurons in preparations containing backlabelled corticotectal neurons. This observation would be in agreement with previous results obtained from burst-firing neurons and regular-spiking neurons (Mason and Larkman, 1990). For an example see Figure 4.8.

At the end of the injected current pulse the membrane potential tended to overshoot (after hyperpolarizing pulses) or to undershoot (after depolarizing pulses) the resting level (see Figure 4.8). Rebound action potentials were not elicited at the offset of a hyperpolarizing pulse (overshoot) in the range of current I used (-0.75nA to +0.75nA), which I limited to less than those values because electrodes showed signs of rectification with long current pulses above these values. Nevertheless it is conceivable that larger currents might have elicited APs, as has been reported previously for tectal neurons (Lopez-Barneo and Llinas, 1988) .

c) Suprathreshold properties :

Burst firing: The obvious electrophysiological criterion that made it possible to distinguish the intrinsic properties of the two populations of projection neurons in my preparation was the ability of **all SC-projecting neurons** to fire action potentials in a burst-discharge in response to injected suprathreshold depolarizing current pulses. On

the other hand, not a single neuron backlabelled from the contralateral hemisphere was found which showed such a burst-firing pattern after intracellular current injection.

A variety of burst-discharge patterns could be found (see Figure 4.9) but a burst usually consists of several fast action potentials riding on a slow depolarizing envelope of membrane potential. The first spike was generally higher and faster than the following spikes which sometimes decremented substantially during a single burst-discharge. Successive spikes always broadened. The latency of activation could vary substantially and bursts could arise abruptly from the voltage baseline. In several cases I also observed that the burst-discharge was a somewhat fragile firing pattern and changed with successive trials. After an initial full burst in response to an injected current pulse the cell later fired only "collapsed bursts", which often only consisted of one initial fast and large spike and a second smaller spike with an extremely slow falling phase (see Figure 4.9).

Ten out of 14 **SC**-cells showed a burst-discharge in response to any suprathreshold current pulse injected. The other four cells fired single spikes in the just suprathreshold range and bursts only in response to larger current injections. This change occurred gradually, with the burst becoming more pronounced as the injected current strength was increased. Nevertheless each cell fired only one burst followed by a number of single action potentials (see Figure 4.9 and also **Chapter 7** Figure 5 B).

The shape of single action potentials (AP) was broadly similar in all pyramidal cells with respect to their overall appearance, (but see below for spike-firing patterns of **SC**-neurons versus **CLH**-neurons), but there were some statistically significant differences between **SC**-neurons and **CLH**-neurons in quantified AP parameters (see

Figure **4.9**: Action potential firing patterns of layer 5 pyramidal neurons projecting to the SC. Various burst-firing patterns were elicited in response to injected depolarizing current pulses of minimal suprathreshold strength (A1, B1, C1). The right-hand traces (A2, B2, C2) show responses to slightly increased current strengths necessary for the recruitment of one additional spike in each case.

The injected current pulse amplitude is indicated in each trace.

A-traces: the corresponding cell morphology is shown in Figure 4.3 plate a.

B-traces: the corresponding cell morphology is shown in Figure 4.3 plate b.

Scale bars in C apply also to A and B.

Action potential firing patterns of layer 5 pyramidal neurons projecting to the SC

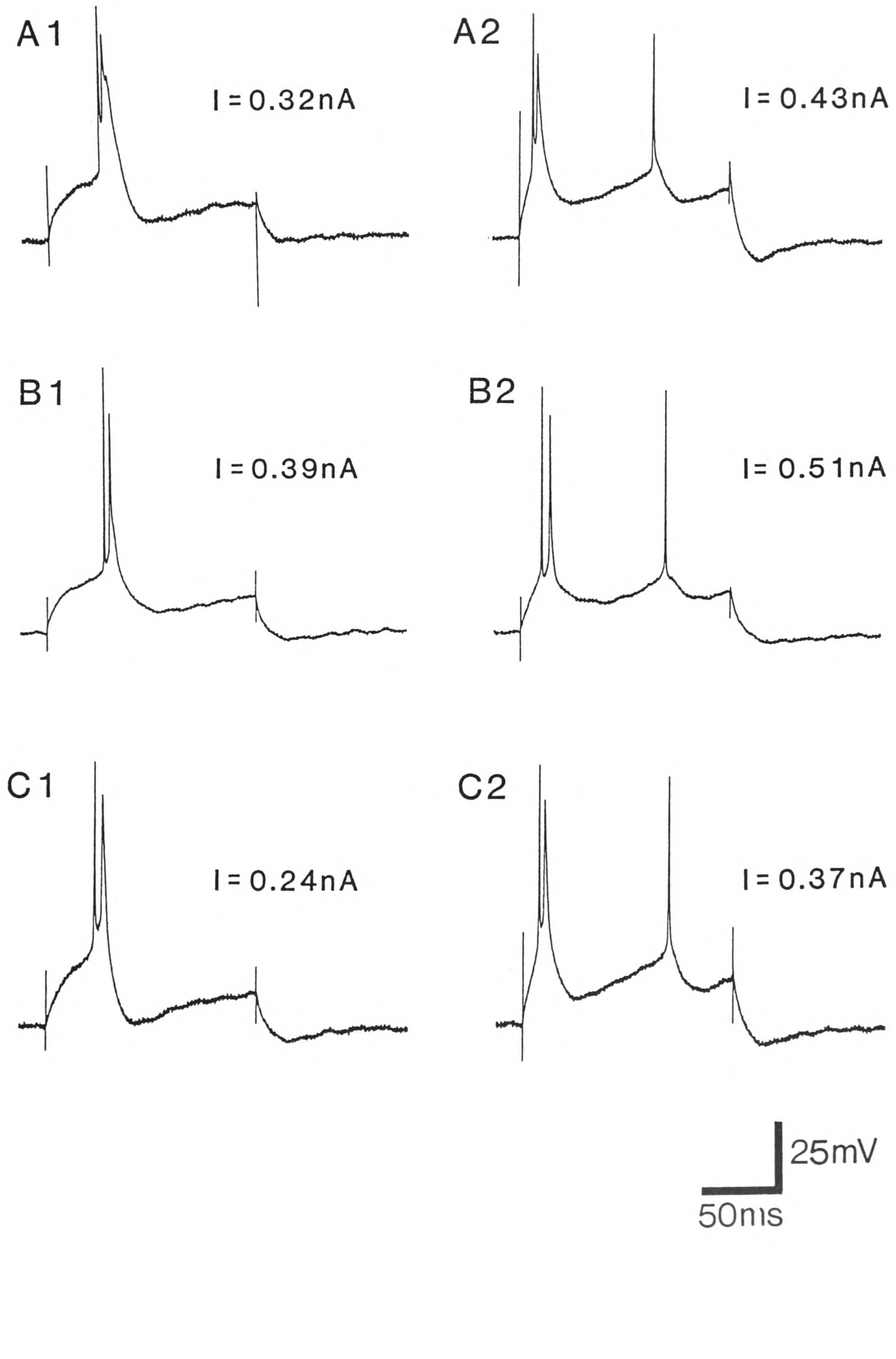

Figure **4.10**: Action potential firing patterns of layer 5 neurons projecting to the CLH. Various regular spike-firing patterns were elicited in response to injected depolarizing current pulses of minimal suprathreshold strength (A1, B1, C1). The right traces (A2, B2, C2) show responses to slightly increased current strengths necessary for the recruitment of one additional spike in each case.

The corresponding current pulse amplitude is indicated in each trace.

A-traces: the corresponding cell morphology is shown in Figure 4.5 plate A.

B-traces: the corresponding cell morphology is shown in Figure 4.5 plate B.

Scale bars in C apply also to A and B.

Action potential firing patterns of layer 5 pyramidal neurons projecting to the CLH

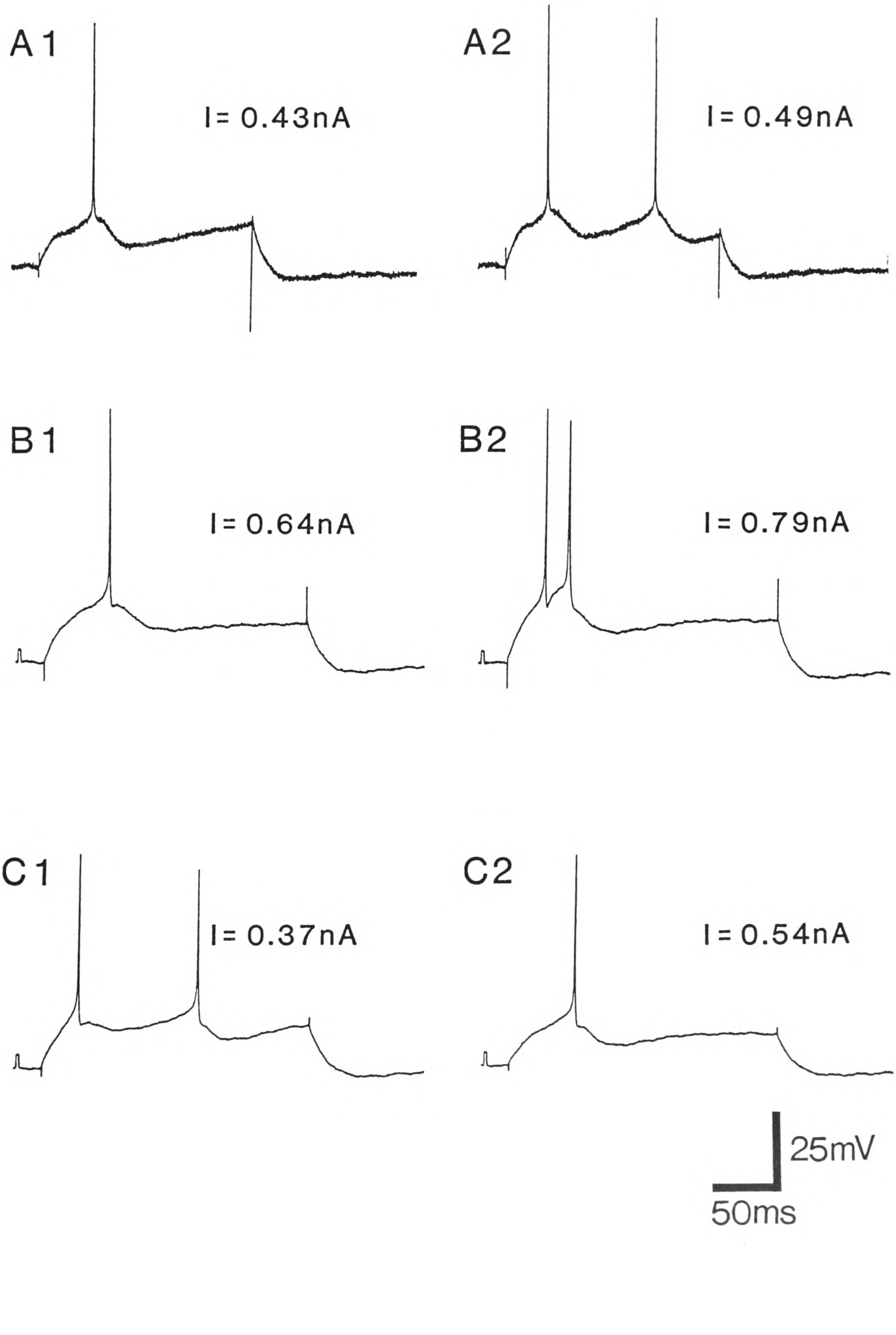

Table 4.2: Action potential parameters from APs of back-labelled layer 5 projection neurons from the visual cortex.

	SC-Cells	CLH-Cells	unlabelled NB	unlabelled B
no. of cells	14	19	17	3
Peak height above threshold /mV	65.5 ± 7.9 +	55.0 ± 4.3	57.1 ± 9.9	67.6
Width of half amplitude /ms	0.63 ± 0.13 □	0.74 ± 0.14	0.72 ± 0.11	0.65
10%/90% rise time /ms	0.22 ± 0.05 ▲	0.25 ± 0.04	0.24 ± 0.04	0.23
90%/10% fall time /ms	0.75 ± 0.14	0.73 ± 0.18	0.74 ± 0.14	0.78
30%/70% rise rate /V/s	299.6 ± 99.3 +	216.6 ± 41.0	224.4 ± 51.6	278.2
70%/30% fall rate /V/s	82.9 ± 21.0 □	67.3 ± 16.2	64.5 ± 11.9	78.4
Rate ratio	3.65 ± 0.52	3.35 ± 0.65	3.50 ± 0.66	3.5

Data in this and subsequent tables are given as mean values ± SD (where possible).Statistical differences (student's t-test) between the SC-neurons and the CLH-neurons are indicated as follows:

+ = $p \leq 0.01$; □ = $p \leq 0.05$; ▲ = $p \leq 0.1$

Table 4.2).

For **all** cells (SC-neurons, CLH-neurons, non-backlabelled regular-spiking cells and non-backlabelled burst-firing cells) the 10/90% rise time of APs was substantially shorter than the 90/10% fall time ($p<0.001$) with the rise time measures being only slightly shorter for **SC**-neurons compared to **CLH**-neurons ($p<0.1$, but see table 4.2). Furthermore there was a significant difference in AP peak amplitude above threshold ($p<0.01$) with **SC**-neurons having higher spikes than **CLH**-neurons. The **SC**-projecting bursters also had a higher 30/70% rise rate and 70/30% fall rate ($p<0.01$) and therefore a shorter width (measured as time from rising phase to falling phase at half peak amplitude) compared to values from **CLH**-projecting nonbursters. Because both the rise rate as well as the fall rate were faster in **SC**-neurons, the ratio of the rise-rate to fall-rate was only slightly different between the two cell groups.

Spike afterpotentials : If single action potentials of the two prelabelled neuronal cell populations were compared it could be seen that APs of both groups were followed by the same sequence of after-potentials. Often the falling phase continued to a value below threshold to form an initial after-hyperpolarisation (i.A.H.P) which was followed by a second depolarizing afterpotential (D.A.P) which again was followed by a late slow A.H.P (l.A.H.P.). These three after-potentials were more clearly distinguished and more pronounced in **CLH**-neurons (see also **Chapter 5,** Figure 5.10).

Repetitive firing : In the range just above threshold, **CLH**-neurons usually fired one or two separated action potentials. As the amplitude of the injected rectangular current

Figure **4.11**: Action potential firing patterns of a non-back-labelled layer 5 twin apical dendrite cell elicited in response to an injected depolarizing current pulse of minimal suprathreshold strength (A). The other traces (B, C, D) show responses to slightly increased current strengths necessary for the recruitment of one additional spike each time.

The corresponding current pulse amplitude is indicated in each trace. The corresponding cell morphology is shown in figure 4.6.

Scale bars in D apply also to A, B and C.

Action potential firing patterns of a non-backlabelled layer 5 pyramidal neuron with a twin apical dendrite

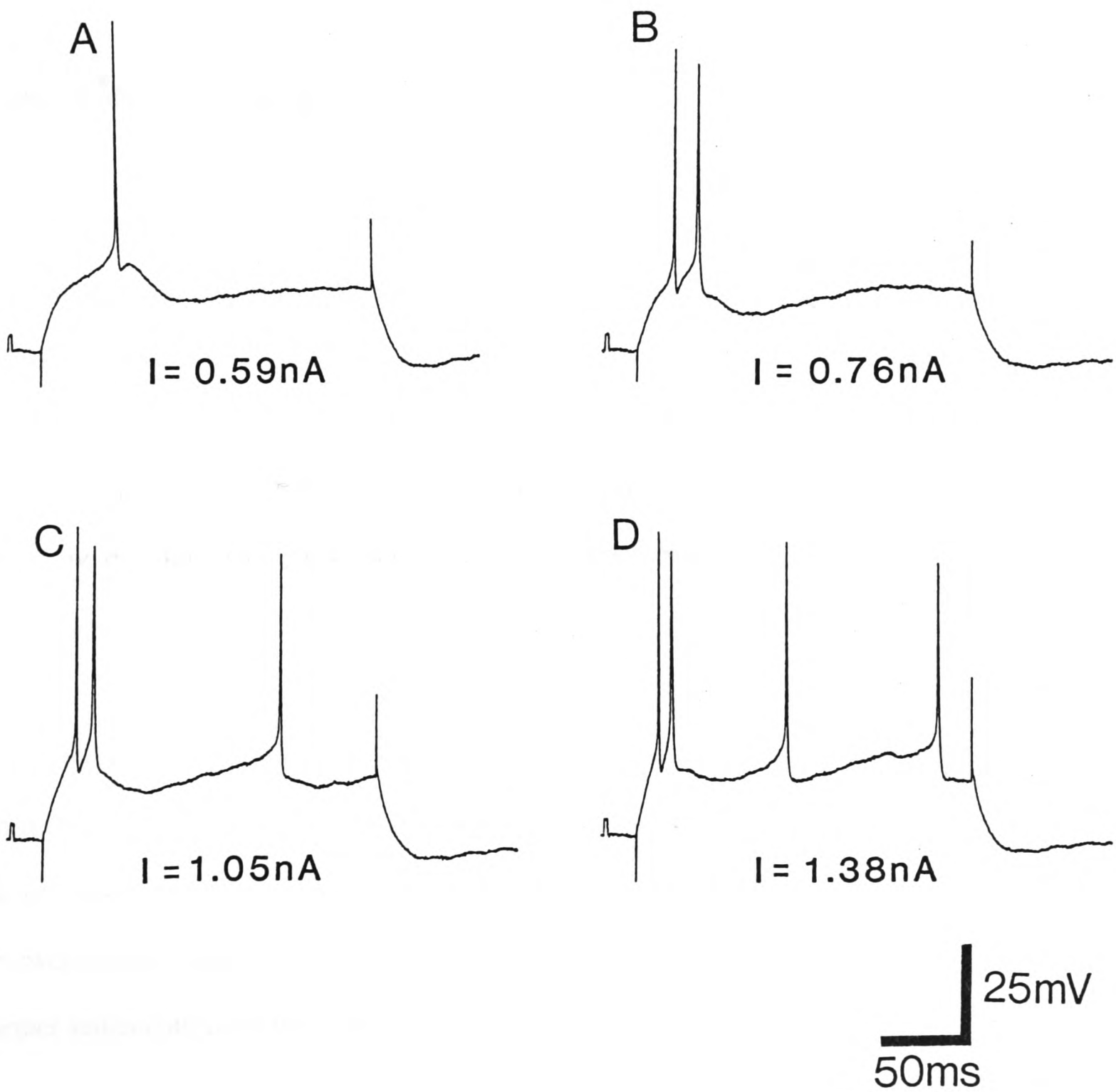

pulse was increased, all cells fired an increasing number of spikes. Although there was considerable variation amongst cells of one group, all **CLH**-neurons showed a gradual increase in spike frequency as the injected pulse strength was augmented. Their firing pattern also showed obvious signs of adaptation with longer interspike intervals after successive spikes. Of the 14 **SC**-neurons described above, 10 fired in bursts and 4 showed a single spike in response to injected current pulses just above threshold.

d) Neurons with a twin apical dendrite:

Two neurons were impaled (in slice preparations containing backlabelled SC-neurons) which differed both in morphology (see Figure 4.6) and electrophysiology from the backlabelled populations. They possessed intermediate values for their input resistance (21.2 MΩ and 20.4 MΩ) and membrane time constant (14.4ms and 13.8ms). They appeared to have less "sag" than the **SC**-neurons and showed pronounced overshoot/undershoot voltage deflections in the subthreshold range tested for the current/voltage relationship (see Figure 4.8c). They fired single action potentials in response to a depolarizing, but only minimal suprathreshold current pulse and always "doublets" if the current strength was slightly increased (see Figure 4.11a,b). An even further increase in amplitude of the injected current pulse elicited additional spikes after substantially longer interspike intervals (see Figure 4.11c). Because only two non-backlabelled neurons of this class were recorded from, it is inappropriate to make further statements about their intrinsic properties.

4.4 Discussion :

The aim of this set of experiments was to explore any correlation between the intrinsic electrophysiological properties, the morphology and the projection target of neurons, which were backlabelled from the site of their axonal termination. The experiments of this chapter demonstrated that in layer 5 of the visual cortex of the rat the corticotectal projection arises from a population of burst-firing neurons of a distinct morphological type, which is characterized by a thick apical dendrite extending towards the pia and reaching into layer 1. On the other hand it was demonstrated, that the interhemispheric projection of layer 5 arises from a population of regular-spiking neurons with a slender morphological appearance, whose apical dendrite does not reach layer 1. The results showed that the two classes of neurons investigated differ significantly in both their subthreshold as well as their suprathreshold properties. Subdivisions of the two groups could not be revealed, but a larger number of cells might have allowed this. The findings thus confirmed those of Larkman and Mason (1990), Mason and Larkman (1990), and Chagnac-Amitai (1990) and extended them to provide the first direct demonstration of a correlation between two cell classes of this kind and the projection target of the cells studied.

The known existence of other projection neurons within other layers of the visual cortex (e.g. projecting to the pons or the LGN) or within the somatosensory cortex (eg. projecting to the pons or via the pyramidal tract) encourages further investigation to see whether other neuronal populations with comparable correlations can be found.

In the following sections it will be discussed to what extent this sample is representative for the two populations of projection neurons studied. The result will then be compared to previous anatomical and physiological studies before the significance of the findings is discussed.

4.4.1 Anatomy :

Possible reasons for a sampling bias :

The results presented in the preceding sections show that corticotectal cells located in layer 5 of the visual cortex are relatively large, burst-firing cells with a long apical dendrite reaching layer 1. It is conceivable that some smaller cells with different electrophysiolgical properties might also participate in this projection but remained undetected because larger neurons were impaled more often. I consider this possibility unlikely for several reasons. Firstly, relatively sharp microelectrodes were used for impalements in this study compared to other combined electrophysiological-morphological studies employing the HRP-technique (e.g. Deschenes et al., 1979; Parnavelas et al., 1983; Mason and Larkman, 1990). Secondly, none of the burst-firing cells found in this study or in any of the previous studies (Chagnac-Amitai et al., 1990; Larkman and Mason, 1990; Mason and Larkman, 1990; Lohmann et al., 1991) had a morphology that was different from that of the SC-neurons examined. Thirdly, all the previous studies of corticotectal cells showed a morphology that is very similar to the thick type found in SC-neurons here (e.g. Klein et al. 1986; Schofield et al.1987). With respect to the interhemispheric projection neurons the possibility of a sampling bias is more difficult to exclude. The variability of measured electrophysiological

parameters was much higher in CLH-cells and the possibility exists that a substantially larger sample would allow some subdivision of that class of neurons, as was hinted by Mason and Larkman (1990). The greater morphological heterogeneity has been noticed before (e.g. Hübener and Bolz, 1988 in rat; Diao and So, 1991 in hamster; Buhl and Singer, 1989 in cat) and supports this idea, and it woud be of interest to see whether there are functional or structural differences in cells of such possible subclasses.

Subpopulations of pyramidal neurons in the infragranular layers of the neocortex :

The investigation of differences in the morphology of cortical pyramidal cells is by no means modern. The existence of two cell types has been mentioned for more than 40 years (Lorente de Nó, 1943; Parnavelas et al., 1977) including the important observation that one type of neurons possessed an extensive apical dendrite and the other one does not. In the motor cortex of cat, different physiological classes of corticospinal cells have been distinguished on the basis of their dendritic morphology (Deschenes et al., 1979, Samejima et al., 1985). Other studies have also pointed out the existence of more than one type of pyramidal neuron in layer 5 of the rat visual cortex. Peters and collaborators (Peters, 1985; Peters et al., 1985, 1987; Peters and Kara, 1985) have emphasized two types of neurons, which they called large- and medium-sized pyramids, based on measurements of the soma size and diameter of the apical dendrite. Their large cell type had an apical trunk which gradually arose from the upper pole of the cell body, whereas the medium sized pyramids showed a more abruptly arising apical dendrite. It is therefore reasonable to assume that their two classes

correspond to the two cell types Larkman and Mason (1990) as well as Chagnac-Amitai et al. (1990) and coworkers have described in combined anatomical-electrophysiological studies which in turn seem to correspond well to the two populations under investigation in this thesis. With respect to the corticotectal cell group this correspondence is more likely because these cells formed a more homogeneous group, especially with regard to the correlation between morphology and action potential firing pattern. (For the interhemispheric projection neurons see below).

The results for the corticotectal group are also strongly supported by morphological observations of corticotectal cells made by Klein et al.(1986) and Schofield et al.(1987) and those of corticotectally and callosally projecting neurons studied by Hübener and Bolz (1988), with the latter authors also indicating a differential intralaminar distribution of these pyramidal cells. They reported that corticotectal cells are located in the superficial portion of layer 5 whereas the interhemispheric cells are found throughout layer 5 and upper layer 6, an observation which was also made in this study (see Figure 4.1). The same intralaminar distribution was also found in a similar rat visual cortex preparation by Hallman et al.(1988).

Comparison of the laminar distribution of cortical projection neurons in other species :

Most efferent projections from the neocortex originate from pyramidal cells located in the infragranular layers (Creutzfeld, 1983) although in higher mammals the majority of corticocortical cells is located in the superficial layers. Some of these cells innervate two projection targets, but these are generally speaking either both subcortical

or both intracortical and not mixed (e.g. Toyama et al., 1969; Toyama et al., 1974; Catsmann-Berrevoets et al., 1980; Wong and Kelly, 1981; Weber et al., 1983).

Cortico-subcortical projections:

For the cortico-mesencephalic projection it has been shown physiologically –by antidromical activation– that two thirds of corticotectal neurons in the cat also project to the pontine nuclei (Baker et al., 1983). The related anatomical evidence for this observation is supportive but less coherent. Keizer et al. (1987) showed by double-labelling studies for the same pathways a much lower percentage (12-60%) of axon collaterals in cat; Hallman et al. (1988) used other fluorescent tracers in a study cortical neurons in rat and showed about the same percentage of neurons double-labelled as expected from the physiological results, with 71% of corticopontine cells sending collaterals to the SC and 81% of corticotectal cells sending collaterals to the pons.

There is also evidence for a differential distribution of projection neurons within a single cortical layer. Hallman et al.(1988) reported that in the rat 80% of all corticotectal and corticopontine neurons are located in the upper two thirds of layer 5. A comparable observation of the distribution of corticotectal cells was previously made in studies of the cat (Kawamura and Konno, 1979) and the macaque monkey (Lund et al., 1975).

There were no differences observed in the intralaminar distribution, if single-labelled neurons neurons projecting to the SC or the pons were compared to a SC-pons double-labelled population (Hallman et al., 1988). Other reports indicate that

corticopontine projecting cells were located even more superficially than corticotectal projection neurons (O'Leary and Stanfield, 1986). All these reports are at odds with two other published studies: Wiesendanger and Wiesendanger (1982) concluded that in rat cortex all corticopontine neurons are located in lower layer 5 and Peters and Kara (1985) described their largest pyramidal cells as being located in the lower portion of layer 5.

It appears that the discrepancy in some results of previous studies may have been caused by different ways of delineating cytoarchitectonic borders of the respective layers which is particularly difficult in rodents.

Interhemispheric projections :

In the visual cortex the distribution of neurons projecting to the contralateral hemisphere is very different from the corticotectal projections in the several species studied so far. It was demonstrated that these interhemispheric fibers originate and terminate for most mammals near the border of area 17, as in the rat (Jacobson and Trojanowski, 1974; Olavarria and Van Sluyters, 1983; Miller and Vogt, 1984; Hübener and Bolz, 1988), the mouse (Olavarria and Van Sluyters, 1984), the rabbit (Swadlow et al., 1978), and the hamster (Dürsteler et al., 1983; Rhoades and Delacroce, 1980; Jen et al., 1984; Diao and So, 1991). In cat it has been described that the main callosal projection of the primary visual cortex originates in layers 2/3 in the lateral portion of area 17 (Innocenti and Fiore, 1976, Shatz, 1977). In primates such projections seem to be sparse from the primary visual cortex (Swadlow, 1983), but if present they are also arise in layers 2/3 (Weyand and Swadlow, 1980; for a review see Swadlow, 1983).

Most of these studies concluded that the majority of callosal connections originate and terminate close to the border of area 17/18, thus representing the vertical meridian of the visual field. Despite this common feature in the organisation of transcallosal connections, the functional significance of the differences in regional and laminar distribution of cells participating in the interhemispheric connectivity remains obscure. (Some aspects of specific functions for the interhemispheric and the corticotectal projections are discussed in **Chapter 8**).

Few, if any, of these interhemispheric projection neurons have subcortically projecting axon collaterals (see Wong and Kelly, 1981 for corticothalamic projection in cat auditory cortex; Catsman-Berrevoets et al.,1980 for corticospinal projection from rat somato-sensory cortex; Weber et al., 1983 for cat corticotectal projection from the visual cortex). Such results have also been corroborated for rat visual cortex preparations, with neither Hallman and coworkers (1988) nor Hübener and Bolz (1988) finding any neurons projecting to the superior colliculus (or the pons) and the contralateral hemisphere, as investiated using fluorescent double labelling techniques. It may therefore be a general principle of cortical organisation that interhemispheric axons do not send collaterals to subcortical targets.

Dendritic morphology of single cells :

With the introduction of fluorescent microspheres for retrograde tracing techniques (Katz et al., 1984) and subsequent intracellular injection of such back-labelled cells or by combining electrophysiology with intracellular dye injection (e.g.

Deschenes et al., 1979) it has been possible to study the morphology of individual cells whose projection site is known.

In 1987 Katz reported that there are obvious distinctions between the dendritic morphology of layer 6 neurons projecting to the claustrum and those that project to the dorsal lateral geniculate nucleus in the cat. In studies of cortical neurons a considerable heterogeneity in the morphology of interhemispheric projecting neurons has been noticed (e.g. Klein et al., 1985, 1986; and Diao and So, 1991 for hamster neocortex, Schofield et al., 1987; Hübener and Bolz, 1988 for rat visual cortex). This is in sharp contrast to observations of a strikingly homogeneous group of corticotectal projection neurons.

In the study of Hallman et al.(1988), the authors described a sample of callosal projection neurons in which no cell had an apical dendrite extending beyond layer 4 and concluded that the observation of an apical dendrite reaching layers 2/3 is sufficient to distinguish corticotectal or corticopontine neurons from callosal projection neurons.

Neither the results from Hübener and Bolz (1988) nor my own observations (see also **Chapter 6**) support this conclusion, because some of the corticocortical cells had relatively long apical dendrites, which reached considerably further than layer 4.

For most layer 5 pyramidal cells the basal and apical oblique dendrites together contribute over 70% of the total dendritic shaft membrane area of the cell (Larkman and Mason, 1990; Larkman, 1991b) and of the oblique dendrites the majority arises close to the soma. The basal dendrites together with the proximal oblique dendrites occupy a roughly spherical volume of cortex around the soma predominantly in layer 5 (Larkman, 1991b), within which they therefore receive most of their synaptic input. On

the other hand the apical dendrite might sample a very different cortical volume. The apical trunk and some distant oblique dendrites can receive inputs from layers 2/3 while the terminal arborisation receives input from layer 1. The different classes of layer 5 neurons will receive different proportions of their input from specific layers which may be functionally very important. Since many local and also extrinsic axons from different sources form synapses in a laminar-specific fashion, it is worth thinking about the functional aspects of such an observation in terms of the different inputs to the dendritic branches (e.g. cholinergic, serotonergic etc.) which might have a modulatory role in cortical function. For a discussion of these aspects see **Chapter 8.**

4.4.2 Electrophysiological properties :

The values for basic cell properties such as resting membrane potential, apparent input resistance, membrane time constant and action potential parameters reported here are within the range of previous results of neocortical neurons ***in vitro*** from various laboratories (e.g. Connors et al., 1982; Stafstrom et al., 1984 ; McCormick et al., 1985; Sutor and Zieglgänsberger, 1987; Bindman et al., 1988; Chagnac-Amitai et al., 1990; Mason and Larkman, 1990). It can therefore be said with confidence that the quality of the intracellular recording was not seriously diminished by the use of the fluorescent tracer CF, which was necessary to obtain morphological information and to confirm the back-labelling of the cells from which recordings were taken.

Evaluation of subthreshold properties :

The membrane time constant (tau_m), measured from the voltage decay following a brief current pulse, was significantly longer for CLH-neurons than for SC-neurons. The measured values will represent the real time constants only if a number of conditions are satisfied (Rall, 1969; Jack, 1979). These include the necessity that the voltage decay is passive, that means not influenced by active conductances. This was clearly not the case in most layer 5 neurons in which the later part of the decay became more rapid than expected from a single exponential and the resting membrane potential was transiently overshot. The same observation was made in an identical preparation by Mason and Larkman (1990) and similar observations have been made from motoneurons *in vivo* (Gustavson and Pinter, 1984; Fleshman et al., 1988). This might have caused some underestimation of the real value of the membrane time constant, although measurements were taken before the onset of the sag was apparent. This problem is minimized by the use of short pulses (Durand et al., 1983).

The apparent input resistance was measured over a voltage range just negative to rest. Values of SC-neurons were significantly lower ($p<0.01$) than those of CLH-neurons, although the presence of sag might have caused some underestimation of the R_{in} value (Fleshman et al., 1988; Mason and Larkman, 1990). Because both types of projection neurons showed some sag the underestimation would have affected both cell groups although not necessarily to the same extent, thus probably influencing the difference between the two groups only a little.

Current/voltage relations: All cells tested showed a decrease in R_{in} when the amplitude of injected current pulses was increased in either the hyperpolarizing or the depolarizing direction. Such inward (or anomalous) rectification has previously been observed in

neocortical neurons (Connors et al., 1982; Staftstrom et al., 1982; Stafstrom et al., 1984; Sutor and Zieglgänsberger, 1987; Bindmann et al., 1988; Avoli and Olivier, 1989; Mason and Larkman, 1990). In the depolarizing direction it is most probably caused by a persistent inward sodium current (Connors et al.,1982; Stafstrom et al., 1984; Stafstrom et al., 1985; Sutor and Zieglgänsberger, 1987). In the hyperpolarizing direction it could be explained by a fast inward potassium current (anomalous rectifier) found in cortex (Spain et al., 1987; Sutor and Zieglgänsberger, 1987) or other brain areas (e.g. Osmanovic and Shefner, 1987; Griffith, 1988). Phenomena similar to the sag and overshoot/undershoot observed in both layer 5 populations studied have been found in a wide variety of neurons (e.g. Halliwell and Adams, 1982; Griffith, 1988; Hounsgaard and Midtgaard, 1988) including those of the mammalian neocortex (e.g.Staftstrom et al., 1982, 1984; Penit-Soria et al., 1987; Spain et al., 1987; Avoli and Olivier, 1989; Connors and Gutnick, 1990). These findings suggest a slow inward rectifier, although other currents such as the M current, the calcium-sensitive potassium current ($I_{K(Ca)}$) and the low threshold calcium current could contribute to the observed voltage deflection. The functional role of such nonlinearities is unclear, but it could be the case that currents such as the anomalous rectifier are involved in spike-frequency adaptation and control of cell excitability after repetitive activation via a regulation of size and duration of spike-afterpotentials. The persistent inward sodium current contributing to non-linearities in the range above resting membrane potential could selectively influence cable properties (Adams and Galvan, 1986; Yoshii et al., 1988).

Suprathreshold properties: Although single action potentials were similar in their general shape, significant differences were detected between the two cell groups studied. A greater rise rate and fall rate was observed in SC-neurons, which therefore

determined the smaller width and the only slightly larger 30%/70% rate ratio of spikes of these cells compared to those of CLH-neurons. The values for action-potential parameters obtained in this study are in good agreement with those from neurons of the rat sensorimotor cortex (McCormick et al., 1985). However all AP-parameters measured (AP peak amplitude, rise and fall time, rise and fall rate, and width) were considerably smaller than those from rat visual cortex published by Mason and Larkman (1990). The values for membrane time constants and cell input resistance were also noticeably smaller than those reported the study by Mason and Larkman (1990).

The main reason for this discrepancy is probably the fact that a new set up was used that was especially assembled for this study. The absence of a conventional air-table, the employment of the epifluorescence compound microscope and an additional crosstable necessary for movement of the complete slice chamber might well have caused some additional mechanical instability. The use of carboxy-fluorescein might also have influenced the membrane characteristics, since it is known that some dye-molecules bind to membraneous proteins (Waggoner, 1978). One additional reason for the discrepancy between the results of this study and results of Mason and Larkman (1990) might be that the latter authors used excessive capacitance compensation throughout the recording duration because they did not continously monitor it during the recording procedure. This may have artifactually boosted the amplitude of APs.

Nevertheless the differences in action potential parameters and subthreshold properties between the two backlabelled cell populations (SC-cells and CLH-cells) investigated in this study are similar to those between slender regular spiking and thick

burst-firing cells reported by Mason and Larkman (1990).

Spike afterpotentials: Single action potentials of cells from both groups were followed by a similar sequence of after potentials. An initial fast A.H.P was followed by an intercalated D.A.P, which in turn was followed by a late A.H.P. This observation has been made in previous studies (McCormick and Prince, 1987; Bindman et al., 1988; Huguenard and Prince, 1988; Mason and Larkman, 1990). The initial A.H.P may be due to activation of a K^+-current (A-current, e.g. Connor and Stevens, 1971; Prince and Huguenard, 1988), the intercalated D.A.P. is caused by Ca^{2+}-currents (e.g.Konnerth et al., 1986; Friedman and Gutnick, 1987; Schwindt et al., 1988) and the late A.H.P is mediated by a calcium dependent K^+-current (e.g. Hotson and Prince, 1980; Lancaster and Adams, 1986). Most of these currents have their main effect on spike repolarisation, but they may also be involved in modulating neuronal spike frequency and its accommodation.

Burst firing: Of the two populations of projection neurons studied in this set of experiments only the SC-neurons fired action potentials in bursts. Such bursts could vary between cells, but all consisted of a number of fast action potentials riding on a depolarizing envelope, which was followed by a slow A.H.P. Various studies have reported burst-firing neurons in neocortex (McCormick et al., 1985; Prince and Huguenard, 1988; Montoro et al., 1988; Connors and Gutnick, 1990; Mason and Larkman, 1990; Lohmann et al., 1991). My observations confirm the finding that the threshold for burst-firing was in some cases greater than that for eliciting single action potentials and that bursting could develop gradually as the injected depolarizing current was increased. Because such a burst-firing pattern could be elicited via intracellular

injection of current and could be changed by changes in the current amplitude injected, I consider it to be generated by intrinsic membrane properties rather than by synaptic input. Transmembrane calcium currents are believed to be involved in generation of bursts in hippocampal CA3 neurons (Wong and Prince, 1978; Johnston et al., 1980) and in neocortical neurons (Deisz and Prince, 1990). Several calcium currents have been found in neocortical neurons (Connors et al., 1982, Stafstrom et al., 1985, Franz et al., 1986; Friedman and Gutnick, 1987; Deisz and Prince 1990) but there is also strong evidence for a sodium component of the depolarizing envelope (Konnerth et al., 1986, Deisz, 1988). The contribution of a potassium current in preventing burst firing became evident via pharmacologial experiments in which blocking of K^+-currents converted regular spiking cells into burst-firing cells (Connors and Gutnick, 1984; Schwindt et al., 1988).

In this study, only the SC-neurons were capable of generating the intrinsic burst-firing pattern. However, previous studies of cell populations other than layer 5 of the visual cortex also found cortical cells that fired action potentials in bursts (Connors et al., 1982; Artola and Singer, 1987; Friedmann and Gutnick, 1987; Montoro et al., 1988; Thomson et al., 1988; Lohmann et al., 1991). The different and partially contradictory findings might be explained in several ways. First, different species were used and different cortical areas were studied. Second, there were differences in the definition of a burst-firing pattern. Third, by the fact that it is impossible to determine the location of the cell from which recordings were taken if the recording electrode is not filled with a dye that allows observation of the recording site and of each recorded cell. If morphological data are not available it is conceivable that impalements achieved in one of the more superficial layers (2/3 or 4) were actually obtained from the apical dendrites of cells located in the deep layers of the cortex. This may have been the case

in early studies by Connors et al. (1982) and McCormick et al. (1985) in which they concluded that a large proportion of their bursting cells were spiny stellate cells of layer 4 although the photographs published in these paper did not definitively prove this hypothesis for such cells in s. Workers in this laboratory frequently obtain impalements of thick apical dendrites in layer 4 and lower layer 2/3 (A. Larkman, personal communication). So far, only two recent studies have provided detailed anatomical descriptions of the pyramidal cell types that were capable of either burst-firing or regular-spike firing (Chagnac-Amitai, 1990; Larkman and Mason, 1990; Mason and Larkman, 1990) and their findings are consistent with mine.

What is the functional significance of bursting? It has been speculated that burst-firing cells recorded in layer 4 (which in fact might have been layer 5 cells impaled in their apical dendrite) receive a strong excitatory thalamic input which may evoke their burst-discharge *in vivo* (McCormick et al., 1985; Prince and Huguenard, 1988). Perhaps such a massive excitation deos affect corticotectal layer 5 cells via the basal and especially proximal oblique dendrites of these neurons. The possibility of a synaptic initiation of burst discharge has been shown by Mason and Larkman (1990), who reported that orthodromic synaptic suprathreshold stimulation of thick layer 5 cells could elicit a burst-discharge in 5 out of 6 cells tested.

If a burst of action potentials (as recorded in the soma) occurs, it is very likely that it will propagate along the axon to its terminal arborizations where it will cause release of transmitter. Burst generation could then provide one way of establishing a secure and profound effect on a target neuron (e.g. via temporal summation of postsynaptic potentials as shown by Miles and Wong, 1986). Such cell interactions

could also be involved in certain kinds of rhythm generation in the cerebral cortex where they could serve as pacemakers. Bursts could be the synchronizing elements for epileptiform discharges (Hablitz, 1986). Another possible functional role of the burst-firing pattern is the initiation of long-term potentiation (Hablitz, 1986; Gamble and Koch, 1987). Mason and Larkman (1990) have also pointed out that burst-firing neurons can fire an initial burst followed by a tonic regular spiking pattern. They propose that this could enable the cell to switch between two operating modes, perhaps regulated via the influence of modulatory transmitters (McCormick and Prince, 1988; Steriade and Llinas, 1988). These activity patterns might therefore have important consequences for the integration performed by cortical microcircuitry.

4.5 Conclusions :

This study has directly demonstrated the existence of a clear correlation between the intrinsic electrophysiological properties, the morphology and the projection target of pyramidal cells in layer 5 of the visual cortex. It was also possible to show that corticotectal projection neurons have different subthreshold and intrinsic suprathreshold membrane properties compared to interhemispheric projection neurons. The differences in the morphological structure will determine the range of specific synaptic inputs available to each cell with the subsequent possibility of different afferent systems causing functional differences between the two groups of projection neurons. The electrophysiological characteristics of the two groups will –together with other yet unknown properties– influence the input-output relations of the neurons to serve their particular functions of which we still know so little.

Chapter 5:

The development of intrinsic electrophysiological properties of pyramidal neurons from layer 5 of the rat visual cortex studied *in vitro*:

5.1 Introduction :

To understand the mechanisms of electrical information processing in neocortical circuits in detail, a precise knowledge of the biophysical properties of neuronal membranes and synapses of the cells involved in this process is required because the way neurons integrate the flow of electrical signals will determine their output and consequently their role within the synaptic circuit.

The spread of current within the dendritic tree as the main information receiving part of a cortical neuron is largely passive. To gain further insight into the physiological role such neurons play, it is therefore essential to determine the passive characteristics such as membrane time constant and cell input resistance. Those data for single nerve cells are of interest because most of the processing of incoming information from other neurons (in the form of synaptic potentials) is a subthreshold event and therefore largely dependent on passive properties. Besides the synaptic location and the degree of activity of synaptic sites, both of which are determinants of a synaptic potential, these properties determine largely the influence such synaptic potentials have on the firing-pattern output of a neuron via their summated response at the somatic membrane.

If the goal of neuroscience is to understand the complex structure of nerve cells, their circuits and their functions in specific regions of the adult brain, it often helps to investigate the properties of the same type of neuron throughout the development of the structure concerned. This could give clues to differentiate between the properties that are intrinsic to the constituents themselves and those which are acquired through interaction with extrinsic factors (see **Chapters 7 and 8** : suggested experiments).

The main period in which pyramidal neurons from the cortex of rodents mature is the early postnatal phase of forebrain development (e.g. Berry et al. 1964, Dobbings 1967, for review see Miller 1988b). Because the bone-structure of the skull is not yet well developed during that period and the main part of the cranium consists of cartilaginous material, it is relatively easy to expose the brain partially or remove it entirely from the skull to have it accessible for experimental investigation.

5.2 Materials and Methods :

Amongst the available experimental techniques, the *in vitro* slice preparation has many advantages for studies of the electroresponsiveness of single cells in the developing cortex. Experimental advantages include accessibility to selected parts of the tissue and the high mechanical stability of the preparation, which is of great importance for intracellular work. The recording site can be more precisely determined and intracellular recordings can be obtained more easily, than in ***in vivo*** experiments. This approach also allows a definite correlation between the physiology and the anatomy of a single neuron by including a suitable marker for intracellular staining in

the electrode filling solution.

There are two intracellular markers commercially available which have been extremely popular for a long time amongst investigators of single cell properties. These are Lucifer Yellow CH (LY) and horseradish peroxidase (HRP). Both meet the general requirements of easy solubility, relative stability during histological processing as well as rapid diffusion and retention within the injected neuron, but they differ substantially in their applicability for the investigation of single cell characteristics. LY has proved to be unsuitable for electrophysiology -the investigation of which was one of the intentions for this study- and it will therefore not be considered further here. The latter (HRP) is commonly used for combined electrophysiological/anatomical investigations of single cells but has several disadvantages, if compared to the more recently available marker, biocytin. Biocytin is a small organic complex formed by biotin and lysine and was introduced to the neuroscience literature about three years ago (Horikawa and Amstrong, 1988). The main advantage of using biocytin rather than HRP is its lower molecular weight (372.5 versus ca. 40000) and its high affinity to avidin (Wright et al., 1952), which can subsequently be coupled to a variety of markers. The low molecular weight and its high charge allow unproblematic iontophoretic ejection using either current polarity from sharp, unbevelled microelectrodes. Biocytin is compatible with all common electrode filling solutions, unlike HRP which seems to be inactivated by salt solutions of high molarity. Biocytin also diffuses rapidly within the injected cell. If the slice is then immersion-fixed and subsequently reacted with the avidin-HRP complex and a chromagen substrate, it provides an image that is similar to the opaque histochemical product of HRP injections. In my experience the only disadvantage biocytin fills have is that they are less reliable in their morphological quality when

Figure **5.1**: Camera lucida drawing of a pyramidal neuron from layer 5 of the rat visual cortex from a postnatal day 17 preparation. The neuron was impaled in conventional living slices (thickness 400μm) and the electrophysiology studied. During the recording procedure the neuron was injected with biocytin which was included in the recording micropipette. The filled neuron was reconstructed from separate drawings. To improve visibility the axon is shown in red on an overlay.

Scale bar =100 μm.

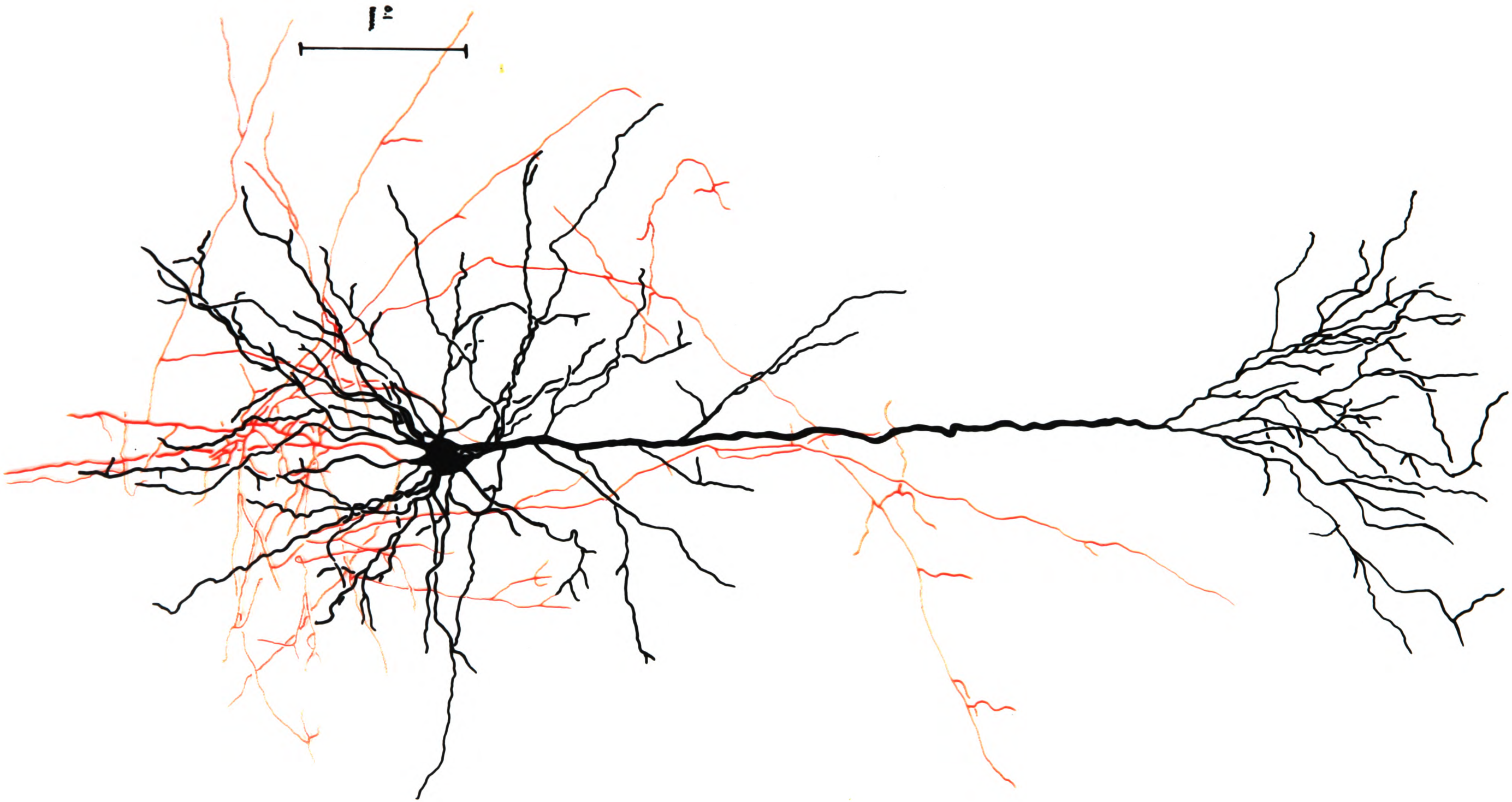

Figure **5.1**: Camera lucida drawing of a pyramidal neuron from layer 5 of the rat visual cortex from a postnatal day 17 preparation. The neuron was impaled in conventional living slices (thickness 400µm) and the electrophysiology studied. During the recording procedure the neuron was injected with biocytin which was included in the recording micropipette. The filled neuron was reconstructed from separate drawings. To improve visibility the axon is shown in red on an overlay.

Scale bar =100 µm.

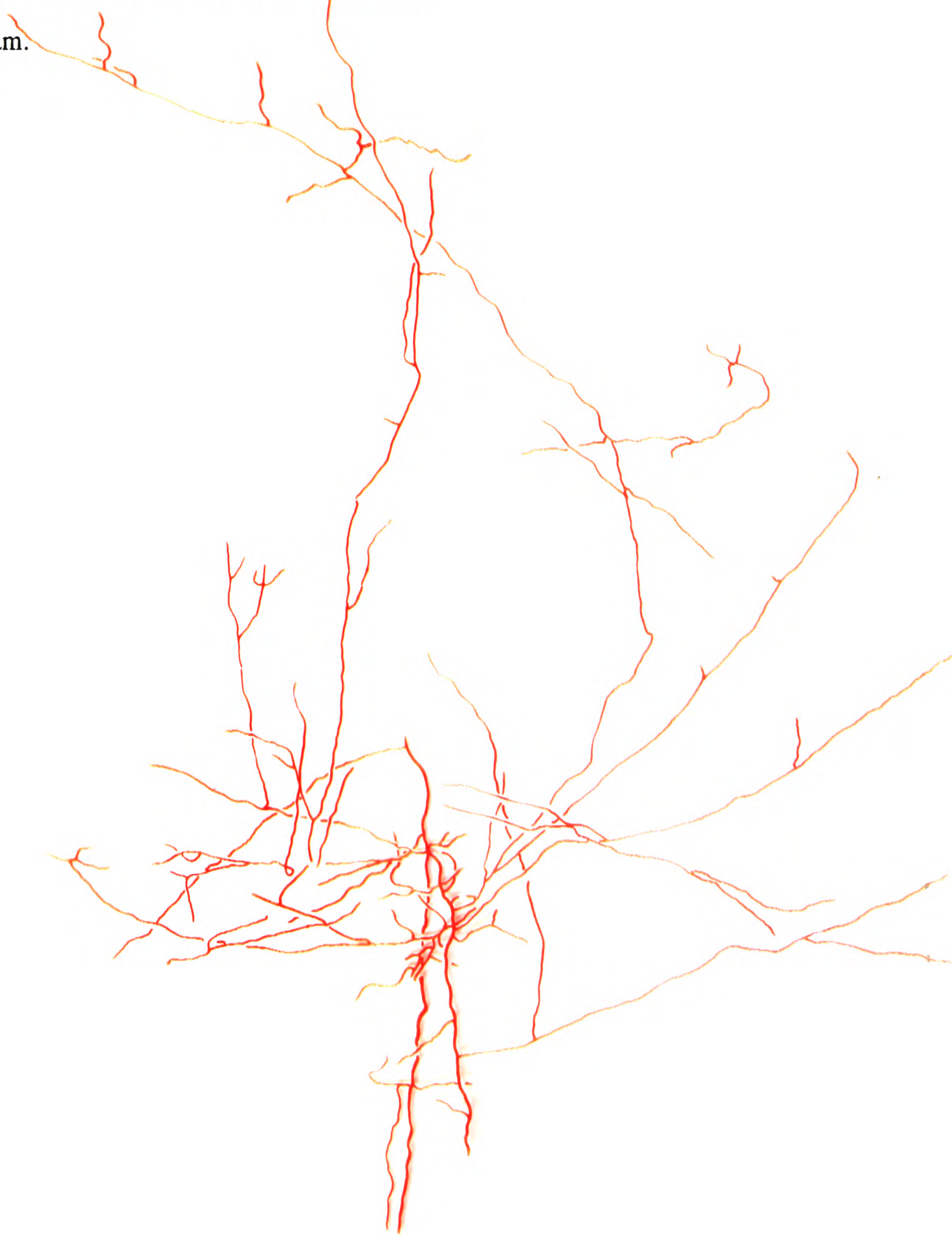

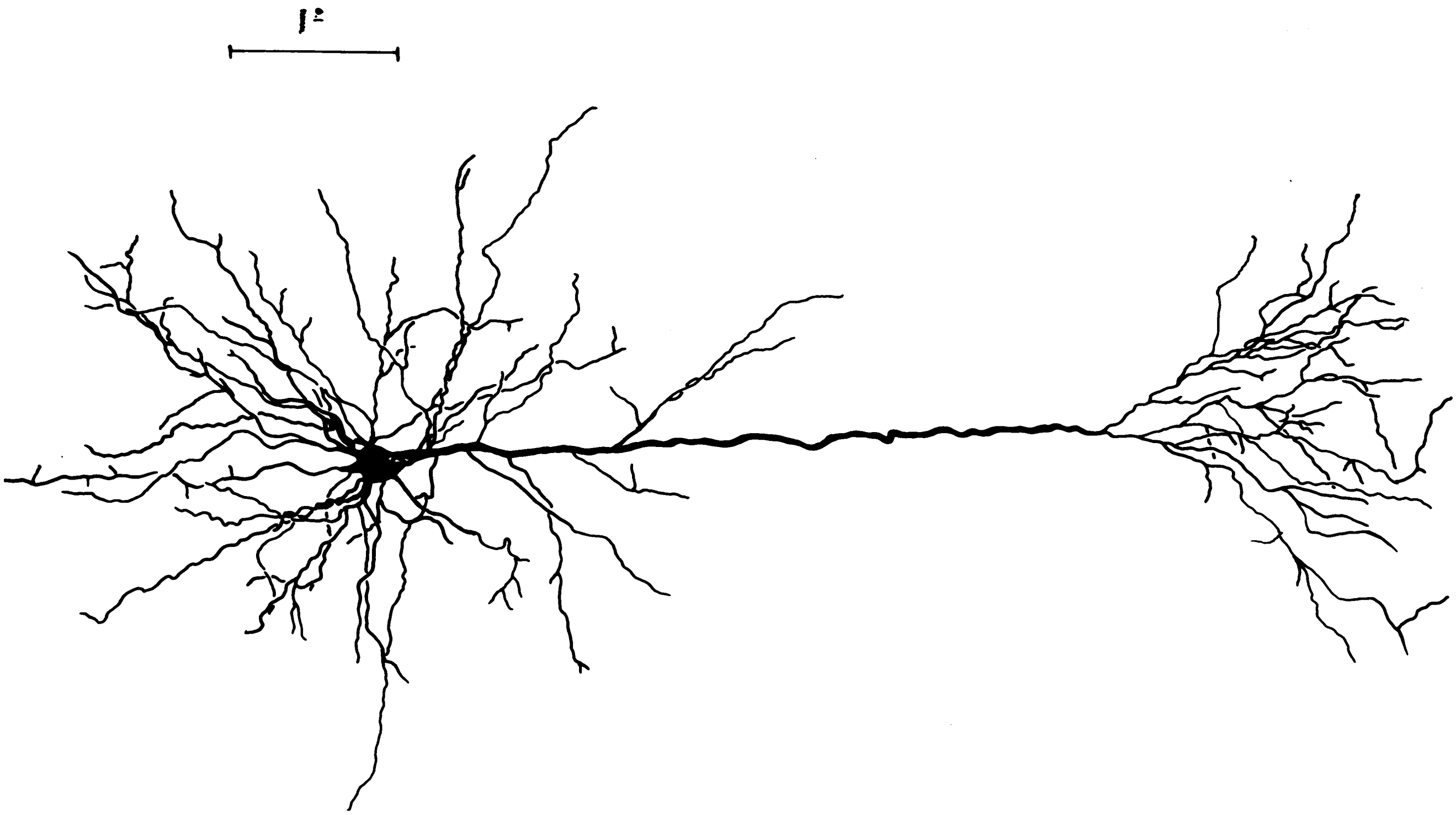

compared to results from HRP fills. The appropriate parameters for the histological reaction of biocytin were established in our laboratory (see **Chapter 3**) and it was possible to obtain comparable results from cells of all age groups used in this set of experiments.

Developmental electrophysiological data could be compared to data from pyramidal neurons from the adult rat visual cortex as collected with the HRP-technique (Larkman and Mason, 1990; Mason and Larkman, 1990; Chagnac-Amitai et al., 1990).

This set of experiments was designed to investigate the changes in the electro-responsiveness of pyramidal neurons from the rat visual cortex throughout the early postnatal period, up to the fourth postnatal week when the neurons are essentially adult. Subthreshold current/voltage relations, action potential parameters and the occurrence and time course of evoked excitatory as well as inhibitory postsynaptic potentials were all investigated using conventional intracellular recording techniques. Many of the features examined changed progressively during this postnatal period of cortical maturation.

Animals of different postnatal ages were assigned to specific groups, each spanning three days only rather than a full week as in previous investigations (McCormick and Prince, 1987; Kriegstein et al., 1987; Luhmann and Prince, 1991). In this way I hoped to make even small changes more apparent and to relate this investigation closely to previous anatomical studies (e.g. Miller, 1981, 1988b) using the same binning width.

Intracellular recordings were obtained using backfilled glass micropipettes containing 2M $KMeSO_4$ enriched with 2% biocytin with a DC-resistance of 70-270 MΩ measured in ACSF. The signal was fed into a bridge circuit, amplified, filtered and stored on disk for later analysis. The location of layer 5 was estimated using depth measures (from the pia) of the presumptive recording site as observed through an inverted microscope equipped with eyepiece graticules. This measure was compared with results from a set of Nissl-stained coronal sections of cortices from animals of varying postnatal ages (see **Chapter 3:** Materials and Methods). After recording from a particular cell the slice was fixed in a solution of 2.5% glutaraldehyde and 1.5% paraformaldehyde in 0.1M PB and subsequently reacted histochemically with a chromagen substrate (Hanker-Yates Reagent, Sigma), so that the location of each neuron and its morphological type could be confirmed (see Figure 5.1). This procedure also allowed to study the morphology of each single cell in detail and it could be drawn using a bright-field microscope (Nikon Optiphot) with a camera lucida attachment. All the cells included in this sample were pyramidal in shape.

5.3 Results :

5.3.1 General findings :

Intracellular recordings from pyramidal cells in layer 5 of adult rodent visual cortex have previously shown that these cells do not fire action potentials spontaneously during intracellular recording at membrane resting potential in the slice preparation (Connors et al., 1982; McCormick et al., 1985; Mason and Larkman, 1990:

Chagnac-Amitai et al., 1990). Nevertheless all those studies reported that cells were capable of generating multiple action potentials in response to injected depolarizing current pulses of sufficient length and amplitude. This was also the case for all the cells in this study. Knowing that such impaled neurons were silent at rest -after an initial injury discharge of action potentials as the electrode penetrated the cell membrane- cells were only accepted for analysis if they had a resting membrane potential more negative than -50mV –without permanently injected negative DC-current– and if they were capable of generating action potentials overshooting the zero potential when stimulated via injection of depolarizing current. Neurons that fired spontaneously at rest were judged to be damaged and were not included in the sample –as were those incapable of generating overshooting action potentials before and at the very end of the recording procedure. The selection criteria mentioned above are similar to those used in comparable studies from adult rodent cortex (Connors et al., 1982; McCormick et al., 1985; Mason and Larkman, 1990) and developing cortex (Kriegstein et al., 1987; McCormick and Prince, 1987; Schwartzkroin, 1982) although the criterion for accepting resting potentials was less stringent for immature neurons if compared to the studies of adult cortical cells.

The success rate for obtaining stable acceptable intracellular impalements was substantially lower in slices from young animals, especially from the two youngest age groups (binned as p6 and p9). This may be the consequence of several factors influencing the success of impalements: firstly, slices of the immature brains tended to flatten considerably in this interface chamber arrangement during the several-hour period of the experiment. This process of "thinning" is most likely caused by a shrinkage of the extracellular space which is relatively larger in immature brain tissue than in more mature brain tissue (Ransom et al., 1985). Because of this phenomenon

the long-term recording stability is decreased, thus causing some problems for experiments involving pharmacology which require lasting impalements for long wash-in/wash-out periods. Secondly it seemed to be more difficult to hold cells immediately after the impalement, even if a relatively large hyperpolarizing DC-holding current was applied to stabilize the membrane potential initially. This observation may also be explained through a greater mechanical fragility of these membranes. Another possible explanation could be that transport mechanisms across the cell membrane are less well developed in immature neurons and such membranes can not yet restabilize the membrane potential sufficiently well as the cell is penetrated. Thirdly one should also take into account that cells from the developing cortex are smaller in size compared to mature pyramidal cells. They might therefore be more susceptible to osmotic changes as they occur during microelectrode impalements.

The vast majority of impalements in this set of experiments was obtained from pyramidal cells, although occasionally nonpyramidal cells were recorded as could be determined from their electrophysiological properties using the criteria of McCormick et al. (1985). Spontaneously active nonpyramidal neurons were found only after the first postnatal week, which seems to correlate well with other indications of a delayed development of inhibitory functions (vide infra: section on synaptic action). The data obtained from such nonpyramidal cells were not included in the present investigation since the intention was to focus on the time course of developmental changes in pyramidal neurons only.

5.3.2 Qualitative morphological observations :

Some general features of developmental changes in layer 5 neurons could be observed when drawings of single cells were made and examined after they had been reacted for the intracellularly injected biocytin and individual cells had subsequently been reconstructed. No attempt was made to quantify the structural changes of cells from this sample (but for comparison see **Chapter 7**), so only a qualitative description is possible.

It was striking to see that those pyramidal neurons were more mature in their appearance than expected from Golgi-stained material in the published literature (Eayrs and Goodhead, 1959; Juraska and Fifkova, 1979a; Miller 1981, 1988b; Petit et al., 1988). There were two types of cells to be found in all the age groups from this set of experiments. One type had an thick apical dendrite that ascended towards the pial surface and terminated there in an arborization extending into layer 1. The other cell type possessed a slender apical dendrite, which did not reach the layer 1 and did not form a terminal arbor (see Figure 5.2). This slender apical dendrite tapered to a very fine diameter somewhere on its way to the more superficial layers until it was impossible to follow it visibly. No cell of this type had an apical dendrite that arborized and terminated in layer 1. Neurons from younger age groups had small somata and obviously shorter dendrites with a smaller number of higher order branches, than seen in cells from the older age groups. The basal dendrites had only a few spines in the two youngest age groups, whereas the spine density on basal dendrtites from neurons of the older groups seemed to be much higher. Although the full extent of the dendritic arborization cells was still much smaller in the age groups of the second postnatal week, they already resembled closely the general appearance of neurons from the adult

Figure **5.2**: Composition of several camera lucida drawings of representative pyramidal neurons from layer 5 of the rat visual cortex from different postnatal stages :

a) neurons from the first postnatal week

b) neurons from the second postnatal week

c) neurons from the third postnatal week.

Two pyramidal neurons are shown from each postnatal stage to demonstrate the two different cell types observed at each postnatal stage used.

All neurons were impaled in living slices (thickness 400µm) and the electrophysiology studied. During the recording procedure each neuron was injected with biocytin. After recording, slices were fixed by immersion in a mixture of paraformaldehyde and glutaraldehyde. After a reslicing procedure to obtain several thin slices (60µm), the injected marker was reacted with a chromagen substrate (see **Chapter 3**: Materials and Methods) to obtain a Golgi-like product which could be drawn using bright field illumination.

Each neuron was reconstructed from separate drawings. For better visibility of the dendritic arborization most of the axonal collaterals are omitted from these reconstructions although they were well preserved as can be seen in figure 5.1.

The main axon is indicated by triangles.

Scale bar in C =100 µm and applies to all cells.

Layer 5 pyramidal neurons of the developing visual cortex

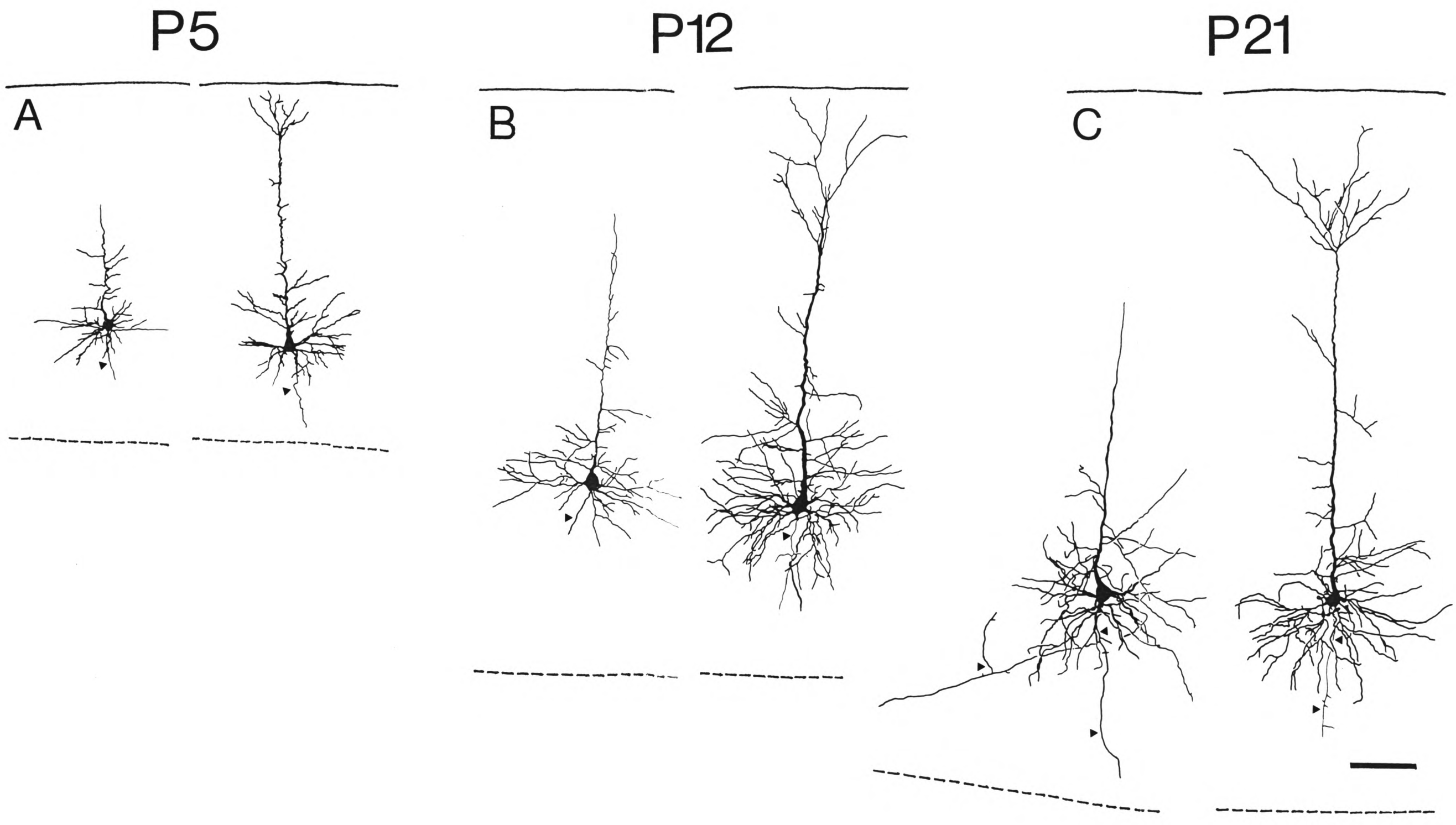

Figure **5.3**: Dye coupling in pyramidal neurons from the developing rat visual cortex. Plates show two representative clusters of pyramidal neurons seen after the slice (in which only a single impalement was obtained) was reacted for intracellularly injected biocytin.

A) Cluster of dye-coupled pyramidal neurons from a brain slice preparation at **p3**. The aggregate of coupled cells consisted in this case of 12 neurons all of which were located in layer 5.

B) Pair of dye-coupled pyramidal neurons from a brain slice preparation at **p15**. At this postnatal stage dye-coupling was rarely seen and, if present, consisted in my experience of a few cells only.

Scale bar in A =100μm and applies also to B.

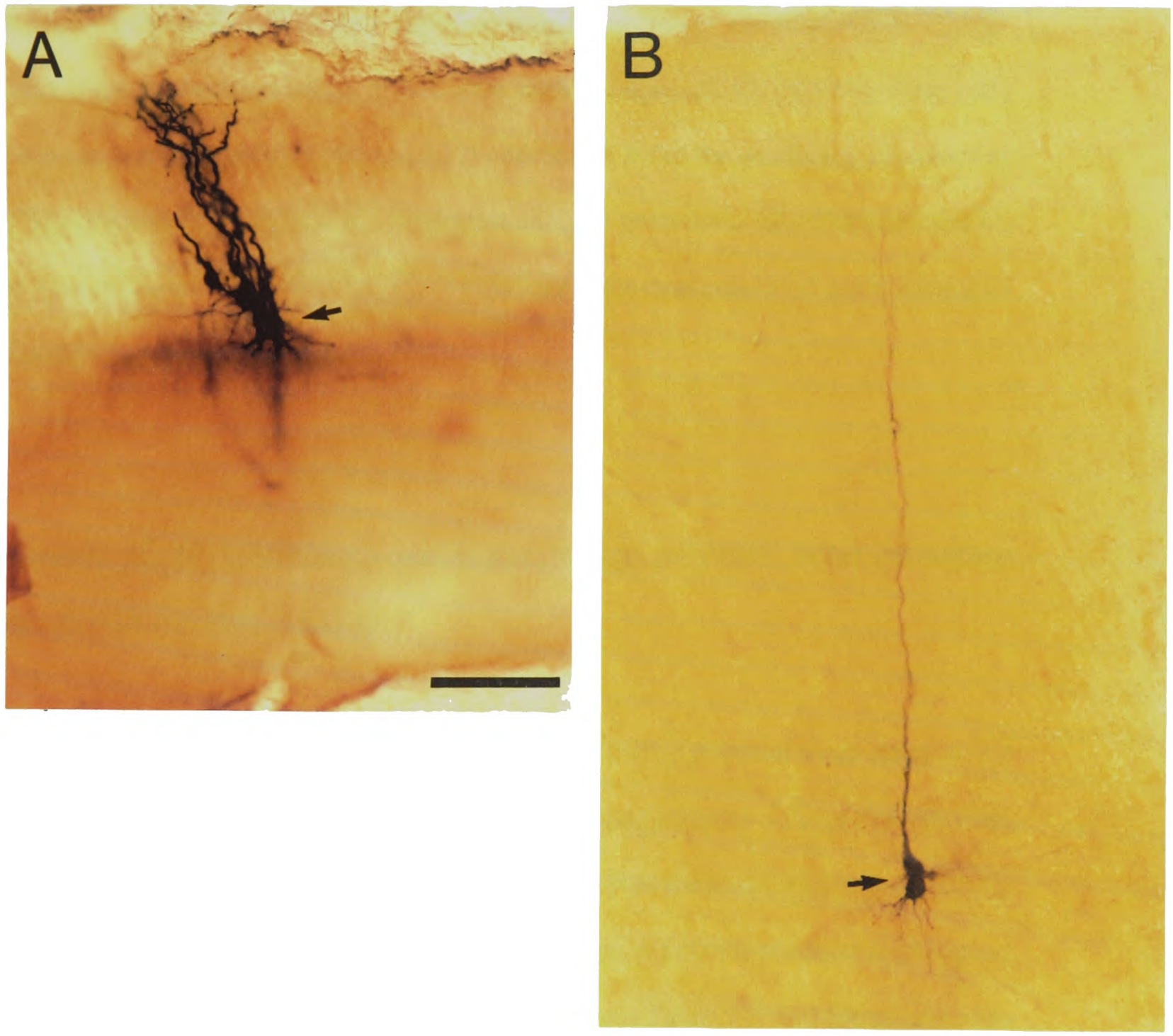
A
B

5.3.3 Electrophysiological observations :

Although we also looked initially at single sweep records from each injected current step and its resulting membrane voltage response, I then decided to work with averaged responses employing signal-averaging software obtained from C.E.D. (Cambridge Electronic Design, U.K.). This method improved the signal to noise ratio of the records considerably and helped in addition to avoid the possibility of selecting an unrepresentative trace for the subsequent analysis procedure. All measurements for the investigation of subthreshold I/V-relations were performed on such averaged responses (vide infra).

a) subthreshold properties: membrane resting potential, input resistance and membrane time constant

Measurements to determine the membrane resting potential were taken at the very end of the recording period from each cell by comparing the voltage reading from within the cell with the value measured immediately after electrode withdrawal, leaving the tip of the electrode still within the slice. The resting membrane potential in immature neurons was less negative than in mature neurons (see Table 5.1) and the progressive postnatal change was significant ($p<0.01$) when the p6-group values (mean 60.1±4.1mV) were compared with the values from the adult group (mean 70.3±5.4) (See Figure 5.6a).

Membrane time constant and input resistance were measured using *short* (0.5

Figure **5.4**: Membrane time constants of pyramidal neurons from the developing visual cortex. Semilogarithmic plots of the voltage decay following brief (0.5ms), hyperpolarizing current pulses injected into

A) a p7-neuron

B) a p12-neuron

C) a p21-neuron

Zero value on the X-axis corresponds to the end of the injected current pulse. The dotted lines (from which time constants were taken) are least-squares fits to the straightest portion of the plots. Values are indicated in each trace. Note the age-related decrease in membrane time constant, which is described in detail in Table 5.1. The current/voltage relations and the morphology of the corresponding cells are shown in figure 5.5.

Inset scale bars in A also apply to B and C.

Membrane time constants of layer 5 pyramidal neurons from the developing cortex

A

P7

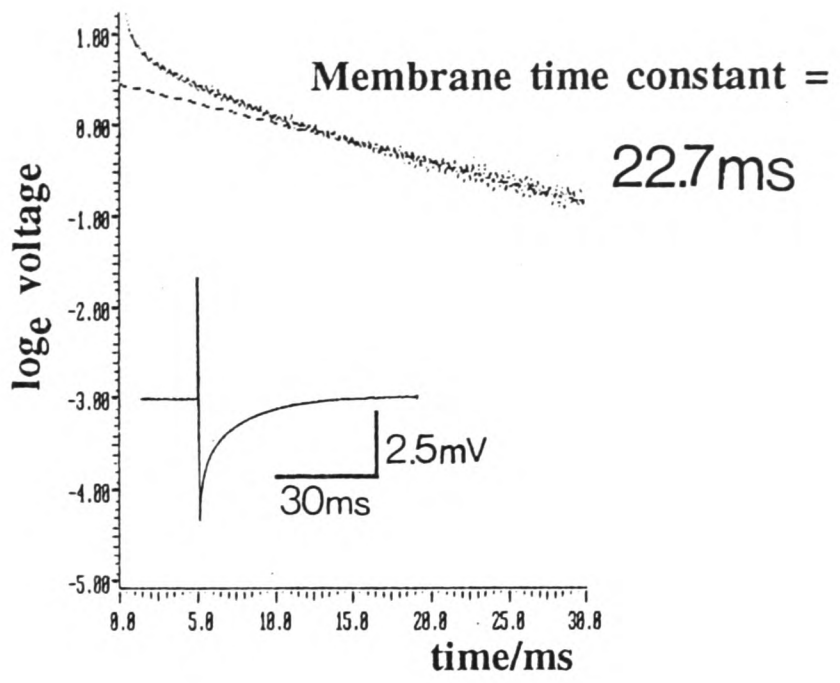

B

P12

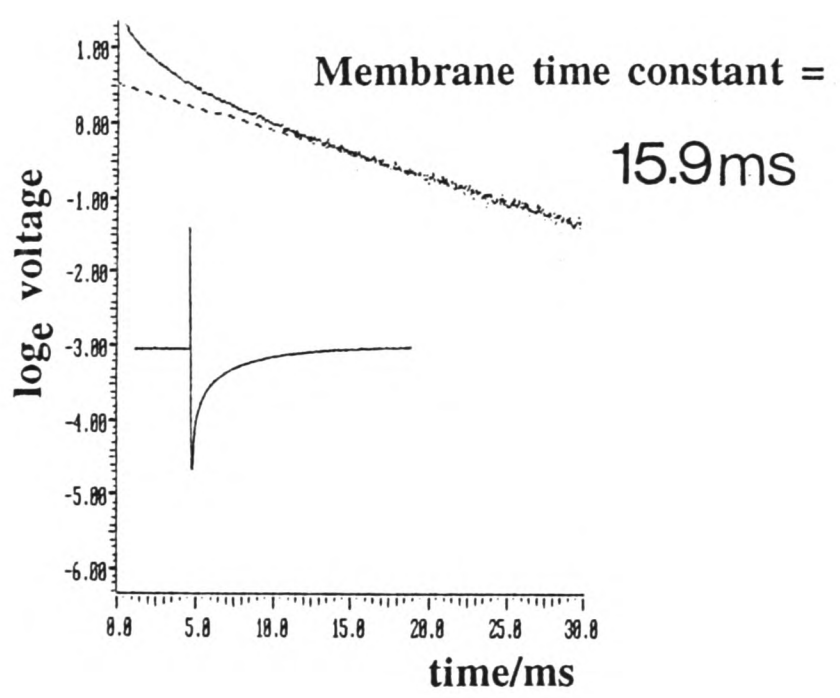

C

P21

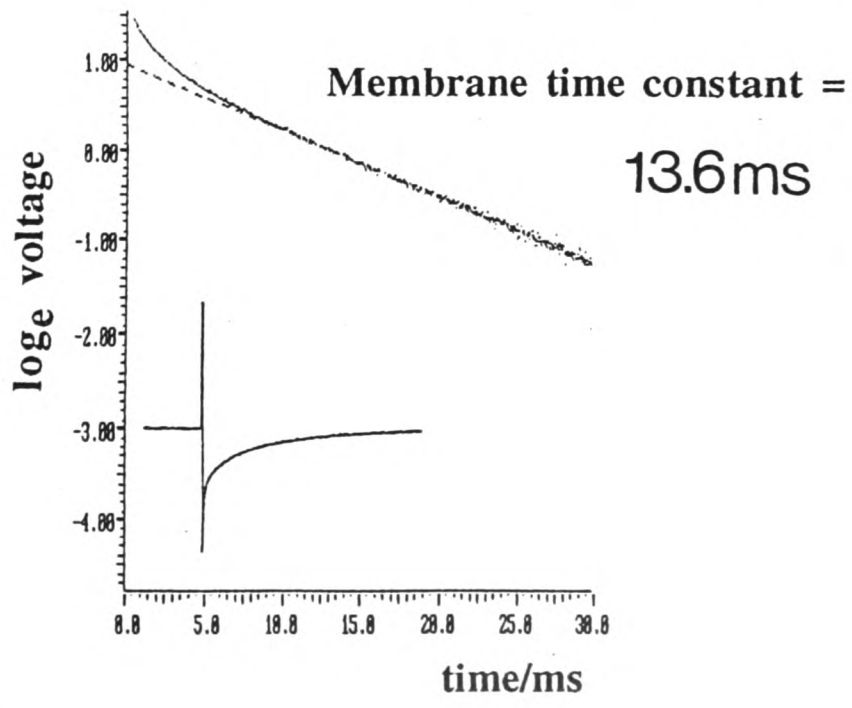

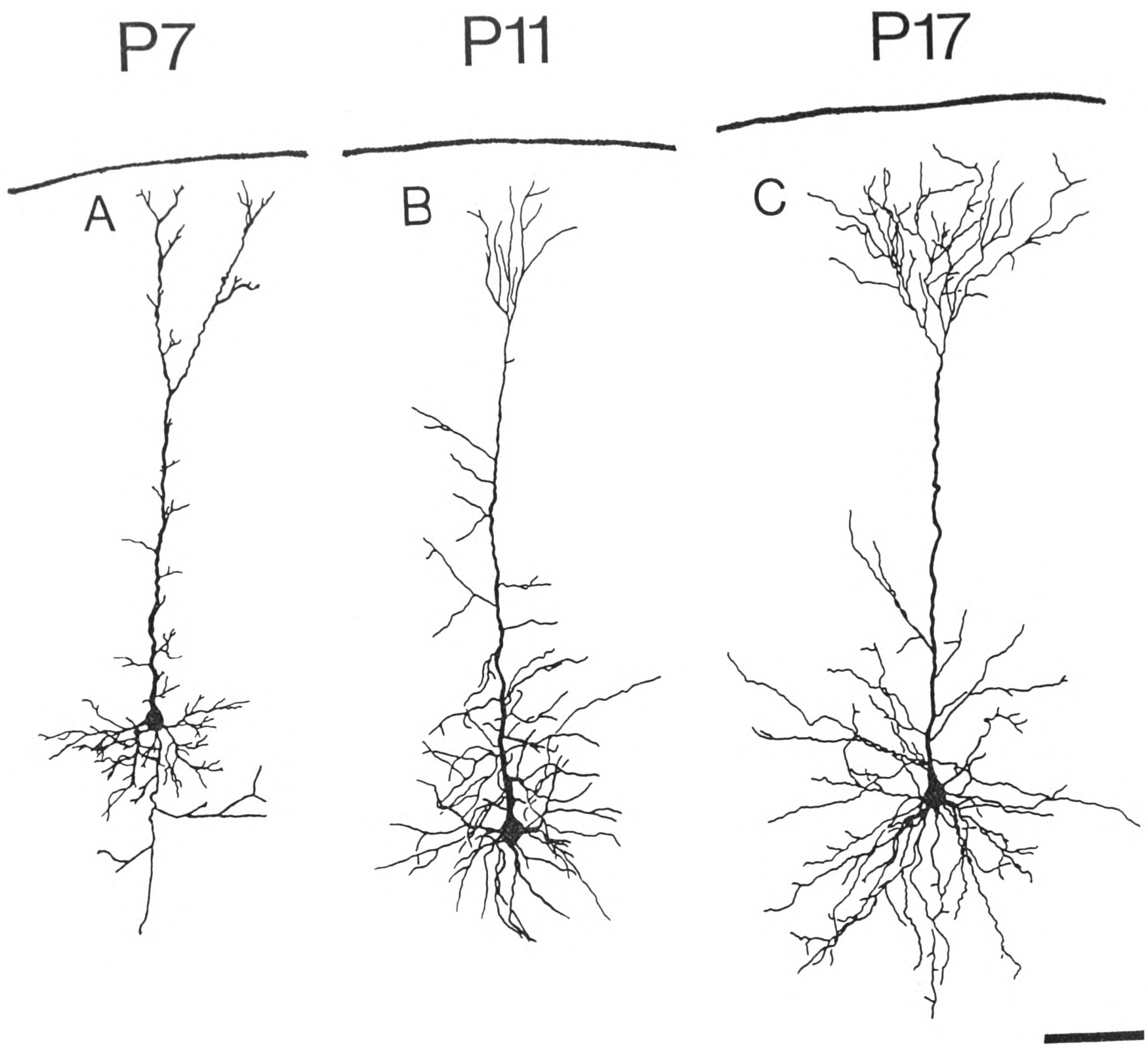

Figure 5.5 : Current/voltage relations of neurons from the developing rat visual cortex as investigated by the response to injected current pulses of identical amplitude. Camera lucida drawings of the neurons are shown on this page. Scale bar in A-C = 100µm. Physiological data are shown on the opposite page. Peak voltage deflection is marked by circles, steady state value by triangles. Correspomding I/V values are plotted to the right. Scale bar in **C** applies to all traces.

A: P7 neuron; Top trace shows voltage response to current pulses of -0.3nA to +0.3nA amplitude as shown in the bottom traces. Membrane resting potential was -70mV; R_{ME} was 224 MΩ.

B:P11 neuron; Top trace shows voltage response to current pulses of -0.3nA to +0.4nA amplitude as shown in the bottom traces. Membrane resting potential was -65mV; R_{ME} was 147 MΩ.

C: P17 neuron; Top trace shows voltage response to current pulses of -0.4nA to +0.4nA amplitude as shown in the bottom traces. Membrane resting potential was -66mV; R_{ME} was 121 MΩ.

Current/voltage relations of layer 5 pyramidal neurons from the developing visual cortex

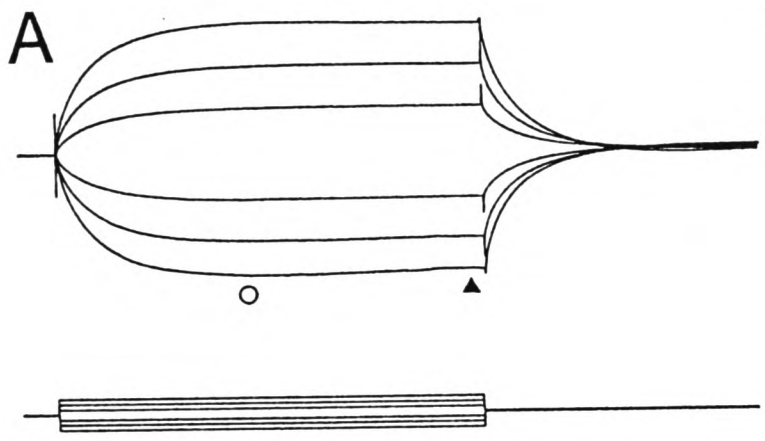

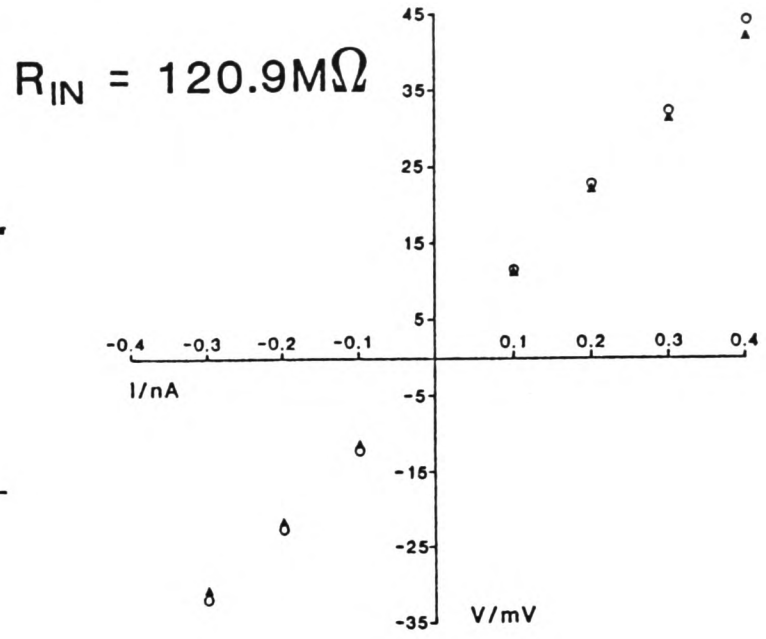

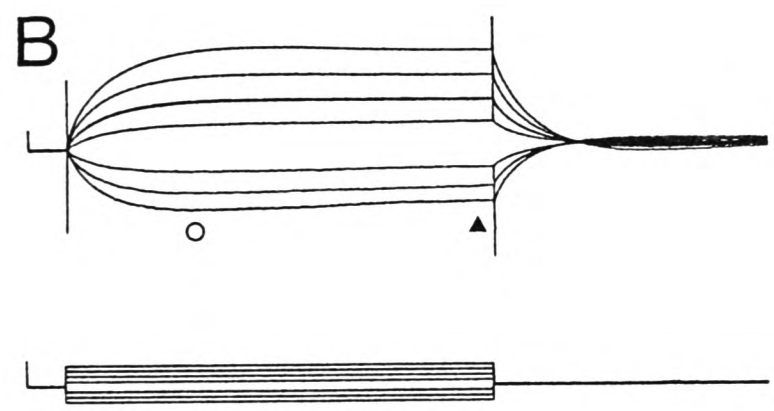

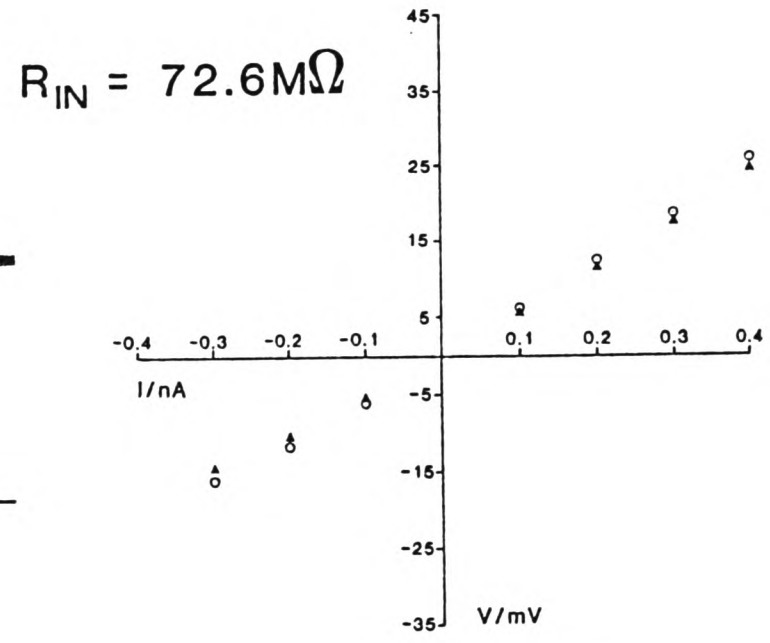

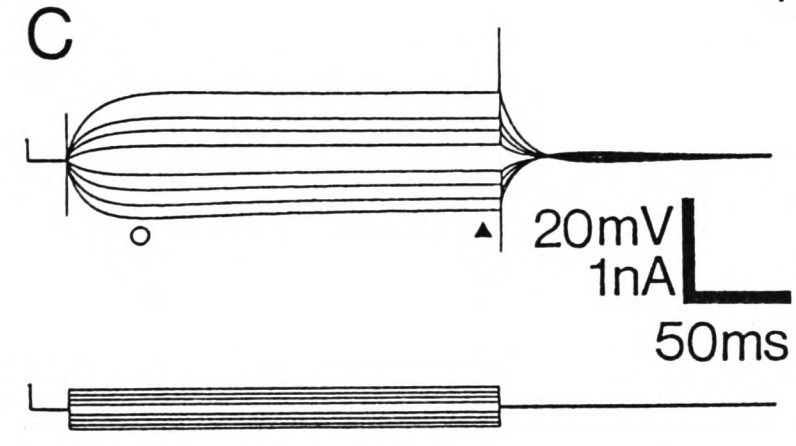

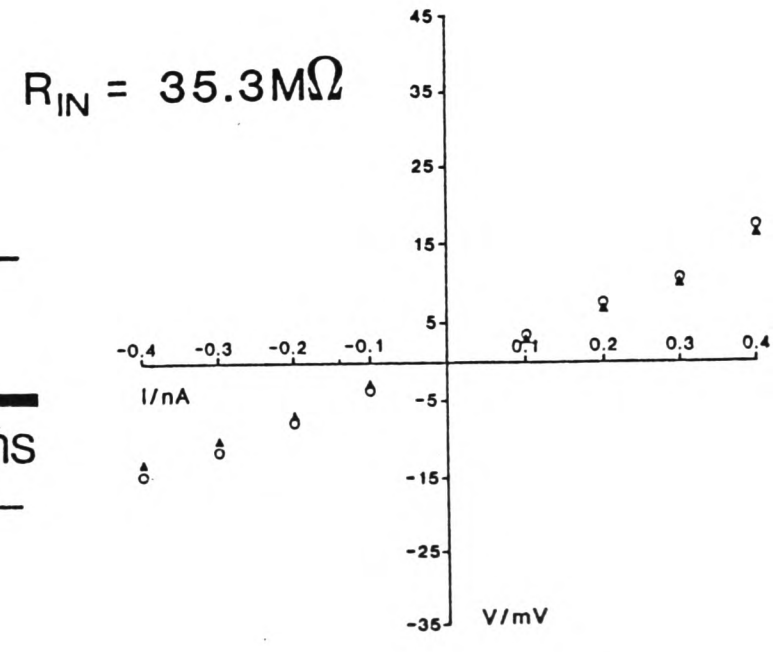

ms) current pulses (for advantages see Iansek and Redman, 1973; Durand et al., 1983) of 0.5nA and 1nA amplitude and of positive or negative polarity. Such pulses were repeatedly injected at 3Hz and the resulting voltage response was digitized at 20 kHz and averaged (n=200) to reduce the electrical background noise. The voltage decay following such an averaged brief pulse of current was then plotted semilogarithmically versus time and a simple regression line fitted selectively through the straightest portion of the data points obtained at late times (see Figure 5.4). This region was chosen to exclude the early period of the voltage decay, which reflects charge redistribution within the neuron itself (Rall, 1969; Durand et al., 1983; Jack et al., 1983). The slope of that regression line was used to calculate the time constant of the cell membrane and the same plots were also used to determine the apparent input resistance using the method of Durand et al., 1983 (based on Iansek and Redman, 1973). Both positive and negative pulses were recorded in each case for two different current pulse strengths and the four obtained values were compared to increase reliability and to assure linearity. All the values were very close to one another so I decided to quote in the following section only those values ± SD which were obtained from the 1.0nA negative current pulses injected.

Both the **membrane time constant** and the apparent **input resistance** decreased significantly with age from 18.1±5.3 ms at **p5** to 11.8±3.0 ms in the **adult** ($p<0.01$) and from 93.0±21.9 MΩ at **p5** to 38.7±11.3 MΩ in the **adult** ($p<0.01$) respectively (see Table 5.1 and also Figure 5.4 and 5.6). This age-related decrease in input resistance could occur because of a progressive increase in cell size, a decrease in specific resistance of the neuronal membrane or both. Assuming very little postnatal change in the specific membrane capacitance the observed decrease in membrane time constant could be explained by a lower specific cell membrane resistivity for older

Table 5.1 Age-related changes of subthreshold properties in pyramidal neurons from the developing visual cortex.

	P_6	P_9	P_{12}	P_{15}	P_{18}	P_{21}	Adult
no. of cells	6	9	8	14	8	10	8
$-V_m$/mV	60.1 ± 4.1 +	65.2 ± 6.0	67.0 ± 7.3	68.3 ± 6.2	69.1 ± 6.1	70.1 ± 6.0	70.3 ± 5.4
R_{in}/MΩ	93.0 ± 21.9 +	76.6 ± 41.6	55.1 ± 18.5	51.0 ± 20.6	45.2 ± 10.6	41.6 ± 13.3	38.7 ± 11.3
time const./ms	18.1 ± 5.3 □	16.2 ± 6.4	14.9 ± 3.5	14.6 ± 4.2	14.4 ± 1.4	14.3 ± 2.7	11.8 ± 3.0

It was tested whether the change from p6 to adult was significant (Students t-test).
Symbols indicating the significance level are placed in the corresponding p6 column.
+ = p≤ 0.01; □ = p≤ 0.05; ▲=p≤ 0.1

Figure **5.6:** Age-related changes in neuronal subthreshold properties of layer 5 pyramidal neurons from the developing rat visual cortex.

Data presented in this and subsequent figures of this chapter give means ± SDs; corresponding values are listed in Table 5.1.

A) Resting membrane potential, as measured immediately after electrode withdrawal

B) Apparent input resistance, obtained from short hyperpolarizing current pulses

C) Membrane time constant, obtained from short hyperpolarizing current pulses

A

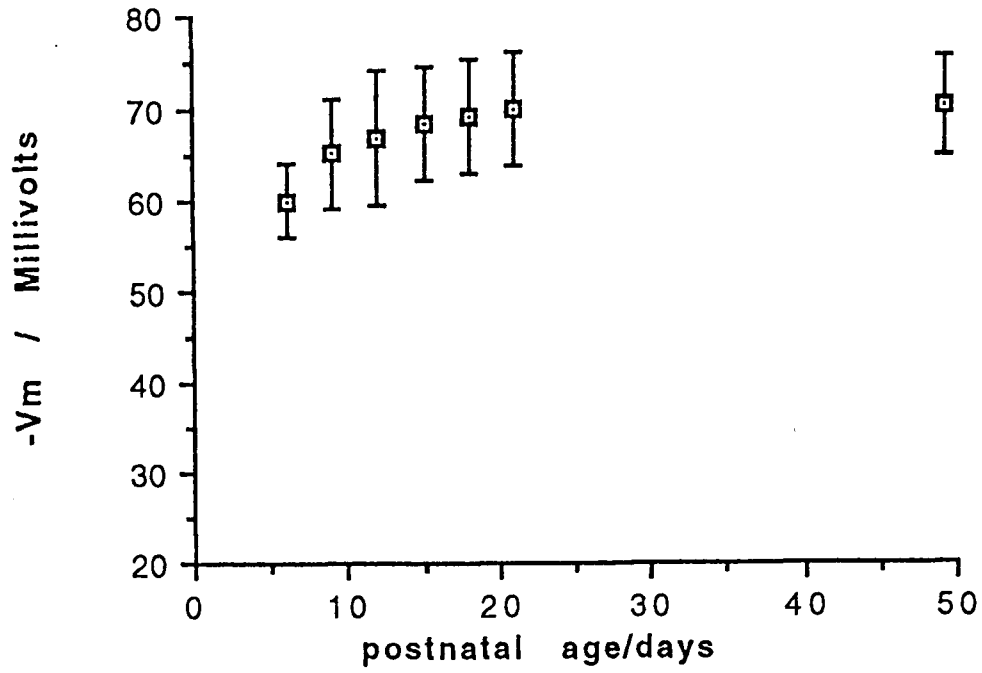
Resting membrane potential
-Vm / Millivolts
80
70
60
50
40
30
20
0
10
20
30
40
50
postnatal age/days

B

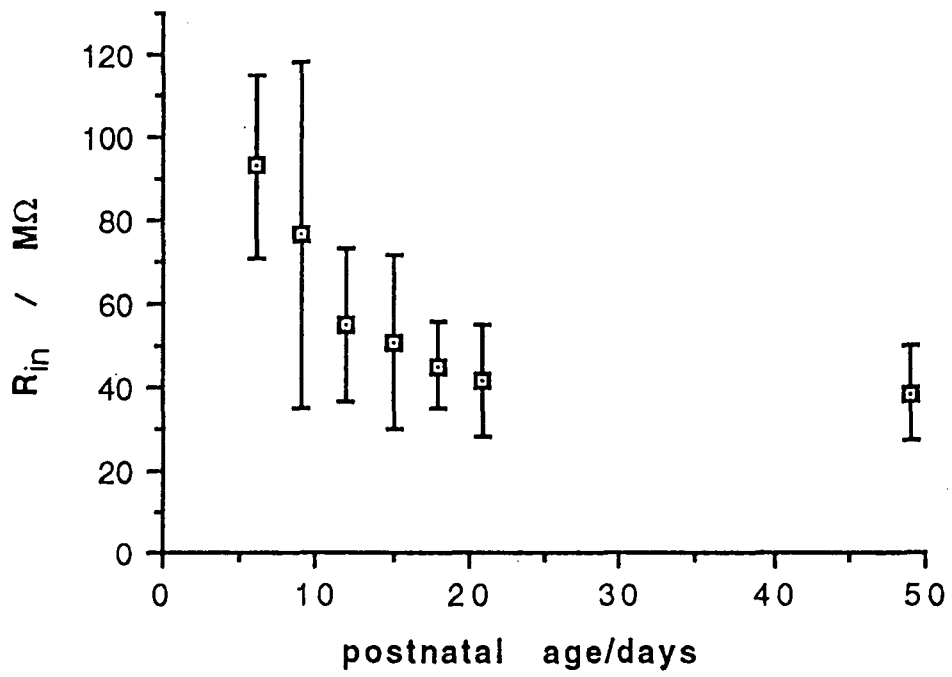
Input resistance from short negative pulses
R_{in} / MΩ
120
100
80
60
40
20
0
0
10
20
30
40
50
postnatal age/days

C

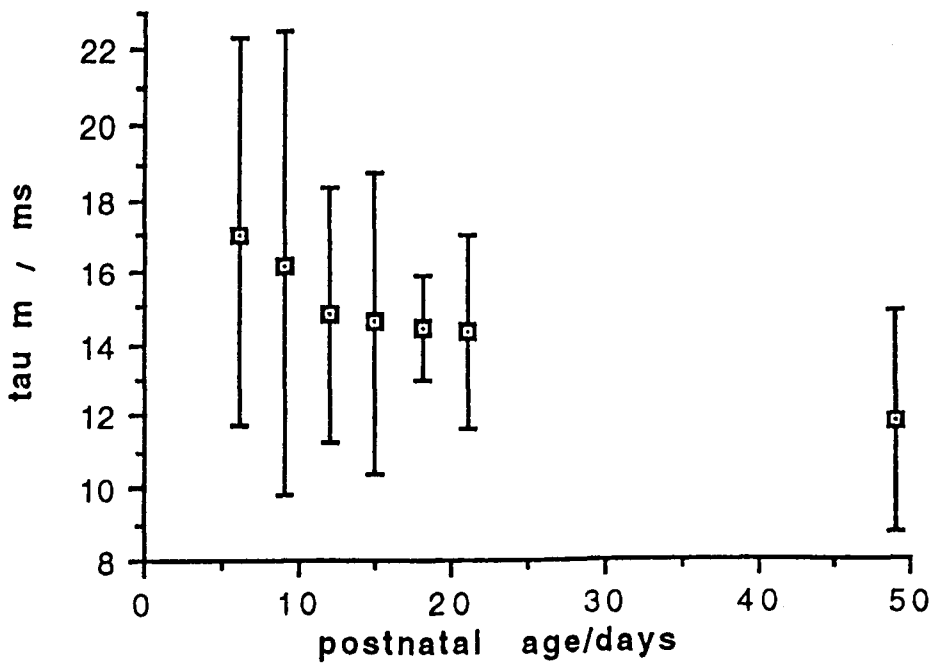
Membrane time constant from short negative pulses
tau m / ms
22
20
18
16
14
12
10
8
0
10
20
30
40
50
postnatal age/days

neurons.

The current/voltage relations of all cells were examined by applying rectangular current pulses of variable amplitude through the recording electrode. For this analysis the maximal and the steady-state voltage response of the neurons to long (t=200 ms) positive or negative current pulses in the hyperpolarizing as well as the subthreshold depolarizing directions were measured in current-steps of 0.1 nA. Because micropipettes showed time-dependent changes in resistance when passing large currents of more than 0.75 nA, procedures requiring measurement of the intracellular potential during current injection were limited to pulses with amplitudes less than such values (usually about –0.70 nA to +0.5 nA or nearest to threshold).

Plots of injected current step amplitudes versus voltage responses obtained from cells of the young groups showed linearity over a wide range which seems to be larger than in data collected from adult animals, although this was not quantified (see Figure 5.5). The slope of this I/V relation decreased during the maturation process and I/V values between -5mV to -10mV from resting potential were also used from this set of data as another measure of slope (=R_{in}) for control purposes. In most of the neurons the slope measured with long small depolarizing current pulses was greater than the slope measured using hyperpolarizing pulses of identical amplitude. A few cells showed an approximately constant slope-value that was independent of the polarity for the current pulse used.

I/V nonlinearities such as inward rectification were observed in many cells from both immature and adult animals as the strength of the injected depolarizing current was

increased (see Figure 5.5, right side). As has been reported previously (Kriegstein et al., 1987) this feature seemed to be more prominent in cells from older age groups (see I/V plots Figure 4.8) although no attempts were made to quantify this.

b) Rectification phenomena :

During long rectangular current pulses of either polarity the membrane potential of neurons initially showed time-dependent rectification and tended to "sag" back towards the membrane resting potential (see Figure 5.5a,b,c and 5.7). I tried to quantify the degree of sag at various postnatal ages by calculating the percentage sag during hyperpolarizing as well as depolarizing current pulses. The percentage sag was determined using the following equation :

Percentage sag = $(100 \times (V_{peak} - V_{steady\ state}) / V_{peak})$ after Stafstrom et al. (1984). For all the cells from which recordings were taken, the percentage sag was relatively independent of the size of the peak voltage deflection or strength of current pulse used. Therefore at least three separate measurements of percentage sag were averaged for each cell, with measurements made from different current strengths and for each current pulse polarity. Depolarizing current pulses where the voltage deflection approached the action potential threshold were omitted from the averaging procedure.

In all but one of the age groups there was a positive correlation between the percentage sag during hyperpolarizing pulses and that during depolarizing pulses (see Table 5.2). The percentage sag increased slightly during maturation but this change was not significant if t-tested. Results are shown in Figures 5.8 a and b.

Time dependent rectification : Measurement and quantification of the "sag"-phenomena and overshoot /undershoot

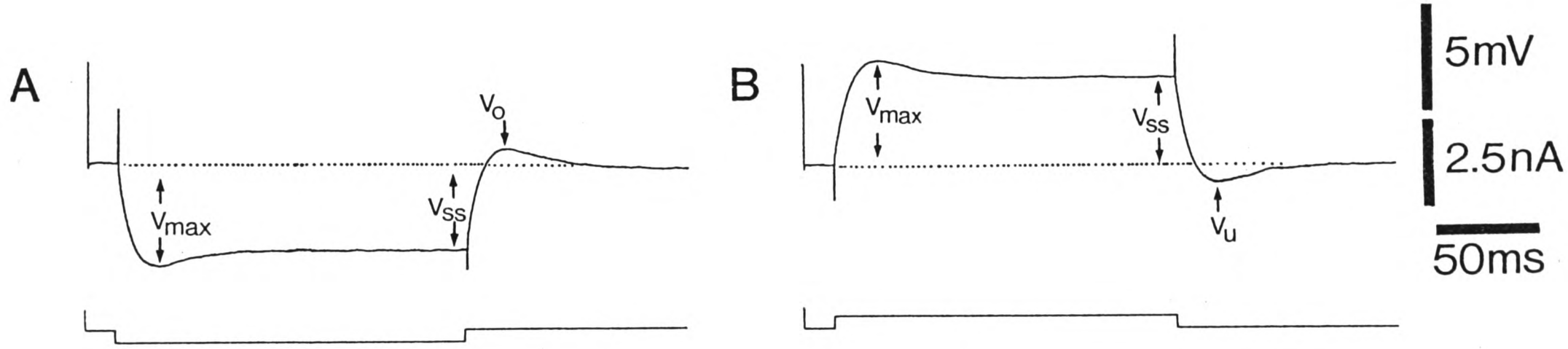

TABLE 5.2	P_6	P_9	P_{12}	P_{15}	P_{18}	P_{21}	Adult
no. of cells	*	9	8	14	8	10	8
% sag depol.	*	4.2 ± 4.6	6.0 ± 4.5	8.4 ± 7.2	8.1 ± 2.9	10.6 ± 10.6	13.4 ± 7.9
% sag hyperpol.	*	4.2 ± 5.3	4.7 ± 2.8	5.5 ± 2.6	10.3 ± 5.4	7.5 ± 4.6	7.2 ± 5.3
% overshoot	*	4.5 ± 6.9	5.7 ± 1.9	5.5 ± 4.1	10.9 ± 4.6	8.1 ± 5.7	10.4 ± 6.8
% undershoot	*	3.7 ± 5.5	5.5 ± 3.0	5.2 ± 3.7	9.2 ± 5.0	7.4 ± 5.6	8.3 ± 6.3

Figure **5.7**: Age-related changes in subthreshold properties of layer 5 pyramidal neurons from the developing rat visual cortex. Quantification of rectification phenomena.

Data presented in this figure give means ± SDs; corresponding values are listed in Table 5.2.

A) Percentage sag during *long* (200 ms) depolarizing pulses calculated by the following equation:

$[100x(V_{max}-V_{steady\ state})/V_{max}]$ after Stafstrom et al. (1984). The percentage sag value was reasonably independent of the size of the maximal voltage deflection at the onset of the current pulse. For each cell at least three sag values were therefore averaged from current pulses of different amplitude. The value closest to threshold was omitted from the averaging procedure.

B) Percentage sag during *long* hyperpolarizing pulses. Calculated as mentioned above.

C) Percentage undershoot after depolarizing pulses i.e. the amount by which the membrane potential became transiently more negative than mebrane resting potential after the depolarizing pulse $[100x(V_{undershoot}/V_{max})]$; see figure in Table 5.2 for illustration. The percentage undershoot was reasonably constant regardless of the current pulse amplitude. Therefore 3 values were averaged from different pulse strengths used.

D) Percentage overshoot after hyperpolarizing pulses. Calculated as mentioned above.

A

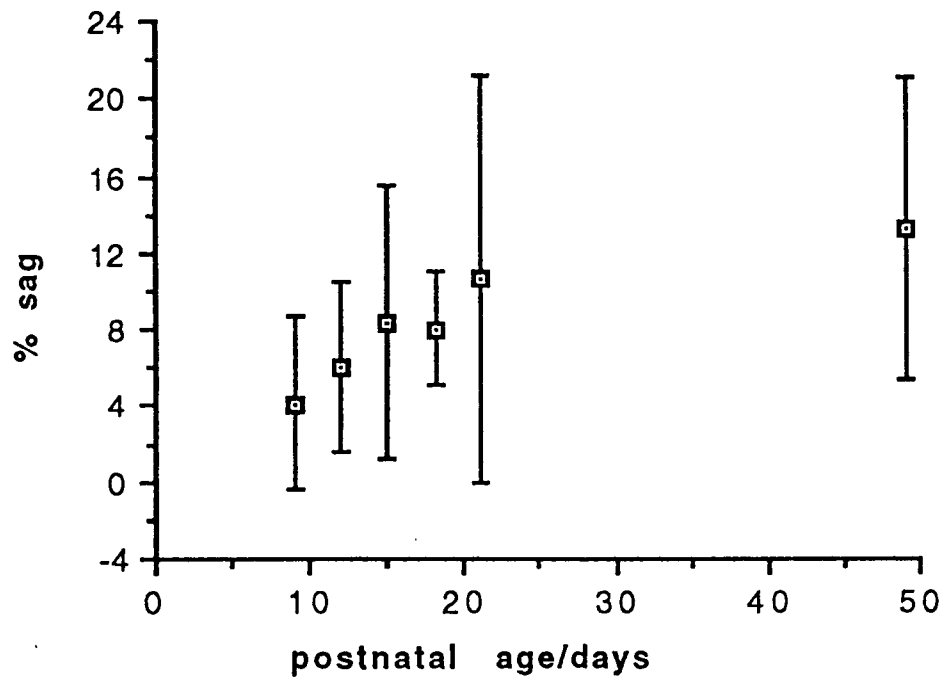
Percentage sag from long depolarizing pulses
% sag
24
20
16
12
8
4
0
-4
0
10
20
30
40
50
postnatal age/days

B

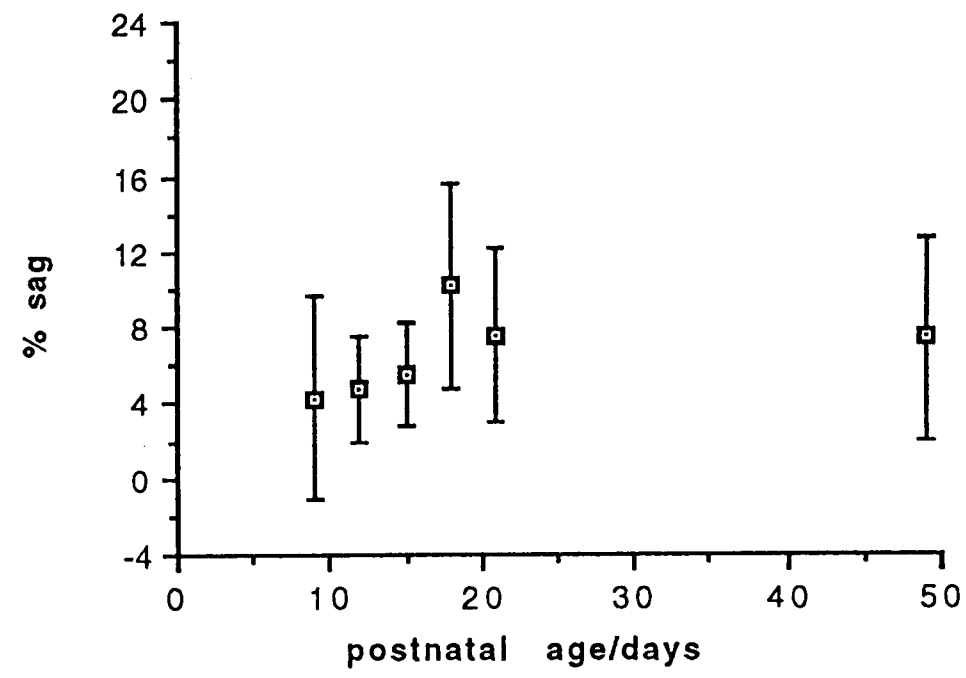
Percentage sag from long hyperpolarizing pulses
% sag
24
20
16
12
8
4
0
-4
0
10
20
30
40
50
postnatal age/days

C

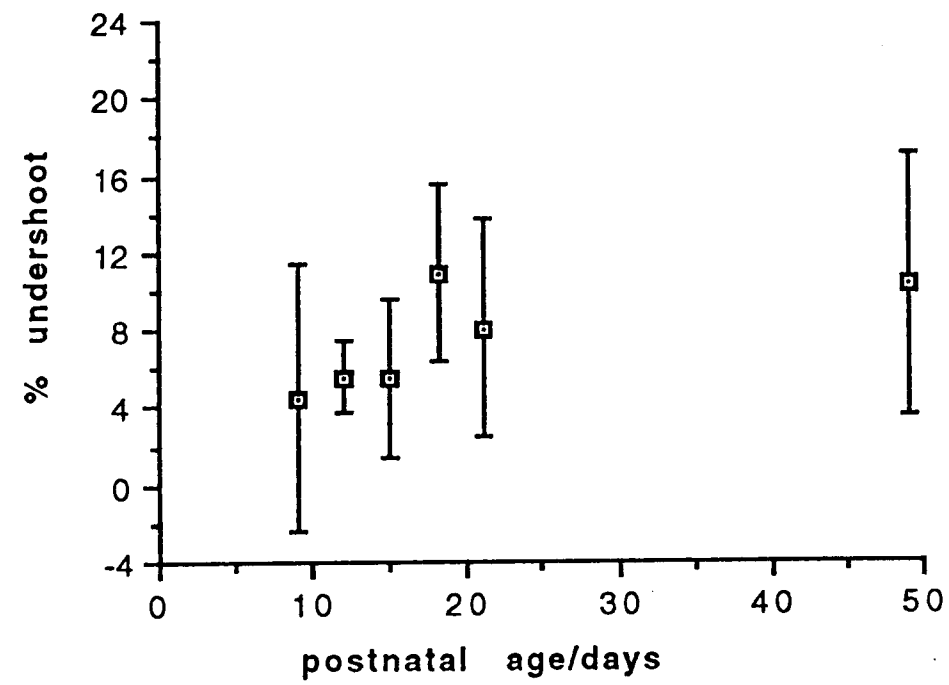
Percentage undershoot (pos. pulses)
% undershoot
24
20
16
12
8
4
0
-4
0
10
20
30
40
50
postnatal age/days

D

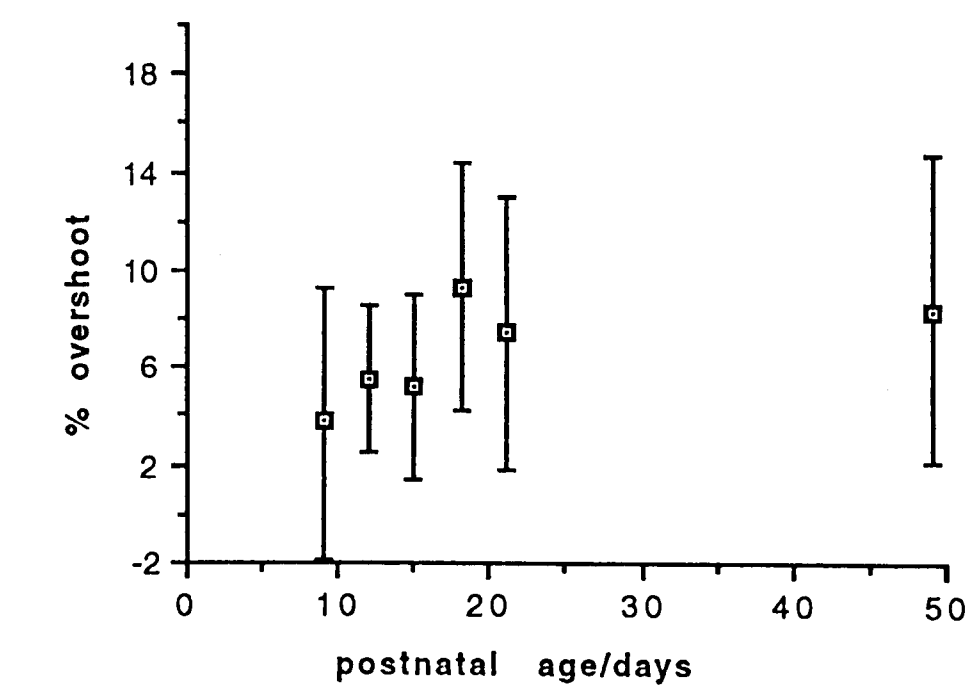
Percentage overshoot (neg.pulses)
% overshoot
18
14
10
6
2
-2
0
10
20
30
40
50
postnatal age/days

The same procedure was applied to analyse another related phenomenon occurring at the end of the injected current pulse (see Figure 5.7). In this case the membrane potential of layer 5 neurons tends to "overshoot" or "undershoot" the resting membrane potential after injection of hyperpolarizing and depolarizing current pulses respectively. In this investigation the overshoot did not trigger action potentials, although it is conceivable that larger or longer pulses might have done so, as known from other neuronal populations (e.g. Lopez-Barneo and Llinas, 1988).

For the later phenomenon a slight trend could be observed indicating an increase of the percentage overshoot/undershoot in both the hyperpolarizing as well as the depolarizing direction during postnatal development (see Figures 5.8 c and d). Nevertheless this change was also insignificant.

These findings are in good agreement with results published from the rat somatosensory cortex (McCormick and Prince, 1987; Kriegstein et al., 1987).

c) Action potential parameters :

Intracellular injection of long rectangular depolarizing current pulses of sufficient length (duration > 200ms) and amplitude could evoke action potentials (APs) in all age groups tested, but the APs of immature pyramidal cells differed in several ways from those obtained from more mature cells (see Figure 5.9).

The peak AP amplitude above threshold (defined below) of the cells from younger animals was substantially smaller (see Table 5.3), APs were significantly longer in duration (see Table 5.3) and slower in both rate of rise and rate of fall (see Table 5.3) than those obtained from cells of the adult group. Therefore width at half-height decreased substantially during maturation (see Figures 5.11). In most cells the threshold voltage relative to the resting membrane potential could readily be seen as a sharp bend in the voltage curve if the response to a pulse of suprathreshold amplitude was recorded and the V trace subsequently displayed at high gain with respect to time (see Figure 5.10). Nevertheless, because this visibly discernible point was not obvious in all cases, threshold was defined objectively as the point where the voltage rise rate exceeds 50V/s, as has been used for the same population of cells in slices from adult animals (Mason and Larkman, 1990). Threshold was less sharply marked in immature cells than in more mature neurons (see Figure 5.10), which possibly reflects a change in Na^+-channel density during early ontogenesis and/or a change in kinetics of the sodium channel complex (e.g. MacDermott and Westbrook, 1986; see discussion). In parallel to the resting membrane potential becoming more negative, threshold also became more negative with age, both in absolute terms and relative to rest (see Figures 5.6a and 5.11a). Simultaneously both AP peak height above threshold and AP peak height above rest increased significantly (see Figure 5.11b and Table 5.3).

d) Action potential firing pattern :

It was always possible to elicit trains of spikes as the injected current amplitude was increased although immature cells tended to inactivate or accommodate quickly

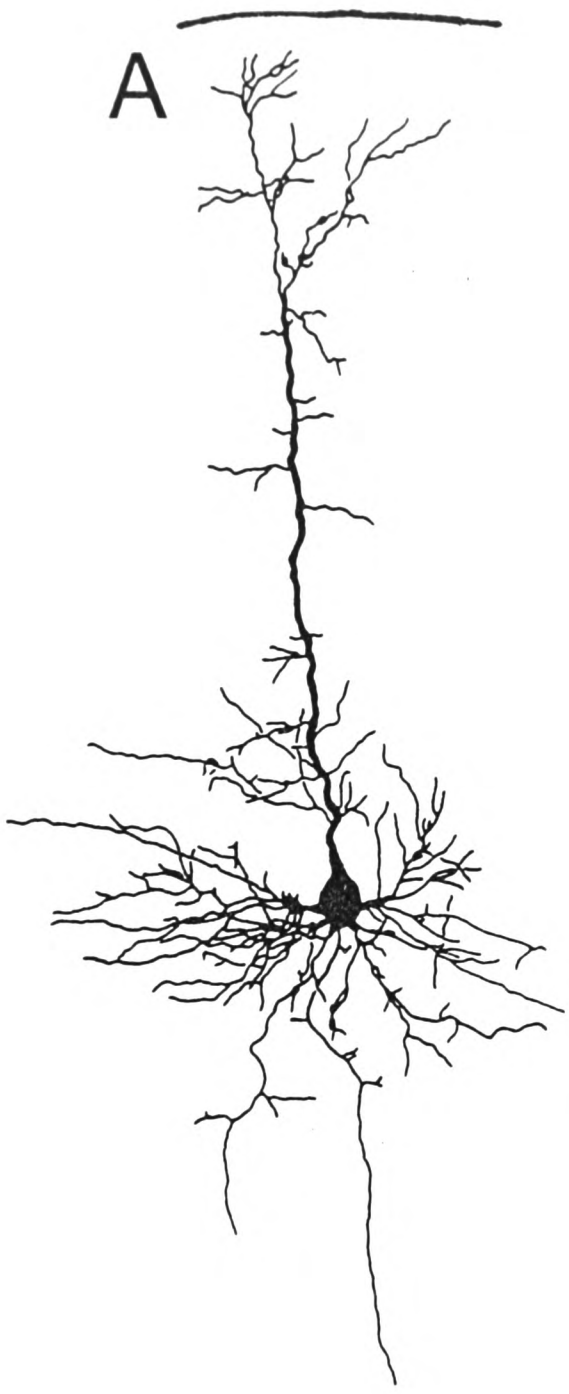

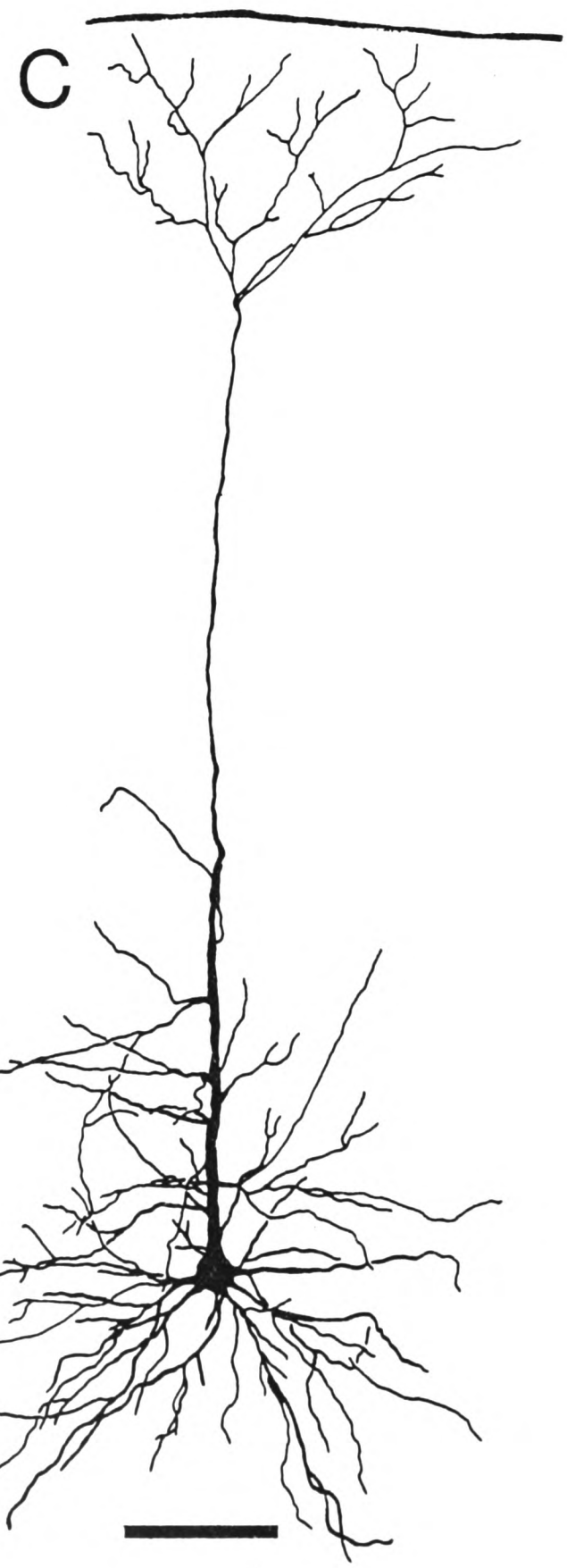

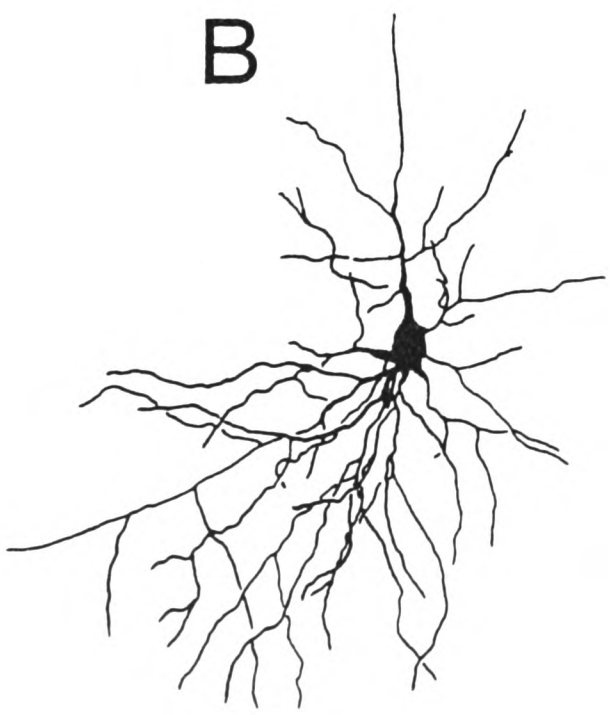

Figure 5.8 Action potentials and corresponding cell morphology of neurons from the developing rat visual cortex:

Scale bar in A-C = 100μm.

A: Non-bursting neuron, p8

B: Regular-spiking neuron, adult

C: Burst-firing neuron, adult

Opposite page:

The left traces show the response to the smallest supra-threshold current pulse. Right traces show the response to a current pulse necessary for the recruitment of a second spike.

Action potential firing patterns of young and adult layer 5 pyramidal neurons of the visual cortex

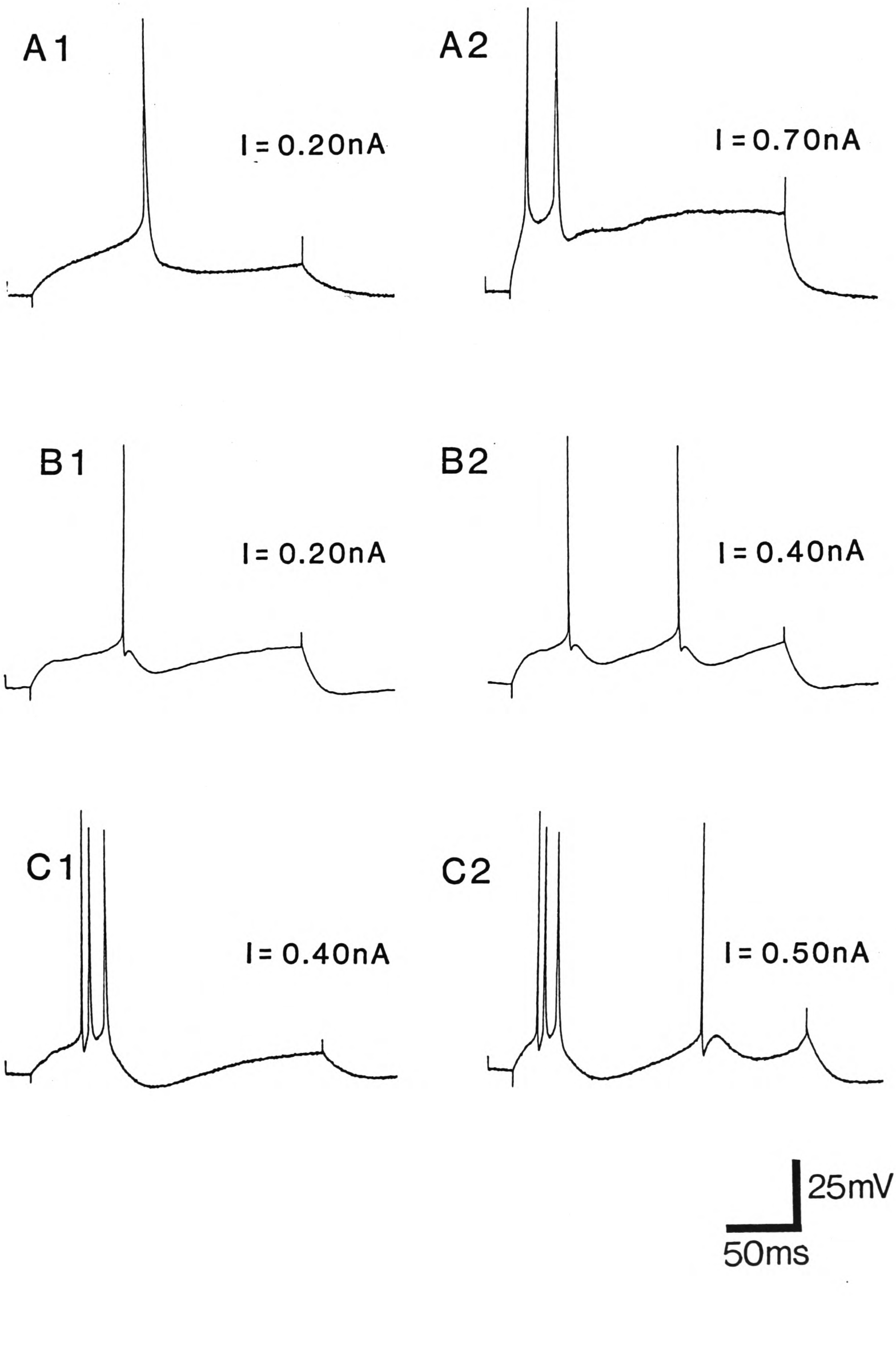

Table 5.3 Age-related changes of action potential parameters in pyramidal neurons from the developing visual cortex.

	P_6	P_9	P_{12}	P_{15}	P_{18}	P_{21}	Adult
no. of cells	6	17	12	17	9	12	8
Threshold above rest /mV	33.3 ± 8.5 +	30.1 ± 9.3	29.7 ± 8.3	26.8 ± 7.3	23.5 ± 7.9	20.5 ± 4.6	18.4 ± 9.3
Peak height above threshold /mV	42.5 ± 9.6 +	48.1 ± 7.2	55.6 ± 6.6	59.9 ± 7.3	60.3 ± 8.4	63.9 ± 9.3	70.1 ± 7.3
Width of half amplitude /ms	1.57 ± 0.37 +	1.44 ± 0.31	1.22 ± 0.37	1.09 ± 0.23	1.01 ± 0.23	0.88 ± 0.22	0.54 ± 0.10
10%/90% rise time /ms	0.43 ± 0.08 +	0.33 ± 0.08	0.26 ± 0.12	0.22 ± 0.05	0.20 ± 0.05	0.20 ± 0.05	0.21 ± 0.03
90%/10% fall time /ms	1.97 ± 0.68 +	1.92 ± 0.49	1.91 ± 0.55	1.71 ± 0.47	1.43 ± 0.35	1.10 ± 0.36	0.57 ± 0.19
30%/70% rise rate /V/s	120.2 ± 68.3 +	143.1 ± 50.2	224.3 ± 79.9	276.0 ± 71.1	298.8 ± 59.5	307.1 ± 72.5	338.0 ± 52.1
70%/30% fall rate /V/s	25.4 ± 8.5 +	26.1 ± 7.9	25.9 ± 6.3	31.4 ± 9.6	36.9 ± 7.9	44.1 ± 10.8	118.2 ± 43.8
Rate ratio	4.0 ± 2.3	5.67 ± 1.87	9.02 ± 3.72	9.17 ± 2.63	8.33 ± 1.95	6.47 ± 2.62	3.17 ± 1.13

It was tested whether the change from p6 to adult was significant (Students t-test).
Symbols indicating the significance level are placed in the corresponding p6 column.
+ = $p \leq 0.01$; □ = $p \leq 0.05$; ▼= $p \leq 0.1$

Figure **5.9:** Age-related changes in neuronal action potential parameters from action potentials recorded in layer 5 pyramidal neurons from the developing rat visual cortex. Data presented in this figure give means ± SDs; corresponding values are listed in Table 5.3.

A) Postnatal change in action potential threshold above rest. Threshold was defined as the point where voltage rise rate exceeds 50V/s.

B) Action potential peak height above threshold.

C) Action potential width, measured as the time between rissing phase and falling phase at half amplitude.

D) Action potential mean rise time measured as time to rise from 10% to 90% of the peak value.

E) Action potential mean fall time measured as time to fall from 90% to 10% of the peak value.

F) Action potential rise rate measured between values of 30% and 70% of the peak amplitude.

G) Action potential fall rate measured between values of 70% and 30% of the peak amplitude.

H) Ratio of rise rate to fall rate.

A

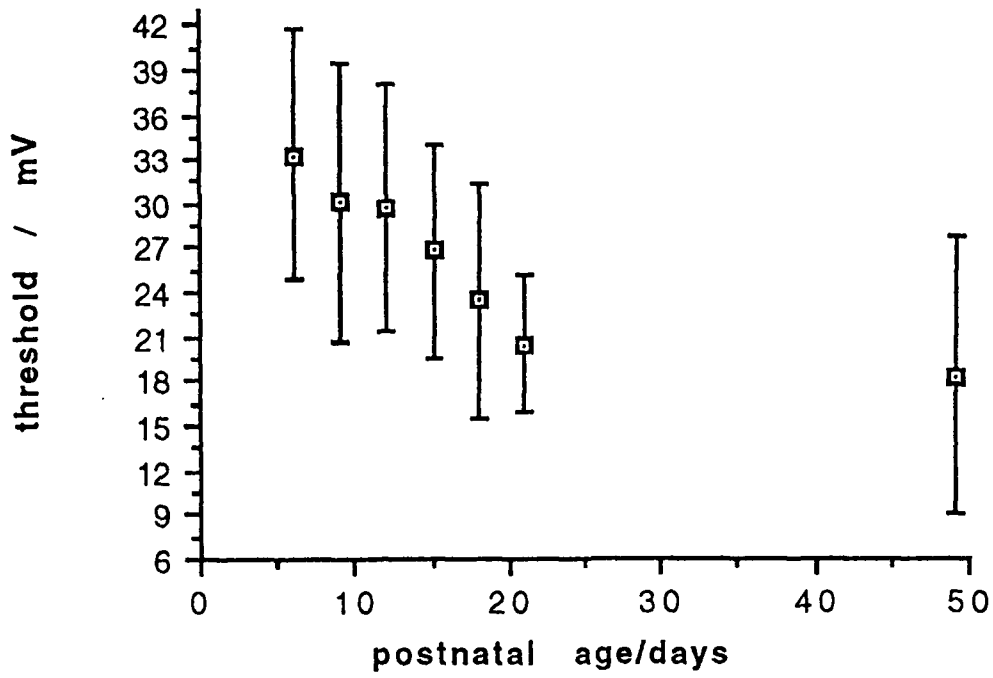
AP threshold above rest
threshold / mV
42
39
36
33
30
27
24
21
18
15
12
9
6
0
10
20
30
40
50
postnatal age/days

B

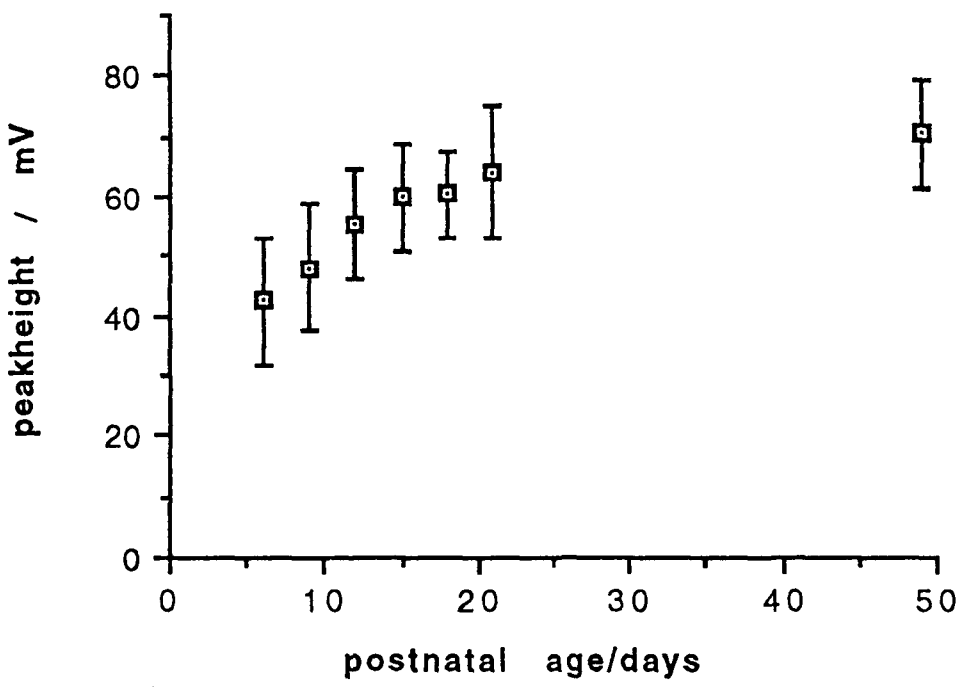
AP peakheight above threshold
peakheight / mV
80
60
40
20
0
0
10
20
30
40
50
postnatal age/days

C

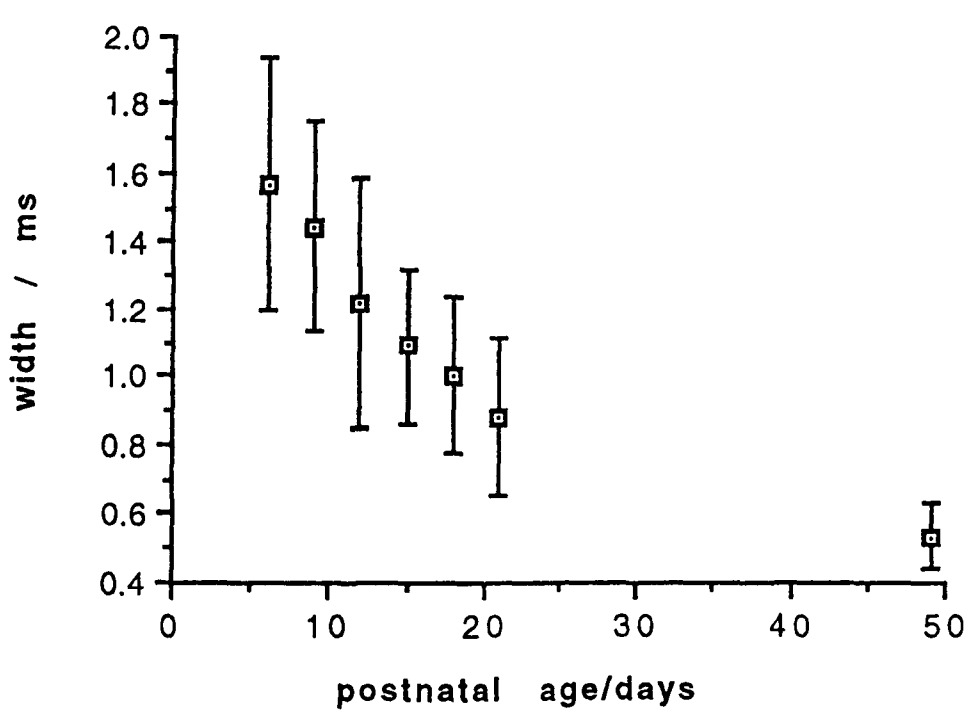
AP width at half amplitude
width / ms
2.0
1.8
1.6
1.4
1.2
1.0
0.8
0.6
0.4
0
10
20
30
40
50
postnatal age/days

D AP mean rise time

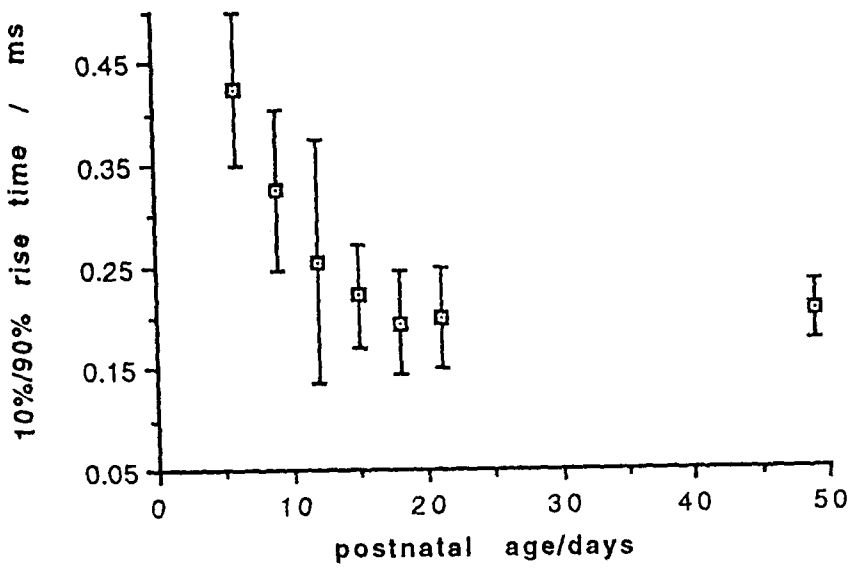

E AP mean fall time

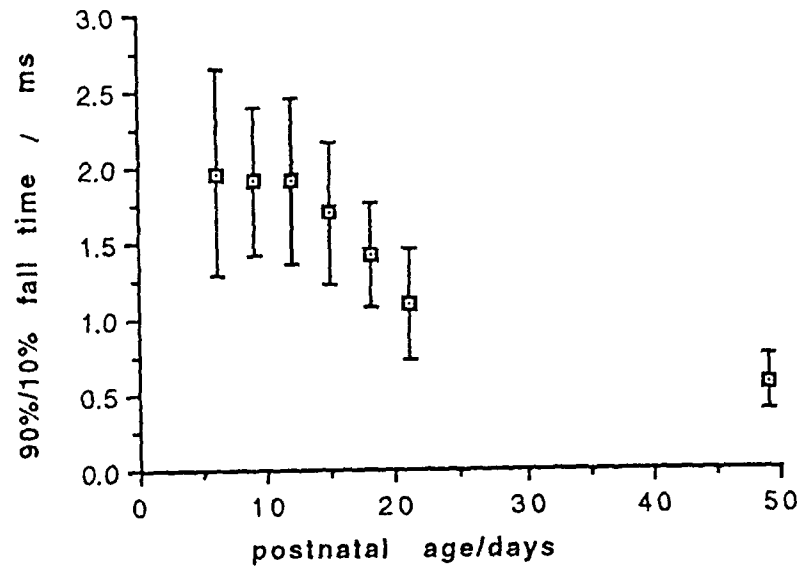

F AP mean rise rate

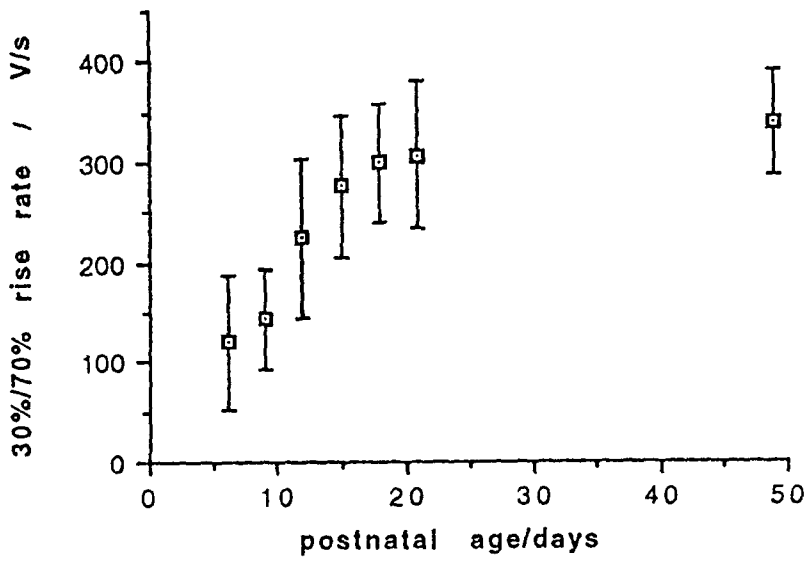

G AP mean fall rate

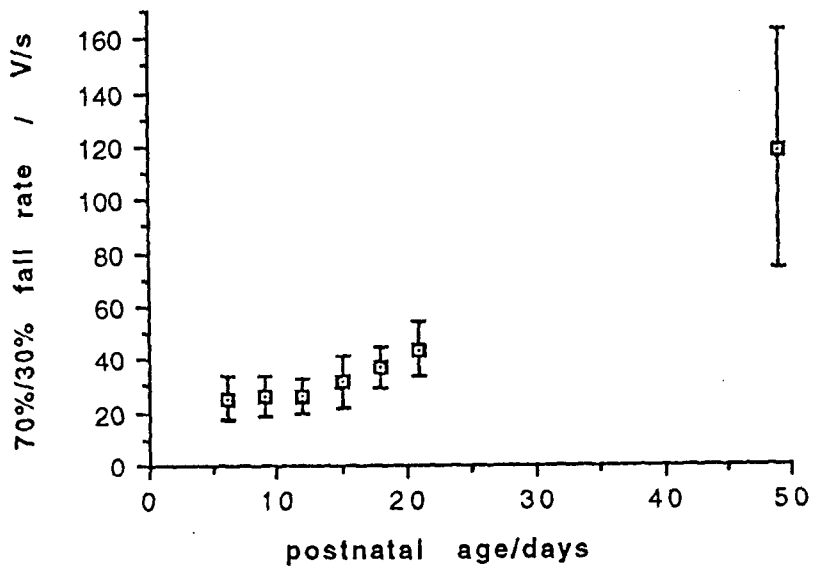

H AP rise rate to fall rate ratio

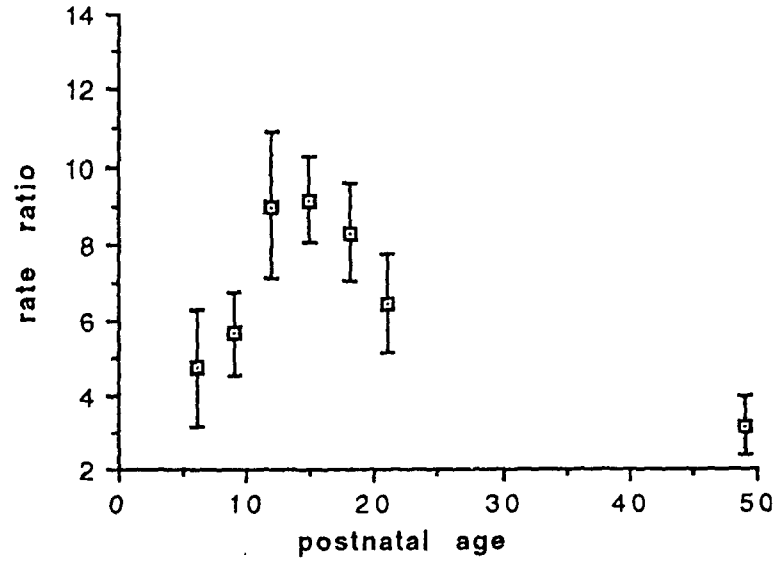

after the onset of the current pulse injected (see Figure 5.9a). Because of this characteristic feature and because of the fact that I used very sharp micropipettes (having sometimes a very high electrode resistance of about 200 MΩ or more and therefore showing signs of rectification throughout the pulse duration) no attempt was made to analyse spike frequency versus current strength.

Each cell from the sample was tested, whether or not it could fire action potentials in bursts. A range of amplitudes of the injected current pulses was used, which was superimposed on different baseline membrane potentials (maintained via steady current injection). In no case before **p15** was it possible to elicit a burst-like discharge pattern even in cells from which trains of action potentials could be recorded. After p15 burst-firing and regular spiking neurons could be distinguished.

e) Spike after potentials :

In cells from very immature age groups a monophasic after-hyperpolarization could be observed following single action-potentials. On the other hand it was obvious that cells in slices obtained from more mature animals had APs which were followed by two phases of hyperpolarizing after-potentials (A.H.P.s) which were separated by a small depolarizing after-potential (D.A.P.). (For illustrations see Figures 5.10 A3 and B3). The duration of A.H.P.s varied in cells from different age groups. They were considerably smaller and shorter in APs of cells from immature cortex but became more pronounced and longer in APs of cells from juvenile and adult cortex. The slow A.H.P. was always present and could last more than 120 ms in mature cells (see Figure

Figure **5.10**: Action potentials and associated phenomena in young and adult layer 5 pyramidal neurons from the rat visual cortex:

A1) Single action potential elicited in a p7 neuron in response to a minimal suprathreshold current injection (I = 0.5nA). Scale bar: see B1; V_m was -62mV; R_{ME} was 168MΩ.

B1) Single action potential elicited in an adult regular spike-firing neuron in response to a minimal suprathreshold current injection (I=0.4nA).V_m was -69mV; R_{ME} was 73MΩ. Scale bar in B1 applies also to A1

A2) and B2) Pre-action potential voltage traces from the figures above shown at higher gain with respect to time and voltage. Arrow indicates the approximate AP-threshold as defined by eye. Note the difference in time course as the voltage rises to values close to the AP- threshold. Scale bar in B2 applies also to A2.

A3) and B3) Post-action potential voltage traces from the figures above showed at higher gain with respect to time and voltage. Note that the trace of the neuron from an adult brain slice (B3) shows clearly 3 afterpotentials. An initial, fast after-hyperpolarisation (i A.H.P.) and a late, slow after-hyperpolarisation (l A.H.P.) with an intercalated depolarizing afterpotential (D.A.P.). The trace recorded in a p7 neuron shows only one afterpotential (the late slow A.H.P.). Scale bar in A3 applies also to B3.

Action potential associated phenomena in young and adult layer 5 pyramidal neurons of the visual cortex

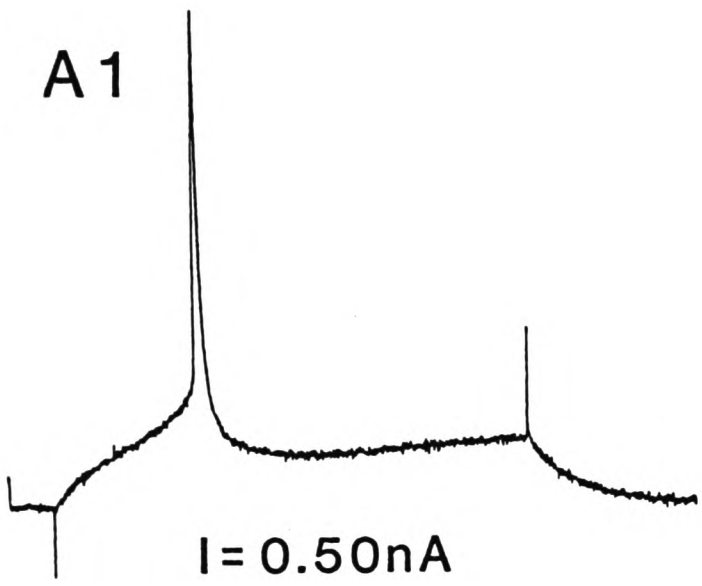

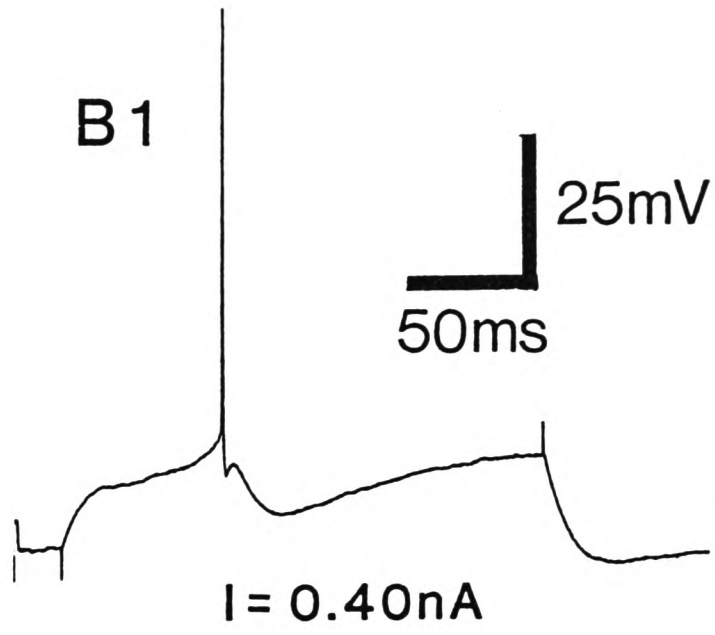

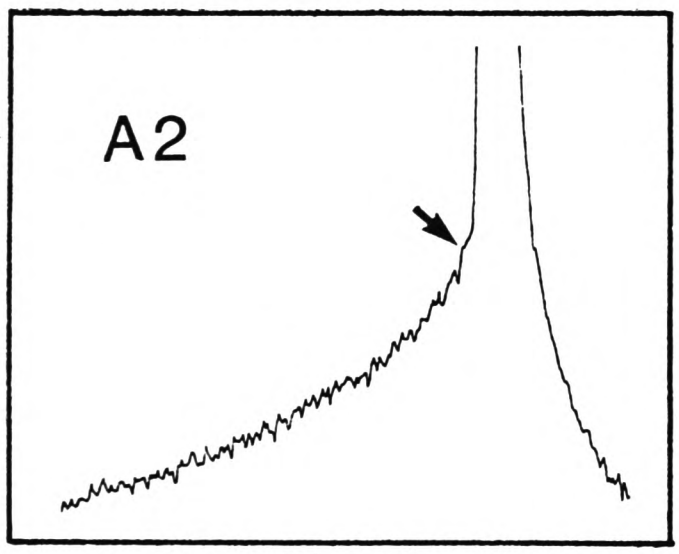

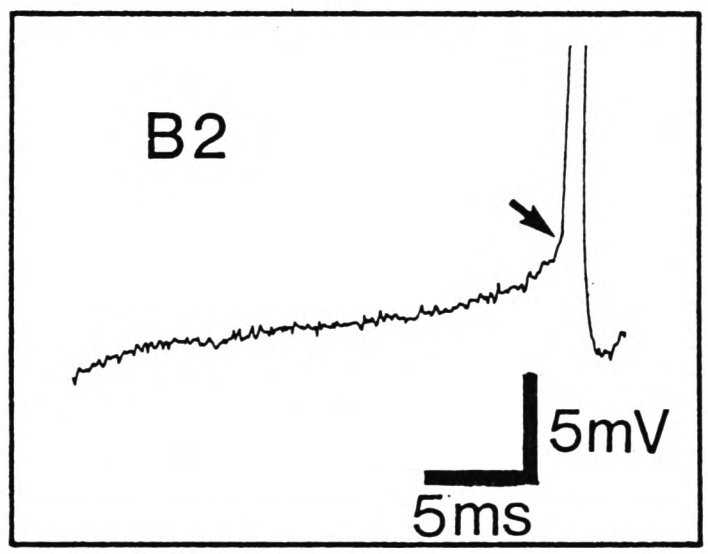

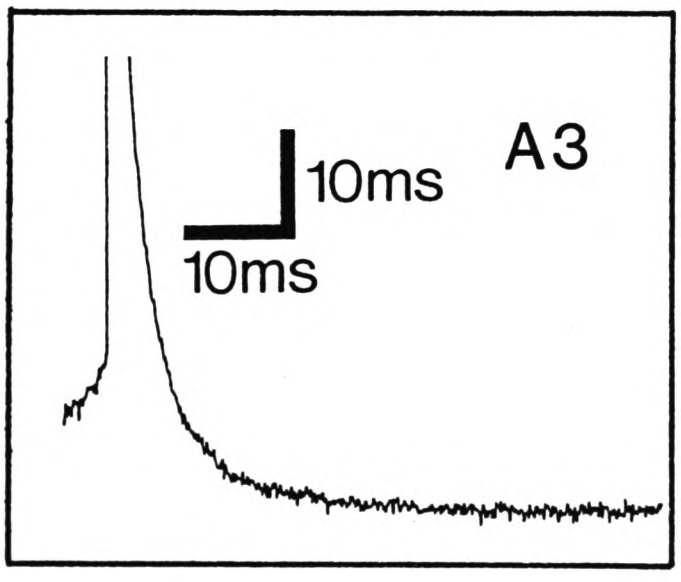

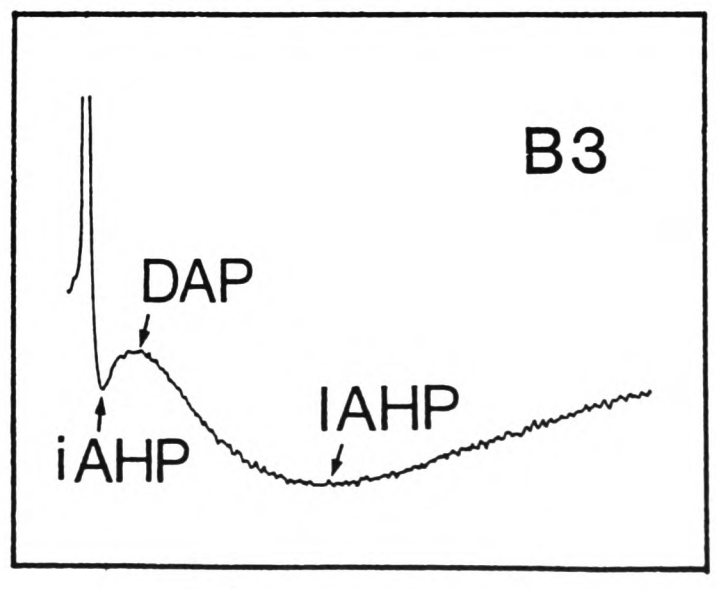

5.9B1 and C1).

The existence of A.H.P.s has previously been investigated in pyramidal cells from rodent brain slice preparations of the hippocampus of adult guinea-pigs (Hotson and Prince, 1980; Brown and Griffith, 1983; Lancaster and Adams, 1986). These studies demonstrated that the two phases of after-hyperpolarisation following such action potentials were due to the activation of Ca^{2+}-dependent K^+ currents (I_c) whereas the intercalated D.A.P. was due to a mixed Na^+/Ca^{2+} current (Konnerth et al., 1986). Detailed studies of these phenomena have also been investigated in the cat (Stafstrom et al., 1984).

F) synaptic physiology :

Classical, fast postsynaptic potentials are generated by a brief injection of current caused by the presynaptic release of packets of quanta of transmitter which act on postsynaptic ion channels. The general pattern of the resulting voltage response is thus a brief rising phase, a peak and a exponential decline towards the resting level. A careful analysis of the time course of such a voltage transient can provide information about electrotonic location of the injected current as well as the cable properties of the postsynaptic cell (Jack et al., 1971; Iansek and Redman, 1973; Jack, 1979).

To look for developmental changes in cell to cell signalling, the time courses of extracellularly evoked postsynaptic potentials were investigated in recordings of the previously described sample of neurons from slices prepared from young and juvenile animals. In further experiments the occurrence and the pharmacology of inhibitory

postsynaptic potentials (i.p.s.p.s) were examined.

General findings: Synaptic potentials could be reliably elicited using a bipolar tungsten electrode driven by a Digitimer DS2 isolated stimulator which delivered a very brief ($t \approx 0.20\mu sec$), adjustable voltage shock (0.1V-100V) to the surface of the slice.

Although initially single sweep records were used from each evoked p.s.p. it was then decided to work with averaged p.s.p.s. employing signal-averaging software obtained from C.E.D. (Cambridge Electronic Design, U.K.). This method improved the signal to noise ratio of the records considerably and helped to avoid the possibility of obtaining an unrepresentative p.s.p. for the subsequent analysis procedure. In general about 25-100 trials of each monosynaptic p.s.p. were averaged and their waveform quantified with respect to the time course.

Excitatory postsynaptic potentials : Depolarizing synaptic potentials could be evoked in **all** cells tested in all different age groups. Extracellular stimulation was successful from a number of places on the slice surface including the white matter, the adjacent grey matter and more superficial cortical layers if the stimulation site was close enough to the recording site. To make the group of stimulated afferent fibers as homogeneous as possible the e.p.s.p.s for analysis were always evoked with the stimulation electrode placed in layer 5, about 250-400μm lateral to the tip of the adjacent recording electrode (Hori et al., 1988). Thereby it was possible to evoke fluctuating e.s.p.s of very small mean amplitude (about 1mV) which were most probably the result of the stimulation of only a few synaptic sites, perhaps originating from a single afferent fiber.

Figure **5.11:** Age-related changes in excitatory synaptic potential shape as recorded in layer 5 pyramidal neurons from the adult and the developing rat visual cortex.

A) Synaptic potential recorded in an adult regular spike firing neuron. Average of 200 single sweeps; stimulus shock strength: 1.65V for ≈20μs; V_m= -70mV; R_{ME}= 88MΩ.

B) Synaptic potential recorded in a p11 regular spike firing neuron. Average of 150 single sweeps; stimulus shock strength: 2.85V for ≈20μs; V_m= -71mV; R_{ME}= 145MΩ.
Note the difference in mean rise time and time course of the falling phase.

Scale bar in B) applies also to A).

Excitatory postsynaptic potentials recorded in pyramidal neurons from the developing visual cortex

By adopting this procedure using small e.p.s.p.s it should have been possible to detect even relatively small changes in the time course of synaptic potentials. Such changes might be hidden if a larger postsynaptic response were recorded, because these usually consist of both an e.p.s.p. and i.p.s.p. or could be composed of many afferents with possibly different properties.

Several characteristic features distinguished the postsynaptic potentials recorded from immature neurons from the postsynaptic potentials recorded in neurons from adult animals. Firstly, it was impossible to elicit the typical depolarizing-hyperpolarizing sequence (usually found in all adult pyramidal neocortical cells; Connors et al., 1988) in any of the evoked p.s.p.s recorded from immature cortical slices before **postnatal day 9,** even if the shock stimulus strength was increased considerably. In **all** the cells obtained from animals from the first postnatal week and those up to p9 only purely depolarizing p.s.p.s. were found at resting membrane potential and all other membrane potentials tested, V_m being manipulated from -47mV to -100 mV by steady current injection. In the original data from averaged synaptic potentials, a shortening of the mean 10%/90% rise time, the mean time to peak and the e.p.s.p. duration (measured as the time at half amplitude) could be observed. Although all these mean values change considerably as cortical maturation progresses, the change was reduced and became insignificant if the values were normalized using the respective cell membrane time constant (see Figures 5.12A-C and a-c). It thus appears that much of the change in e.p.s.p time course was due to a reduction in membrane time constant which changes itself significantly throughout the same period (see Figure 5.6 above). If the membrane potential was shifted to more depolarized levels (by DC-current injection a gradual increase in p.s.p.-amplitude could be observed at all postnatal ages studied.

Figure **5.12:** Age-related changes in excitatory synaptic potential shape indices as measured from synaptic potentials recorded in layer 5 pyramidal neurons from the adult and developing rat visual cortex.

A) Changes in mean synaptic potential rise time measured between 10% and 90% of the e.p.s.p. peak amplitude.

a) mean rise time values normalized by the respective membrane timeconstant.

B) Mean synaptic potential width measured as time at half amplitude.

b) mean half width values normalized by the respective membrane time constant.

C) Mean e.p.s.p. time to peak.

c) mean time to peak values normalized by the respective membrane time constant.

Note that the trend observed in the original data disappeared after values were normalized with the respective membrane time constants of the cells from which records were taken.

A Mean rise time of synaptic potentials

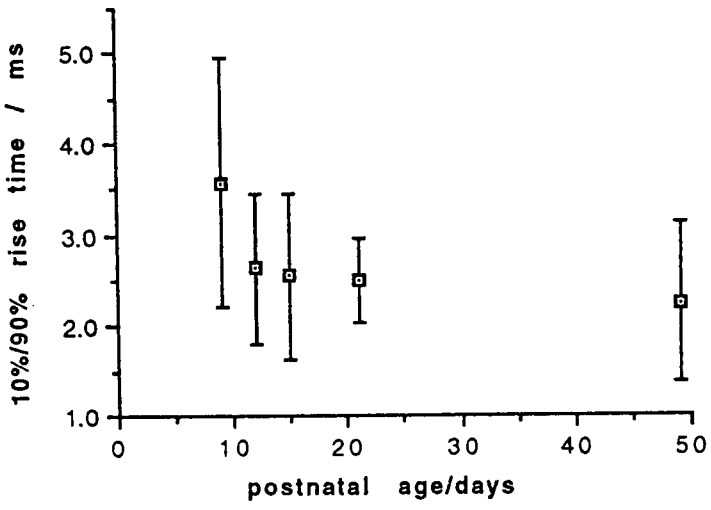

a Normalized synaptic rise time

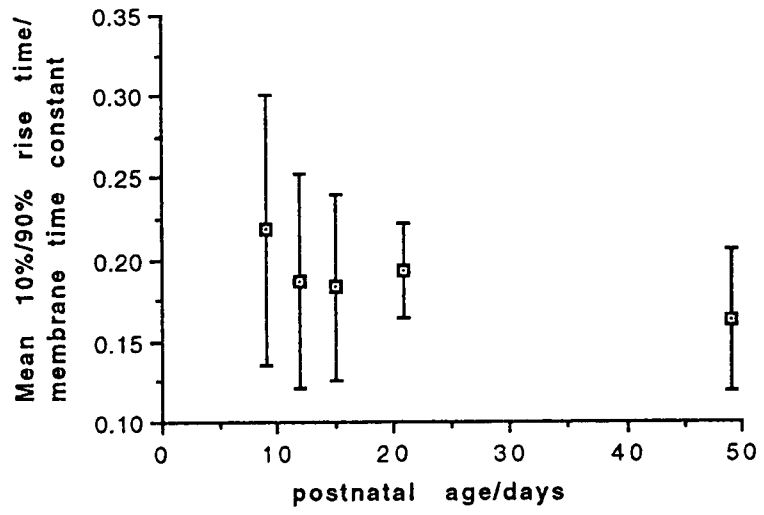

B Synaptic potential width at half amplitude

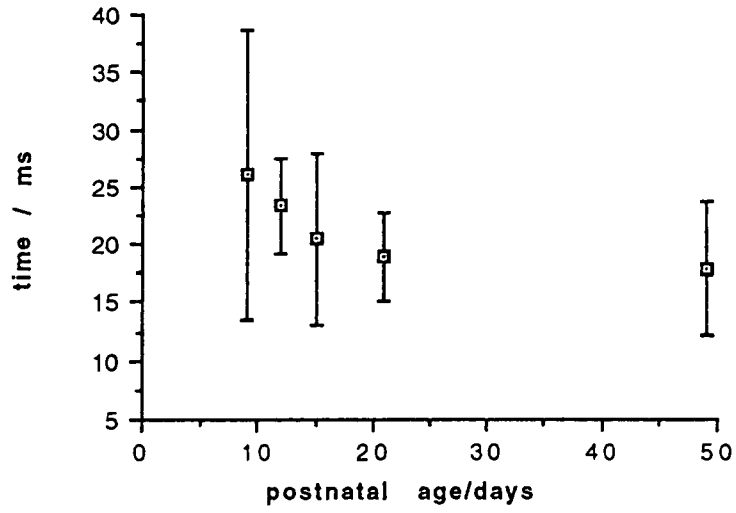

b Normalized synaptic potential width at half amplitude

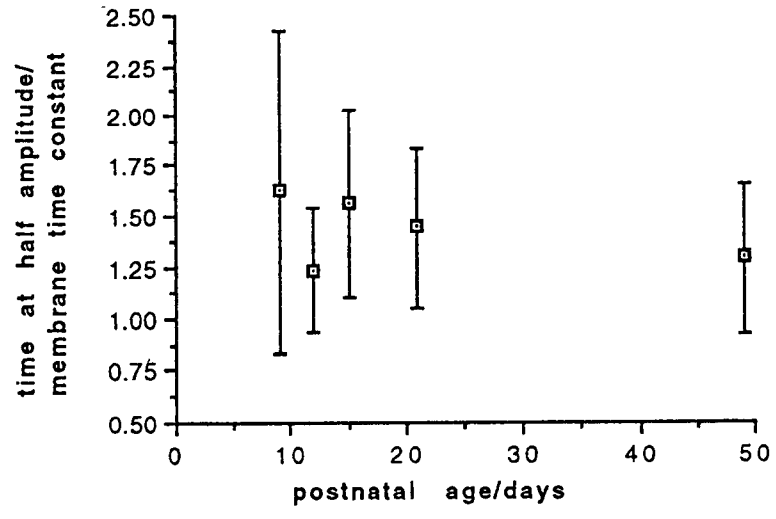

C Synaptic potential mean time to peak

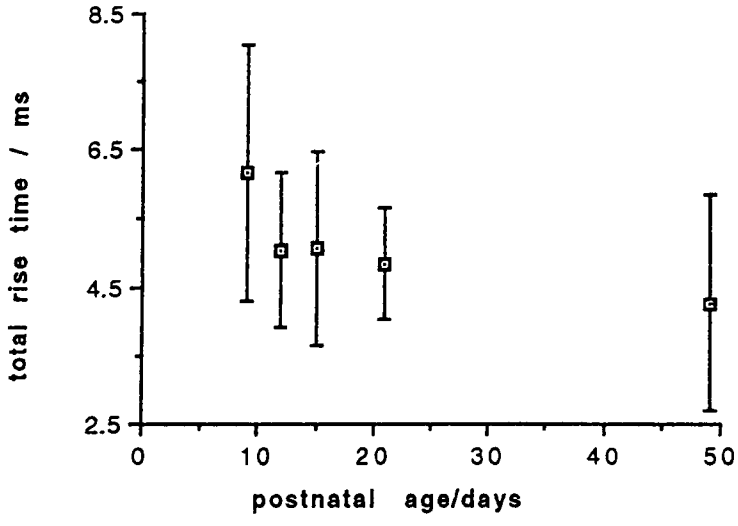

C Synaptic potential mean total rise time normalized

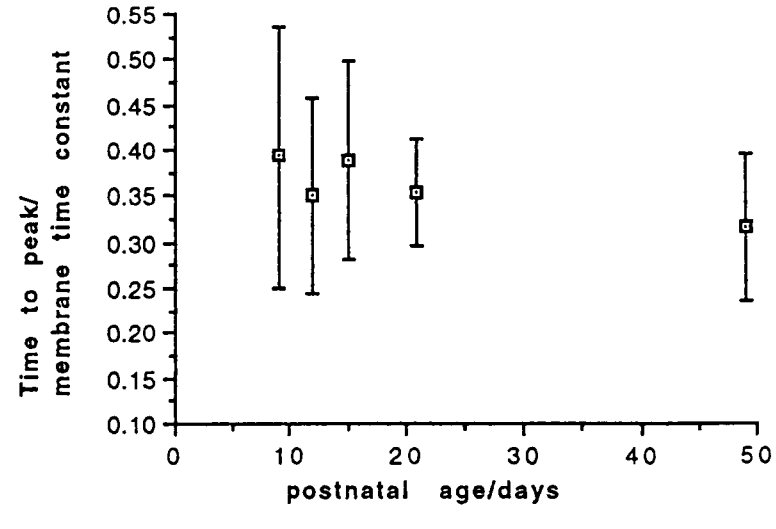

The amplitude of the e.p.s.p. could also be increased to threshold, if the stimulus intensity was increased. Occasionally an action potential was triggered off such an evoked e.p.s.p.

Inhibitory postsynaptic potentials: All p.s.p.s evoked in cells from preparations before p9 were depolarizing in action (vide supra). It might have been possible that $E_{Cl} \leq E_m$ and therefore the expected i.p.s.p active was present but hidden or depolarizing. I therefore tested **the same p.s.p.** at a more hyperpolarized or depolarized V_m (the resting membrane potential was manipulated to values up to about –47mV) but still no hyperpolarizing action was detectable. To make sure that the failure to detect any i.p.s.p.s was not due to some inadequate stimulus strength, some loss of a few hyperpolarizing events in the averaged response or some very early fatigue of i.p.s.p.s which might not occur in e.p.s.p.s, another protocol was adopted to look for i.p.s.p.s separately. From the beginning of the recording period (for synaptic potentials) the ACSF was modified to contain 20mM CNQX (6-cyano-7-nitroquinoxaline-2,3-dione) and 25mM D–AP5 (D-2-amino-5-phosphonovaleric acid). These two pharmacological agents block selectively glutamate-mediated excitatory synaptic transmission, so it was possible to look specifically for i.p.s.p.s during stimulation of the slice at various sites with high shock-intensities (up to 50V). Nevertheless it was still impossible to elicit any p.s.p. of hyperpolarizing action in any cell from animals younger than p9 (see Figure 5.13a).

After p9, all the evoked i.p.s.p.s showed a strong voltage dependence with a substantial increase in amplitude as V_m was manipulated to more depolarized values. (see Figure 5.13b and c). I.p.s.p.s could be evoked in cells (n=12) of the second

Figure **5.13:** Age related changes in inhibitory synaptic potentials as observed in synaptic potentials recorded from layer 5 pyramidal neurons at various postnatal stages. All traces shown were recorded from neurons bathed in modified ACSF containing 25μM CNQX and 50mM APV to block glutamatergic excitatory transmission.

A) Traces from potentials of a p8 neuron; extracellular shock stimulation of the slice failed to elicit any p.s.p. at various membrane potentials tested.
V_m was -64mV; R_{ME} was 92MΩ.

B) Traces from recordings of a p9 neuron; extracellular shock stimulation of the slice succeeded in eliciting an i.p.s.p. which reversed at a membrane potential of -66mV. Averages of 35 single sweeps of p.s.p.s recorded at various membrane potentials (values are indicated in the figure in -mV) are superimposed.
V_m was -63mV; R_{ME} was 139MΩ.

C) Traces from a recording of a p17 neuron; extracellular shock stimulation of the slice succeeded in eliciting an i.p.s.p. which reversed at a membrane potential of –65mV. Averages of 35 single sweeps of p.s.p.s recorded at various membrane potentials (values are indicated in the figurein in -mV) are superimposed.
V_m was -65mV; R_{ME} was 128MΩ.

D) Two traces from a recording of an adult neuron; extracellular shock stimulation of the slice succeeded in eliciting an i.p.s.p. which reversed at a membrane potential of –68mV.Averages of 35 single sweeps of p.s.p.s recorded at two different membranepotentials are superimposed. Note the different time scale.
V_m was -79mV; R_{ME} was 106MΩ.

Note that the time course of the i.p.s.p. recorded art p9 is consideraby slower than the time course of the i.p.s.p. recorded in the p17 or adult neuron. All i.p.s.p.s recorded in young and juvenile neurons showed a short latency and were monophasic. In i.p.s.p.s recorded in adult brain slice preparation an additional late hyperpolarizing component is present, which arises at a longer latency and slows down the repolarization of the initial, fast i.p.s.p. thus changing its time course (indicated by arrow).
Scale bar in c applies also to a and b.

Inhibitory postsynaptic potentials recorded in pyramidal neurons from the developing visual cortex

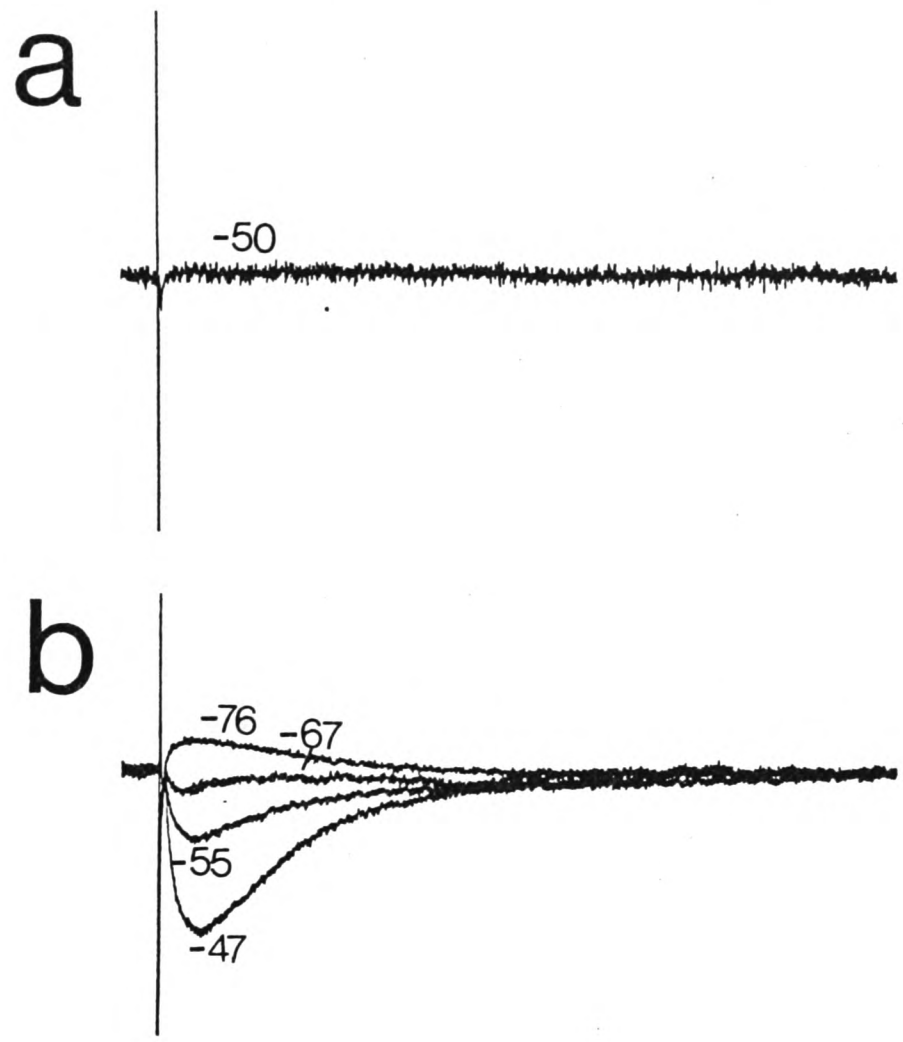

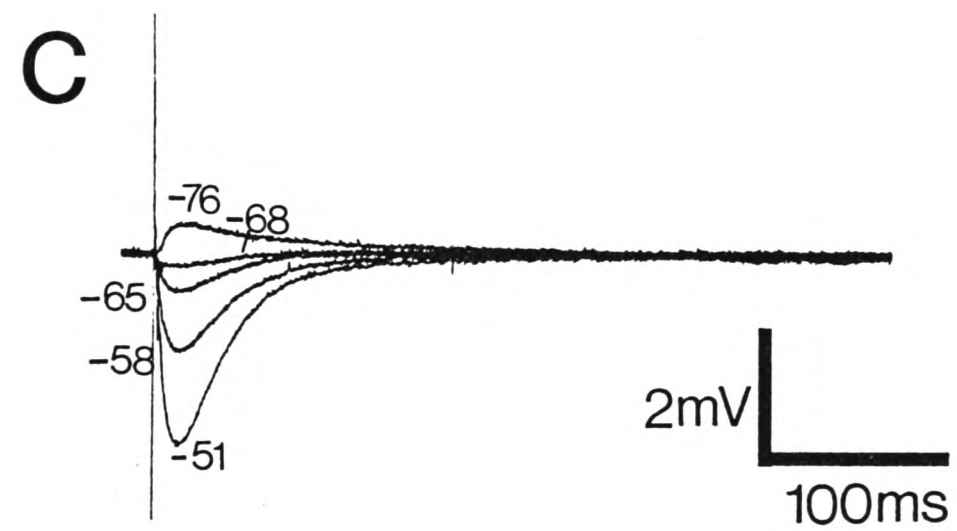

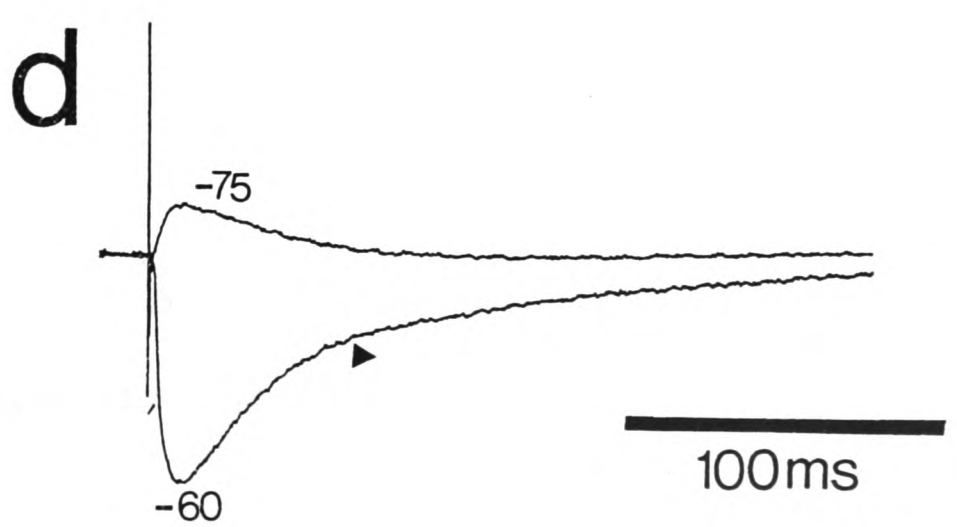

postnatal week and these were tested for their reversal potential. This was found to be around –70±6.32mV which is close to the presumed chloride equilibrium potential and indicated that the i.p.s.p.s might be mediated through the $GABA_A$ receptor complex. The latter assumption was confirmed as these i.p.s.p.s were abolished by application of 50μM bicuculline-methiodide to the bathing solution (n=4). A late i.p.s.p. component, which is thought to be $GABA_B$ receptor mediated (Connors et al., 1988), was only apparent in cells from adult brain slices (see Figure 5.13d).

After postnatal day 9 I did not have great difficulty in eliciting either e.p.s.p.s or i.p.s.p.s but as a general rule it can be said that the stimulus-shock-strength had to be higher for eliciting i.p.s.p.s.

The general conclusion is that excitatory postsynaptic potentials (e.p.s.p.s) alone can be evoked via extracellular shock-stimulation in the slice preparation from cortex of the very early postnatal period.

5.4 Discussion :

The results of this set of experiments indicate that intrinsic properties of pyramidal neurons from layer 5 of the rat visual cortex change significantly during the early postnatal period.

In the first part of this discussion some general aspects of the generation of the neocortex will be discussed, followed by a description of the differentiation process of

single cortical neurons with respect to changes in their somadendritic structure and their axonal arborizations. A detailed understanding of the structural changes of neurons during maturation is helpful because it parallels the changes in electrophysiological properties throughout the same period and might have some influence on them. In the second part, changes in the electrophysiological properties of cortical pyramidal cells will be discussed. The findings presented in the preceding sections of this chapter will be compared to data obtained in other studies of neuronal maturation as reported in published literature. Finally, some of the functional consequences of developmental changes are discussed with reference to the maturation process observed *in vivo*.

Generation of the cortex (see also General Introduction) :

The pyramidal neurons of the visual cortex are generated within the last week of gestation. The neurons destined for the infragranular layers are generated around embryonic days 15 to 17. After their last mitotic cycle, cells migrate towards the pial surface to transiently form the cortical plate. This process is not yet finished at birth and it is therefore impossible to differentiate between separate cortical laminae before the last generated cells (later to be neurons of the superficial layers) have almost finished their migration period, which continues well into the first postnatal week (see Nissl-plates).

To avoid pooling of different neuronal populations, thereby being of different maturity, I have limited this study to the phase of cortical development commencing at postnatal day 6, when the two infragranular layers can be distinguished from the cortical plate (see also Juraska and Fifkova, 1979a). I am well aware of the fact that the

earliest stages of neuronal differentiation of layer 5 cells are thus missingfrom my sample, but I wanted to avoid investigating a mixture of neuronal populations. Furthermore the existence of dye coupled neurons in early stages of postnatal corticogenesis casts doubt on electrophysiological data collected from these stages. A brief anatomical description follows for completeness.

As postmitotic immature neurons migrate towards their final location, which presumptive layer 5 pyramidal cells reach around p1, they show very little signs of structural differentiation and appear as virtually branchless cells (e.g. Miller, 1988b; Petit et al., 1988). All subtypes of cortical pyramidal neurons at this stage possess a prominent pial process and have also a trailing process. The pial process (the former guiding process) will transform into the apical dendrite, whereas the former trailing process differentiates into the axon and grows actively towards a target structure (Peters and Feldman, 1973). It is not clear when structural differentiation starts in these neurons, and what factors influence this phenomenon, but a gradual process has been described:

Morphological differentiation of single neurons:

The anatomical development of pyramidal cells from the rat cerebral cortex has been previously investigated in a number of studies using techniques for either the light microscope, the electron microscope or a combination of both (e.g. Ramon y Cajal, 1911; Eayrs and Goodhead, 1959; Berry and Rogers, 1965; Berry, 1974; Parnavelas and Lieberman, 1979; Miller, 1981; Miller and Peters, 1981; Juraska, 1982; Juraska

and Fifkova, 1979a,b ; Petit et al., 1988; reviewed by Jones, 1981; Miller, 1988b). The morphological differentiation encompasses, among many ultrastructural changes the extension of neuronal processes and the formation of synaptic connections. These two points will be emphasized here.

Most of the morphological changes occur within the first four postnatal weeks, after which neurons are thought to be morphologically virtually adult-like (Jacobson, 1963; Jacobson and Trojanowski, 1975; Kristt, 1978; Wise et al., 1979; Miller, 1981; Miller and Peters, 1981; Blue and Parnavelas, 1983; Miller, 1988b). Cell body growth seems to be slow within the first postnatal week, is most rapid during weeks 2 and 3, and by the end of week 4 the cell bodies have adult size (Mathers, 1978; Miller 1981,1988b, see also results in **Chapter 6**). Within that period the cell body volume increases about 2.5 to 4 fold. The growth of pyramidal cells from the infragranular layer 5 is **not** synchronized with that of the superficial layers 2/3 (a finding that was already described by Ramon y Cajal, 1906 [as mentioned by Lorente de Nó, 1943]), which can be accounted for by the difference in generation-time and perhaps different migration schemes (Bayer and Altman, 1991).

The generation of layer 5 cell precedes that of cells for the supragranular layers by about three days. Consequently layer 5 neurons start to increase in somatic size earlier and also attain their mature size about three days earlier than cells from layers 2/3 (Butler and Caley, 1972; Parnavelas and Lieberman, 1979; Miller, 1988b). Although there are reports of somatic spines to be found within the first postnatal week (Marin-Padilla, 1972; Juraska and Fivkova, 1979a; Miller, 1981), I was unable to confirm this in any of the cells studied in this sample. The failure to detect any such spines might be

explained in several ways. First, the spines may be transient thus occurring only briefly during early development. Second, the sample from the first postnatal week was small in size (n=6) in this set of experiments. Thirdly, the intracellular staining procedure might have failed to fill and visualize such processes. Finally, the spines might be fragile and might have been lost during the period of slice maintenance *in vitro*.

There is an enormous increase in neuropil volume during early cortical development which also accounts for most of the increase in cortical thickness that has been observed (see also Nissl-study in **Chapter 3:** Material and Methods) and causes a shift of the location of cortical layer 5 with respect to the position to the pial surface.

A large contribution to this increase in neuropil is made by the prolific development of neuronal dendrites throughout this early postnatal period. The developmental changes have been shown to consist of : *de novo* production of primary dendrites, extension of existing dendrites, growth of additional dendritic branches and a massive generation of spines on those dendrites (for a review see Miller, 1988b).

The apical dendrite is already a prominent morphological feature of cells from the earliest postnatal stages. It is thought that it develops from the guiding process of the migrating neuron (Peters and Feldman, 1973). Therefore it should be present and visible in all neurons that have completed their migration. The next obvious sign of neuronal structural differentiation is the appearance of the primary basal dendrites (p1 to p3). Only later do a number of primary oblique dendrites arise from the apical dendrite and higher-order dendritic branches arise all over the neuron, thus causing a tremendous gain in dendritic complexity. A transient exuberant production of primary

dendrites has also been described around p6 (Miller, 1981). Some dendritic growth continues at the tip of each dendrite well into adult life (Juraska, 1982).

Dendritic growth cones have been seen in Golgi preparations from young age groups and also in intracellularly injected neurons from the developing cortex (see **Chapter 6**), but they disappear by the beginning of the third postnatal week (Wise et al., 1979; Miller, 1981; Juraska, 1982).

Several studies have tried to quantify this change in dendritic structure (Eayrs and Goodhead, 1959; Juraska and Fifkova, 1979a; Wise et al., 1979; Miller, 1981; Juraska, 1982). Despite different ways of assessing the change in complexity, they all come to the conclusion that denditic growth is slow in the first postnatal week, increases significantly during postnatal weeks 2 and 3 and seems to be complete at the beginning of the fourth week. The surprising fact of an existing transient overproduction of primary basal dendrites in week 2 (Miller, 1981) could reflect the pruning or retraction of connections that were not successful in establishing sufficient synaptic support.

The morphological essence of this maturation period is a significant increase in neuronal surface area as well as an increase in structural complexity which also indicates important changes made in the connections between cells.
The morphological changes described in this section are paralleled and might even be influenced by significant changes in the electrophysiological properties, some of which I have investigated and will discuss in the following section.

Developmental changes in neuronal electroresponsiveness :

The complementary physiology and morphology of neurons from postnatal rat visual cortex has been studied in this thesis to provide data describing the early postnatal development of pyramidal neurons in the visual cortex and to provide further insight into cellular and synaptic properties of developing neurons.

The results of this study demonstrate that the intrinsic electrophysiological properties of layer 5 pyramidal neurons from the rat visual cortex undergo significant changes during the early postnatal period. Action potentials become larger, faster and briefer during a phase in which the membrane time constant shortens and the cell input resistance decreases. In addition, it was demonstrated that the time-course of extracellularly evoked postsynaptic potentials in these cells also becomes more rapid. First, the quality of the preparation will be evaluated before the results relating to subthreshold properties are discussed; this section is then followed by a discussion of the changes in action potential parameters. Finally the observations made of synaptic potentials during cortical development will be discussed.

General aspects of neuronal development :

Several previous studies have investigated the time-course of postnatal changes of subthreshold properties and action potential parameters in a variety of preparations from neurons of the rodent central nervous system (Schwarzkroin, 1982; Schwarzkroin and Kunkel, 1982 for rabbit hippocampus *in slices*; Gardette et al., 1985 for rat intra-

cerebellar nuclei *in slices*; Westbrook and Brenneman, 1984; MacDermott and Westbrook, 1986 for mouse spinal cord *in culture*; Walton and Fulton, 1986; Fulton, 1987 for neonate rat spinal cord *in slices*; Hamill et al., 1986; Huguenard et al., 1988 *from acutely dissociated cells* from rat cortex; Kriegstein et al.,1987; McCormick and Prince, 1987 for rat sensorimotor cortex *in slices*).

The values for basic cell properties such as membrane resting potential, input resistance, mebrane time constant and AP parameters from this study are in good agreement with data obtained from these studies. I am therefore confident that cells in my preparations for intracellular recording were in good condition and can furthermore be compared to data obtained from adult cortical cells studied previously in this laboratory (Larkman and Mason, 1990; Mason and Larkman, 1990; Mason et al., 1991).

Subthreshold properties:

Membrane resting potential: The membrane resting potential of layer 5 neurons became progressively more negative with time.

Membrane time constant: The time constant measure was taken from an analysis of a voltage decay from short hyperpolarizing current pulses, which avoids some of the time-dependent non-linearities, which develop during the long pulses (Durand et al.,1983, see also **Chapter 4**: discussion).

The membrane time constant decreased substantially within the investigated postnatal period from an average value of 18.1±5.3 ms at p6 to around 11.8±3.0 ms in the adult group. As long as a approximatly constant specific membrane capacitance (C_m) is

assumed (normal C_m values are thought to be around 1μF/cm^2; Cole, 1972; Jack, 1979) this change can most probably be attributed to a change in the related specific membrane resistivity (R_m) since the membrane time constant is the product of R_m and C_m. Such a decrease in R_m could be explained by the progressivly increasing insertion of ionic channels (which are open near V_m) into the neuronal membrane, an assumption that is supported by findings of related changes in Na^+- and K^+- conductance (Prince and Huguenard, 1988).

Input resistance: The apparent input resistance (R_{in}) was measured using the same short current pulses (of negative polarity) which were used for time constant measurements. The short pulses minimized the time-dependent non-linearities which are observed if longer current pulses are used.

The apparent input resistance decreased throughout the postnatal period studied. The observed decrease was most dramatic during the first two postnatal weeks. This progressive change is correlated with a simultaneous increase in cell body size, total membrane surface area, and cell volume, changes which also occurs mainly within the first two postnatal weeks (Miller, 1981; for details see **Chapter 6:** discussion).

The high input resistance of cells from younger cells could be due to both the smaller size of the neurons and their higher R_m. There may also be some change in cytoplasmic composition (and therefore resistivity, R_i) but this effect will be small. McCormick and Prince (1987) have argued that higher input resistances and longer membrane time constants (see below) could increase the responsiveness of immature neurons to imposed depolarizations. Such cells will tend to be electrotonically short and any synaptic activity will be prolonged. This could compensate for the rather

poorly developed synaptic inputs in very young postnatal stages (Kristt, 1978; Blue and Parnavelas, 1983; Kriegstein et al., 1987; McCormick and Prince, 1987; Prince and Huguenard, 1988; and own observations).

Suprathreshold properties :

Burst-firing and regular spike-firing pattern: Cells which showed a burst-firing pattern in response to a suprathreshold stimulus were first encountered at p15 in this sample of neurons. This is surprisingly late in cortical development. Because it is known that such a burst-firing pattern is a somewhat fragile property, it is conceivable that some burst-firing cells existed already but were not detected. On the other hand, my observation correlates well with previous reports on a late appearance of this phenomenon (Kriegstein et al., 1987). A further evaluation of this finding is given in

Because of the latter finding and because the number of neurons in each group was relatively small and because of the fact that it was impossible to recover all cells histologically, I did not attempt to subdivide even the older neurons into sub-classes (e.g.of tufted and untufted morphology). Nevertheless it would be interesting to follow the development of electrophysiological properties in the sub-classes separately.

Parameters of single action potentials:

Action potential threshold above rest became progressively more negative with postnatal age. This change is all the more striking if the simultaneous change in resting

membrane potential to more negative values is taken into account. The 10%/90% rise-time decreased to about half and the equivalent fall-time decreased to about one quarter during the first three postnatal weeks. The 30/70% rise-rate increased about threefold, whereas the fall-rate increased almost fivefold. These changes are probably primarily caused by an enormous increase in ion channel density during that period, as shown via [^{3}H]-saxitoxin-binding studies (Baumgold et al., 1983) or [$^{22}Na^+$] ion-flux assays (Courand et al., 1986). They are **not** caused by a maturational change of channel kinetics as shown "cell-attached-patch-clamp" studies (Hamill et al., 1986; Huguenard et al., 1986). The insertion of ion channels occurs at different rates for different ion channels and differs between neuronal classes (Prince and Huguenard, 1988). These changes are responsible for the large decrease in spike duration from 1.57±0.37 ms in the p6 group to 0.54±0.10 ms in the cell group from adults and for the repetitive firing properties (see below). The AP-peak amplitude above threshold also increased significantly, an observation that is related to the changes in sodium conductance (Hondeghem, 1978) and to the number of channels, since the channel kinetics do not change (see above).

Studies from both invertebrate neurons (e.g. Ribera et al., 1981; Goodman and Spitzer, 1981) as well as some vertebrate neurons (Bader et al., 1983) have indicated that the ionic mechanism of AP-generation changes from primarily Ca^{2+}-mediated to predominantly Na^+-mediated. However the available data from rodent neocortical neurons (Franz et al., 1986; McCormick and Prince, 1987) indicate that Na^+ is the dominant ion for AP-generation throughout the whole postnatal developmental period.

Afterpotentials: Single action potentials from immature cells were followed by

afterpotentials which changed in waveform during development. In neurons in slices from adult animals it is possible to discriminate three afterpotentials; an initial fast A.H.P. and a late slow A.H.P. -both separated by an intercalated D.A.P. Of those, the initial A.H.P. and the D.A.P. were pronounced only at later developmental stages (see Figure 5.10). This observation has been made in previous studies (McCormick and Prince, 1987; Huguenard et al., 1988).

The observation concerning the initial A.H.P. is in agreement with a retarded development of delayed rectifier potassium channels (Prince and Huguenard, 1988) and perhaps the absence of another potassium current (the A-current) which is involved in this phenomenon in the adult (Connor and Steven, 1971; Prince and Huguenard, 1988). The intercalated D.A.P. is caused by calcium currents (e.g. Konnerth et al., 1986; Friedman and Gutnick, 1987; Schwindt et al., 1988) and the late A.H.P.is due to an calcium dependent potassium current (Hotson and Prince, 1980; Lancaster and Adams, 1986). Changes of the latter two have not yet been studied during development. All these currents have an effect on spike repolarization and may also modulate neuronal spike frequency and its accommodation.

Synaptic potentials:

Excitatory synaptic potentials: Great effort was made to employ very slow stimulus repetition rates to avoid presynaptic depression as well as postsynaptic desensitization during the recording procedure, because it has previously been shown that the amplitude of synaptic potentials is very dependent on stimulus frequency in recordings

from young cells (Kriegstein et al., 1987). I was able to demonstrate that e.p.s.p. waveforms became more rapid during development, but that most of this change was due to the decrease in time constant that occurred during the same postnatal period. It was also observed that e.p.s.p.s could be elicited at all the postnatal stages studied and that depolarization of the membrane resting potential caused an increase in amplitude. This observation has been reported in previous studies and it was suggested that voltage activated NMDA-receptor mediated currents are involved in this prolongation (e.g. Jones and Baughman, 1988; Thomson et al., 1988; own observations). Recently the e.p.s.p.-voltage dependence has been investigated in detail (Deisz et al., 1991) and it was concluded that in addition to the NMDA-receptor mediated prolongation, a mixed calcium/sodium mediated process can be found in cortical neurons that enhances the amplitude of single e.p.s.p.s with depolarizations.

Even when i.p.s.p.s could be detected, the stimulus strength required to reliably trigger an e.p.s.p. was always less than that necessary to elicit i.p.s.p.s.

Inhibitory postsynaptic potentials: It was demonstrated that in layer 5 pyramidal cells from the visual cortex i.p.s.p.s appear relatively late in postnatal cortical development. This finding of a delayed development of inhibitory synaptic action is in good agreement with studies made in neurons from other brain areas (Schwartzkroin, 1982; Mueller et al., 1983; Schwartzkroin and Kunkel, 1983; Harris and Teyler, 1983; Michaelson and Lothman, 1989). Although whole-cell patch clamp studies have recently demonstrated an early GABA-ergic inhibition in immature hippocampal neurons (Zhang et al., 1990), I am confident that this was not the case here. Each depolarizing p.s.p. recorded in neurons from the first postnatal week was tested at various membrane potentials and did not show any sign of reversal. Furthermore,

after the slices were treated with 25μM CNQX and 50μM APV to block glutamatergic e.p.s.p.s., it was still impossible to find any p.s.p. whatsoever at any membrane potential tested in cells recorded in slices from brains before p9.

Very recent reports on the maturation of the GABA-ergic system studied in a large sample of neurons from the rat neocortex, (Luhman and Prince, 1991) have also confirmed that i.p.s.p.s could be elicited in only 3.6% of impaled cells within the first ten postnatal days. It seems likely, therefore, that inhibitory synaptic function develops relatively late in the rat visual cortex.

Chapter 6:

Projection neurons in layer 5 of the immature visual cortex: distinct morphological types can be distinguished within the first postnatal week

6.1 Introduction :

There appear to be at least two distinct pyramidal neuronal populations present in layer 5 of the adult rodent visual cortex which differ in their morphological features and project to different projection sites (e.g. Schofield et al., 1987; Hallman et al., 1988; Hübener and Bolz, 1988). Moreover further studies have recently demonstrated that at least two morphologically distinct pyramidal cell types in layer 5 have different intrinsic physiological properties (for cat motorcortex see Deschenes et al., 1979; for rat visual and somatosensory cortex see Larkman and Mason, 1990; Mason and Larkman, 1990; Chagnac-Amitai et al., 1990). In rat visual cortex these two cell populations differed primarily in the following features: the cells of one population always had a thick apical dendrite ascending towards the pial surface and forming an obvious tuft in layer 1, while the cells of the other group had a more slender apical dendrite, which terminated in layers 2/3 without forming such a terminal tuft. This morphological classification aligned closely with the physiological classification into burst-firing neurons and regular spiking neurons (non-bursters) respectively.

Using intracellular recording techniques combined with a retrograde tracing technique I was able to show (see **Chapter 4**) that pyramidal cells projecting to the superior colliculus (SC) are characterized by a thick apical dendrite and can unequivocally be classified as burst-firing neurons, whereas cells projecting to the contralateral hemisphere (CLH) possess a slender apical dendrite and could be classified as regular-spiking cells (for details see **chapter 4**). It was also demonstrated that back-labelled neurons of the two populations have also different intrinsic physiological properties, such as membrane time constant, input resistance and action potential parameters, which are also correlated with this morphological distinction. Furthermore it was shown that such electrophysiological differences between layer 5 pyramidal neurons, which allow such a classification, were only discernible after the second week of postnatal cortical development (see **Chapter 5**).

The intention for the experiments presented in this section was to find out whether significant differences in morphology can be observed before the electrophysiological differentiation into bursters and non-bursters occurs in these neurons. To investigate the morphology of pyramidal projection neurons in early postnatal cortical development, retrogradely labelled neurons of layer 5 of rat visual cortex were studied in a fixed slice preparation via intracellular injection and subsequent photoconversion of *Lucifer Yellow* (LY).

One question to be answered was whether the previously described characteristics of adult cell morphology (see Larkman and Mason, 1990; Larkman, 1991a; and **Chapter 4**) are already present in early stages of cortical development or whether those features emerge some time after birth. It is conceivable that the projection neurons of both groups look more similar or even identical in early

developmental stages. If the answer to the latter question were yes it would be of interest to find out when the characteristic differences appear in cortical development. The morphology of the slender cell type might arise from something close to the thick cell type morphology e.g. by specific pruning of the terminal tuft.

On the other hand it is conceivable that the emergence of two morphological cell types is a "side effect" of another developmental change, as for example the increase in thickness of the grey matter, simply leaving the apical dendrite of the CLH-projecting cell population behind as the cortical depth increases. Last but not least, it is also conceivable that a terminal tuft never develops in cells that project to the contralateral hemisphere.

6.2 Materials and Methods :

Twelve rats were used in this set of experiments. The third postnatal day (p3) was chosen for the injection of tracer because it had previously been reported to be the earliest possible stage at which cortical cells *in vivo* can be labelled reliably via retrogradely transported tracers injected into the rat SC (Thong and Dreher, 1986, 1987; Richburg and Kirby, 1989; but see DiI study on hamster by Rhoades et al., 1991) or into the other cortical hemisphere (Miller and Vogt, 1984; Miller, 1986b; but see also O'Leary et al., 1990 for recent DiI studies). Because animals at that age are very small in size –having then a total body weight of only 5 grams– and no stereotaxic atlas or equipment is available for such early developmental stages, a non-stereotactic surgical procedure was developed for the back-labelling operations (**Chapter 3**: Materials and Methods and Appendix 5). After the injection of tracer a survival period

Figure **6.1**: Pyramidal neurons from layer 5 of the developing visual cortex filled intracellularly with Lucifer Yellow (LY) which was injected under visual control into individual neurons in fixed slices. This set of plates illustrates that it was clearly possible to differentiate between back-labelled and non-back-labelled neurons when they were filled with LY.

Plates on the *left* side show neurons with the filter block appropriate for the excitation wavelength of LY whereas plates on the *right* side show corresponding photographes with the filter block changed to the appropriate wavelength for the excitation of rhodamine fluorescence. Small arrows in A, C, E, and G point at the main axon; Big arrows in B, D, F, and H, point at the same cells shown in the corresponding *left* side plates.

Plates A) and C) show intracellularly injected neurons from **p5** which both were clearly non-back-labeled as can be seen in the corresponding plates B) and D).

Plates E) and G) both show LY filled neurons from **p5** which were both unequivocally back-labelled as can be seen in corresponding plates F) and H).

Scale bar in H =50μm and applies to all plates.

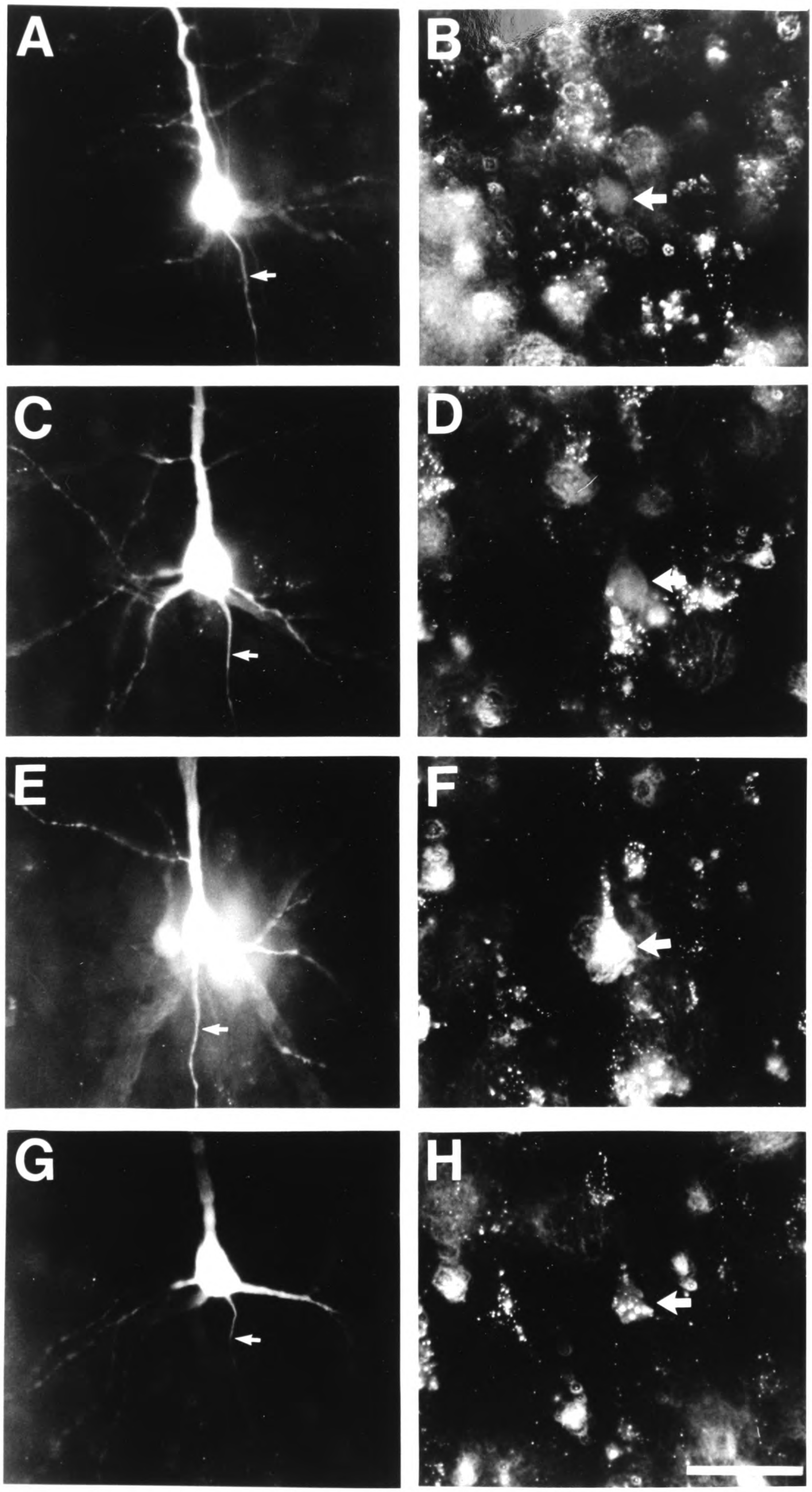
A
B
C
D
E
F
G
H

between two and seven days was allowed before slices were prepared. The brains of animals were perfusion-fixed and coronal slices (150 µm thickness) of the visual cortex prepared with the aid of a microtome with a vibrating blade. Individual backlabelled cells were then injected intracellularly with LY as described in the Materials and Methods section of **Chapter 3**.

Filling of cells was judged to be complete when the dye had spread into the terminal processes of dendrites as well as the main axon and some axonal collaterals. Cell bodies were accepted for injection only if located at depths of 50-100µm below the cut surface of the slice to ensure that the morphology of individual neurons was as complete as possible within these relatively thin slices. Photoconversion of successfully filled single neurons was carried out according to the method described by Buhl and Lübke (1989) (see **Chapter 3**: Materials and Methods).

Two groups of projection neurons (SC-cells and CLH-cells) were investigated, each at two postnatal stages. For each of the 4 cell groups, 3 animals were sacrificed at **p5** and at **p10**. Animals of all groups had undergone operations for tracer injection at **p3**. A total of more than 120 back-labelled layer 5 neurons was filled successfully in both groups at both dates. Additionally approximately 90 non-backlabelled cells were filled in the same experiments. Observations from these immature back-labelled neurons were also compared to those made from cortical neurons obtained in living slice preparations of adult animals (see **Chapter 4**).

After intracellular injection with LY, cells were photoconverted and subsequently 12 back-labelled neurons from p5 and another 16 backlabelled neurons from p10 drawn under high magnification (1250x) using a microscope equipped with a

camera lucida attachment. All quantitative measurements were made from these drawings and the results from both groups of projection neurons were compared within the respective back-labelled groups as well as between both groups at both stages (p5 and p10). These results were also compared with morphological data from similar but non-back-labelled adult cells obtained previously in this laboratory (Larkman and Mason, 1990; Larkman, 1991a).

6.3 Results :

As in the slice preparations from adult rat visual cortex, all cells back-labelled via the tracer injection into the ipsilateral SC were exclusively located in layer 5 of the visual cortex and formed an uninterrupted narrow band of neurons (see Figure 6.2B) that extended from medial to lateral throughout the whole cortical visual areas 17, 18a and 18b and extended further medially as well as further laterally beyond their borders.

In a second set of experiments neurons in the visual cortex were back-labelled after tracer injection into area 17 of the contralateral hemisphere. Back-labelled CLH-neurons were distributed across all layers except layer 1 in preparations of the homotopic cortical area 17 (see Figure 6.2A), a finding that is similar to the observations made in preparations of the adult rodent visual cortex (see **Chapter 4**).

6.3.1 General morphological observations :

Even in the youngest animals in this study, prelabelled at **p3** and studied at **p5**, rhodamine beads could be seen in a large number of neurons in layer 5 of the coronal

Figure **6.2:** Coronal slices from the developing visual cortex which contained pyramidal neurons back-labelled by injection of fluorescent microspheres into either A) the **contralateral hemisphere** or B) the **superior colliculus** (as seen in fixed slices).

Plates show the equivalent medial part of area 17 with the medial border between area 17 and 18b to the right side. Cortical laminae are approximately indicated on the right side of plate A.

A) Slices with back-labelled CLH-neurons. A high number of labelled neurons is visible in the developing layers 2/3 and in layer 5. Note the high number of backlabelled cells which was always present in lower part of the developing superficial layers 2/3. Layer 4 and the upper portion of layer 5 can be recognized as a zone containing only a few back-labelled neurons.

B) Slices with back-labelled SC-neurons. Note that back-labelled neurons were exclusively located in layer 5 with a higher number of neurons found in the upper portion of the layer.

Scale bar in b =100μm and applies to both plates.

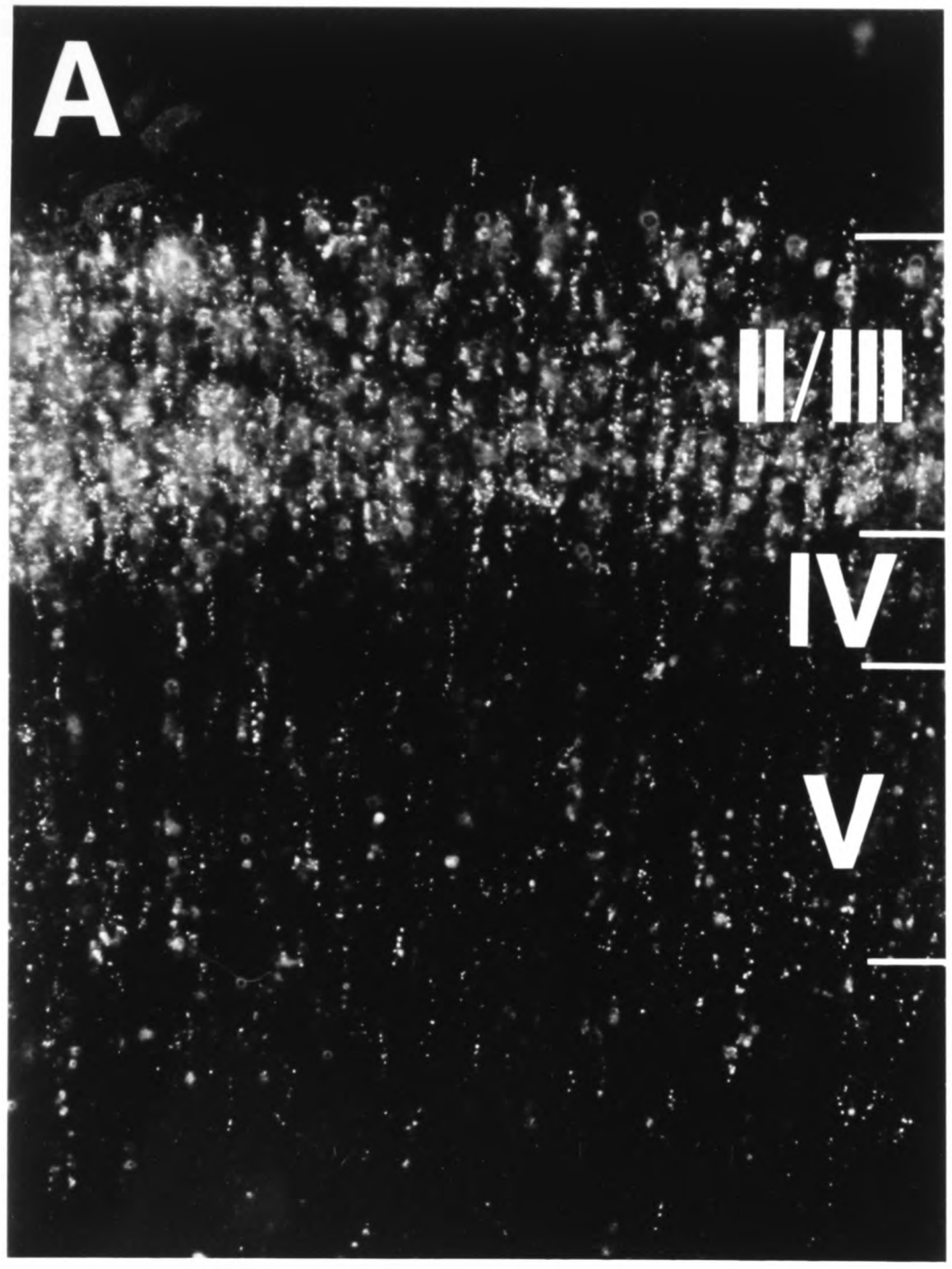
A
II/III
IV
V

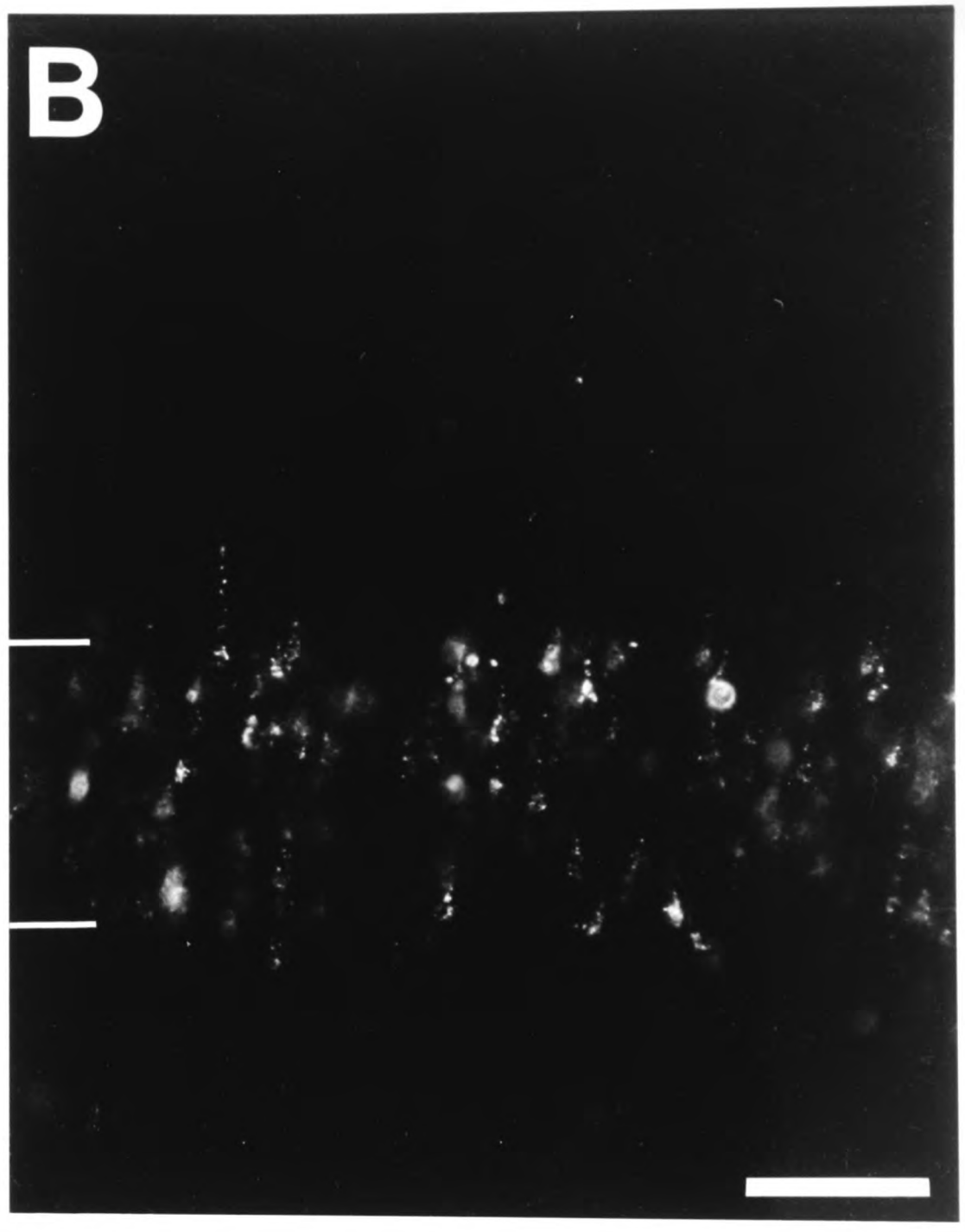
B

Figure **6.3:** General features of pyramidal neurons from layer 5 of the developing visual cortex as seen in LY filled neurons after photoconversion of injected cells in fixed slices. Plates illustrate also the quality of the LY-photoconversion product.

A) High power magnification of a neuronal soma with a prominent apical dendrite that is gradually emerging at the upper pole of the soma; Several oblique dendrites can be seen originating from the apical dendrite and primary basal dendrites can be seen arising from the cell body. The main axon is indicated by a black arrow.
   Scale bar in D equals 20µm

B) High power view of a branch point of a bifurcating apical dendrite. The spine density is relatively low ; single spines are indicated by hollow arrows.
   Scale bar in D equals 10µm.

C) High power view of a main axon. Axonal varicosities can be seen at points were axon collaterals are given off. Individual varicosities are indicated by arrowheads.
   Scale bar in D equals 20µm

D) High power view of a terminal ending of a dendrite, which ends with a growth cone like structure.
   Scale bar equals 10µm

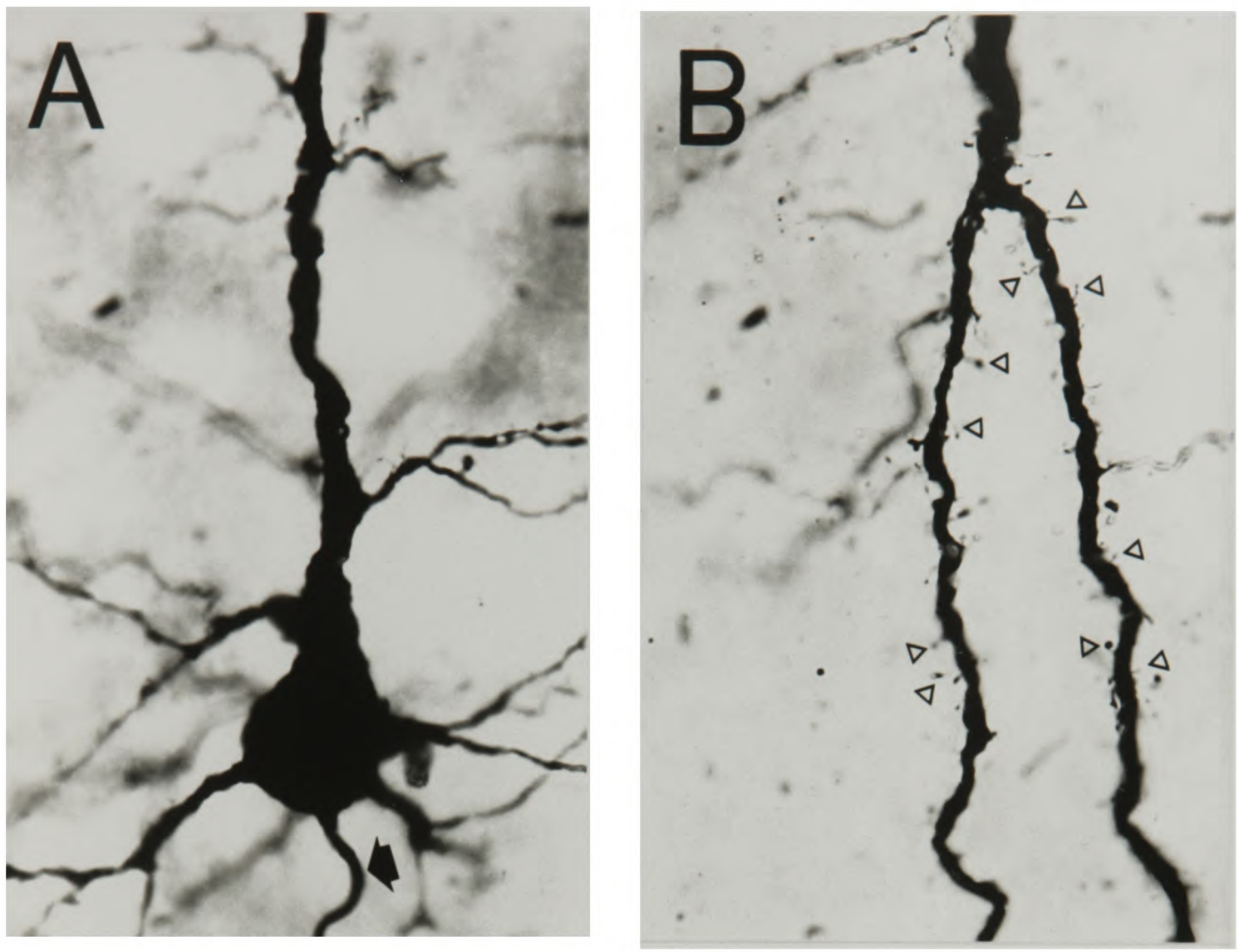
A
B
C
D

Figure **6.4:** General features of layer 5 pyramidal projection neurons injected in fixed slices from the developing visual cortex in early corticogenesis (at **p5**).

A) Group of four pyramidal neurons back-labelled from the ipsilateral SC after intracellular injection with LY. Note the prominent apical dendrite ascending towards the pial surface and terminating in form of a tuft in layer 1. The asteriks markes a neuron that is also shown in figure 6.5.

B) Group of three pyramidal neurons back-labelled from the CLH after intracellular injection with LY. Note that these neurons have only thin apical dendrites ascending towards the pial surface which taper on their way and terminates without forming an elaborate arborization

Scale bar in B= 80µm and applies also to A.

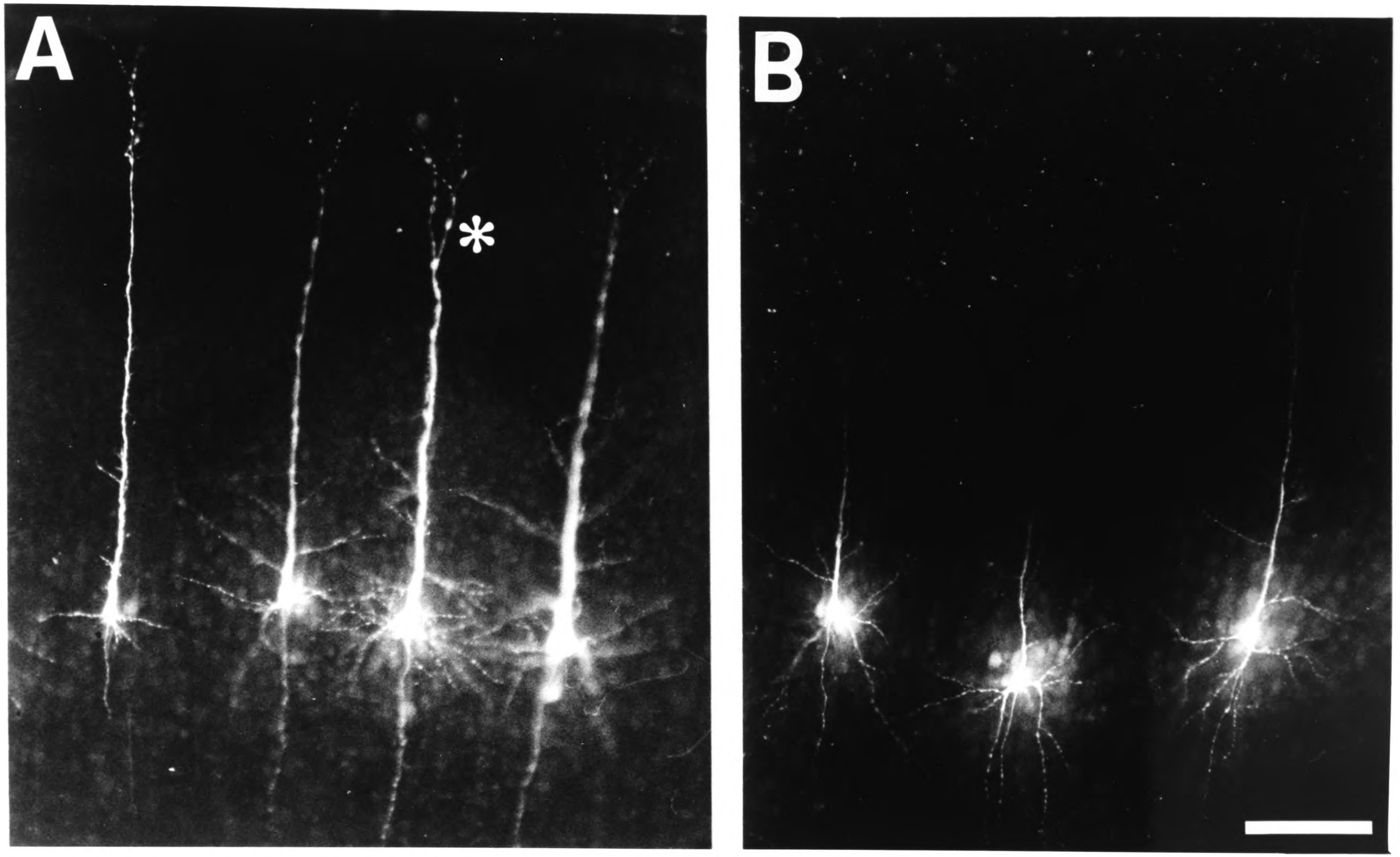
A
*
B

Figure **6.5:** Photo-montage of a SC-projecting neuron from the developing visual cortex (at **p5**) after intracellular LY injection in fixed slices.

This neuron was back-labelled from the ipsilateral SC after tracer injection at p3. Note the prominent apical dendrite ascending towards the pial surface. It gives off several oblique stem dendrites, most of which are located proximal to the soma, before bifurcating and forming a terminal tuft in layer 1. Most basal and oblique dendrites show varicosities but only a few spines at this stage in cortical development. The axon is indicated by a white arrow.

Scale bar = 50μm.

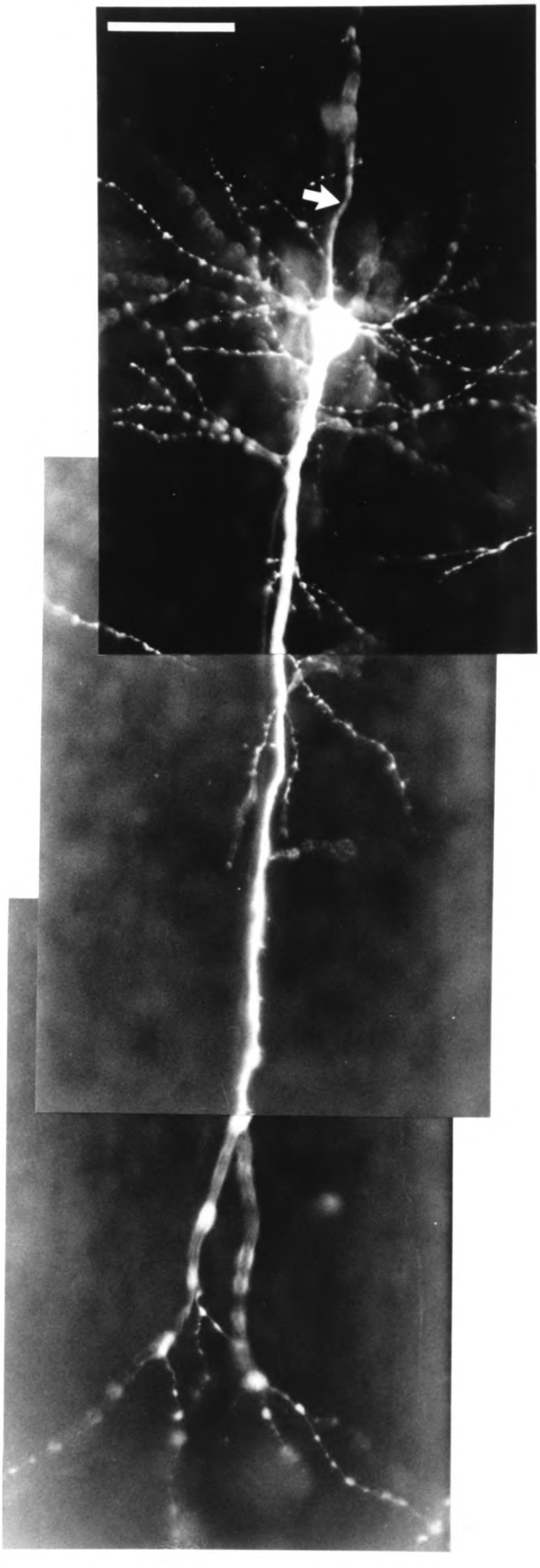

slice (see Figure 6.2), although the number of retrogradely transported beads found within each single cell was lower than in cells from adult animals treated in the same fashion .

All the back-labelled layer 5 pyramidal neurons that were injected with LY could readily be categorized and assigned to one of two morphologically distinct groups.In the first group all the cells were characterized by a morphology, which was similar to the type of cells with a thick apical dendrite reaching layer 1 (as described in **chapter 4**). The cells of the second group could be characterized as belonging to the type with a slender apical dendrite (also described in **chapter 4**). In contrast to neurons from the first group, their apical dendrite ascended towards the upper border of the cortical plate (which at that postnatal stage is about to transform into layers 2/3) but tapered gradually without forming a dendritic tuft in layer 1.

In general, all neurons had several (between 3 and 7) basal dendrites covered with dendritic varicosities (see Figure 6.5) and only a few spines (see Figure 6.3B). All the dendrites from both the basal as well as the oblique trees showed a dichotomic branching pattern (Figure 6.3B). No case of a trichotomic branchpoint was found. Most of the dendrites and also some of the axonal branches showed growth cone like structures (see Figure 6.3.D) at their terminal endings. The main axon showed often swellings at branch points where axon collaterals arose (Figure 6.3C).

6.3.2 Neurons back-labelled from the superior colliculus :

In all groups investigated (p5, p10 and adult) retrogradely labelled corticotectal cells were confined to a narrow band extending from medial to lateral throughout layer

Figure **6.6:** Four plates illustrating the somata of two representative corticotectally projecting neurons from the developing visual cortex as seen after LY injection in fixed slices prepared at **p5**.

A) Soma of the same neuron that is completely reconstructed in figure 6.5. Note the thick apical dendrite, which does not taper visibly as it ascends. The small white arrow points to the main axon.

B) Corresponding photograph to A, after the filter block was changed to the wavelength appropriate for rhodamine excitation. Fluorescent microspheres are clearly visible and extend also into the apical dendrite.

C) Soma of another SC-projecting neuron from the same preparation. Note the thick proximal part of the apical dendrite, which geradually emanated from the upper pole of the soma. The white arrowpoints to the main axon.

D) Corresponding photograph to C, after the filter block was changed to the wavelength appropriate for rhodamine excitation. Microspheres are clearly seen and extend into the apical dendrite.

Scale bar in D= 50μm and applies also to A, B, and C.

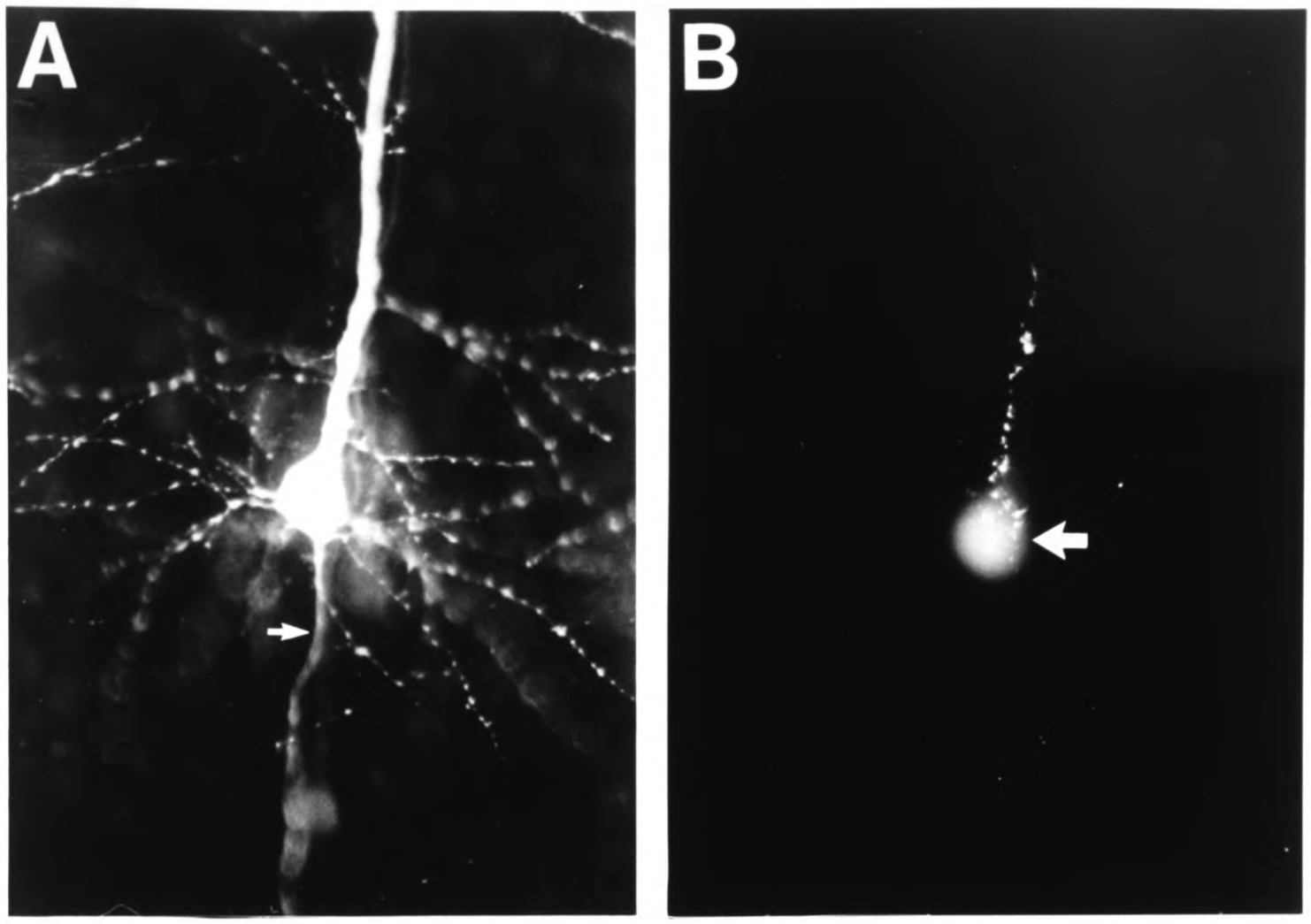
A
B
C
D

Figure **6.7**: Representative **p5** SC-projecting neurons from layer 5 of the rat visual cortex studied in a fixed slice preparation. Composition of several camera lucida drawings.

SC-neurons were drawn after intracellular injection and photoconvertion of LY. All SC-cell show an apical tuft that arborizes in layer 1. Oblique branches are given off by the apical dendrite and arise predominantly close to the soma. Some of the proximal oblique dendrites are as long as some of the basal dendrites with whom they form a "sampling unit" for synaptic input (see text).

Solid triangles point to the main axon; Hollow triangles point to axon collaterals.

Scale in E = 100μm and applies to all drawings.

P5 neurons backlabelled from the SC

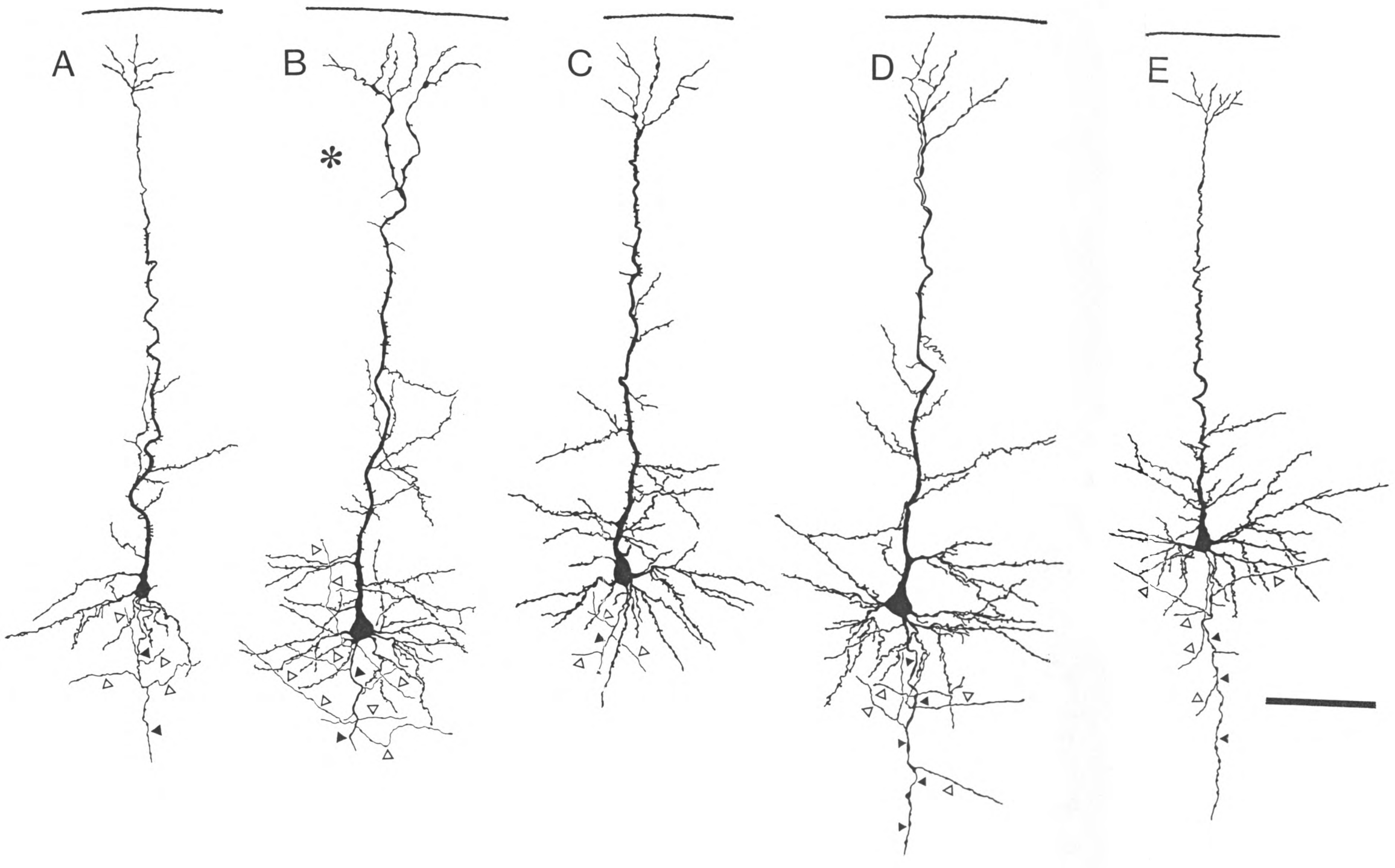

Figure **6.8:** Somata of two representative corticotectally projecting neurons from the developing visual cortex as seen after LY injection at **p10**.

A) Soma of a typical SC-neuron. Note the thick proximal part of the apical dendrite, which geradually emanats from the soma. The white arrow points to the main axon.

B) Corresponding photograph to A, after the filter block was changed to the wavelength appropriate for rhodamine excitation. The big white arrow points to the soma of the filled neuron seen in A. Some microspheres are clearly visible as is the somatic shape of the neuron.

C) Soma of another SC-projecting neuron from the same preparation. Note the thick apical dendrite, which does not taper visibly on its way towards the pial surface. The small white arrow points to the main axon.

D) Corresponding photograph to C, after the filter block was changed to be appropriate for rhodamine excitation. The big white arrow points to the soma of the filled neuron shown in C. Fluorescent microspheres are visible in the soma and also extend into the apical dendrite.

Scale bar in D= 50μm and applies also to A, B, and C.

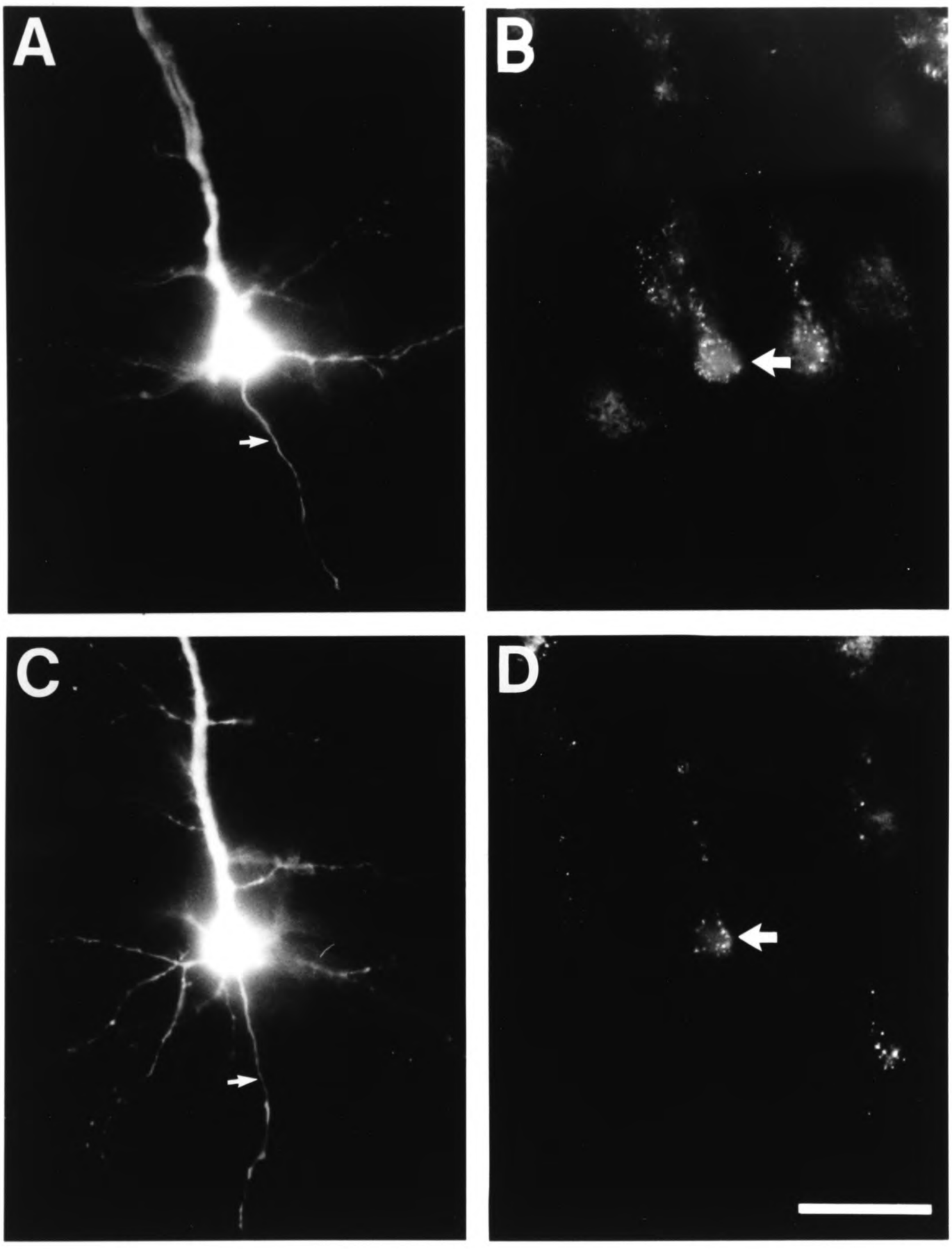
A
B
C
D

Figure **6.9**: SC-projecting cells from layer 5 of the rat visual cortex studied in a fixed slice preparation prepared at **p10**. Composition of several camera lucida drawings.

SC-neurons were drawn after intracellular injection and photoconvertion of LY. All SC-cells show an apical tuft that formed a terminal arborization in layer 1. Most of the stem segments of oblique dendrites, given off by the apical dendrite, arise proximal to the soma. The neuronal appearance is more mature compared to the p5 SC-neurons seen in figure 6.7 as can also be seen in the morphological data obtained from these cells (Table 6.1 and 6.2), Note that the dendritic spine density is considerably higher in these p10 SC-neurons than in SC-neurons from the p5 sample.

Solid triangles point to the main axon; Hollow triangles point to axon collaterals.

Scale in E = 100μm and applies to all drawings.

P10 neurons backlabelled from the SC

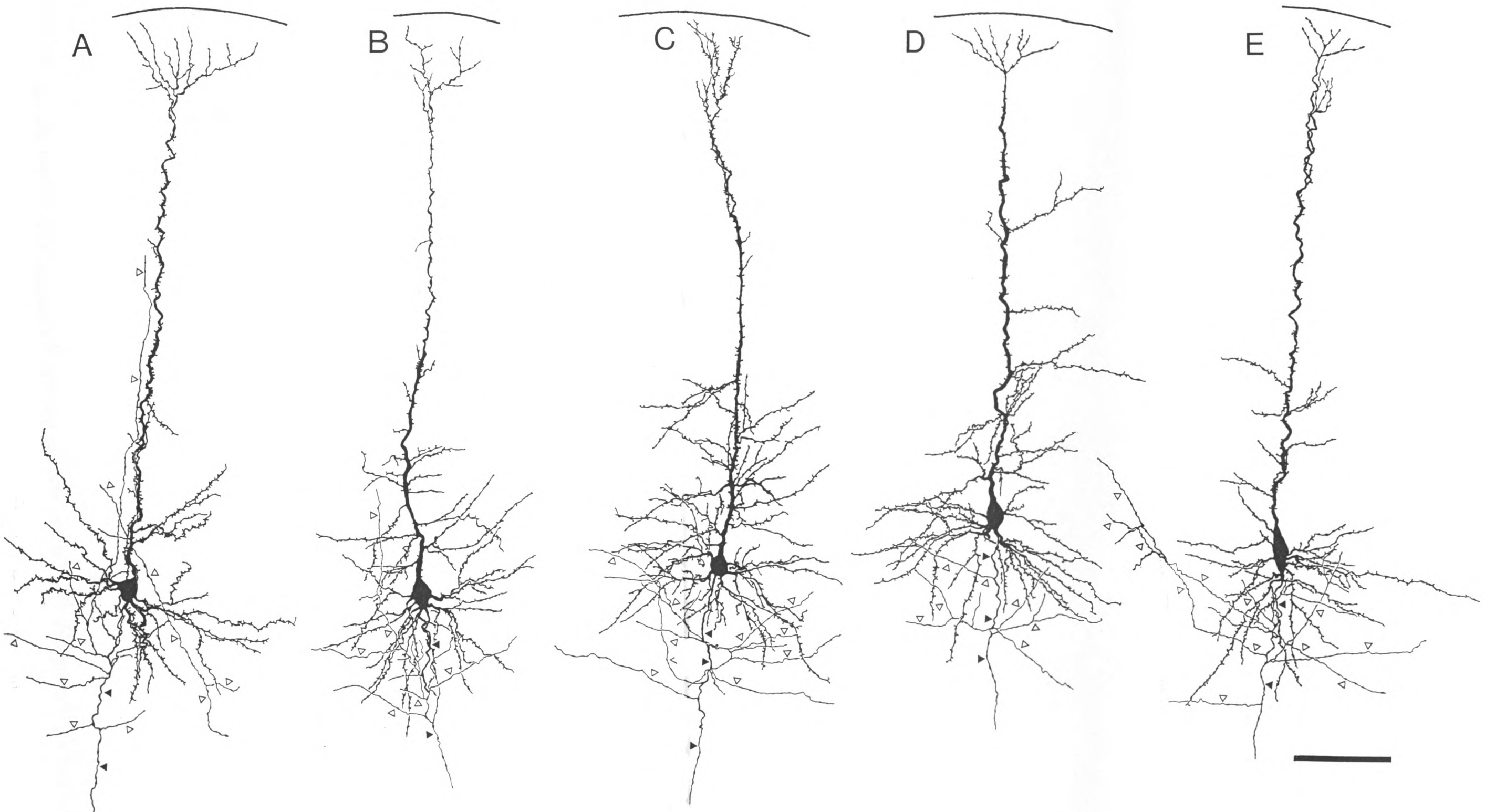

5 of the visual cortex (see Figure 6.2B) as delineated from a set of Nissl stained coronal sections in control animals (not shown). In none of the animals (at p5 or p10) there was a population of corticotectally projecting cells located in any other layer of the cortex. Moreover, all corticotectal neurons subsequently filled with LY formed a remarkably homogenous group with similar basic morphological features (see Figure 6.4A, 6.7 for **p5** and 6.9 for **p10**) common for all age groups studied. Neurons of this type were characterized by the following features: a soma that was substantially higher than wide (21.1±3.5μm height versus 15.57±3.6μm width at **p5** [see Figure 6.6] and 23.4±3.1μm height versus 15.4±3.6μm width at **p10** [see Figure 6.8], for comparison see table 6.1) and by the appearance of a thick apical dendrite which emanated as an elongation of the upper part of the soma.

At **p5**, cells of the corticotectal group had some four (4.4±0.8) primary basal dendrites, which were relatively short and showed many branching points. If counted at **p10** the number of primary basal denrites had increased significantly to 6.5±1.8 (see table 6.1). Single basal dendrites showed many bifurcations and all basal dendrites together gave rise to a large total of terminal tips 20.6±6.1 at **p5** compared to 25.7±5.2 at **p10**. This increase was insignificant. The thick apical dendrite ascended straight towards the pial surface and gave rise to several oblique branches (11.6±3.6 at **p5** and 11.0±5.8 at **p10**) , which were mainly located proximally in layers 5 and 4 with only a few more in the developing supragranular layers (see Figure 6.5).

Each of the primary oblique dendrites had only very few, if any, branching points and therefore gave rise to only a few tips. All oblique dendrites of a cell had an average total of 18.2±6.5 tips at **p5** versus 18.2±10.9 tips at **p10**,thus indicating that there was no noticeable increase in the number of branch points between the two age groups. The apical dendrite tapered only a little on its way before it formed a terminal

tuft in the upper part of the developing layers 2/3, which always extended into layer 1 (see Figure 6.5). The tuft was extended over a wider area and had more branches in animals of the **p10** group and adult animals compared to the SC-cells of the **p5** group. The total number of all tips from basal plus oblique dendrites increased between **p5** and **p10** from 38.8±10.26 to 43.8±14.39, although this change was insignificant.

The terminal tuft appeared well developed in both age groups but it seemed to become more elaborate between **p5** and **p10**. This is reflected in the increase in the number of tips counted at **p5** (8.0±2.1) compared to those counted at **p10** (10.3±1.4) although this change was only marginally significant (see Table 6.1).

6.3.3 Neurons back-labelled from the contralateral hemisphere :

In the young animals (**p5** and **p10**), just as in the adults (see **Chapter 4**), interhemispherically projecting cells could be found in all layers of the visual cortex except layer 1 (see Figure 6.2A). The density of prelabelled cells was highest in the developing supragranular layers 2/3 and in layer 5, with only a few cells to be found in layers 4 and 6. Every filled prelabelled cell could unequivocally be assigned to a group in which no cells had a thick apical dendrite arborizing in layer 1 (see Figure 6.4B and 6.11 for **p5**, 6.13 for **p10**). Just one injected cell backlabelled from the other hemisphere had an apical dendrite that reached layer 1, but this dendrite was thin and formed only three thin terminal branches there. Surprisingly this cell was the one of the p 10 CLH-cell group, that also had the highest number of basal dendritic tips as well as the highest number of oblique dendrites and oblique tips and the highest number of total

Figure **6.10:** Somata of four representative back-labelled interhemispherically projecting neurons from the developing rat visual cortex at p5 as seen after LY injection into CLH-neurons in fixed slices. Several neurons are shown from this preparation to illustrate the heterogeneity of CLH-neurons. Small white arrows point to the main axon (*left side plates*); Big, white arrows point to the corresponding somata (*right side plates*) after the filter was changed to the wavelength appropriate for rhodamine excitation.

A) Vertically elongated, ovoidal soma of a CLH-neuron. Note that the apical dendrite emerges almost abruptly from the upper pole of the soma.

B) Corresponding photograph to A. Fluorescent microspheres are visible within the soma.

C) Triangular shaped soma of another neuron CLH-projecting neuron from the same preparation. Note the thick proximal part of the apical dendrite, which geradually emanated from the soma. Basal dendrites extend predominantly laterallly.

D) Corresponding photograph to C. Fluorescent microspheres are clearly visible and they also extend into the apical dendrite.

E) Soma of another CLH-neuron with few, short basal dendrites. Note the apical dendrite which tapers close to the soma.

F) Corresponding photograph to E.

G) Circular shaped soma of an CLH-neuron with a curved apical dendrite.

F) Corresponding photograph to E.

Scale bar in H= 50μm and applies also to all other plates.

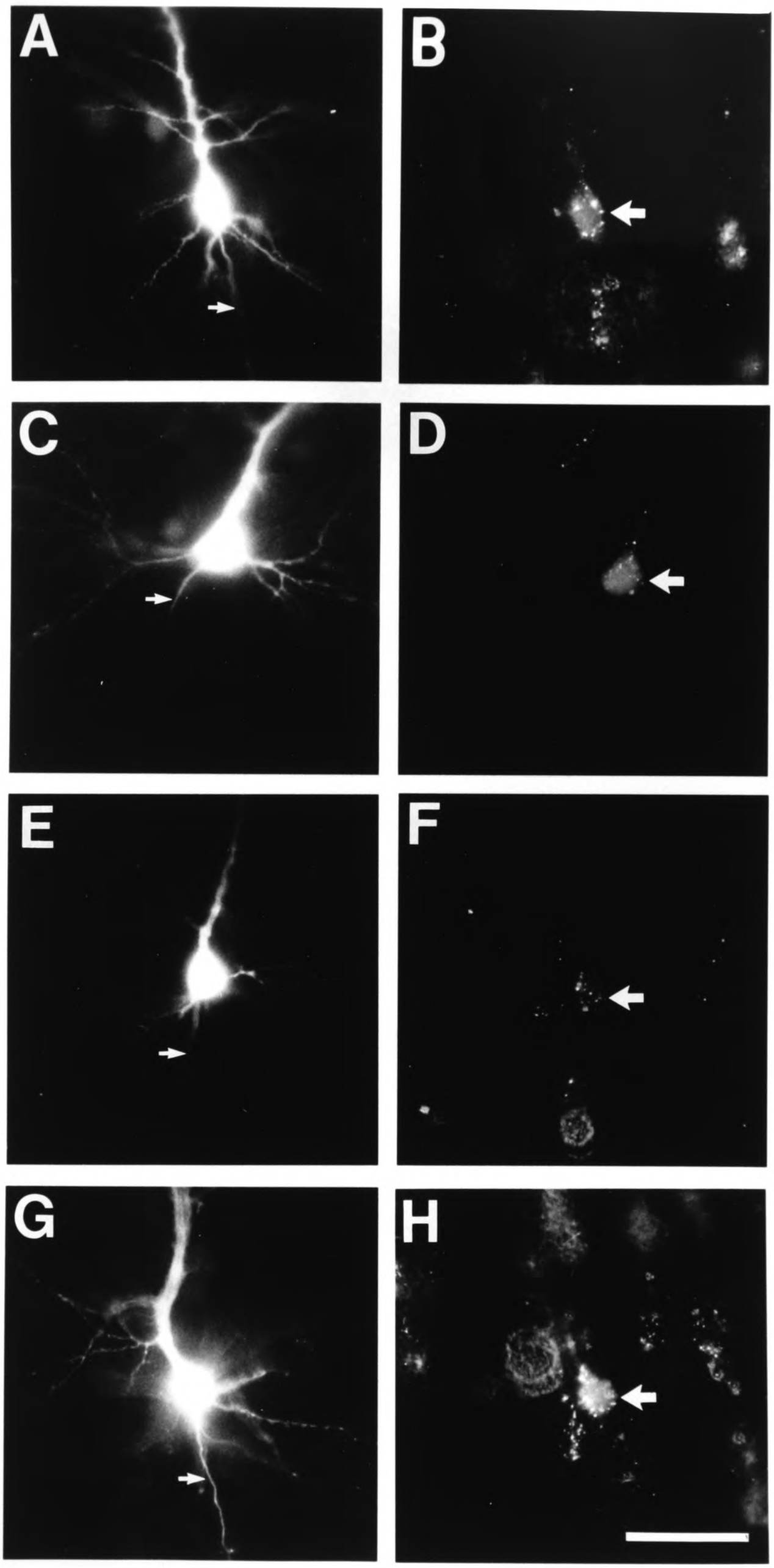
A
B
C
D
E
F
G
H

Figure **6.11**: CLH-projecting cells from layer 5 of the immature rat visual cortex. Composition of several camera lucida drawings of representative back-labelled p5 neurons.

CLH-neurons were drawn after intracellular injection and photoconvertion of LY. All CLH-cells show a thin ascending apical dendrite which terminates without forming a terminal tuft below the pial surface without reaching layer 1. A stem segments of oblique dendrites are given off by the apical dendrite.

Solid triangles point to the main axon; Hollow triangles point to axon collaterals.

Scale in E = 100µm and applies to all drawings.

P5 neurons backlabelled from the CLH

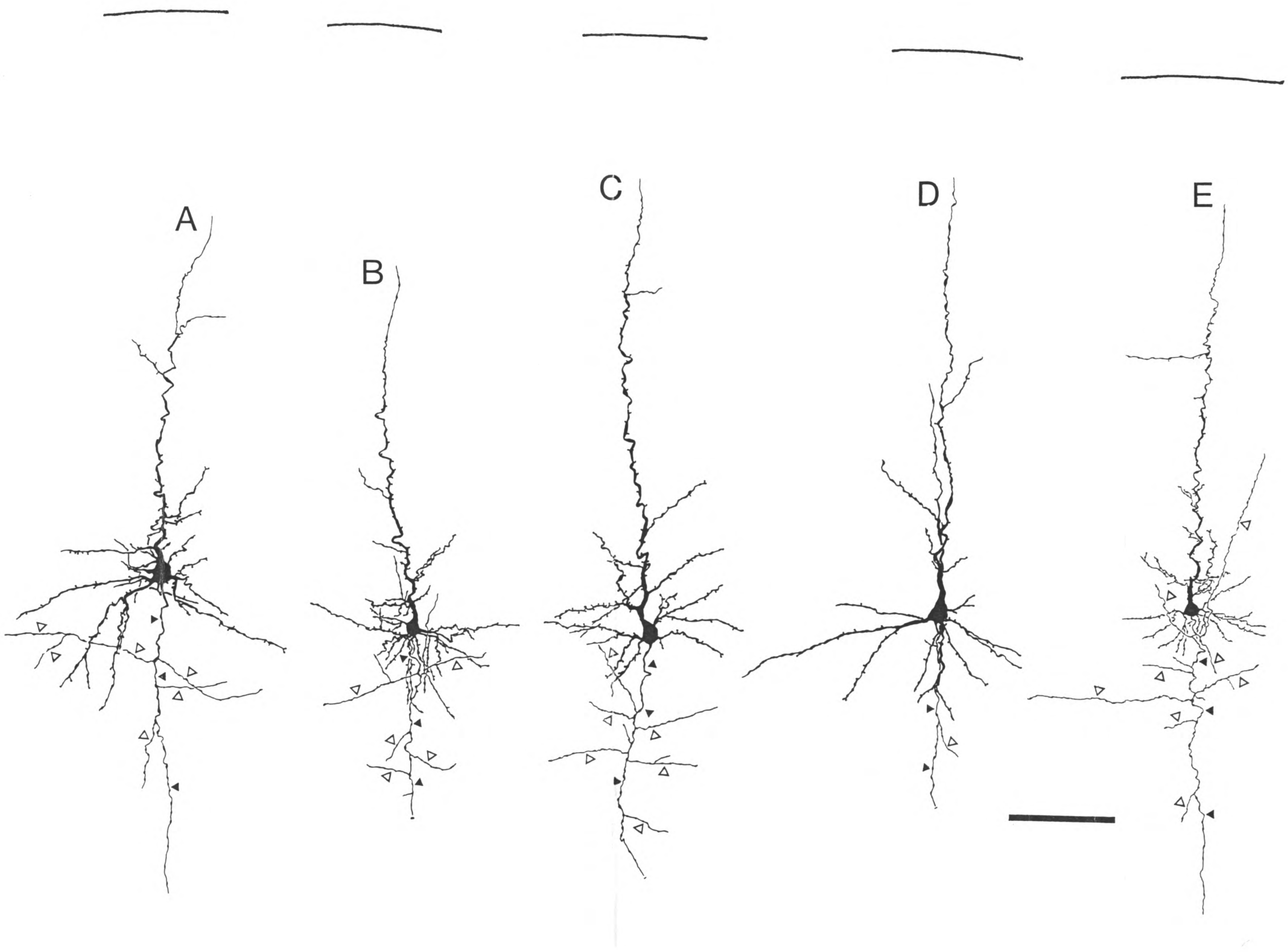

Figure **6.12:** Somata of four representative back-labelled inter-hemispherically projecting neurons from the developing rat visual cortex as seen after LY injection at **p10**. Several neurons are shown to illustrate the heterogeneity of somata of CLH-neurons. Small white arrows point (*inleft side plates*) to the main axon; Big, white arrows (*in right side plates*) point to the corresponding somata after the filter was changed to be appropriate for rhodamine excitation.

A) Soma of a CLH-neuron. Note that the apical proximal part of the apical dendrite is thick and emerges gradually from the upper pole of the soma. It then tapers considerably at a point where it gives of oblique branches and curves.

B) Corresponding photograph to A. Microspheres are clearly visible within the soma and initial segment of the apical dendrite.

C) Oviodal shaped soma of another CLH-projecting neuron which shows only a few stem segments of basal dendrites. Note the apical dendrite, which abruptly forms at the pial pole of the soma.

D) Corresponding photograph to C. Microspheres are clearly visible in the soma and also in the apical dendrite.

E) Soma of another CLH-neuron with basal dendrites extending mainly laterally. Note the apical dendrite which forms abruptly to starts of thick and then tapers considerably.

F) Corresponding photograph to E showing the back-labelling.

G) Another ovoidal soma of an CLH-neuron with a few basal stem segments only. Note that the axon arises from a protrusion, which also forms a basal dendritic stem segment.

H) Corresponding photograph to G showing the back-labelling.

Scale bar in H= 50µm and applies also to all other plates.

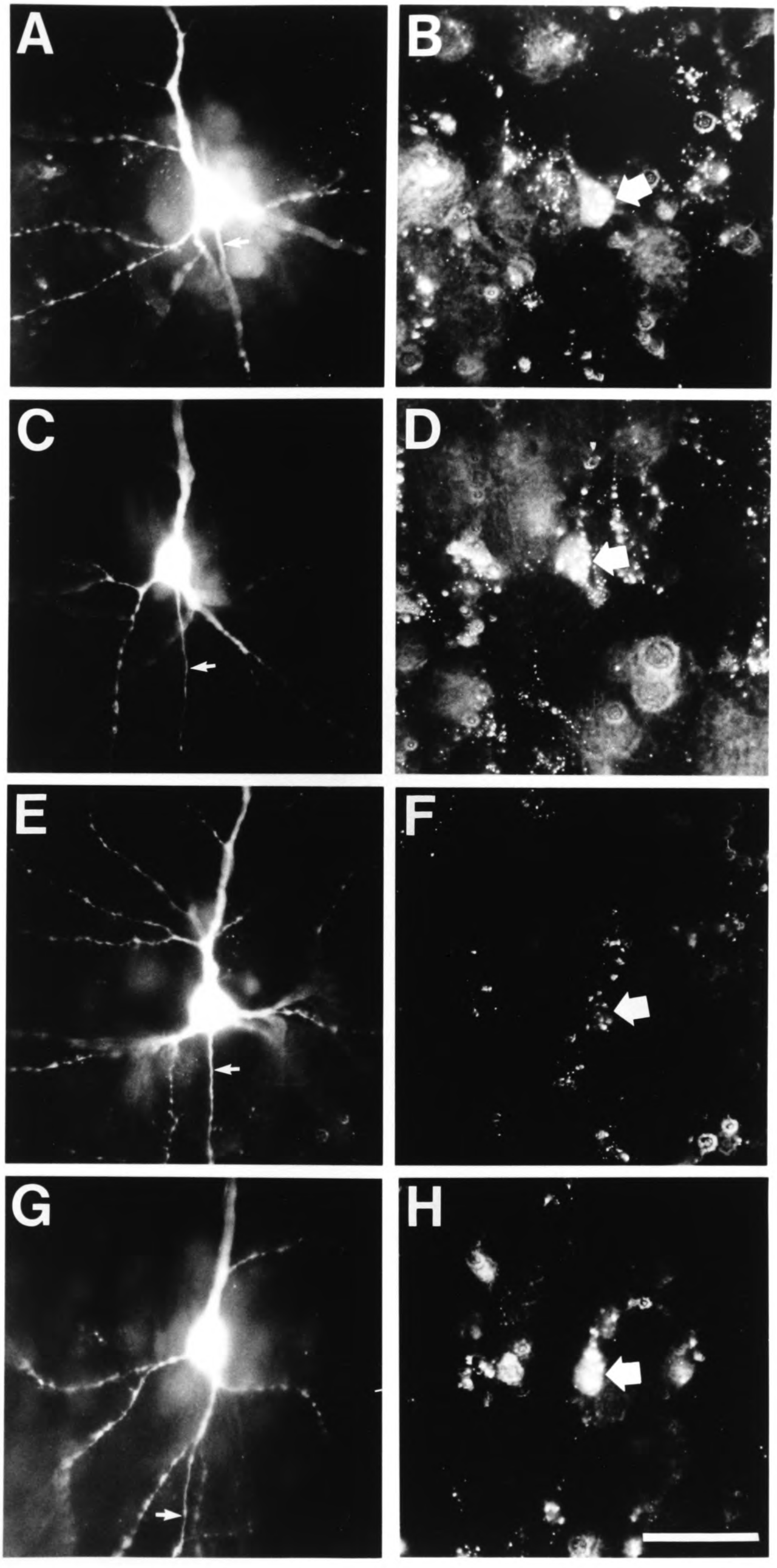
A
B
C
D
E
F
G
H

Figure **6.13**: CLH-projecting cells from layer 5 of the rat visual cortex studied in a fixed slice preparation. Composition of several camera lucida drawings of representative neurons from p10.

Cells were drawn after intracellular injection and photoconvertion of LY. All CLH-cells show a thin apical dendrite which terminates below layer 1 as it ascends towards the pial surface. A few oblique branches, which arise mostly close to the soma, are given off by the apical dendrite. The appearance of these neurons is more mature compared with the p5 CLH-neurons, as can also be seen in data listed in Table 6.1 and 6.2.

Solid triangles point to the main axon; Hollow triangles point to axon collaterals.

Scale in E = 100μm and applies to all drawings.

P10 neurons backlabelled from the CLH

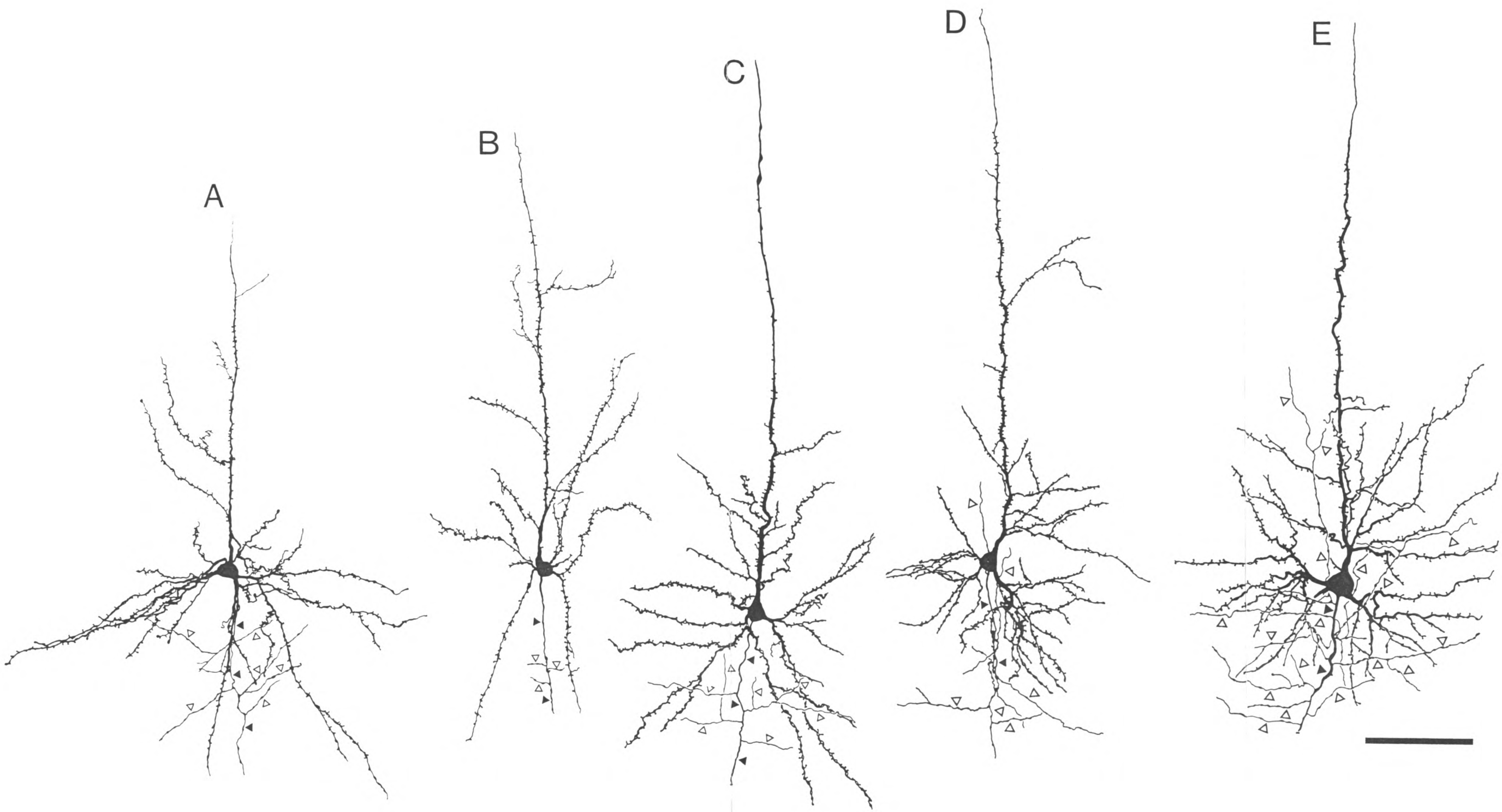

tips.

The cell somata of the CLH-projecting group were generally smaller than the cells categorized in the corticotectal group, although there was a considerable overlap in soma size (see figures 6.10 for **p5** and 6.12 for **p10**; see also Table 6.1). In addition the following morphological features could be observed in back-labelled interhemispheric neurons: cells had few primary basal dendrites (4.4±0.8 at **p5** and 4.0±0.8 at **p10**) with only a few dendritic branches, which seemed in most cases to extent over a longer distance than those of corticotectal projection neurons. The total number of tips made by all the basal dendrites increased slightly but significantly from 12.8±2.2 at **p5** to 16.5±4.1 at **p10** but was at both dates significantly lower than in SC-projecting neurons ($p< 0.05$ at **p5**, $p<0.01$ at **p10**).

Neurons of the CLH-projecting group had the general appearance of the slender type (see Figures 6.11 and 6.13), with a thin apical dendrite that tapered on its way towards the pial surface. This apical dendrite could generally not be followed visibly into layer 1 (only one single exception), but ended somewhere below in the superficial layers 2/3 without forming a visible tuft.

Interhemispheric projecting cells had significantly ($p<0.05$) fewer primary oblique dendrites than corticotectal neurons (7.0±1.4 at **p5** and 7.2±2.1 at **p10**) and none of the primary oblique dendrites branched extensively, thus having only 9.2±2.8 tips at **p5** and 9.7±2.3 tips at **p10**. Both measures were significantly smaller than those from SC-neurons ($p<0.05$ at **p5** and **p10**). The total number of tips formed by all basal dendrites as well as all oblique dendrites increased only insignificantly from p5 to p10, possibly because of the time window being too small to detect any developmental

Figure **6.14**: Four plates to illustrate the obvious difference in soma-dendritic morphology of layer 5 projection neurons from the visual cortex at **p5**. Two neurons back-labelled via injection of tracer into either the CLH (A and B) or into the SC (C and D) were intracellularly injected with LY and subsequently photoconverted in a fixed slice preparation.

Neurons from each group differ already at this postnatal stage significantly in some of their morphological features. (see also data in Tables 6.1and 6.2). The most obvious difference is in the shape of the soma and the way each soma gives rise to its apical dendrite. Interhemispheric neurons have a small cell body and a slender apical dendrite which arises more abruptly from the upper pole of the cell body, whereas corticotectally projecting neurons (C, D) have a thick apical dendrite which emerges more gradually from the cell body.

Scale bar in D = 25μm and applies to all plates.

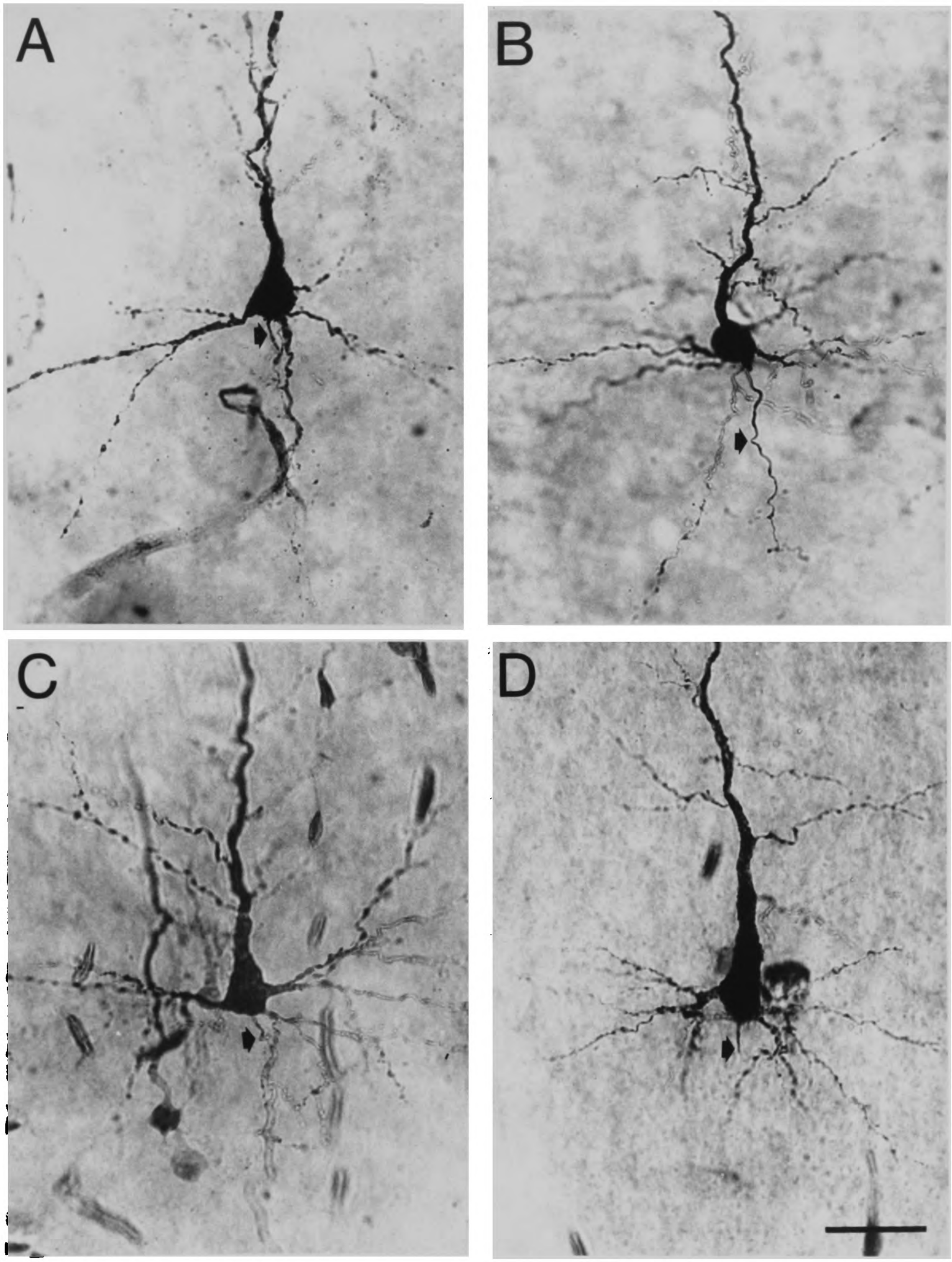
A
B
C
D

Figure **6.15**: Four plates to illustrate the pronounced difference in soma-dendritic morphology of layer 5 projection neurons from the visual cortex at **p10**. Two neurons back-labelled via injection of tracer into either the CLH (A and B) or into the SC (C and D) are shown which were intracellularly injected with LY which was subsequently photoconverted.

Neurons from the two groups differed significantly in some of their morphological features. (see data in Tables 6.1and 6.2). The most obvious difference was in the size and shape of the soma and the way each soma gave rise to its apical dendrite. Some of these features can be seen on the plates shown: It can clearly be seen that interhemispheric neurons have a small cell body and a slender apical dendrite. Corticotectally projecting neurons (C, D) have a thick apical dendrite which emerges more gradually from the cell body. More stem segments of basal dendrites can be seen in these SC-neurons than in the CLH-neurons and their basal dendrites branch more often closely to the soma.

Scale bar in D = 25μm and applies to all plates. The black arrow points at the axon in each plate.

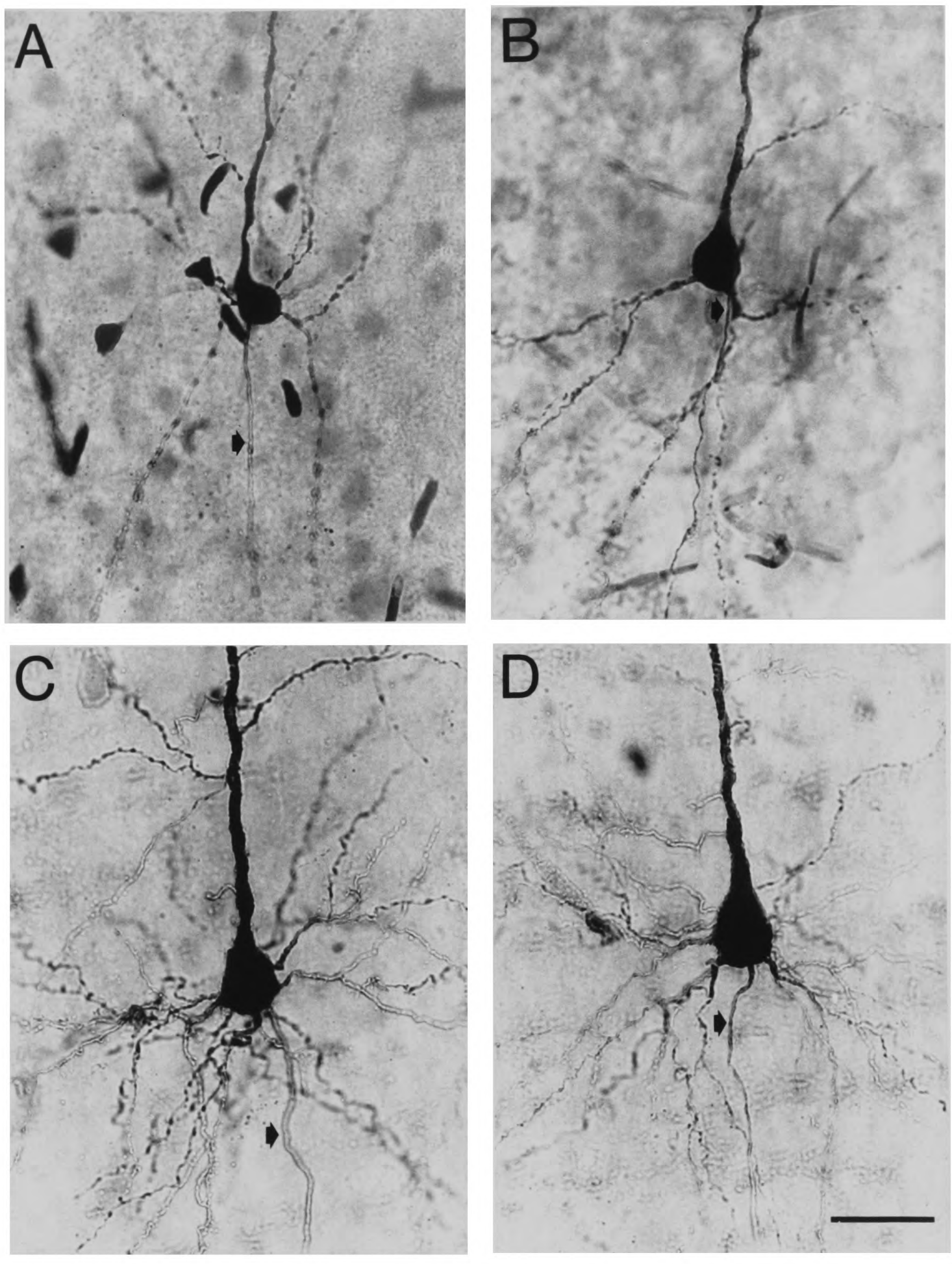
A
B
C
D

Table 6.1 Morphological data of back-labelled projection neurons from the immature visual cortex: Neuronal Somata

p5

	SC-CELLS	CLH-CELLS
no. of cells	5	5
Soma height/ μm	21.1 ± 3.5 □	15.0 ± 2.5
Soma width/ μm	15.6 ± 3.6 ▲	13.6 ± 1.8
Ratio h/w	1.38 ± 0.12 +	1.11 ± 0.07

p10

	SC-CELLS	CLH-CELLS
no. of cells	6	7
Soma height/ μm	23.4 ± 3.1 □	17.9 ± 3.5
Soma width/ μm	15.4 ± 1.3 ▲	18.0 ± 3.7
Ratio h/w	1.50 ± 0.24 +	1.01 ± 0.17

a

	Tufted Bursters	Untufted regular spikers
no. of cells	11	10
Soma height/ μm	24.5 ± 4.9 □	19.8 ± 3.0
Soma width/ μm	18.1 ± 3.3	19.3 ± 3.9
Ratio h/w	1.36 ± 0.19 □	1.05 ± 0.20

+= $p \leq 0.01$; □=$p \leq 0.05$; ▲=$p \leq 0.1$

Table 6.2 Morphological data of back-labelled projection neurons from the immature visual cortex: Dendritic structure

p5

	SC-CELLS	CLH-CELLS
n (basal stem segments)	4.6 ± 0.5	4.4 ± 0.8
n (basal tips)	20.6 ± 6.1 □	12.8 ± 2.2
n (oblique stem segments)	11.6 ± 3.6 □	7.0 ± 1.4
n (oblique tips)	18.2 ± 6.5 □	9.2 ± 2.8
n (total tips)	38.8 ± 10.3 □	22.0 ± 4.5
n (tuft tips)	8.0 ± 2.1	-

p10

	SC-CELLS	CLH-CELLS
n (basal stem segments)	6.5 ± 1.8 □	4.0 ± 0.8
n (basal tips)	25.7 ± 5.2 +	16.5 ± 4.1
n (oblique stem segments)	12.7 ± 4.9 □	7.2 ± 2.1
n (oblique tips)	19.8 ± 9.5 □	9.7 ± 2.3
n (total tips)	47.8 ± 12.4 +	26.2 ± 6.0
n (tuft tips)	10.3 ± 1.5	-

a

	Tufted Bursters	Untufted Regular Spikers
n (basal stem segments)	5.8 ± 1.8 □	4.4 ± 0.7
n (basal tips)	34.6 ± 5.7 □	25.8 ± 5.4
n (oblique stem segments)	12.0 ± 2.0 ▲	8.9 ± 4.9
n (oblique tips)	24.6 ± 3.1 □	13.7 ± 7.0
n (total tips)	65.0 ± 6.8 □	40.8 ± 6.8

+= $p \leq 0.01$; □=$p \leq 0.05$; ▲=$p \leq 0.1$

changes and perhaps also because of the relatively small sample size. Nevertheless this measure was also significantly lower than in the corticotectal projecting neurons ($p<0.02$ at p5 and p10).

Two non-back-labelled pyramidal cells with inverted morphology (see drawing Figure 6.15) were also found in preparations containing the neurons backlabelled from the CLH. Both cells had an apical dendrite, which also arborized at its end, but its terminal tuft was located within the white matter because of its unusual orientation. A most interesting observation in these cases was that the axon descended towards the white matter, thus following the apical dendrite in its path, giving off many collaterals while still within the dendritic field of the same cell (see Figure 6.16).

6.3.4 Observations of other neurons from the same preparations :

In all the slices containing back-labelled cells I also deliberately filled many pyramidal cells layer 5 which were not prelabelled (about 90 cells compared to more than 120 back-labelled cells injected). In slices of SC- or CLH-injected animals I attempted to look at cells closely intermingled with the population of filled backlabelled cells. A few of the injected non-back-labelled cells showed a morphology of the thick type, which I was unable to distinguish from the SC-back-labelled population. On the other hand the appearance of most of the non-back-labelled cells fitted well into the group of cells of the slender type, lacking a thick apical dendrite. In two cases non-back-labelled 'twin apical trunk' cells were filled, with an ascending apical dendrite that bifurcated in layer 4. From there, both apical branches ran closely together towards the

Figure **6.16**: Inverted pyramidal cells from layer 5 of the developing rat visual cortex. Composition of camera lucida drawings of two representative **p10** neurons. Scale in B = 100μm and applies to both drawings. Solid triangles point to the main axon; Hollow triangles point to axon collaterals.

Both cells were drawn after intracellular injection and photoconvertion of LY in fixed tissue. Each inverted neuron shows clearly an apical tuft that arborizes in layer 6 in A and at the layer 6/white matter border in B. Oblique branches given off by the apical dendrite arise at several points along its path and are as long as some of the basal dendrites.Cell B was back-labelled from the CLH, whereas cell A was unlabelled in a SC-preparation.

P10 inverted pyramidal neurons

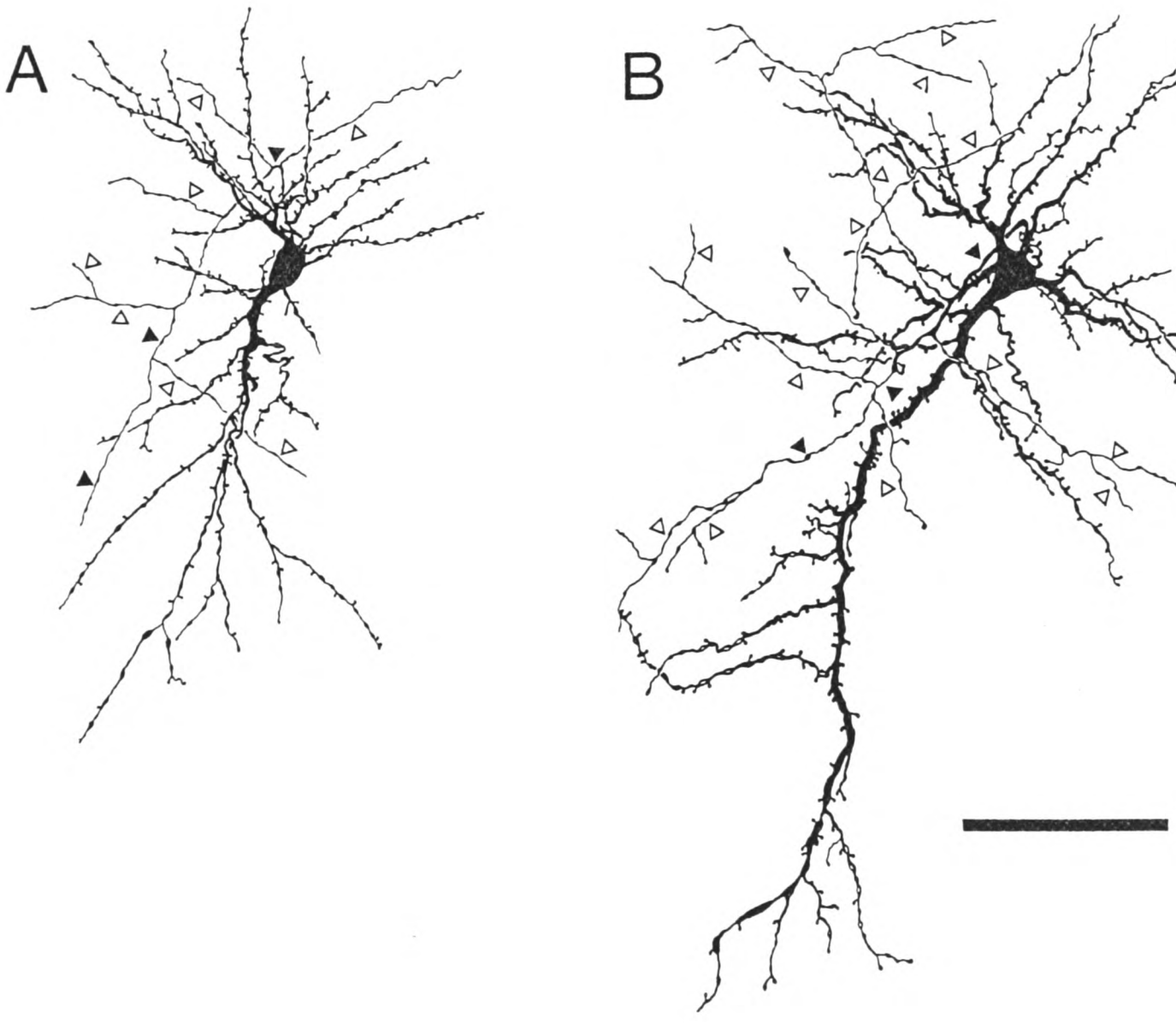

Figure **6.17**: Two plates to illustrate the soma-dendritic morphology of an inverted CLH-projection neuron from the visual cortex at **p10**.

The most obvious striking difference between this CLH-neuron and other normally oriented CLH-neurons is in the shape of the soma and the way this soma gives rise to its apical dendrite and axon. Interhemispheric neurons usually have a small cell body and a slender apical dendrite which arises more abruptly from the pial pole of the cell body, whereas this CLH-neuron has a thick apical dendrite which emerges more gradually from the cell body.

The axon (plate A) leaves at the lower pole of the neuron to turn then abruptly in its direction (see black arrow) to head towards the white matter following the course of the apical dendrite (see also Figuren 6.16). It also gives rise to several axon collaterals thus located within the range of apical dendritic branches. The axonal branch points can be recognized as varicosities in the main axon (indicated by arrowheads).

Scale bar in B = 10μm and applies to both plates.

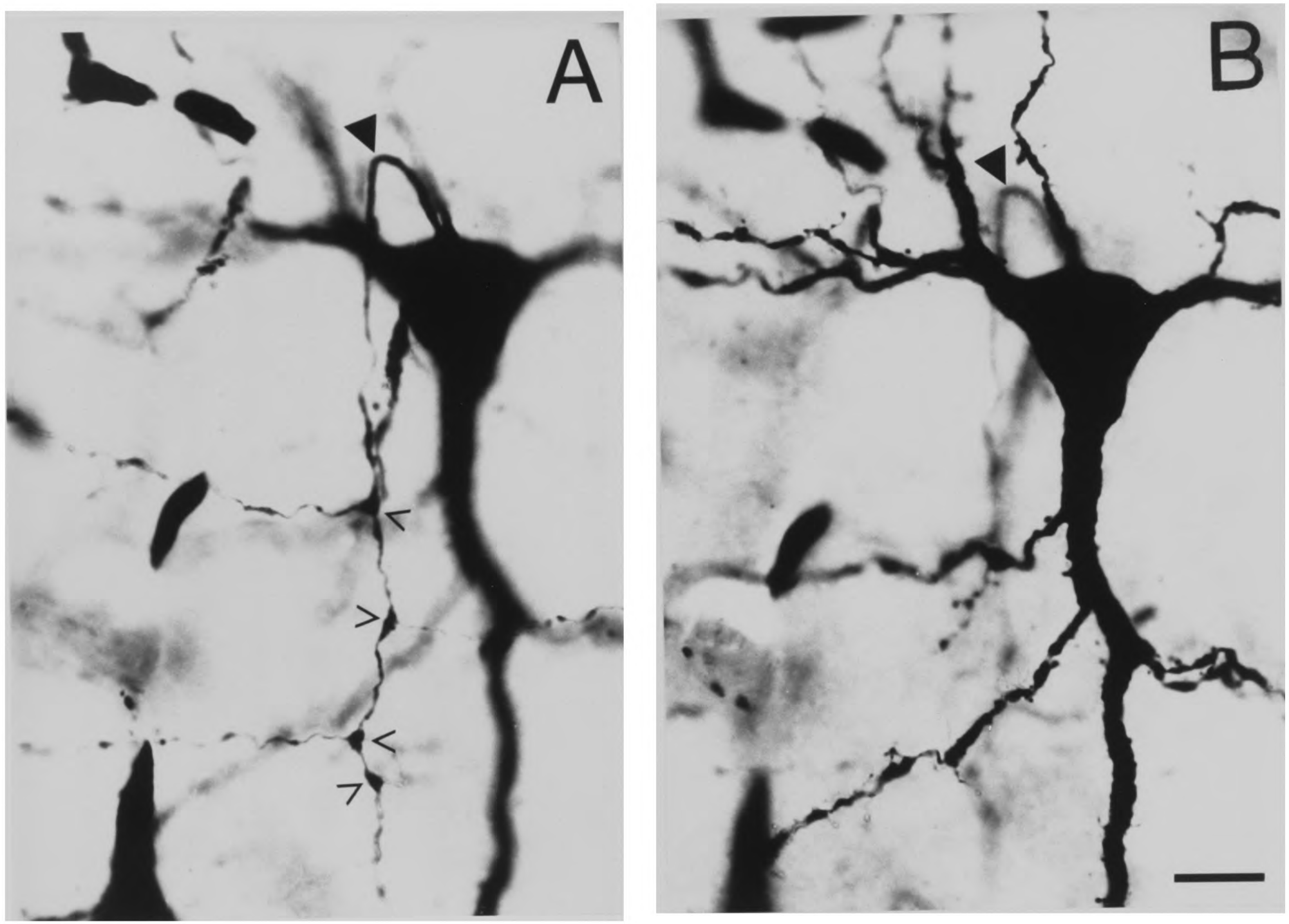
A
B

surface to arborize in layer 1 forming tufts similar to those of the corticotectally projecting neurons.

Non-back-labelled cells were also filled in the slices from animals in which cells had been back-labelled from the opposite hemisphere. About one third of the non-backlabelled cells had a morphology of the slender type and were indistinguishable from the filled cells backlabelled from the CLH. The other two thirds of non-backlabelled cells which were filled had a morphology of the thick type described before.

In addition (as in the two other cells mentioned above) it was not possible to confirm any back-labelling in cells with twin apical dendrites (n=3) in either of these preparations. Furthermore it was not possible to demonstrate any SC-back-labelling in pyramidal neurons with inverted morphology (Miller, 1988a; Bueno-Lopez et al., 1991), although the number of such cells (n=2) in this sample was much too small to be definite about the finding.

6.4 Discussion :

It can be concluded that the significant anatomical differences between SC or CLH projecting neurons can be clearly distinguished at p5 and p10. The morphology obtained from individual back-labelled cells injected with LY allows the two populations to be clearly classified into slender and thick pyramidal cells of the types described by Larkman and Mason (1990) and Larkman (1991a). To demonstrate that the result from the p5 or p10 CLH-group is not an artifact due to differences in the

Figure **6.18**: Plate showing two layer 5 pyramidal neurons from the developing rat visual cortex after intracellular injection with LY at p5.

The photograph depicts two filled adjacent neurons in a fixed slice preparation from the rat visual cortex which contained back-labelled CLH-neurons. This figure illustrates that non-back-labelled neurons with an apical dendrite could also be filled in these preparations. The missing apical dendrite in the CLH-neuron to the left is therefore not an artifact introduced by the slicing procedure but a finding that reflects a morphological difference between the two cell classes studied.

Scale bar =100µm.

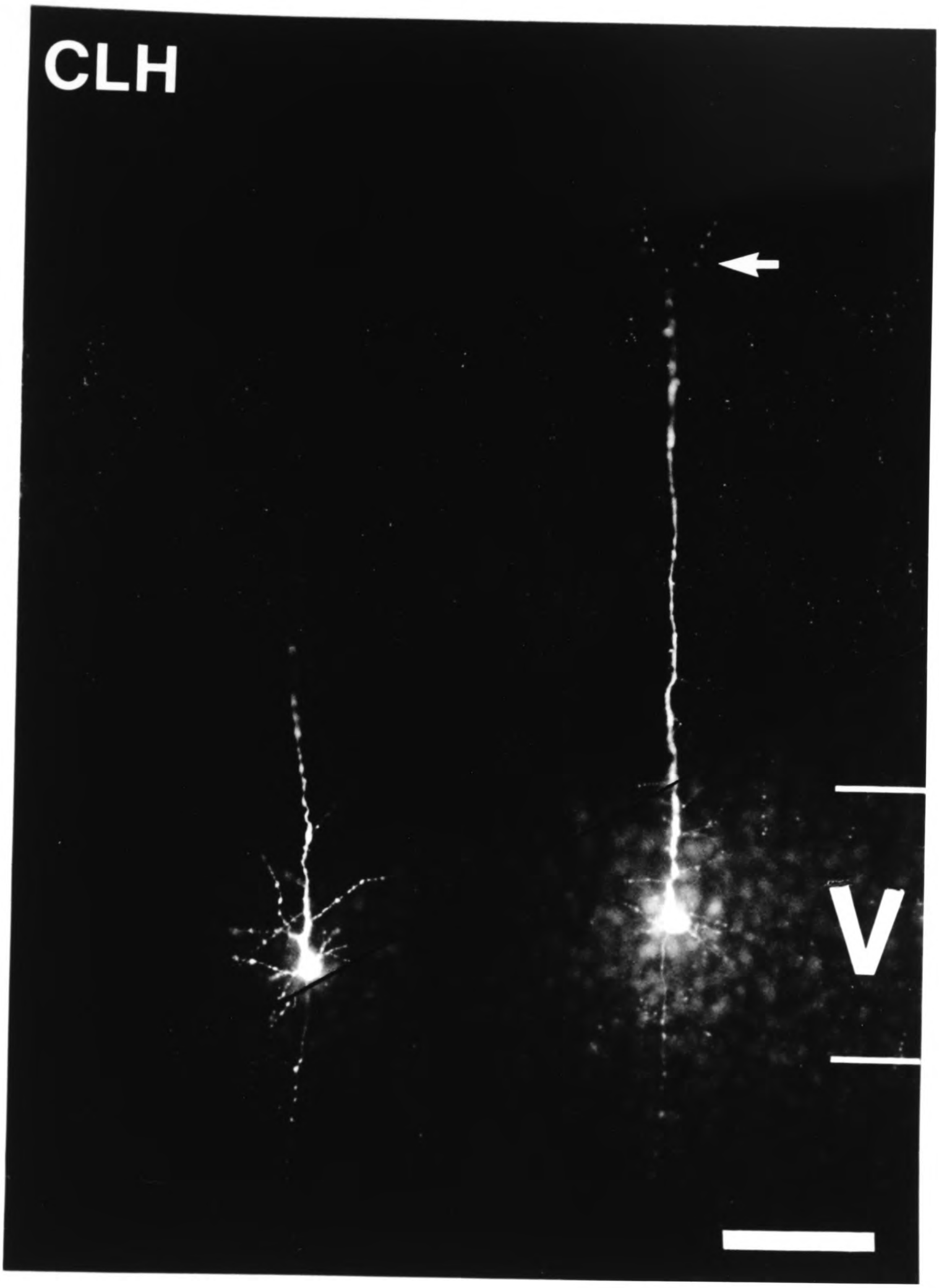
CLH
V

slice-preparation, which might have cut off the apical dendrites, I have also filled tufted neurons (non-back-labelled) in preparations containing back-labelled CLH-neurons (see Figure 6.18).

The pyramidal neurons from both groups already showed within the first postnatal week the main characteristic features of neurons described in similar preparations from adult visual cortex (e.g. Hübener and Bolz, 1988; Larkman, 1991a). At neither of the dates investigated (p5 and p10) could I find cells of both morphological types or intermediate types or entirely different types amongst a group that was prelabelled from the single injection site (SC or CLH) investigated in separate experiments.

Injections of other pyramidal cells that were not back-labelled but were closely intermingled with the population of back-labelled cells also revealed neurons of the same classes of morphological appearance as those from back-labelled cells within the same experiment. Thus not all cells of the thick type were back-labelled from the SC nor were all cells of the slender type backlabelled from the CLH but fewer thick ceels remained unlabelled after an SC-injection than did slender cells after a CLH-injection.

Several possible explanations can account for the fact that these cells were not back-labelled. Firstly it is conceivable that these cells projected to the target structure but were not back-labelled, perhaps because their axon did not ramify within the actual injection site. This might very well be the case for callosal projecting cells which are known to project homotopically or heterotopically or both (e.g. ; Miller and Vogt, 1984a; Miller, 1988b). The same is also possible for the population of corticotectal cells because tracer injections did not fill the entire SC, but this argument is less

powerful for this case because it is known that there is a high precision of visual projection within the corticotectal pathway (e.g. Hoffmann et al., 1972). This means that corticotectal cells located closely together in the cortex should project to neighbouring areas in the target (SC). Therefore neighbouring cells projecting to neighbouring target regions should either both be labelled or unlabelled unless of course the topography is very imprecise at early developmental stages.

The second possible explanation is that cells of a homogeneous morphological type project to different targets. This also seems to be quite likely, because several previous studies have revealed that many subcortically projecting cells that send their axon to a single target in the adult (e.g. the superior colliculus or the pyramidal tract) send axon collaterals simultaneously to both subcortical targets in early developmental stages (see e.g. O'Leary and Stanfield, 1985; Stanfield and O'Leary, 1986; O'Leary and Terashima, 1988; O'Leary et al., 1990). After selective axon elimination during cortical maturation they might therefore still belong to one morphologically homogeneous group, although only one population will be back-labelled.

Thirdly it is conceivable that a proportion of the axons of one population of cells –although later projecting to one of the investigated targets– has not yet reached the injection site and cannot be retrogradely labelled. This is likely because efferent fibers innervating one structure can reach the target sequentially rather than simultaneously, as it is known from the retinofugal system. This assumption may account for the relatively high number of non-back-labelled pyramidal neurons with similar morphology to the back-labelled neurons in brain slice preparations from young animals.

The most important finding is the **striking coherence** in the morphological appearance of each group of projection neurons and its early differentiation for all the

injected cells.

Because of the short time span between the prelabelling operation and slice preparation for LY-injection it is possible that cells in rat visual cortex projecting to the superior colliculus or the contralateral hemisphere acquire their characteristic morphological features prior to and therefore possibly independent of the innervation of the projection site. The most interesting open question that remains now to be answered is: how and when do cells in a single layer, generated at virtually the same time in early corticogenesis become structurally differentiated and send their axons to innervate the appropriate targets? In addition, the specific functional correlate of such a morphological difference between projection neurons, which can be observed across various species, remains an enigma to be solved.

Chapter 7:

Juvenile superior colliculus projecting neurons from layer 5 of the rat visual cortex studied *in vitro:*

7.1 Introduction :

The aim of this set of experiments was to investigate the action potential firing patterns of juvenile neurons projecting to the superior colliculus. Such projection neurons fire action potentials in a burst-pattern in brain slice preparations from the the adult animal (see **Chapter 4**). They also are of a distinct morphological type, which is already recognizable very early in postnatal cortical development (see **Chapter 6**). On the other hand it was observed that such intrinsic bursts of action potentials could not be found in layer 5 neurons before postnatal day 15 (**p15**) in neurons from the developing visual cortex (see **Chapter 5**).

This raises the question whether SC-projecting cells from the same preparation at a particular postnatal day around p15 are a physiologically homogeneous group and display similar action potential firing patterns or whether these cells differ in their intrinsic properties.

To this end 28 backlabelled neurons projecting to the superior colliculus (SC-neurons) were studied in a series of experiments investigating subthreshold properties

and characteristic action potential parameters. One third of the cells recorded in this study were classified as "bursters" (see Table 7.1: SC-cells B) whereas two thirds were classified as "non-bursting" neurons (see Table 7.1: SC-cells NB). Both types of action potential firing patterns could be found in slices prepared from a single animal, indicating that the observed difference can occur within a neuronal population of a certain postnatal age and is not due to a consistent difference between animals of different postnatal maturational stages.

Observations of the individual cell morphology, as revealed by intracellular injection of *carboxyfluorescein* (CF) during the recording period, did also not allow a morphological distinction between the two groups of SC-cells (B and NB) on the basis of qualitative anatomical features.

7.2 Materials and Methods :

Cortical layer 5 neurons were back-labelled by incorporation of rhodamine-conjugated microspheres after injection of tracer solution into the SC and retrograde transport of the beads to the neuronal somata. Because I did not have access to a stereotaxic frame for juvenile animals and there is no atlas available for the stereotactic coordinates for the juvenile postnatal stages required for the back-labelling procedure, a different protocol was adopted:

Animals underwent surgery between **p3** and **p5**. The tracer injections were performed under visual control rather than stereotactically, but the superior colliculus can clearly be visualized at this postnatal stage when the dorsal aspect of the mesencephalon is exposed. Animals were allowed to survive for about ten days

before brain slices were prepared at **p15** or **p16,** an age at which both bursting and non-bursting layer 5 pyramidal neurons had been found. Because of the long survival period after the surgery, particular care was taken to avoid any infections during the operation procedures (for details describing the operation procedure, the preparation of slices, the chamber configuration, the use of fluorescent tracer and the techniques employed for electrophysiological recording: see **Chapter 3** Materials and Methods).

Individual back-labelled SC-neurons were impaled in a living brain slice preparation in an interface slice chamber that was attached to an epifluorescence microscope (for configuration of the set up see **Chapter 3**). The physiological properties of each cell were charaterized using potassium methylsulfate electrodes also containing 1.25% CF to study the morphology of cells from which records were taken. After a successful recording period each single cell was also completely filled with CF. Each cell was photographed using a low-power objective to reveal its general morphology immediately after electrode withdrawal. The cell body of each cell was subsequently examined for back-labelling using a high power objective (Nikon x40 ELWD).

7.3 Results :

From 14 animals a total of 28 unequivocally backlabelled SC-neurons were recorded. In addition data were collected from more than 30 non-backlabelled neurons recorded in the same slice preparations, but most of those cells were not analysed further.

Ten of the back-labelled SC-neurons fired action potentials in a burst-firing pattern,

the remaining 18 SC-neurons fired action potentials in a non-bursting pattern.

In the following section a brief morphological description of the SC-neurons is followed by a comparison of the data obtained from the two groups of backlabelled SC-neurons.

7.3.1 Qualitative anatomical observations :

All the cells back-labelled via injection into the SC were located exclusively in layer 5 of the ipsilateral cortical hemisphere (See Figure 7.1 B). As in the adult animals, the population of SC-neurons formed a continuous band of cells that extended from medial to lateral throughout the visual areas (stretching from the medial portion of area 29 to the lateral part of area 41 and possibly extending even further than this).

All the back-labelled SC-neurons, whether "bursters" or "non-bursters", had a similar morphology with the following characteristic features (see Figure 7.1 A and 7.2 B/C) : a large soma that was vertically elongated and a thick apical dendrite that arose gradually from the upper (pial) pole of the soma. This apical dendrite ascended straight towards the pial surface to branch extensively near the border of layers 2/3 and layer 1. These branches bifurcated manyfold and formed an elaborate tuft in layer 1 which stretched laterally over a distance of about 200µm (See Figure 7.2 A).

The quality of the preparation and the completeness of the intracellular dye injection is demonstrated in tyoical examples in Figures 7.1A and 7.2A and B where,

Figure **7.1**: Morphology of a representative juvenile (p15) pyramidal neuron projecting to the SC as seen after intracellular injection with carboxyfluorescein (CF) after recording in a living brain-slice preparation.

A) Overview of the injected SC-cell located in layer 5 showing its general soma-dendritic morphology. The soma gives rise to a prominent apical dendrite, which can easily be recognized as it ascends towards the pial surface to form a terminal tuft in layer 1. Several oblique branches are given off by the apical dendrite the majority of which arises proximal to the neuronal cell body. There are many basal dendrites which bifurcate in the immediate proximity to the cell body, to form a dense skirt of branches. The descending axon (indicated by a white arrow) can also be seen. It gives off axonal collaterals most of which are directed laterally.

B) The corresponding picture as seen with the filter block appropriate for the wavelength for rhodamine fluorescence. It can be seen that corticotectally projecting neurons are exclusively located in layer 5 with a high proportion of the back-labelled cells being located in the superficial portion of layer 5.

Scale bar in B = 100μm and applies also to A.

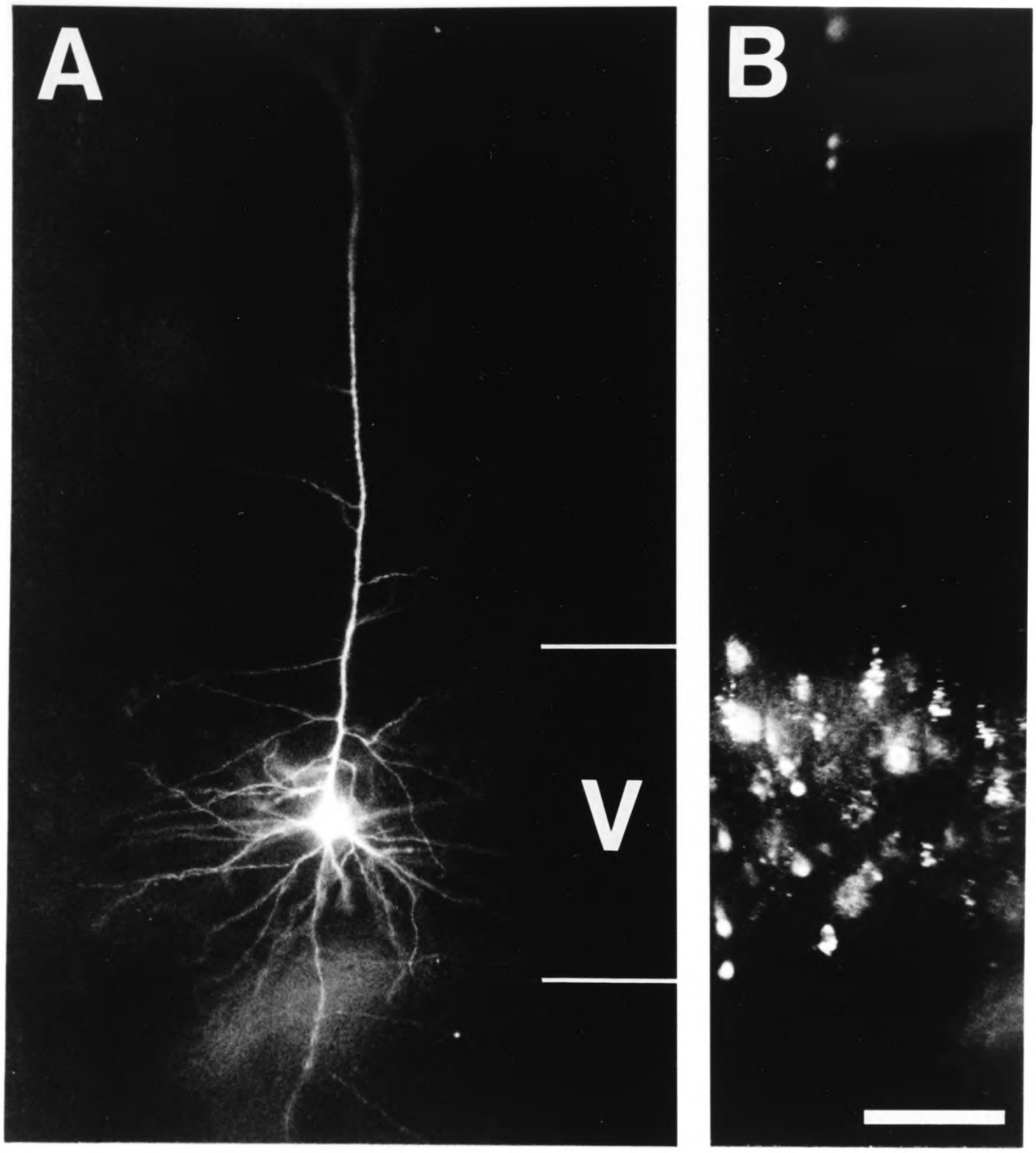
A
B
V

Figure **7.2**: Three plates illustrating the morphological quality of fills obtained by intracellular injection of CF into cells from which recordings were taken in the conventional 400µm living brain slice preparations from juvenile brains prepared at p15/p16.

A) Terminal tuft of a juvenile SC-projecting neuron. This terminal tuft shows many dendritic branch points and branches extend laterally for about 200µm to each side. A few single spines can also be seen on these branches. The pial surface is indicated by a hatched line.

B) Soma of the SC-projecting neuron which is also shown in figure 7.1. The elaborate system of basal dendritic branches is clearly visible as is the high number of proximal oblique dendrites contributing to an almost spherical cortical volume that is sampled by them. The main axon is indicated by a white arrow.

C) Same cell as in B, shown after the filter set was changed to the wavelength appropriate for rhodamine excitation.
Scale bar in C = 50 µm and applies also to A and B.

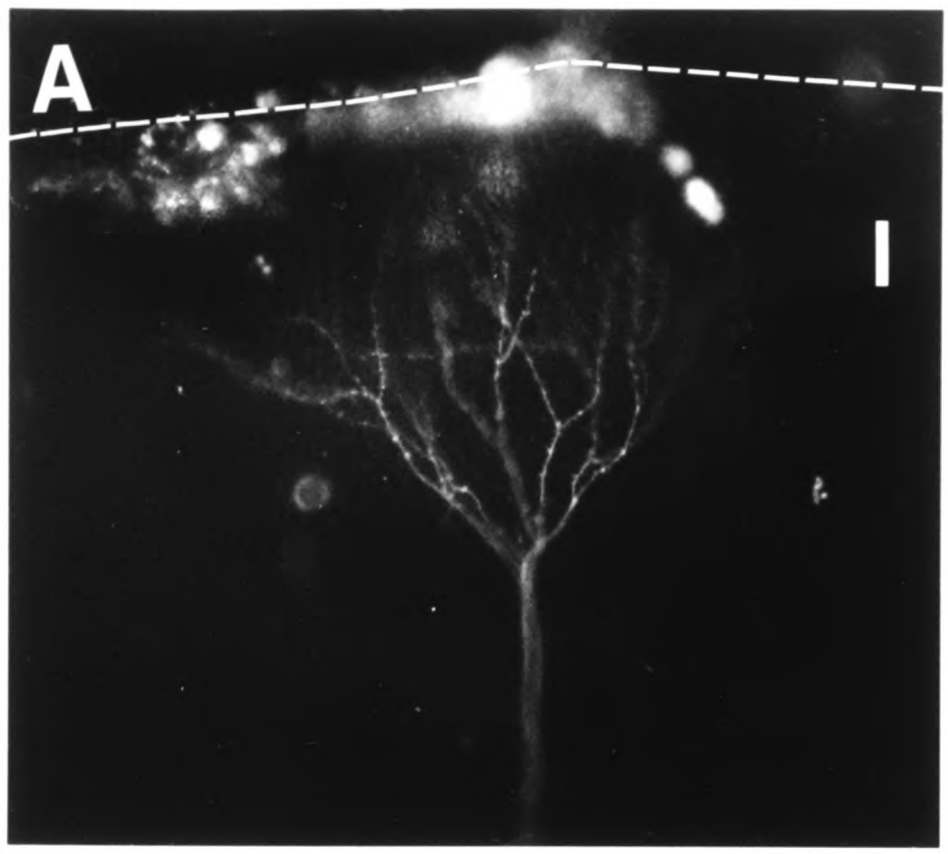
A
I

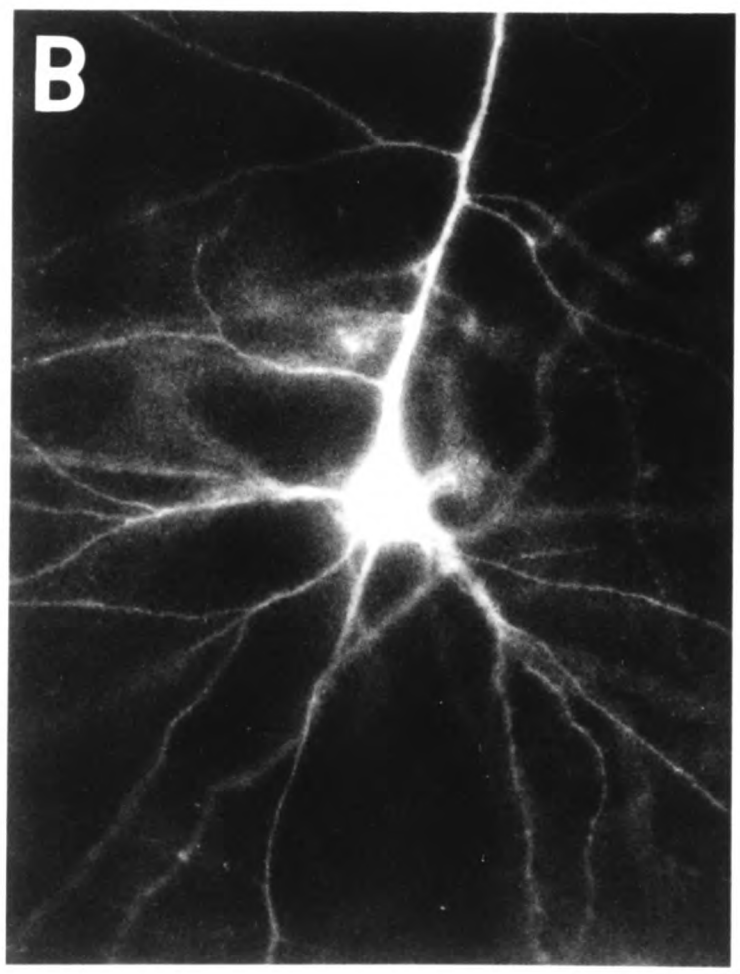
B

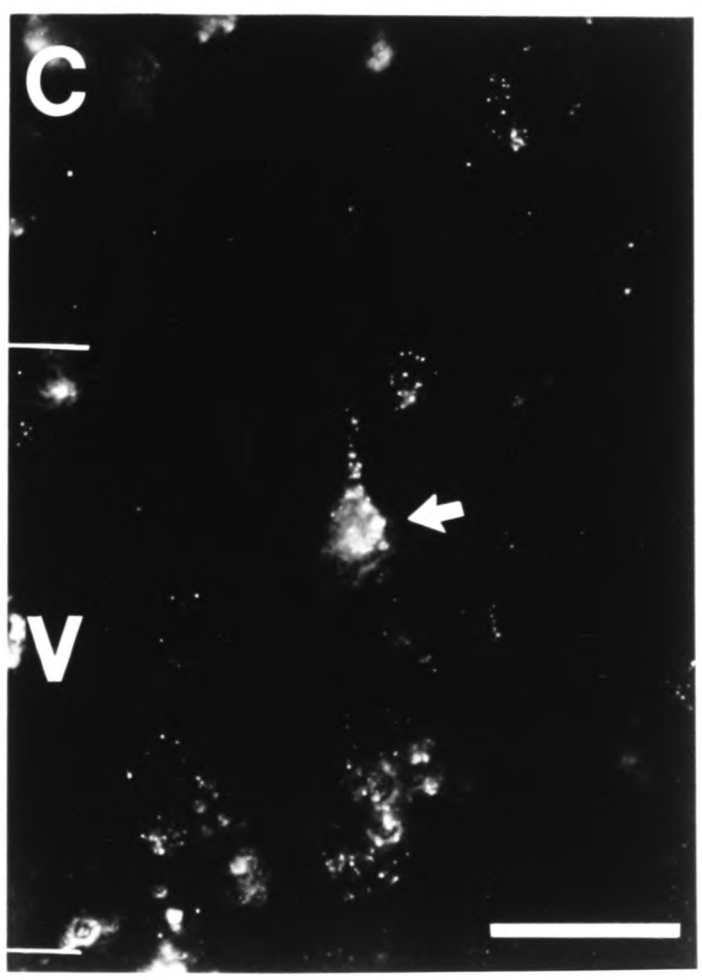
C
V

besides the basal dendritic skirt and the oblique branches of the apical dendrite, axon collaterals and an extensive terminal arborization including spines are visualized. I am therefore confident that the morphology of the cells injeced was as complete as possible within the 400µm slice and physiological differences between cells were not caused by damage of the cell membrane or selective loss of dendritic branches during the preparation of slices.

All the back-labelled SC-neurons had 3-7 stem segments of basal dendrites which were relatively short and possessed many dichotomous branch points and therefore a high number of branches. This dendritic skirt in the vicinity of the cell body sampled an almost spherical volume of cortex centered around the soma.

The apical dendrite also gave rise to a high number of branches. Most oblique branches from the apical trunk were located proximally and contributed towards the same "spherical volume". Only a small number of oblique branches was located more superficially (see Figure 7.1 A).

There was **no discernible qualitative morphological difference** between SC-neurons which fired action potentials in bursts and those which fired action potentials in a non-bursting pattern (See below: Electrophysiological section and Figure 7.6).

7.3.2 Electrophysiological results :

a) General findings :

All cells analysed from this set of experiments were capable of firing trains of action potentials overshooting the zero potential if stimulated by intracellular suprathreshold current injection. None of the cells fired action potentials spontaneously at membrane resting potential.

Subthreshold properties :

Resting potential: The membrane resting potential (V_m) did not differ between the bursting and non-bursting back-labelled SC-neurons and was in both groups around –65mV. The values were slightly but not significantly different from those of adult cells (see Table 7.1)

Membrane time constant: The membrane time constant was measured from the averaged voltage response to a series of 0.5ms current pulses of -1.0nA amplitude. The measured voltage was plotted semilogarithmically versus time and the membrane time constant calculated from the slope of a regression line fitted through the straightest portion of the data points obtained at late times as described previously (see Figure 7.3 and **Chapter 4:** results section for a more detailed description). The membrane time constant of the group of non-bursting SC-neurons (12.4±3.8ms) did not differ significantly from the values of bursting neurons (11.4±4.4ms). However, the non-bursting SC-neurons alone had a mean membrane time constant that was just statistically significantly longer ($p<0.05$) than that of mature SC-neurons from adult preparations (see Table 7.1).

Figure **7.3**: Membrane time constants of back-labelled SC-projecting neurons from the juvenile visual cortex. Semilogarithmic plots of the voltage decay following brief (0.5ms), hyperpolarizing current pulses injected into A) a burst-firing SC-neuron B) a non burst-firing -neuron. Inset scale bars in A apply also to B.

Zero value on the X-axis corresponds to the end of the injected current pulse. The dotted lines (from which time constants were taken) are least-squares fits to straightes portion of the plots.

Membrane time constants from juvenile layer 5 pyramidal neurons projecting to the SC

A

SC-projecting and still non bursting neuron

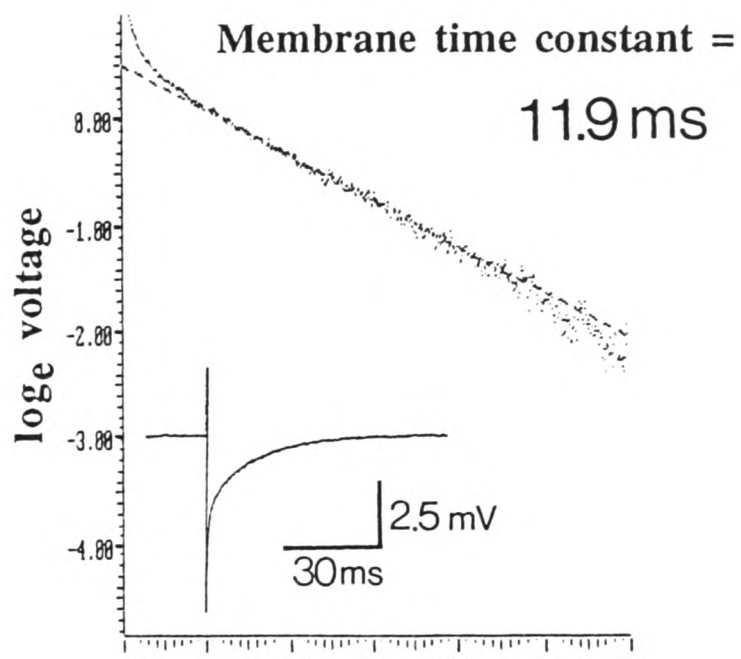

B

SC-projecting and burst-firing neuron

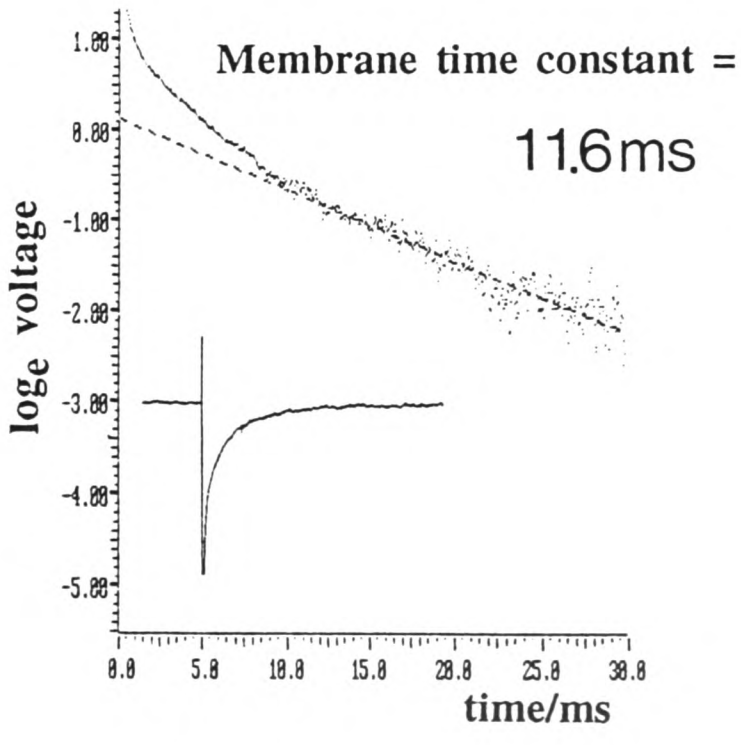

Figure **7.4**: Current/voltage relationships of two SC-projecting neurons from the juvenile visual cortex. Voltage responses (*left side top traces*) to long (t=200ms) current pulses (*left side bottom traces*) injected into **the cells.**

A1) a burst-firing SC-neuron.

A2) a non-burts-fifing SC-neuron.

B) a non-labelled regular spike-firing neuron.

The voltage response was measured at its peak (hollow circles) and just before the end of the of the current pulses. Both values were plotted against injected current (*right side plots*) in A1, A2, B. Scale bars in B apply also to A1 and A2. For the action potential firing patterns see figure 7.5.

Note that the only visible difference between the burst-firing SC-neuron (A1) and the non-burst-firing SC-neuron (A2) is a stronger depolarizing "sag" and a more pronounced overshoot/undershoot voltage deflection (in A1) at the end of the current pulses injected. Neither input resistances nor time constants differed significantly between the two groups.

Current/voltage relations of juvenile layer 5 pyramidal neurons projecting to the SC

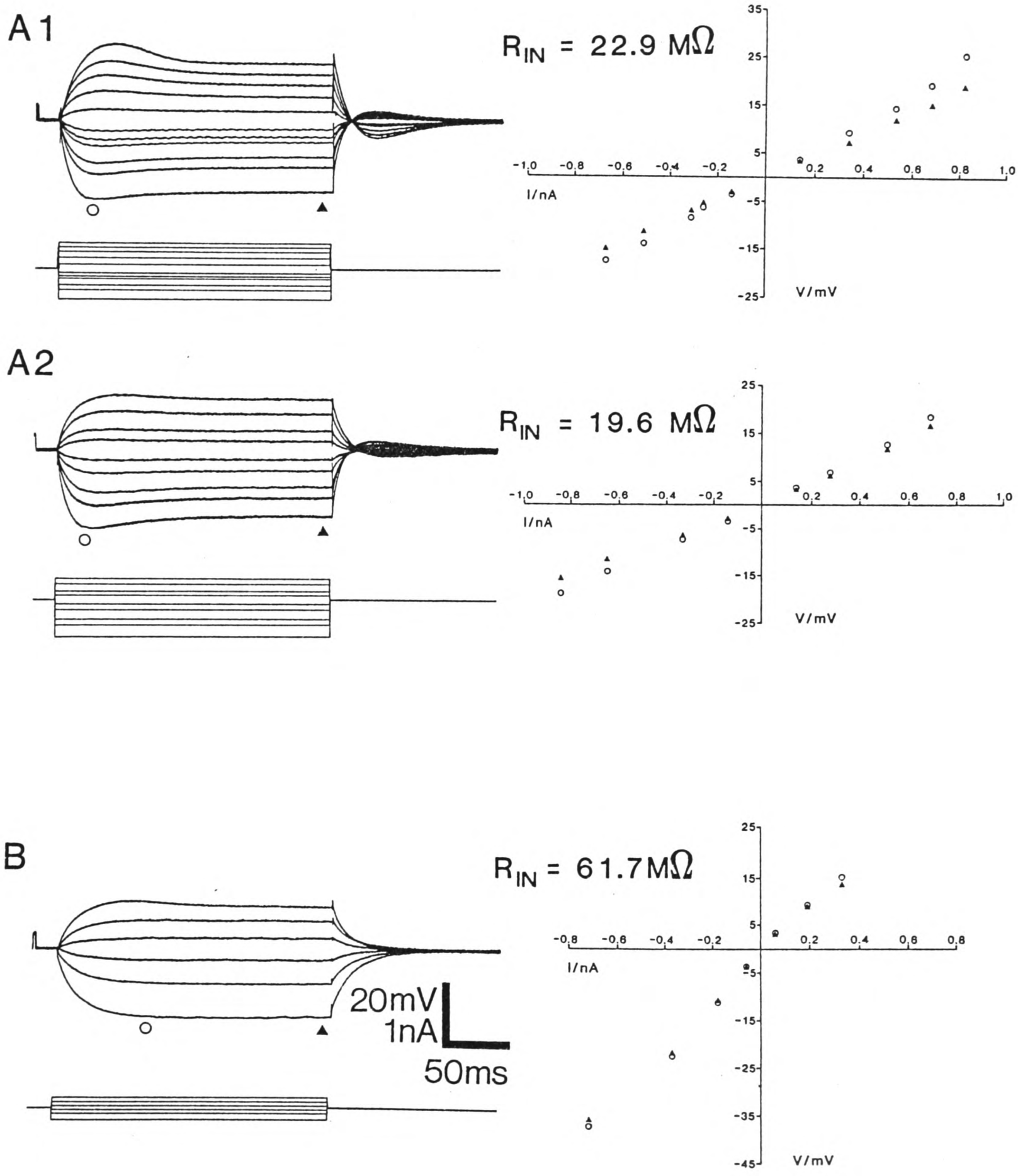

Table 7.1: Subthreshold properties of two groups of juvenile back-labelled layer 5 neurons projecting to the SC.

	P_{15}		Adult
	SC-CELLS$_B$	SC-CELLS$_{NB}$	SC-CELLS
no. of cells	10	18	11
$-V_m$ /mV	65.6 ± 4.5	65.4 ± 4.3	68.6 ± 3.1
R_{in} /MΩ	18.2 ± 2.9	19.6 ± 2.8	14.3 ± 4.6
time constant /ms	11.4 ± 4.4	12.4 ± 3.8	9.1 ± 3.1

Data in this and subsequent tables are given as mean values ± SD. Statistical differences (student's t-test) between the SC-neurons and the CLH-neurons are indicated as follows:

+ = $p \leq 0.01$; □ = $p \leq 0.05$; ▲ = $p \leq 0.1$

Current voltage relations: To test the possibility that both groups might differ in the sub-threshold range of their I/V relations, long ($t \leq 200ms$) current pulses of positive and negative polarity (-0.7nA to +0.7nA) were injected into each neuron and the voltage responses to each pulse averaged (See Figure 7.4, left side). The apparent input resistance (R_{in}) was measured from the voltage range negative to rest using values of a steady-state voltage deflection between -5mV and –10mV. There was no detectable difference between the two groups of SC-neurons with both neuronal samples having an R_{in} value of about 19 MΩ, a value that is still significantly higher ($p<0.01$) than the input resistance of SC-projecting neurons from adult brains (see Table 7.1 and **Chapter 4**).

During the initial phase of long current pulses the membrane potential tended to "sag" back towards the resting level. No difference in the occurrence of this phenomenon was apparent between the two groups of juvenile SC-neurons (see Figure 7.4 A1 and A2 and corresponding cells in Figure 7.6) and no attempt was made to quantify this observation.

At the end of the injected current pulse the membrane potential tended to overshoot (after negative pulses) or undershoot (after positive pulses) the membrane resting potential. There was also no apparent difference between the two groups of SC-neurons. As in the SC-neurons investigated in slices from adult animals (see **Chapter 4**) no rebound action potentials were triggered from such an off-response following a hyperpolarizing pulse over the current range that was applied.

b) Suprathreshold properties:

Burst-firing: Ten out of 28 back-labelled SC-neurons studied in detail fired action potentials in a burst in response to depolarizing current pulses whereas the remaining 18 SC-neurons did not fire a burst but displayed a regular spike-firing pattern (See Figure 7.5).

Both types of action potential firing patterns were found in SC-neurons impaled in **the same slice preparations** prepared from one animal (see Figure 7.5 and corresponding cells in Figure 7.6). A variety of burst-discharge patterns could be observed (see Figure 7.7) which suggests that the development of a burst-firing pattern evolves gradually from a preceding regular spiking pattern. In such burst-firing SC-neurons from juvenile brains a burst consisted normally of just two clustered spikes, the first of which was considerably higher and faster than the second, which always had a prolonged falling phase. Typically the second spike was triggered before the membrane had completely repolarized after the first spike, thus linking the two spikes by an interspike-interval depolarized with respect to the membrane threshold potential. Additional spikes could be recruited separately if the amplitude of the injected current pulse was increased and such additional spikes occurred after a much greater interval than those during the preceding cluster (see Figure 7.5 B).

In the non-bursting SC-neurons single action potentials could be elicited by injection of a just suprathreshold current and a gradually increasing number of spikes could be evoked by an increase in injected current strength (see Figure 7.5 A).

As in SC-neurons from slices of adult animals, action potentials in both groups had substantially shorter rise times than fall times. The detailed investigation of action

Figure **7.5**: Various action potential firing patterns elicited in juvenile SC-projecting neurons in response to an injected depolarizing current pulses of minimal suprathreshold strength (A1, B1). The lower traces (A2, B2 etc.) show a slightly increased current strengths necessary for the recruitment of one additional spike each.

Scale bars in B4 apply also to all other traces. The injected current pulse amplitude is indicated in each case.

A-traces: Non burst-firing SC-neuron the corresponding cell morphology is shown in Figure 7.6 *in the left plate.* Vm was -73mV; RME was 89MΩ.

B-traces: Burst-firing SC-neuron the corresponding cell morphology is shown in Figure 7.6 *in the right plate.* Vm was -72mV; RME was 94MΩ.

Action potential firing patterns of juvenile layer 5 pyramidal neurons projecting to the SC

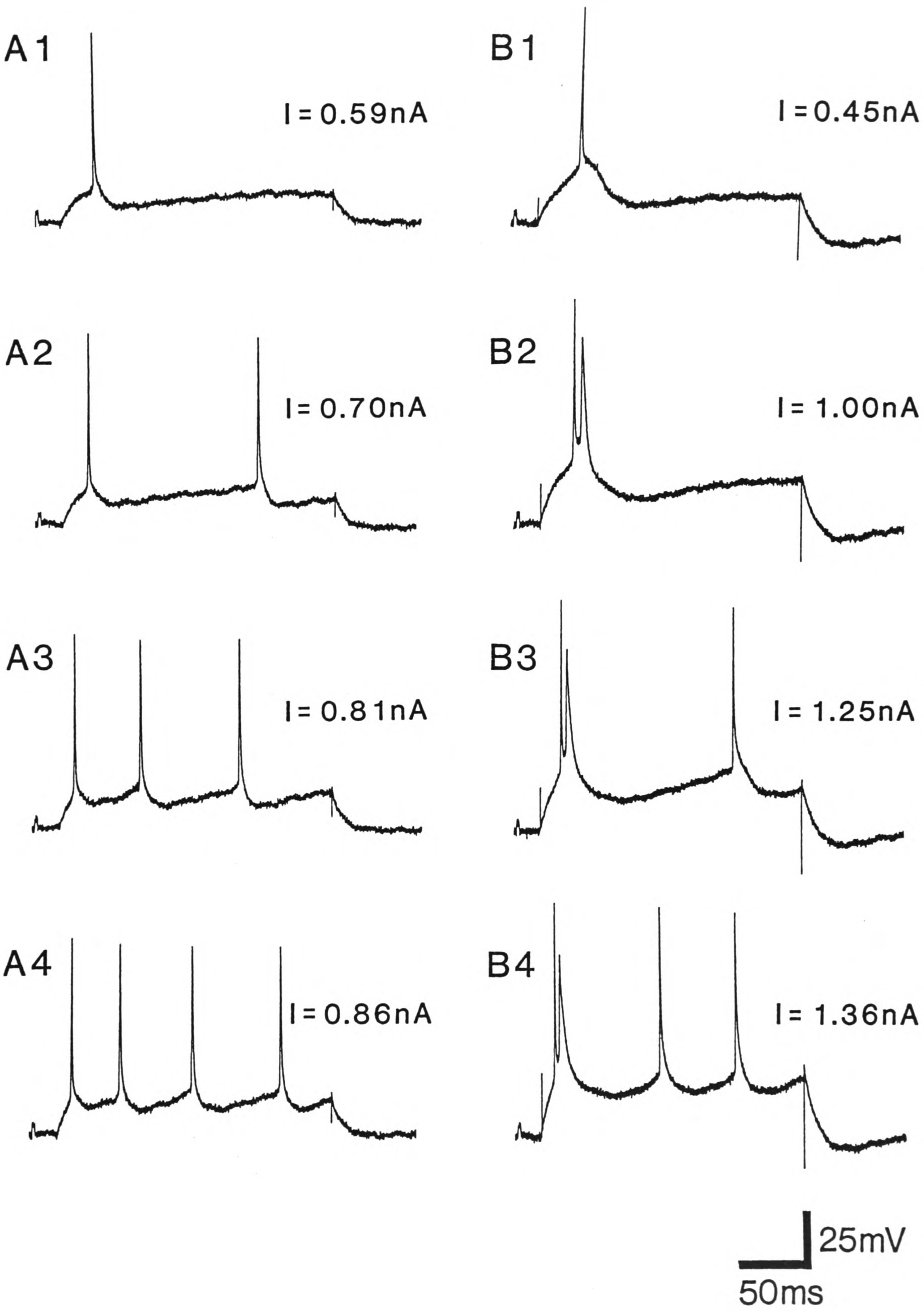

Figure **7.6**: Juvenile layer 5 pyramidal neurons from the visual cortex which were back-labelled from injections into the SC. These photo-montages show two SC-neurons which differed in their action potential firing pattern but did not differ significantly in their intrinsic electro-physiological properties.

Left side plate: P15 SC-neuron which fired action potential in in a regular spiking pattern after intracellular injection of suprathreshold current pulses (see figure 7.5 A1-A4)

Right side plate: P15 SC-neuron which fired action potential in a burst after intracellular injection of suprathreshold current pulses (see figure 7.5 B1-B4).

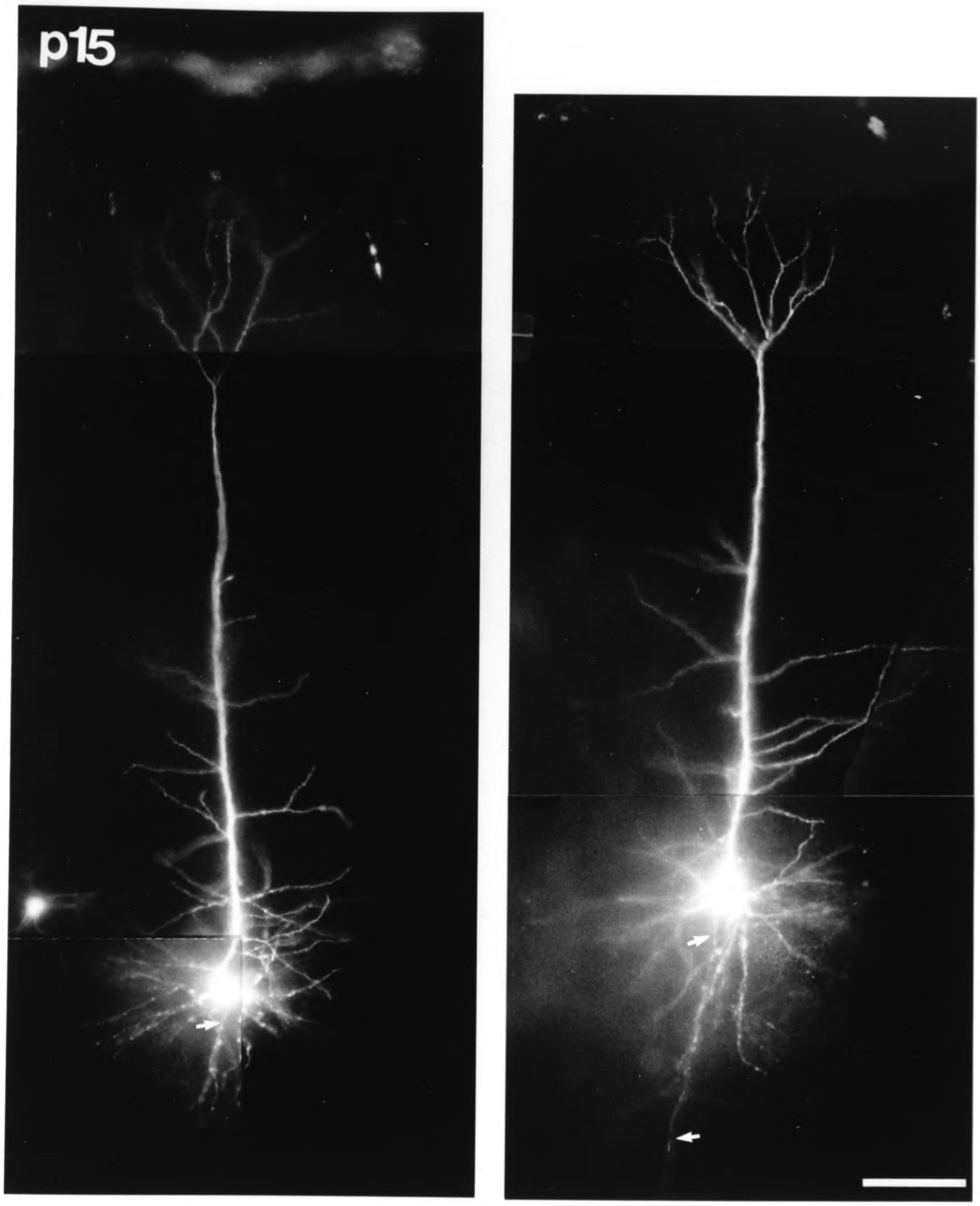
p15

Different action potential burst firing-patterns in juvenile cortical neurons projecting to the SC

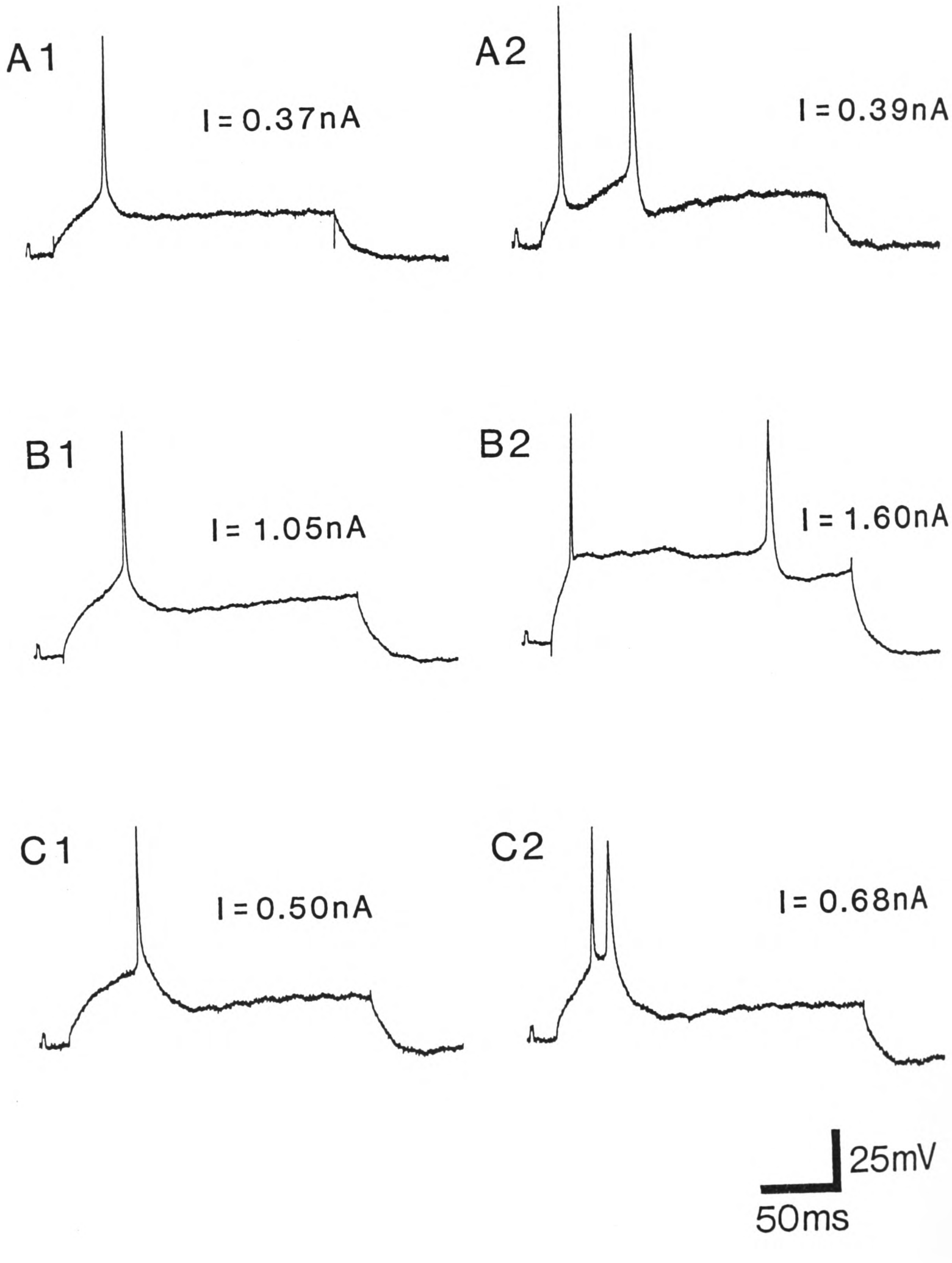

Figure 7.7: Various action potential firing patterns elicited in juvenile cortical SC-neurons in response to an injected depolarizing current pulses of minimal suprathreshold strength (A1, B1, C1). The right traces (A2, B2, C2) show slightly increased current strengths necessary for the recruitment of one additional spike, thus forming a "burst". Scale bars in C apply also to A and B. The injected current pulse amplitude is indicated in each trace.

Table 7.2: Action potential parameters from APs of juvenile back-labelled layer 5 neurons projecting to the SC.

	P_{15}		Adult
	$SC\text{-}Cells_B$	$SC\text{-}Cells_{NB}$	SC-Cells
no. of cells	10	18	14
Peak height above threshold /mV	61.1 ± 7.5	59.8 ± 7.3	65.5 ± 7.9
Width of half amplitude /ms	0.96 ± 0.13 ▼	1.10 ± 0.20	0.63 ± 0.13
10%/90% rise time /ms	0.20 ± 0.04 □	0.27 ± 0.04	0.22 ± 0.05
90%/10% fall time /ms	1.50 ± 0.42	1.93 ± 1.01	0.75 ± 0.14
30%/70% rise rate /V/s	288.9 ± 72.7	240.4 ± 75.8	299.6 ± 99.3
70%/30% fall rate /V/s	42.8 ± 14.3 ▼	33.9 ± 11.7	82.9 ± 21.0
Rate ratio	6.93 ± 0.91	7.66 ± 2.94	3.65 ± 0.52

Data in this and subsequent tables are given as mean values ± SD.Statistical differences (student's t-test) between the SC-neurons and the CLH-neurons are indicated as follows:

+ = $p \leq 0.01$; □ = $p \leq 0.05$; ▼ = $p \leq 0.1$

potential parameters (see Table 7.2) reveals that the main difference between the single action potentials of both groups of SC-neurons was a significantly longer rising phase in non-bursting SC-neurons as well as a slower falling rate, thus causing a difference in width at half amplitude. No other parameters showed a significant difference.

Spike afterpotentials: If single action potentials were compared from both groups of SC-neurons similar afterpotentials could be observed. The long latency slow after-hyperpolarization (l A.H.P. see **Chapter 5**) could be seen in all cells and was pronounced. If present, the initial after-hyperpolarization (i A.H.P.) was hardly visible but it was in most cases hidden by a depolarizing after-potential (D.A.P.) that was continuous with the falling phase of the action potential (Figure 7.5 B1). Because these phenomena are less well developed in young and juvenile neurons and not as clearly distinguishable in bursting neurons as in regular spiking neurons (Mason and Larkman 1990) the observation was not pursued further.

Repetitive firing: All bursting SC-neurons were capable of firing additional trains of action potentials if stimulated with suprathreshold current pulses of sufficient length and amplitude (see Figure 7.6). Non-bursting SC-neurons showed a gradual increase in spike-frequency. They usually needed a smaller increase in current injection for the recruitment of additional spikes. Both groups of SC-neurons showed signs of adaptation with increasing interspike intervals after each successive spike.

7.4 Discussion :

In this set of experiments, juvenile neurons back-labelled from the SC were investigated by means of intracellular recording and dye injection.
Amongst the 28 SC-neurons studied, about one third was found to fire action potentials in bursts whereas the other two thirds fired action potentials in a non-bursting pattern. The analysis of subthreshold properties such as membrane resting potential, membrane time constant and apparent input resistance did not reveal any significant differences between the two groups of SC-neurons. Nevertheless if the values of both groups are compared to data from an identical slice preparation of adult cortex, differences can be shown which indicate that these cells are not yet fully developed (See Table 7.1 and 7.2).

It could be demonstrated that the only difference between the two groups of SC-neurons is in the action potential firing pattern action potential waveform. This suggests that this observation of suprathreshold differences between juvenile SC-neurons is due to genuine variability within the same neuronal population at the same age rather than being due to individual differences in maturity between individual animals.

In a comparison of action potential parameters between the juvenile non-bursting SC-neurons and the juvenile burst-firing SC-neurons only the rise time and the fall rate were found to be significantly different. This finding is interesting because it suggests that the difference in firing pattern is not due to factors that grossly determine the waveform of single action potentials. This idea is supported by previous findings (Hamill et al., 1986; Huguenard et al., 1986,1988; Prince and Huguenard, 1988) which have pointed out that the kinetics of sodium and potassium

currents do not change significantly during postnatal development so that changes in action potential rise time and fall time are primarily dependent on changes in channel density. This latter idea has been supported by sodium flux studies (Courand et al., 1986) and studies of toxin-binding to the sodium receptor (Baumgold et al., 1983). Based on pharmacological investigations of depolarizing currents underlying the burst-firing pattern, it was suggested that a calcium activated potassium current controls the generation of a depolarizing Ca^{2+}/Na^{+}- envelope underlying the bursts (Deisz, 1988; Deisz and Prince, 1990). It would therefore be of great interest to study the development of such a current and the factors controlling its prominence.

It would also be of great interest to investigate whether there is a correlation between the time of eye opening in these animals, at around p13 in Wistar rats, and a possible effect thereof on the onset of bursting (for further discussion see: **Chapter 8**).

It thus appears that the AP difference found in SC-projecting cells around **p15** in this set of experiments simply reflects the fact that the non-bursting SC-cells are in a less mature state than the burst-firing SC-cells.

Chapter 8:

General conclusion

The experiments carried out for this thesis have investigated pyramidal neurons located in layer 5 of the rat visual cortex in both living and fixed brain slice preparations.

First, results were presented from a set of experiments employing the combination of conventional *in vitro* intracellular recording and dye-injection techniques with retrograde tracing. This combination made it possible to characterize directly both the intrinsic electrophysiological properties and the morphological features of individual back-labelled neurons. Two populations of projection neurons were investigated in layer 5 of the rat primary visual cortex. It was shown that corticotectal projection neurons (SC-neurons) as well as interhemispheric projection neurons (CLH-neurons) form two homogeneous morphological groups, each distinct from neurons of the other group. The main characteristic anatomical feature of corticotectal projection neurons was a prominent thick apical dendrite which terminated in an extensive arborisation in layer 1. All interhemispheric neurons had a slender apical dendrite that tapered, did not form a terminal tuft and did not reach layer 1.

The neurons of both groups also differed significantly in their electrophysiological properties in both the subthreshold and suprathreshold range. In particular the firing-pattern of action potentials revealed striking differences between the groups, with corticotectal projection neurons firing bursts of action potentials whereas interhemispheric projection neurons displayed a regular spike-firing pattern. These

results indicate that a distinct dendritic morphology can be characteristic for one particular group of cortical projection neurons and may reflect differences in the mixture of afferent information these cells receive.

The difference in laminar distribution between populations of projection neurons as well as the specific intralaminar location of the neuronal cell body and the arrangement of its dendrites will determine the different types of inputs each efferent neuron receives. It is known that various inputs to the visual cortex are segregated by their laminar organisation, e.g. fibres originating in the dorsal lateral geniculate nucleus terminate primarily in layers 4 and lower 3 with a less dense innervation of layers 1 and 6 (Ribak and Peters, 1975; Herkenham, 1980; Sefton and Dreher, 1985). Non-specific thalamic afferents end mainly in layers 2/3 and 1 (Jones, 1985; Zilles, 1990). Fibers from the nucleus thalamis posterior project to upper layer 5 and 1 (Herkenham, 1980) and interhemispheric connections terminate predominantly in layers 2/3 and 5 (Miller and Vogt, 1984a and 1984b; Miller, 1988). Ascending fibres mediating noradrenergic and serotonergic input to the occipital cortex terminate predominantly in layer 1 and the superficial layers, cholinergic fibers terminate both superficially and deeper (with a peak in layer 4), whereas the dopaminergic system has its main input directly to the infragranular layers (for review see Zilles et al., 1990). Local intracortical projections are also laminar specific (Burkhalter, 1989).

These observations may be of particular interest with respect to the information a cell receives via its apical dendrite as it traverses across the various layers. One should also take into account the variation in spine density along the dendrite, which has been reported in various rodents (Valverde, 1967; Marin-Padilla and Stibitz, 1968; Larkman, 1991c) as well as in man (Marin-Padilla, 1967). It has already been demonstrated that

different classes of corticospinal neurons in the cat can be influenced selectively via stimulation of afferents to the molecular layer (Chen and Towe, 1985) which might be mainly modulatory in effect.

A modulatory input to one layer might specifically change the firing-output of neurons in response to synaptic stimulation of fibres terminating in a particular layer. Such an influence has been reported from *in vivo* studies of the dopaminergic innervation of neurons of the rat prefrontal area (Ferron et al., 1984). These neurons changed in their spontaneous spike firing frequency after stimulation of the ventral tegmental area.

The possibility of such a "functional tuning" might also selectively apply to the corticotectal cells of this study, because of their extensive terminal tuft in layer 1. Interhemispheric neurons which lack a terminal tuft and hence do not receive synaptic input from fibres terminating in layer 1 are less likely to be influenced by "non-specific" modulation, e.g. via serotonergic input.

Compared to the cells projecting to the contralateral hemisphere via the corpus callosum the corticotectal cells from the sample investigated in this thesis formed physiologically a more homogeneous group. This has also been reported from ***in vivo*** studies investigating the properties in neurons of both cell populations by single unit recording.

Several authors have investigated the receptive field properties of corticotectal neurons in various species (for cat see e.g. Palmer and Rosenquist, 1974; Harvey,

1980; for monkey see e.g. Finlay et al., 1976; for rodents see e.g. Lemmon and Pearlman, 1981; Swadlow, 1988). It has been reported that in cat the cells projecting to the SC are mainly special complex cells, which are driven by input from both eyes with almost equivalent strength (Palmer and Rosenquist, 1974). In cat (but not in monkey) they are frequently selective for the directions of image motion. They do not show obvious length summation within the receptive field, are orientation selective but respond prefertially to small moving spots as stimuli. The latter finding has also been described in hamster (Klein et al., 1986). Nevertheless Weyand et al.(1986) found also standard complex cells amongst corticotectal projection neurons in the cat. Therefore corticotectal cells are most likely involved in information processing concerned with movement perception rather than analysis of shape (see Harvey, 1980). In higher mammals, such as cat and monkey, these neurons are considered to play a part, via their input to the SC, in the control of eye movements and visually guided motor activity.

The sample of interhemispheric projection neurons formed a more heterogeneous group with respect to their morphology as well as their physiological characteristics. One group of callosally projecting cells, namely those interconnecting representations of the central visual field, are thought to function both in fusion of the two hemifields and in stereopsis. It is therefore not surprising that these neurons were found to form a more heterogeneous group, which has been noted both functionally and morphologically (e.g. Mitchell and Blakemore, 1970; Harvey, 1980; Blakemore et al.,1983; Buhl and Singer, 1989; Diao and So, 1991).

Nevertheless it should be noted that it is very difficult to compare such findings

from higher mammals with well developed vision to the situation in rodents, because functional speculations in the former are often related to the fact that central vision is more acute than peripheral vision, which is not so clearly the case in rodents.

The variation in ganglion cell density across the retina in the rat (ranging from about 1000/mm^2 to 6000/mm^2, Dreher et al., 1984) is relatively small compared to the figures for other species, which can have a much higher centre/periphery ratio than 6:1. A ratio of of about 80:1 has been reported in the cat (Rowe and Stone, 1976) and values of about 300:1 were demonstrated in monkey (Rolls and Cowey, 1970). In addition, it is worth noting that the size of dendritic arborisations of rat retinal ganglion cells –which reflect the size of the receptive field centres of these cells– does not change with variation in retinal ganglion cell density (Dreher et al., 1985) and there seems to be no apparent increase in receptive field size of single units recorded in rat visual cortex with increasing retinal eccentricity (Goodale and Carey, 1990). Visual acuity is approximately 1 cycle/degree and therefore about 50 times worse than in primates (Dean, 1978, 1990)

Thus it seems that the rat has less need for mechanisms to bring stimuli into position on the central retina for the purpose of identifying that stimulus visually. It might therefore be speculated that the rat visual system serves more the purpose of localizing a stimulus within the visual space with less emphasis on a central specialization for identification of stimuli.

Second, the development of pyramidal neurons during the first three postnatal weeks was studied using intracellular recording techniques combined with the injection

of an intracellular marker (biocytin) which allowed the morphological description of the neurons from which records were taken (**Chapter 5**). It was demonstrated that both subthreshold properties (such as membrane time constant and input resistance) and action potential parameters (such as peak amplitude, rise time and fall time and related rates) changed significantly throughout the period investigated. It was also noticed that a burst-firing pattern could not be found before postnatal day 15, a time in development which is of interest because of its close relation to the time when the animals open their eyes (around p13).

The results from **Chapter 5** and the purely anatomical investigation of layer 5 pyramidal projection neurons (in **Chapter 6**) indicate that the changes in neuronal electroresponsiveness are paralelled by anatomical maturation, indicated by a significant increase in somatic size and the progressive differentiation of the dendritic processes. The latter observation suggests an enormous increase in complexity of cortical connectivity and thereby cellular interaction throughout the period studied. Additionally the majority of synaptic sites is located on the dendritic spines, whose number increases significantly throughout this postnatal period (for a review see Miller, 1988b).

Finally data were presented in **Chapter 7** from an investigation of back-labelled corticotectal neurons at postnatal days 15 and 16. This postnatal stage of development is of interest because it is the period when layer 5 projection neurons were found to start to segregate into two physiologically distinct burst-firing and regular-spiking types (see **Chapter 5**).

Corticotectal projection neurons around postnatal day 15 were studied to investigate the development of bursting in a further series of experiments on neurons prepared

from the juvenile visual cortex (see **Chapter 7**). It could be shown that both types of firing patterns and intermediate stages were present in neurons from a single preparation of backlabelled SC-neurons This suggests that there is a gradual change from the non-bursting mode to the burst-firing mode in cells from a single SC-projecting neuronal population. Further investigation of currents underlying this phenomenon is necessary to reveal whether a particular current can be found that is responsible for the switch to the burst-firing pattern. If so, it would be interesting to see whether changes in the amplitude or time course of such a current can be detected, which might reflect a change in channel density within the membrane or a change in channel kinetics. Such a process could be studied in whole cell patch clamp experiments on acutely dissociated back-labelled neurons or through a combination of that technique with receptor binding studies, if specific ligands were available.

It would also be of great interest to see whether the change is influenced by intrinsic factors (meaning here: within the neuron). It is also conceivable that this change is initiated by cellular interaction (eg. via ingrowing fibres triggering the expression of channel proteins) or extrinsic factors such as changes in the pattern of afferent activity caused by the opening of the eyes. The latter possibility could be studied in several ways: first, the animal could be dark-reared or eyelid-sutured to see whether the occurrence of bursting would shift towards later times. Second, TTX-silencing of cellular activity of retinofugal projections might prevent some input necessary for the differentiation process. Finally, the reverse could be tried by artificially activating retinofugal fibres by implanting stimulation electrodes thus causing some additional input to the cortex, which might trigger an earlier occurrence of the burst-firing phenomenon.

References :

A

Adams, P.R., Brown, D.A., and Constanti, A. (1982) :
M-currents and other potassium currents in bullfrog sympathetic neurones
J. Physiol., **330** : pp. 537-572

Adams, P.R., and Galvan, M. (1986) :
Voltage-dependent currents of vertebrate neurons and their role in membrane excitability
in : Advances of Neurology, **44:** pp.137-170
Raven Press, N.Y.

Aghajanian, G.K., and Rassmussen, K. (1989) :
Intracellular studies in the facial nucleus illustrating a simple new method for obtaining viable motoneurons in adult rat brain slices
Synapse, **3** : pp. 331-338

Angevine, J.B., and Sidman, R.L. (1961) :
Autoradiographic study of cell migration during histogenesis of cerebral cortex in the mouse
Nature, **192** : pp. 766-768

Angevine, J.B., and Sidman, R.L. (1962) :
Autoradiographic study of histogenesis in cerebral cortex in the mouse
Anat. Rec., **142** : p. 210

Artola, A., and Singer, W. (1987) :
Long-term potentiation and NMDA receptors in rat visual cortex
Nature, **330** : pp. 649-652

Avoli, M., and Olivier, A. (1989) :
Electrophysiological properties and synaptic responses in the deep layers of the epileptogenic neocortex *in vitro*
J. Neurophysiol, **61** : pp. 589-606

Axelrad, H. (1974) :
Postnatal evolution of functional activity in rat cerebral cortex
Ontogenesis of the Brain, pp. 363-370
(Ed. Jilek, L., and Trojan, S.)
Prague: Universitas Pragensis Press

B

Bader, C.R., Bertrand, D., Dupin, E., and Kato, A.C. (1983) :
Development of electrical membrane properties in cultured avian neural crest
Nature, **305** : pp.808-810

Baker, J., Gibson, A., Mower, G., Robinson, F., and Glickstein, M. (1983) :
Cat visual corticopontine cells project to the superior colliculus
Brain Res., **265** : pp. 227-232

Baumgold, J., Zimmerman, I., and Bambrick, L. (1983) :
Appearances of [^{3}H] saxitonin binding sites in developing rat brain.
Dev. Brain Res., **9** : pp.405-407.

Bayer , S., and Altman, J. (1991) :
Neocortical Development
Raven Press, N.Y.

Bechterew, W. (1894) :
Die Leitungsbahnen in Gehirn und Rückenmark :
Ein Handbuch für das Studium des Nervensystems.
Besold, Leipzig.

Berlin, R. (1858) :
Beiträge zur Strukturlehre der Großhirnwindungen.
Junge, Erlangen.

Berry, M. (1974) :
The cerebral cortex of the rat
in : Aspects of Neurogenesis, Vol.2, pp. 8-67
(Ed. Gottlieb, G.)
Academic Press, N.Y

Berry, M., Rogers, A.W., and Earys, J.T. (1964) :
Pattern of cell migration during cortical histogenesis
Nature, **203** : pp.591-593

Berry, M., and Rogers, A.W. (1965) :
The migration of neuroblasts in the developing cerebral cortex
J. Anat., **99** : pp. 691-709

Berry, M.S., and Pentreath, V. W. (1976) :
Criteria for distinguishing between monosynaptic and polysynaptic transmission
Brain Res., **105** : pp.1-20

Bindman, L.J., Meyer, T., and Prince, C.A. (1988) :
Comparison of the electrical properties of neocortical neurones in slices in vitro and in the anaesthetized rat
Exp. Brain Res., **69** : pp.489-496

Blakemore, C.B., Diao, Y., Pu, M., Wang, Y., Xiao, Y. (1983) :
Possible functions of the interhemispheric connections between visual cortical areas in the cat
J. Physiol., **337**, : pp. 331-349

Blue, M.E., and Parnavelas, J.G. (1983) :
The formation and maturation of synapses in the visual cortex of the rat I.Qualitative analysis
J. Neurocytol., **12** : pp. 599-616.

Boulder Committee (1970) :
Embryonic vertebrate central nervous system: revised terminology
Anat. Rec., **166** : pp.257-262.

Brodmann, K. (1903) :
Beiträge zur histologischen Lokalisation der Großhirnrinde
Erste Mitteilung. Die Regio Rolandica
J. Physiol. Neurol., **2** : pp.79-132

Brodmann, K. (1909) :
Vergleichende Lokalisationslehre der Großhirnrinde in ihren Prinzipien dargestellt auf Grund des Zellenbaues
Barth, Leipzig.

Brodmann, K. (1912) :
Neue Ergebnisse über die vergleichende histologische Lokalisation der Großhirnrinde mit besonderer Berücksichtigung des Stirnhirns.
Anat. Anz., **41** (Suppl.) : pp. 157-216.

Brown, D.A., and Griffith, W.H. (1983) :
Calcium-activated outward currents in voltage-clamped hippocampal neurones of the guinea-pig
J. of Physiol., **337** : pp.287-301

Brückner G., Mares, V., Biesold, D. (1974) :
Neurogenesis of the visual system in the rat : An autoradiographic investigation
J. Comp. Neurol., **166** : pp. 245-256

Bueno-Lopez, J.L., Reblet, C., Lopezz-Medina, A., Gomez-Urqujo, S.M., Grandes, P., Gondra, J., and Hennequet, L. (1991) :
Targets and Laminar distribution of projection neurons with inverted morphology in rabbit cortex
Eur. J. Neurosci., **3** : pp. 415-430

Buhl, E.H., and Schlote, W. (1987) :
Intracellular Lucifer Yellow staining and electron microscopy of neuronesin slies of fixed epitumourous human cortical tissue
Acta Neuropath., **75** : pp. 140-146

Buhl, E.H., and Lübke, J. (1989) :
Intracellular Lucifer Yellow injection in fixed brain slices combined with retrograde tracing,
light and electron microscopy
Neurosci., **28** : pp.3-16

Buhl, E.H., and Singer, W. (1989) :
The callosal projection in cat visual cortex as revealed by a combination of retrograde tracing
and intracellular injection
Exp. Brain Res., **75** : pp. 470-476

Burkhalter, A. (1989) :
Intrinsic connections of rat primary visual cortex: laminar organization of axonal projections
J. Comp. Neurol., **255** : pp. 171-186

Butler, A.B., and Caley, D.W. (1972) :
An ultrastructural and radioautography study on the migrating neuroblast in hamster
Brain Res., **44** : pp. 83-97

C

Campbell, A.W. (1905) :
Histological Studies on the Localisation of the Cerebral Function
Cambridge University Press, London.

Catsman-Berrevoets, C.E., Lemon, R.N., Verburgh, C.A., Bentivoglio, M., and Kuypers, H.G.J.M. (1980) :
Absence of callosal collaterals derived from rat corticospinal neurons :
Exp. Brain Res., **39** : pp. 433-440

Caviness, V.S.Jr. (1982) :
Neocortical histogenesis in normal and reeler mice; a developmental study based upon [^{3}H]-thymidine autoradiography
Dev. Brain Res., **4** : pp. 293-302

Caviness, V.S., and Rakic, P. (1978) :
Mechanisms of cortical development: a view from mutations in mice
Annu. Rev. Neurosci., **1** : pp.297-326

Chagnac-Amitai, Y., Luhmann, H.J., and Prince, D.A. (1990) :
Burst generating and regular spiking layer 5 pyramidal neurons of rat neocortex have different morphological features.
J. Comp. Neurol., **296** : pp. 598-613

Chamberlin, N.L., Traub, R.D., and Dingledine, R. (1990) :
Role of EPSPs in initiation of spontaneous synchronized burst firing in rat hippocampal neurons bathed in high potassium.
J. Neurophysiol., **64** : pp. 1000-1018

Chen, Z., and Towe, A.L. (1985) :
Influence of molecular layer on pyramidal tract neurons
Exp. Neurobiol., **88** : pp. 218-228

Chun, J.J. , and Shatz, C.J. (1989) :
Interstitial cells of the adult neocortical white matter are the remnant of the early generated subplate neuron population
J. Comp. Neurol., **282** : pp. 555-569

Cole, K.S. (1972) :
Membranes, Ions and Impulses: A Chapter of Classical Biophysics
University of California Press, Berkely

Coleman, P.D., Flood, D.G., Whitehead, M., Emerson, R. (1981)
Spatial sampling by dendritic trees in the visual cortex
Brain Res., **214** : pp. 1-21

Connor, J.A., and Stevens, C.F. (1971) :
Voltage clamp studies of a transient outward membrane current in gastropod neural somata
J. Physiol., **213** : pp. 21-30

Connors, B.W., Gutnick, M.J., and Prince, D.A. (1982) :
Electrophysiological properties of neocortical neurons *in vitro*
J. Neurophysiol., **48** : pp. 1302-1320

Connors, B.W., Benardo, L.S., and Prince, D.A. (1983) :
Coupling between neurons of the developing rat neocortex
J. Neurosci, **3** : pp. 773-782.

Connors, B.W., and Gutnick, M.J. (1984) :
Neocortex: cellular properties and intrinsic circuitry.
In : Brain Slices
(Ed. I. Dingledine), pp. 313-339.
Plenum, N.Y.

Connors, B.W., and Gutnick, M.J. (1990) :
Intrinsic firing patterns of diverse neocortical neurons.
TINS, **13** : pp. 99-104

Connors, B.W., Malenka, R.C., and Silva, L.R. (1988) :
Two inhibitory postsynaptic potentials, and $GABA_A$ and $GABA_B$ receptor mediated responses in neocortex of rat and cat
J. Physiol., **406** : pp. 443-468

Courand, F., Martin-Moutot, N., Koulakoff, A., and Berwald-Neffer, Y. (1986) :
Neurotoxinsensitive sodium channels in neurons developing in vivo and in vitro
J. Neurosci., **6** : pp. 192-198

Crepel, F., and Penit-Sonas, J. (1986) :
Inward rectification and low threshold calcium conductance in rat cerebellar Purkinje cells: An in vitro study
J. Physiol., **372** : pp. 1-23.

Creutzfeldt, O.D. (1983) :
Cortex Cerebri
Springer-Verlag, Berlin, Heidelberg, New-York, Tokyo.

Crill, W.E., and Schwindt, P.C. (1983) :
Active currents in mammalian central neurons.
TINS, **6** : pp. 236-240

Crunelli, V., Forde, S., and Kelly, J.S. (1983) :
Blockade of amino acid-induced depolarisation and inhibition of excitation post-synaptic potentials in rat dentate gyrus.
J. Physiol., **431** : pp. 627-640

D

Dean, P. (1978) :
Visual acuity in hooded rats: effect on superior collicular or posterior neocortical lesions
Brain Res., **156** : pp. 17-31

Dean, P. (1990) :
Sensory cortex: Visual perceptual functions
Chapter 12 in : the Cerebral Cortex of the Rat, pp. 275-307
(Eds. Kolb, B., and Tees, R.C.)
The MIT Press, Cambridge MA

Deisz, R.A., and Prince, D.A. (1987) :
Effect of D890 on membrane properties of neocortical neurons
Brain Res., **442** : pp. 63-73

Deisz, R. (1988) :
The current components of intrinsic bursting neurones of the guinea pig neocortex
Pflügers Archiv, **411**, Suppl.1: R 126

Deisz, R., and Prince, D.A. (1990) :
Analysis of current components underlying the bursting pattern of neocortical neurons
personal communication; (submitted for publication)

Deisz, R.A., Fortin, G., and Zieglgänsberger,W. (1991) :
Voltage dependence of excitatory postsynaptic potentials of rat neocortical neurons
J. of Neurophysiol., **65** : pp. 371-382

Deiters, O.F.K. (1865) :
Untersuchungen über Gehirn und Rückenmark des Menschen und der Säugethiere
(ed. M. Schultze).
Vieweg, Braunschweig

Deschenes, M., Labelle, A., and Landry, P. (1979) :
Morphological characterisation of slow and fast pyramidal tract cells in the cat
Brain Res., **178** : pp. 251-274

Diao, Y.,So, K. (1991) :
Dendritic morphology of visual callosal neurones in the golden hamster
Brain Behav. Evol., **37** : pp. 1-9

Dobbings, J. (1967) :
Growth of brain
Science Journal, **3** : pp. 81-90

Dreher, B., Potts, R., Ni, S., Bennet, M. (1984) :
The development of heterogeneities in distribution and soma sizes of rat retinal ganglion cells
In : Development of the visual pathways in mammals : pp. 39-58
(Eds. Stone, J., Dreher, B., and Rappaport, D.)
Alan Liss, N.Y.

Dreher, B., Sefton, A., Ni, S., Nisbett, G. (1985) :
The morphology, number and distribution of the class I cells of the albino and hooded rat
Brain Behav.Evol., **26** : pp. 10-48

Dürsteler, M.R., Blakemore, C.B., and Garey, L.Y. (1979) :
Projection to the visual cortex in the golden hamster
J. Comp. Neurol., **183** : pp. 185-204.

Durand, D., Carlen, P.L., Gurevich, N., Ho, A., Kunov, H. (1983) :
Electrotonic parameters of rat dentate granule cells measured using short current pulses and HRP staining
J. of Neurophysiol., **50** : pp. 1080-1097

E

Eayrs, J.T., and Goodhead, B. (1959) :
Postnatal development of the cerebral cortex of the rat
J. Anat., **93** : pp. 385-402

Edinger, L. (1896) :
Vorlesungen über Bau der nervösen Centralorgane des Menschen und der Thiere
Vögel, Leipzig

Ehrenberg, C.G. (1833) :
Notwendigkeit einer feineren mechanischen Zerlegung des Gehirns und der Nerven
Poggendorff's Ann. Phys. Chem., **28:** pp. 449-465

Ehrenberg, C.G. (1836) :
Beobachtung einer bisher unbekannten auffallenden Struktur des Seelenorgans bei Menschen und Tieren.
Abh. Akad. Wiss. Berlin (Phys. Math. Kl.), *1836* : pp. 665-723

Ehrlich, P. (1868) :
Über die Methylenblaureaction der lebenden Nervensubstanz.
Dtsch. Med. Wochenschau **12** : pp. 49-52

Espinoza, S.G., Thomas, H.C. (1983) :
Retinotopic organisation of striate and extrastriate visual cortex in the hooded rat
Brain Res., **272** : pp. 137-144

F

Ferron,A., Thierry, A. M., Le Dourain, C., and Glowinski, J. (1984) :
Inhibitory influence of the mesocortical dopaminergic system on spontaneous activivity or excitatory response induced from the thalamic mediodorsal nucleus in the rat medial prefrontal cortex
Brain Res., **302** : pp. 257-265

Flechsig, P. (1898) :
Neue Untersuchungen über die Markbildung in den menschlichen Großhirnlappen
Neurol. Zbl., **17** : pp. 977-996.

Fleshman, J.W., Segev, I., and Burke, R.E. (1988) :
Electrotonic architecture of type-identified a-motoneurons in the cat spinal cord
J. Neurophysiol., **60** : pp. 60-85.

Franz, P., Galvan, M., and Constanti, A. (1986) :
Calcium-dependent potentials and associated inward currents in guinea pig neocortical neurons in vitro
Brain Res., **366** : pp. 262-271

Frenac, Y., and Imbert, M. (1984) :
Development of neuronal selectivity in primary visual cortex of cat
Physiol. Rev., **64** : pp. 325-420

French, C.R., and Gage, P.W. (1985) :
A threshold sodium current in pyramidal cells in rat hippocampus
Neuroscience Letters, **56** : pp. 289-293.

Finlay, B., Schiller, and Volman S. (1976) :
Quantitative studies of single cell properties in monkey striate cortex IV, Corticotectal cells
J. Neurophysiol. **39** : pp. 1352-1361

Friedman, A., and Gutnick, M.J. (1987) :
Low-threshold calcium electro-genesis in neocortical neurons
Neurosience letters, **81** : pp. 117-122

Fujita, S. (1963) :
The matrix cell and cytogenesis in the developing central nervous system
J. Comp. Neurol., **120** : pp. 37-42

Fujita, S. (1964) :
Analysis of neuron differentiation in the central nervous system by tritiated thymidine autoradiography
J. Comp. Neurol., **122** : pp. 311-328

Fulton, B.P. (1987) :
Postnatal changes in conduction velocity and soma action potential parameters of rat dorsal root ganglion neurones
Neurosci. Lett., **73** : pp.125-130

G

Gamble, E., and Koch, C. (1987) :
The dynamics of free calcium in dendritic spines in response to repetitive synaptic input
Science, **236** : pp. 1311-1315

Gardette, R., Debono, M., Dupont, J.-L., and Crepel, F. (1985) :
Electrophysiological studies on the postnatal development of intracerebellar nuclei neurons in rat cerebellar slices maintained in vitro. II. Membrane conductances
Dev. Brain Res., **20** : pp. 97-106

Gilbert, C.D., and Kelly, J.P. (1975) :
The projections of cells in the different layers of the cat's visual cortex
J. Comp. Neurol., **163** : pp.81-106

Gilbert, C., and Wiesel, T.N. (1979) :
Morphology and intracortical projections of functionally characterized neurons in the cat visual cortex
Nature, **280** : pp. 120-125

Goldmann, P., and Nauta, W. (1977) :
Columnar distribution of catico-cortial fibres in the frontal, essociation, lymbic and motor cortex of the developing rhesus monkey.
Brain Res., **122** : pp. 393-413

Golgi, C. (1873) :
Sulla sostanza grigia del cervello.
Gaz. Med. Ital. Lombardia, **6** : pp. 244-246.
(Quoted from Opera Omnia, 1903, Vol.1, pp. 91-98, Hoepli, Milan.)

Golgi, C. (1883) :
Sulla fina anatomia degli organi centrali del sistema nervoso..
Riv. Sper. Freniatr. Med. Leg. Alienazioni Ment., **9** : pp. 1-17, 161-192, 385-402
(Quoted from Opera Omnia, 1903, Vol.1, pp. 295-375, Hoepli, Milan.)

Golgi, C. (1885) :
Sulla fina anatomia degli organi centrali del sistema nervoso.
Riv. Sper. Freniatr. Med. Leg. Alienazioni Ment., **11** : pp. 7-123, 193-220

Golgi, C. (1884) :
Recherches sur l'histologie des centres nerveux
Arch. Ital. Biol., **4** : pp. 92-123

Golgi, C. (1886) :
Sur l'anatomie microscopique des organes centraux du système nerveux.
Arch. Ital. Biol., **7** : pp. 15-47

Golgi, C. (1894) :
Untersuchungen über den feineren Bau des centralen und peripherischen
Nervensystems.
Fischer, Jena.

Goodale, M.A., and Carey, D.P. (1990) :
The role of cerebral cortex in visuomotor control
Chapter 13 in : The Cerebral Cortex of the Rat, pp.309-340
(Eds. Kolb, B., and Tees, R.C.)
The MIT Press, Cambridge MA

Goodman, C.S., and Spitzer, N.C. (1981) :
The development of electrical properties of identified neurones in grasshopper embryos
J. Physiol., **313** : pp. 385-403

Grace, A.A., and Llinas, R. (1985) :
Morphological artifacts induced in intracellularly stained neurons by dehydration:
circumvention using rapid dimethyl sulfoxide clearing
Neurosci., **16** : pp. 461-475

Graham, J., Lin, C.S., and Kaas, J.H. (1979) :
Subcortical projections of six visual areas in the owl monkey *Aortus trivirgatus*
J. Comp. Neurol., **187** : pp.557-580

Griffith, W.H. (1988) :
Membrane properties of cell types within guinea pig basal forebrain nuclei in vitro
J. Neurophysiol., **59** : pp. 1590-1612

Gustafsson, B., and Pinter, M.J. (1984) :
Relations among passiv electrical properties of lumbar a-motoneurones of the cat
J. Physiol., **356** : pp. 401-431

Gutnick, M.J., and Prince, D.A. (1981) :
Dye coupling and possible electronic coupling in the guinea-pig neocortical slice
Science, **211** : pp.67-70

Gutnick, M.J., Lobel-Yaakot, R., and Rimon, G. (1985) :
Incidence of neuronal dye-coupling in neocortical slices depends on the plane of section
Neurosci., **15** : pp. 659-666

Gutnick, M.J., and Yarom, Y. (1989) :
Low threshold calcium spikes, intrinsic neuronal oscillation and rhythm generation in the CNS
J. Neurosci. Meth., **28** : pp. 93-99

H

Hablitz, J.J. (1986) :
Mechanisms regulating synchronization of hippocampal epileptiform activity
in Calcium: Electrogenesis and Neuronal Functioning
(Eds. Heinemann, Klee, M., Neher, E., Singer, W.), .
Exp. Brain Res., Suppl. Series 14, pp. 337-344

Halliwell, J.V., and Adams, P.R. (1982) :
Voltage-clamp analysis of muscarinic excitation in hippocampal neurons.
Brain Res., **250** : pp. 71-92

Hallman, L.E., Schofield, B.R., and Lin, C.-S. (1990) :
Dendritic morphology and axon collaterals of corticotectal, corticopontine , and callosal neurons in layer V of the primary visual cortex of the hooded rat
J. Comp. Neurol., **272** : pp. 149-160

Hamill, O.P., Huguenard, J.R., Enayati, E.F., and Prince, D.A. (1986) :
Development of Na^+ conductance in neocortical neurons of the rat
Soc.Neurosci. Abstr., **12** : p. 950

Harris, K.M., and Teyler, T.J. (1983) :
Evidence for late development of inhibition in area CA1 of the rat hippocampus
Brain Res., **268**, pp. 339-343

Harvey, A.R. (1980) :
A physiological analysis of subcortical and comissural projections of areas 17 and 18 of the cat
J. Physiol., **302** : pp . 507-534

Herkenham, M. (1980) :
Laminar projections of thalamic projections to the rat neocortex
Science, **207** : pp.532-535

Hicks, S.P., and D'Amato, C.J. (1968) :
Cell migrations to the isocortex in the rat
Anat. Rec., **160** : pp. 619-634

Hoffmann, K.P. (1973) :
Conduction velocity in pathways from retina to superior colliculus in the cat: a correlation with receptive-field properties
J. Neurophysiol., **36** : pp. 409-424

Holländer, H. (1974) :
On the origin of the corticotectal projection of the cat
Exp. Brain Res., **21** : 433-440

Hondeghem, L.M. (1978) :
Validity of V_{max} as a measure of the sodium current in cardiac and nervous tissue
Biophys. J., **23** : pp. 147-152

Hori, N., Akaike, N., and Carpenter, D.O. (1988) :
Piriform cortex brain slices: techniques for isolation of synaptic inputs
J. Neurosci. Meth., **25** : pp.197-208

Horikawa, K., and Armstrong, W.E. (1988) :
A versatile means of intracellular labeling: injection of biocytin and its detection with avidin conjugates.
J. Neurosci. Meth. **25** : 1-1.

Hotson, J.R., Prince, D.A., and Schwartzkroin, P.A. (1979) :
Anomalous inward rectification in hippocampus neurons
J. Neurophysiol., **42** : pp. 889-894

Hotson, J.R., and Prince, D.A. (1980) :
A calcium-activated hyperpolarization follows repetitive firing in hippocampal neurons
J. Neurophysiol., **43** : pp.409-419

Hounsgaard, J., and Midtgaart, J. (1988) :
Intrinsic determinants of firing pattern in Purkinje cells of the turtle cerebellum *in vitro*
J. Physiol., **402** : pp. 731-749

Hübener, M., and Bolz, J. (1988) :
Morphology of identified projection neurons in layer 5 of rat visual cortex
Neurosci. Lett., **97** : pp. 76-81

Huguenard, J.R., Hamill, O.P., Enayati, E.F., and Prince, D.A. (1986) :
Development of Na^+ conductance in neocortical neurons of the rat
Soc. Neurosci. Abstr., **12** : p.950

Huguenard, J.R., Hamill, O.P., and Prince, D.A. (1988) :
Developmental changes of Na+ conductances in rat neocortical neurons:
appearance of a slowly inactivating component
J. Neurophysiol., **59** : pp. 778-795

Huguenard, J.R., Hamill, O.P., and Prince, D.A. (1989) :
Sodium channells in dendrites of rat cortical pyramidal neurons
Proc. Natl. Acad. Sci. USA, **86** : pp. 2473-2477 (Neurobiology)

Huttenlocher, P.R. (1967) :
Development of cortical neuronal activity in the neonatal rat
Experimental Neurol., **17** : pp. 247-262

I

Iansek, R., and Redman, S.J. (1973) :
An anaysis of the cable properties of spinal motoneurons using a brief intracellular current pulse
J. Physiol., **234** : pp. 613-636

Iansek, R., and Redman, S.J. (1973) :
The amplitude, time course and charge of unitary excitatory post-synaptic potentials evoked in spinal motoneurone dendrites
J. Physiol., **234** : pp. 665-688

Innocenti, G. (1980) :
The primary visual pathway through the corpus callosum:
morphological and functional aspects in the cat.
Arch. Ital. de Biol., **118** : pp. 124-188

Innocenti, G., and Fiore, L. (1976) :
Morphological correlates of visual field transformation in the corpus callosum
Neurosci. Lett., **2** : pp. 245-252

Ivy, G.O., and Killackey, H.P. (1982) :
Ontogenetic changes in the projections of neocortical neurons
J. Neurosci., **2** : pp. 735-743

J

Jack, J.J.B. (1979) :
An Introduction to Linear Cable Theory
Chapter 24 in : Neurosciences : The Fourth Study : pp. 423-437
(Eds. Schmitt, F.O., and Worden, F.G.)
The MIT Press, Cambridge, Massachusetts and London, England

Jack, J.J.B., Miller, S., Porter, R., and Redman, S.J. (1971) :
The time course of excitatory post-synaptic potentials evoked in spinal motoneurones by group Ia afferent fibres
J. Physiol., **215** : pp. 353-380

Jack, J.J.B., Redman, S.J., Wong, K. (1981) : The components of synaptic potentials evoked in cat spinal motoneurones by impulses in single group Ia afferents
J. Physiol., **321** : pp.65-96.

Jack, J., Noble, D., Tsien, R. (1983) :
Electrical current flow in excitable tissue
Oxford University Press

Jacobson, S. (1963) :
Sequences of myelinization in the brain of the albino rat. A: Cerebral cortex, thalamus and related structures
J. Comp. Neurol., **121** : pp.5-29

Jacobson, S., and Trojanowski, J.Q. (1974) :
The cells of origin in the corpus callosum in the rat, cat, andrhesus monkey
Brain Res., **74** : pp. 149-155

Jacobson, S., and Trojanowski, J.Q. (1975) :
The appearance of dendrites of callosal and corticothalamic neurons in somatosensory cortex of immature rats demonstrated by horseradish peroxidas
Adv. Neurol., **12** : pp.319-333

Jen, L.S., So, K., Xiao, Y., Diao, Y., Wang, Y., and Pu, M. (1984) :
Correlation between the visual callosal connections and the retinotopic organisation in the striate-peristriate border region in the hamster. An anatomical and physiological study
Neurosci., **13** : pp.1003-1010.

Jones, E.G. (1984) :
Laminar distribution of cortical efferent cells
Chapter 16 in : Cerebral Cortex Vol.I: pp.521-553
Eds. Peters, A. and Jones, E.G.
Plenum N.Y.

Jones, E.G. (1976) :
Commisural, cortico-cortical and thalamic "columns" in the somatic sensory cortex of primates
In : Afferent and Intrinsic Organization of Laminated Structures in the Brain :
(Ed.Creutzfeldt, O.D.)
Exp. Brain Res., Suppl.1 : pp. 309-316

Jones, E.G. (1981) :
Development of connectivity in cerebral cortex
in: Studies in Developmental Neurobiology
(ed. Cowan, W.M.) pp. 354-394.
Oxford University Press, Oxford

Jones, E. G. (1985) :
The Thalamus
Plenum, N.Y.

Jones, K.A., and Baughman, R.W. (1988) :
NMDA and non-NMDA-receptor components of excitatory synaptic potentials recorded from cells in layer 5 of rat visual cortex
J. Neurosci., **8** : pp.3522-3534

Juraska, J.M. (1982) :
The development of pyramidal neurons after eye opening in the visual cortex of the hooded rat:
A quantitative study
J. Comp. Neurol., **212** : pp. 208-213

Juraska, J.M., and Fifkova, E. (1979a) :
A Golgi study of the early postnatal development of the visual cortex of the hooded rat
J. Comp. Neurol., **183** : pp. 247-256

Juraska, J.M., and Fifkova, E. (1979b) :
An electron microscope study of the early postnatal development of the visual cortex of the hooded rat
J. Comp. Neurol., **183** : pp. 257-268

K

Katz, L.C., Burkhalter, A., and Dreyer, W.J. (1984) :
Fluorescent latex microspheres as a retrograde neuronal marker for *in vivo* and *in vitro* studies of visual cortex
Nature, **310** : pp. 498-500

Katz, L.C. (1987) :
Local circuitry of identified projection neurons in cat visual cortex brain slices
J. Neurosci., **7** : pp. 1223-1249

Kawamura, K. , and Konno, T. (1979) :
Various types of corticotectal neurons in cat as demonstrated by means of retrograde axonal transport of horseradish peroxidase
Exp. Brain Res., **35** : 161-175

Keizer, K., Kuypers, H.G.J.M., and Ronday (1987) :
Branching cortical neurons in cat which project to the colliculi and to the pons:
a retrograde fluorescenct double-labeling study
Exp. Brain es., **67** : pp.1-15

Klein, B.G., Mooney, R.D., Fish, S.E., and Rhoades, R.W. (1986) :
The structural and functional characteristics of striate cortical neurons that innervate the superior colliculus and the lateral posterior nucleus in hamster
Neurosci., **17** : pp. 57-78

Kölliker, A., von (1849) :
Neurologische Bemerkungen
Z.Wiss. Zool. Abt. A., **1** : pp 135-166

Kölliker, A., von (1852) :
Handbuch der Gewebelehre des Menschen. 2. Aufl., pp. 274, 275, 306.
Leipzig, Engelmann, 2 Bd.

Konnerth, A., Lux, H.D., and Heinemann, U. (1986) :
Ionic Properties of Burst Generation in Hippocampal Pyramidal Cell Somata in vitro
Ca^{2+} Electrogenesis and Neuronal Functions
(Eds. Heinemann, U., Klee, M., Neher, E., and Singer, W.)
Exp. Brain Res.Suppl.Series 14,

Kriegstein, A.R., Connors, B.W. (1986) :
Cellular Physiology of the Turtle Visual Cortex : Synaptic Properties and Intrinsic Circuitry
J. Neurosci., **6** : pp.178-191

Kriegstein, A.R., Suppes,T., and Prince, D.A. (1987) :
Cellular and synaptic physiology and epileptogenesis of developing rat neocortical neurons in vitro
Dev. Brain Res., **34** : pp.161-171

Kriegstein, A.R., Blanton, M.G., and LoTurco, J.J. (1989) :
Whole-cell voltage-clamp of synaptic currents recorded from morphologically identified neurons in slices of rat neocortex
Soc. of Neurosc. Abstracts, **15**, No. 516.10

Kristt, D.A. (1978) :
Neuronal differentiation in somato-sensory cortex of the rat
I. Relationship to synaptogenesis in the first postnatal week
Brain Res., **150** : pp.467-48.

Kuhnt, U., Kelly, M.J., and Schaumberg, R. (1979) :
Transsynaptic transport of porcion-yellow in the central nervous system
Exp. Brain Res., **35** : pp. 371-385

L

Lancaster, B., and Adams, P.R. (1986) :
Calcium-dependent current generating the afterhyperpolarization of hippocampal neurons
J. of Neurophysiol., **55** : pp. 1268-1282.

Larkman, A., (1991a) :
Dendritic morphology of pyramidal neurones of the visual cortex of the rat:
I.Branching pattern
J. Comp. Neurol., **306** : pp. 307-319

Larkman, A. (1991b) :
Dendritic morphology of pyramidal neurones of the visual cortex of the rat:
II. Parameter correlations
J. Comp. Neurol., **306** : pp. 320-331

Larkman, A. (1991c) :
Dendritic morphology of pyramidal neurones of the visual cortex of the rat:
III. Spine distribution
J. Comp. Neurol., **306** : pp. 332-343

Larkman, A., Mason, A., and Blakemore, C. (1988) :
The in vitro slice preparation for combined morphological and electrophysiological studies of rat visual cortex
Neurosci. Res., **6** : pp. 1-19

Larkman, A., and Mason, A. (1990) :
Correlations Between Morphology and Electrophysiology of Pyramidal Neurons in Slices of Rat Visual Cortex : I. Establishment of Cell Classes
J. Neurosci., **10** : pp. 1407-1414

Legg, C.R., Mercier, B., and Glickstein, M. (1989) :
Corticopontine projection in the rat: The distribution of labelled cortical cells after large injections of Horseradish Peroxidase in the pontine nuclei
J.Comp.Neurol., **286** : pp. 427-441

Lemmon V., and Pearlman, A.L. (1981) :
Does laminar position determine the receptive field properties of cortical neurons ?
J. Neurosci., **1** : pp. 83-93

Lewis, W.B., and Clarke, H. (1878) :
The cortical lamination of the motor area of the brain
Proc. Roy. Soc. (London), **27** : pp. 38-49

Llinas, R., and Nickolsen, C. (1971) :
Electrophysiological properties of dendrites and somata in alligator Purkinje cells
J. Neurophysiol., **34** : pp.532-551

Llinas, R., and Sugimori, M. (1979) :
Calcium conductances in Purkinje cell dendrites: their role in development and integration.
Prog. Brain Res., **51** : pp.323-334

Llinas, R., and Sugimori, M. (1980) :
Electrophysilogical properties of in vitro Purkinje cell somata in mammalian cerebellar slices
J. Physiol., **305** : pp. 171-195

Llinas, R., and Lopez-Barneo, J. (1988) :
Electrophysiology of mammalian tectal neurons in vitro. II. Long-term adaptation
J. Neurophysiol., **60** : pp. 869-878

Lohmann, H., Rörig, B., and Algür, Y. (1991) :
Correlation of physiological and morphological properties of pyramidal cells in extrastriate cortex of the rat in vitro
Proceedings of the german neurobiol.-conf., Göttingen : p. 233
Thieme-Verlag

Lopez-Barneo, J., and Llinas, R. (1988) :
Electrophysiology of mammalian tectal neurons in vitro. I. Transient ionic conductances
J. of Neurophysiol., **60** : pp.853-568

Lorente de No, R. (1943) :
Cerebral cortex: Architecture, intracortical connections, motor projections
Chapter XV in : Physiology of the Nervous System, 2nd ed., pp. 274-313
Fulton, J.F.
Oxford University Press, Oxford

Luhmann, H.J., and Prince, D.A. (1991) :
Postnatal maturation of the GABAergic system in rat neocortex
J. Neurophysiol., **65** : pp. 247-263

Lund, J. S., Lund, R. D., Hendrickson, A.E., Bunt, A.H., and Fuchs, A.F. (1975) :
The origin of efferent pathways from the the primary cortex, area 17, of the macaque monkey as shown by retrograde transport of horseradish peroxidase
J.Comp. Neurol., **164** : pp. 287-304

Luskin, M.B., and Shatz, C.J. (1985) :
Studies of the earliest generated cells of the cats visual cortex: cogeneration of subplate and marginal zones
J. Neurosci., **5** : pp. 1062-1075

Luskin, M.B., Pearlman, A.L., and Sanes, J.R. (1988) :
Cell lineage in the cortex of the mouse studied in vivo and in vitro with a recombinant retrovirus
Neuron, **1** : pp. 635-647

Lynch, G. and Schubert, P. (1980) :
The use of in vitro brain slices for multidisciplinary studies of synaptic function
Ann. Rev. Neurosci., **3**: pp. 1-22

M

MacDermott, A.B., and Westbrook, G.L. (1986) :
Early development of voltage-dependent sodium currents in cultered mouse spinal cord neurons
Dev. Biol., **113** : pp. 317-326

Magalhaes-Castro, H.H., Saraiva, P.E., and Magalhaes-Castro, B. (1975) :
Identification of corticotectal cells of the visual cortex of cats by means of horseradish peroxidase
Brain Res., **83** : pp. 474-479

Marin-Padilla, M. (1967) :
Number and distribution of spical dendritic spines of the layer 5 pyramidal cells in man
J. Comp. Neurol., **131** : pp. 475-490

Marin-Padilla, M. (1971) : Early prenatal ontogenesis of the cerebral cortex (neocortex) of the cat (*Felix domestica*): A Golgi study. I. The primordial neocortical organization
Z.Anat. Entwickl.-Gesch., **134** : pp. 117-145

Marin-Padilla, M. (1972) :
Prenatal ontogenetic history of the principal neurons of the neocortex of the cat (*Felix domestica*): A Golgi study II. Developmental differences and their significance
Z.Anat. Entwickl.-Gesch., **136** : pp. 125-142

Marin-Padilla, M., and Stibitz, G.R. (1968) :
Distribution of the spical dendritic spines of layer 5 pyramidal cells of the hamster neocortex Brain Res., **11**: pp. 580-592

Martin, K.A.C., and Whitteridge, D.
The relationship of receptive field properties to the dendritic shape of neurons in the cat striate cortex
J. Physiol., **356** : pp. 291-302

Mason, A., and Larkman, A.U. (1990) :
Correlations between morphology and electrophysiology of pyramidal neurons in slices of rat visual cortex: II. Electrophysiology
J. Neurosci., **10** : pp.1415-1428

Mason, A., Nicoll, A., and Stratford, K. (1991) :
Synaptic transmission between individual pyramidal neurons of the rat visual cortex *in vitro*
J. Neurosci., **11** : pp. 72-84

Mathers, L.H. (1978) :
Postnatal dendritic development in the rabbit visual cortex
Brain Res., **168** : pp. 21-99

Mathers, L.H., Chow, K.L., Spear, P.D., and Grobstein, P. (1974) :
Ontogenesis of receptive fields in the rabbit striate cortex
Exp. Brain Res., **19** : pp. 20-35

Mauss, T. (1908) :
Die faserarchitektonische Gliederung der Großhirnrinde bei den niederen Affen
J. Psychol. Neurol., **13** : pp.263-325

McConnel, S.K. (1988) :
Development and decicion-making in the mammalian cerebral cortex
Brain Res. Rev., **13** : pp. 1-23

McCormick, D.A., Connors, B.W., Lighthall, J.W., Prince, D.A. (1985) :
Comparative electrophysiology of pyramidal and sparsely spiny stellate neurons of the neocortex
J. Neurophysiol., **54** : pp.782-806

McCormick, D.A., and Prince, D.A. (1987) :
Post-natal development of electrophysiological properties in rat cerebral cortical pyramidal neurones
J.Physiol., **393** : pp. 743-762

McCormick, D.A., and Prince, D.A. (1988) :
Noradrenergic modulation of firing pattern in guinea pig and cat thalamic neurons,*in vitro*
J. Neurophysiol., **59** : pp. 978-996

Meynert, T. (1867-1868) :
Der Bau der Großhirnrinde und seine örtlichen Verschiedenheiten,
nebst einen pathologisch-anatomischen Corollarium.
Vierteljahresschr. Psychiatr. 1867, **1**: pp. 77-93; 125-217 and 1868 **2** : pp.381-403
3 : 88, 133

Meynert, T. (1869-1872) :
Von Gehirne der Säugethiere.
Handbuch der Lehre von den Geweben des Menschen und der Thiere
(ed. Stricker) **2** : pp. 694-808

Michaelson, H.M., and Lothman, E.W. (1989) :
An in vivo electrophysiological study of the ontogeny of excitatory and inhibitory processes in the rat hippocampus
Dev. Brain Res., **47** : pp. 113-122

Miles, R., Wong, R.K. (1986) :
Excitatory synaptic interactions between CA3 neurons in the guinea-pig hippocampus
J. Physiol., **373** : pp.397-418

Miller, M. (1981) :
Maturation of rat visual cortex: I. A quantitative study of Golgi-impregnated pyramidal neurons
J. Neurocytol., **10,** : pp. 859-878

Miller, M. (1986) :
Maturation of rat visual cortex: III. Postnatal morphogenesis and synaptogenesis of local circuit neurons
Dev. Brain Res., **25** : pp.271-285

Miller, M. (1986) :
The nigration and differentiation of GABA immunoreactive neurons in rat visual cortex as demonstrated by a combined Immunocytochemical-autoradiographic technique
Dev. Brain Res., **28** : pp.41-46

Miller, M. (1988a) :
Maturation of rat visual cortex: IV. The generation, migration , morphogenesis , and connectivity of atypically oriented pyramidal neurons
J. Comp. Neurol., **274**, : pp. 387-405

Miller, M. (1988b) :
Development of projection and local circuit neurons in neocortex
In : Cerebral Cortex Vol.VII, pp.133-175
(Eds. Peters, A., and Jones, E.G.)
Plenum, N.Y.

Miller, M., Peters, A. (1981) :
Maturation of rat visual cortex II. A combined Golgi-electron microscope study of pyramidal neurons.
J. Comp. Neurol., **203** : pp. 555-573

Miller, M., and Vogt, B.A. (1984a) :
The postnatal growth of the callosal connections of primary and secondary visual cortex in the rat
Dev. Brain Res., **14** : pp. 304-309

Miller, M., and Vogt, B.A. (1984b) :
Direct connections of rat visual cortex with sensory, motor and association cortices
J. Comp. Neurol., **226** : pp.184-202

Miller, M., and Vogt, B.A. (1984c) :
Heterotopic and homotopic callosal connections in rat visual cortex
Brain Res., **297** : pp.75-89

Mitchell, D.E., and Blakemore, C.B. (1970) :
Binocular depth perception and the corpus callosum
Vision Res., **10** : pp. 49-54

Montoro, R.J., Lopez-Barneo, J., and Jassik-Gerschenfeld, D. (1988) :
Differential burst firing modes in neurons of the mammalian visual cortex in vitro
Brain Res., **460** : pp.168-172

Mueller, A.L., Taube, J.A., and Schwartkroin, P.A. (1984) :
Development of hyperpolarizing inhibitory postsynaptic potentials and hyperpolarizing response to GABA in rabbit hippocampus studied *in vitro*
J. Neurosci., **4** : pp. 860-867

N

Nauta, W.J.H. and Bucher ,V.M. (1954) :
Efferent connections in the striate cortex of the albino rat
J.Comp.Neurol., **100** : pp. 257-281

O

O'Leary, D.D.M, and Stanfield, B.B. (1985) :
Occipital cortical neurons with transient pyramidal tract axons extend and maintain collaterals to subcurtical but not to intracortical targets
Brain Res., **336** : pp. 326-333

O'Leary, D.D.M, and Stanfield, B.B. (1986) :
A transient pyramidal tract projection from the visual cortex in hamster and its removal by selective axon collateral elimination
Dev. Brain Res., **27** : pp. 87-99

O'Leary, D.D.M., and Terashima, T. (1988) :
Cortical axons branch to multiple subcortical targets by interstitial axon budding: implications for target recognition and "waiting periods"
Neuron, **1** : pp. 901-910

O'Leary, D.D.M., Bicknese, A.R., DeCarlos. J.A., Heffner, C.D., Koester, S.E. Kutka, L.J., and Terashima, T. (1990) :
Target selection by cortical axons: alternative mechanisms to establish axonal connections in the developing brain
Cold Spring Harbor Symp. Quant. Biol., **LV** : pp.453-468
CLH Press

Olavarria, J.O., and van Sluyters, R.C. (1983) :
Widespread callosal connection in infragranular visual cortex of the rat
Brain Res., **279** : pp. 233-237

Olavarria, J.O., and van Sluyters, R.C. (1984) :
Callosal connections of the posterior neocortex in normal eyed, congenitally anophtalmic and neonatally enucleated mice
J. Comp. Neurol., **230** : pp. 249-268

Osmanovic, S.A., and Shefner, S.A. (1987) :
Anomalous rectification in rat locus coeruleus neurons
Brain Res., **417** : pp. 161-166

P

Palmer , L.A., and Rosenquist, A.C. (1974) :
Visual receptive fields of single striate cortical units projecting to the superior colliculus in cat
Brain Res., **67** : pp. 27-42

Parnavelas, J.G., Liebermann, A.R., and Webster , K.E. (1977) :
Orgenization of neurons in the visual cortex, area 17, in the rat
J. Anat., **124** : pp. 305-322

Parnavelas, J.G., Liebermann, A.R. (1979) :
An ultrastructural study of the maturation of neuronal somata in the visual cortex of the rat
Anat. and Embryol., **157** : pp.311-328

Parnavelas, J.G., Burne, R.A., and Lin, C.-S. (1983) :
Distribution and Morphology of functionally identified neurons in the visual cortex of the rat.
Brain Res., **261** : pp.21-29

Penit-Soria, J., Audinat, E., and Crepel, F. (1987) :
Excitation of the rat prefrontal cortical neurons by dopamine: an *in vitro* electrophysiological study
Brain Res., **425** : pp. 263-274

Peters, A. (1980) :
Morphological correlates of epilepsy: cells in the cerebral cortex.
Antiepileptic Drugs : Mechanisms of action; pp. 21-48
(Ed. Glaser, G.H., Peury, J.K., Woodburn, D.M.)
Raven Press, New York

Peters, A. (1984) :
The visual cortex of the rat
Chapter 2 in : Cerebral Cortex Vol III. pp. 19-80
(Ed. Peters, A. and Jones, E.G.)
Plenum, N.Y.

Peters, A., and Feldman, M. (1973) :
The cortical plate and molecular layer of the late rat fetus
Z. Anat. Entwickl.-Gesch., **141** : pp. 3-37

Peters, A. and Jones, E.G. (Eds.) (1984)
Cerebral Cortex
Volume I. Cellular Components of the Cerebral Cortex
Plenum, N. Y.

Peters A. and Jones, E.G. (Eds.) (1985a)
Cerebral Cortex
Volume II. Cellular Properties
Plenum, N.Y.

Peters A. and Jones, E.G. (Eds.) (1985b)
Cerebral Cortex
Volume III. Visual Cortex
Plenum, N.Y.

Peters, A., and Kara, D.K. (1985) :
The neuronal composition of area 17 of rat visual cortex : I. The pyramidal cells
J. Comp. Neurol., **234** : pp. 218-241

Peters, A., Kara, D.K., Harriman, K.M. (1985) :
The neuronal composition of area 17 of rat visual cortex : III. Numerical considerations
J. Comp. Neurol., **238** : pp. 263-274

Peters, A., Proshauer, H., Feldmann, L.M., and Kimerer, L. (1979) :
The projection of the lateral geniculate nucleus to area 17 of the rat cerebral cortex
J. Neurophysiol., **8** : pp.331-335

Petit, T.L., Le Boutellier, J.C., Gregorio, A., and Libstug, H. (1988) :
The pattern of dendritic development in the cerebral cortex of the rat
Dev. Brain Res., **41** : pp. 209-219

Pockberger, H. (1991) :
Electrophysiological and morphological properties of rat motor cortex neurons in vivo
Brain Res., **539** : pp.181-190

Price, J., and Thurlow, L. (1988) :
Cell lineage in the rat cerebral cortex: a study using retroniral-mediated gene transfer
Development, **104** : pp. 473-482

Prince, D.A., and Gutnick, M.J. (1972) :
Neuronal activities in epileptogenic foci of immature cortex
Brain Res., **45** : pp.455-468

Prince, D.A., and Huguenard, J.R. (1988) :
Functional properties of neocortical neurons
in : Neurobiology of Neocortex : pp. 153-176
(ed. Rakic, P., and Singer,S.)
John Wiley & Sons Ltd., Chichester

Purpura, D.P., Snofer, R.J., and Scarff, T. (1965) :
Properties of synaptic activity and spike potentials of neurones in immature neocortex
J. Neurophysiol., **28** : pp.925-942

Purpura, D.P. (1969) :
Stability and seizure susceptiblity of immature brain.
in : Basic Mechanism of the Epilepsies , pp. 481-514
(ed. Jasper, H.H., Ward, A.A., Pope, A.)
Little , Brown & Company, Boston.

R

Rakic, P. (1988) :
Intrinsic and extrinsic determinants of neocortical parcellation : a radial unit model
in : Neurobiology of Neocortex, pp. 5-27
(Eds. Rakic, P., and Singer, W.)
John Wiley &Sons Ltd., Chichester

Rall, W. (1969) :
Time constants and electrotonic length of membrane cylinders and neurons
Biophys.J., **9** : pp. 1483-1508

Ramirez J.J., Sonal Jhaveri, Hahm J., and Schneider G.E. (1990) :
Maturation of projections from occipital cortex to the ventrolateral geniculate and superior colliculus in postnatal hamsters
Dev. Brain Res., **55** : pp. 1-9

Ramon y Cajal, S. (1891) :
Sur la structure de l'ecorce cerebrale de quelques mammifères
La Cellule, **7** : pp. 125-176

Ramon y Cajal, S. (1894) :
La fine structure des centre nerveux.
Proc. Roy. Soc. (London), **55** : pp. 444-468

Ramon y Cajal, S. (1909-1911) :
Histologie du système Nerveux de l'Homme et des Vertebres
Maloine, Paris

Ramon y Cajal, S. (1954) :
Neuron Theory or Reticular Theory? Objective Evidence of the Anatomical Unity of Nerve Cells
Consejo Superior de Investigaciones Cientificas, Madrid

Remak, R. (1841) :
Anatomische Beobachtungen über das Gehirn, das Rückenmark und die Nervenwurzeln
Müller's Arch. Anat. Physiol. Wiss. *1841* : pp. 506-522

Ransom, B.R., Yamate, C.L., and Connors, B.W. (1985) :
Developmental studies on brain extracellular space: activity-dependent K+–accumulation and shrinkage.
In : Ion Measurements in Physiology and Medicine, pp.206-213
(ed. Kessler M.)
Springer-Verlag, Berlin, Heidelberg

Redman, S., and Walmsley, B. (1983) :
The time course of synaptic potentials evoked in cat spinal motoneurones at identified group Ia synapses
J. Physiol., **343** : pp.117-133

Reid, K.H., Edmonds, H.L., Schurr, A., Tseng, M.T., and West, C.A. (1988) :
Pittfalls in the use of brain slices
Prog. Neurobiol., **31** : pp. 1-18

Remak, R. (1841) :
Anatomische Beobachtungen über das Gehirn, das Rückenmark und Nervenwurzeln
Müllers Arch. Anat Physiol. Wiss., *1841* : pp. 506-522

Retzius, M.G. (1893) :
Die Cajalschen Zellen der Großhirnrinde beim Menschen und bei Säugethieren.
Biol. Untersuch. N.F., **4** : pp. 1-9

Retzius, M.G. (1896) :
Das Menschenhirn: Studien in der makroskopischen Morphologie
Norstedt, Stockholm.

Ribak, C.E., and Peters, A. (1975) :
An autoradiographic study of the projections from the lateral geniculate body of the rat
Brain Res., **92** : pp. 341-368

Ribera, A.B., O'Dowd, D.K., and Spitzer, N.C. (1981) :
Maturation of outward currents in amphibian spinal neurons developing in culture
Soc. Neurosci. Abstr., **12** : p.951

Richards, C.D. (1981) :
The preparation of brain tissue slices for electrophysiological studies
Chapter 4 in : Electrophysiology of Isolated CNS-Preparations, pp.107-132
(Ed. Kerkut, G.A. and Wheal, H.V.)
Academic Press, N.Y.

Richburg, F.A., and Kirby, M.A. (1989) :
Development of the corticotectal projection in the neonatal rat
Soc. Neurosci. Abstr., **15** : p. 1337

Rhoades, R.W., and Delacroce, D.D. (1980) :
Visual callosal connections in the golden hamster.
Brain Res., **190** : pp.248-254

Rhoades, R.W., Figley,B., Mooney, R.D., and Fish, S.E. (1991)
Development of the occipital corticotectal projection in the hamster
Exp. Brain Res., **86** : pp. 373-383

Rolls, E.T., and Cowey, A. (1970) :
Topography of the retina and striate cortex and its relation ship to visual acuity in
rhesus monkeys and squirrel monkeys
Exp. Brain Res., **10** : pp. 298-310

Ross, W.N., SalzbergB.M., Cohen, L.B., Grinvald, A., Davila, H.V., Waggoner,
A.S. and Wang, C.H. (1977) :

Changes in absorption, fluorescence , dichroism, and birefringence in stained giant axons:
Optical measurement of the membrane potential
J. Membrane Biol., **33** : pp. 141-183

Rowe, M.H., and Stone, J. (1976) :
Properties of ganglion cells in the visual streak of the cat's retina
J. Comp. Neurol., **169** : pp. 99-126

S

Samejima, A., Yamamoto, T., Ito, J., and Oka, H. (1985) :
Two groups of corticofugal neurons identified with the pontine stimulation in the cat parietal assoziation cortex. An intracellular HRP study.
Brain Res., **347** : pp. 117-120

Sauer, F.C. (1935) :
Mitosis in the neural tube
J.Comp. Neurol., **62** : pp. 377-405

Schmitt, F.O., Dev, P., and Smith, B.H. (1976) :
Electrotonic processing of information by brain cells
Science, **193** : pp. 114-120

Schobert, W., and Winkelman, E. (1975) :
Der visuelle Kortex der Ratte; Cytoarchitectonik und stereotaktische Parameter
Z. mikrosk.-anat. Forsch., **89** : pp.431-446

Schofield,B.R., Hallman, L.E., and Lin, C.-S. (1987) :
Morphology of corticotectal cells in the primary visual cortex of the hooded rat
J. Comp. Neurol., **261** : pp. 85-97

Schurr, A., Reid, K.H., Tseng, M.T., and Edmonds, H.L.Jr. (1984) :
The stability of the hippocampal slice preparation: an electrophysiological and ultrastructural analysis
Brain Res., **297** : pp. 357-362

Schwartzkroin, P.A. (1981) :
To slice or not to slice
Chapter 2 in : Electrophysiology of Isolated CNS-Preparations : pp.15-49
(Ed. Kerkut, G.A. and Wheal, H.V.)
Academic Press, Lonndon

Schwartzkroin, P.A. (1982) :
Development of rabbit hippocampus: physiology
Dev. Brain Res., **2** : pp. 469-486

Schwartzkroin, P.A., Kunkel, D.D. (1982) :
Electrophysiological and morphology of the developing hippocampus of fetal rabbits
J. Neurosci., **2** : pp. 448-462

Schwindt, D.C., Spain, W.J., Foehring, R.C., Stafstrom, C.E., Chubb, M.C., and Crill,W.E. (1988) :
Multiple potassium conductances and their functions in neurons from cat sensimotorcortex
in vitro
J. Neurophysiol., **59** : pp. 424-449

Schwob, J.E., Haberly, L.B., and Price, J.L. (1984) :
The development of physiological responses of the piriform cortex in rats to stimulation of the lateral olfactory tract
J. Comp. Neurol., **223** : pp. 223-237

Sefton, A.J., Mackay-Sim, A., Baur, L.A., and Cottee, L.J. (1981) :
Cortical projections to visual centers in the rat: An HRP study.
Brain Res., **215** : pp. 1-13

Sefton, A.J., and Dreher, B. (1985) :
Visual System
In : The rat nervous system, Vol.I: Forebrain and Midbrain
(Ed. Paxinos, G.)
Academic Press, Sydney

Shatz, C.J. (1977) :
Anatomy of interhemispheric connections in the visual system of Boston siamese and ordinary cats
J. Comp. Neurol., **173** : pp. 497-518

Shimada, M., and Langman, J. (1970) :
Cell proliferation , migration and differentiation in the cerebral cortex of the golden hamster
J. Comp. Neurol., **139** : pp. 227-244

Sidman, R.L., and Rakic, P. (1973) :
Neuronal migration, with special reference to developing human brain: a review
Brain Res., **62** : pp. 1-35

Sloper, J.J. (1972) :
Gap junctions between dendrites in the primate neocortex
Brain Res., **44** : pp. 641-646

Sloper, J.J. and Powell, T.P.S. (1978) :
Gap junctions between dendritic and somata of neurones in the primate sensorimotor cortex
Proc. Roy. Soc. Lond. (Biol.), **203** : pp. 39-47

Snead III, O.C., and Stephens, H.I. (1983) :
Ontogeny of cortical and subcortical electro-encephalographic events in unrestrained neonatal and infant rats
Exp. Neurol., **82** : 249-269

Spain, W.J., Schwindt, P.C., and Crill, W.E. (1987) :
Anomalous rectification in neurons from cat sensorimotor cortex in vitro
J. Neurophysiol., **57**, pp. 1555-1574

Spatz, W.S. (1976) :
The laminar distribution of neurons projecting onto the visual area MT
Exp. Brain Res., Suppl.1: pp. 305-308

Spitzer, N.C. (1982) :
The development of electrical excitability
In : Neuronal-Glial Cell Interrelationships pp. 77-91
(ed. Sears, T.A.)
Springer, New York

Strafstrom, C.E., Schwindt, P.C., and Crill, W.E. (1982) :
Negative slope conductance due to a persistant subthreshold sodium current in cat neocortical neurons in vitro
Brain Res., **236** : pp.221-226

Stafstrom, C.E., Schwindt, P.C., Flatman, J.A., and Crill, W. E. (1984) :
Properties of subthreshold response and action potential recorded in layer 5 of cat somatosensory cortex in vitro
J. Neurophysiol., **52** : pp. 244-263

Stafstrom, C.E., Schwindt, P.C., Chubb, M.C., and Crill, W. E. (1985) :
Properties of persistent sodium conductance and calcium conductance of layer V neurons from cat sensorimotor cortex in vitro.
J. Neurophysiol., **53** : pp.153-170.

Steriade, M. and , Llinas, R. (1988) :
The functional states of the thalamus and the associated neuronal interplay
Physiol. Rev., **68** : pp. 649-742

Stewart, W.W. (1978) :
Neuronal mapping: A photooxidation reaction makes Lucifer Yellow usefull for electron microscopy
Science, **217** : pp.953-955

Stewart, W.W. (1981) :
Lucifer Dyes – highly fluorescent dyes for biological tracing
Nature, **292** : pp. 17-21

Sutor, B., and Zieglgänsberger, W. (1987) :
A low voltage activated, transient calcium current is responsible for the time dependent inward rectification of rat neocortical neurons *in vitro*
Pflügers Arch., **410** : pp. 102-111

Swadlow, H., Weyand, T, and Waxman, S. (1978) :
The cells of origin of the corpus callosum in rabbit visual cortex
Brain Res., **156** : pp. 129-134

Swadlow, H. (1983) :
Efferent systems of the primary visual cortex: a review of structure and function
Brain Res. Rev., **6** : pp. 1-24

Swadlow, H. (1988) :
Efferent neurons and suspected interneurons in binocular visual cortex of the awake rabbit :
Receptive fields and binocular properties
J. Neurophysiol., **59** : pp.1162-1187

T

Takahshi, K., Wakamori, M., and Akaike, N. (1989) :
Hippocampal CA 1 pyramidal cells of rats have four voltage-dependent calcium conductances
Neurosci. Lett., **104** : pp. 229-234

Tauchi, M., and Masland, R.H. (1984) :
The shape and arrangement of the cholinergic neurons in the rabbit retina
Proc. Roy. Soc.B (London), **223** : pp. 101-119

Thomson, A.M. (1986) : A magnesium-sensitive post-synaptic potential in rat cerebral cortex resembles neuronal responses to n-methylaspartate
J. Physiol., **370** : pp. 531-549

Thomson, A.M., Girdlestone D., and West, D.C. (1988) :
Voltage dependent currents prolong single-axon postsynaptic potentials in layer III pyramidal neurons in rat neocortical slices
J. Neurophysiol., **60** : pp.1896-1907

Thong I.G. and Dreher B. (1986) :
The development of the corticotectal pathway in the albino rat
Dev. Brain Res., **25** : pp. 227-238

Thong I.G. and Dreher B. (1987) :
The development of the corticotectal pathway in the albino rat: transient projections from the visual and motor cortices
Nsci. Lett., **80** : pp. 275-282

Toyama, K., Matsunami, K., and Onuo, T. (1969) :
Antidromic identification of association, commissural and corticofugal efferent cells in cat visual cortex
Brain Res., **14** : pp. 513-517

Toyama, K., Matsunami, K., Onuo, T., and Tokashiki, S. (1974) :
An intracellular study of neuronal organisation in the visual cortex
Exp. Brain Res., **21** : pp.45-66

V

Valentin, G.G. (1836) :
Über den Verlauf und die letzten Ende der Nerven.
Nova Acta Phys.-Med. Acad. Leopoldina, Breslau, **18** : pp. 51-240

Valenzeno, D.P., and Pooler, J.P. (1978) :
Inhibition and enhancement of photochemical modification of lobster axon membranes sensitized by dyes or optical probes
Biophys. J., **21** : 43a.

Valverde, F. (1967) :
Apical dendritic spines of the visual cortex and light deprivation in the mouse
Exp. Brain Res., **3** : pp. 337-352

Valverde, F. (1985) :
The organizing principles of the primary visual cortex in the monkey
Chapter 6 in : Cerebral Cortex Vol.III : Visual Cortex,pp. 207-257
(Eds. Peters, A. and Jones, E.G.)
Plenum, N.Y.

Verley, R. (1977) :
The post-natal development of the functional relationships between the thalamus and the cerebral cortex in rats and rabbits
Electroenceph. and Clin. Neurophys., **43** : pp.679-690

Verley, R., and Axelrad, H. (1975) :
Postnatal ontogenesis of potentials elicited in the cerebral cortex by afferent stimulation
Neurosci. Lett., **1** : pp. 99-104

Vogt, O. (1903) :
Zur anatomischen Gliederung des Cortex Cerebri
J. Psychol. Neurol., **2** : pp.160-180

Vogt, C., and Vogt, O. (1919) :
Allgemeinere Ergebnisse unserer Hirnforschung.
J. Psychol. Neurol., **25** : pp.279-462

W

Waggoner, A.S. (1979) :
Dye indicators of membrane potential.
Ann. Rev. Biophys. Bioeng., **8** : pp.47-68

Walton, K., and Fulton, B.P. (1986) :
The ionic mechanism underlying the firing properties of the rat neonatal motoneurones studied in vitro.
Neurosci., **19** : pp.669-683

Weber, J.T., Rieck, R.W., and Gould, H.J. (1983) :
Interhemispheric and subcortical collateralsof single cortical neurons in the adult cat
Brain Res., **276** : pp. 333-338

Westbrook, G.L., and Brenneman, D.E. (1984) :
The development of spontaneous activity in spinal cord culture.
in Dev. Neurosci.: Physiol. Pharm. and Clinical Aspects, pp. 11-17
(ed. Caciagli, F., Giacobini, E., Paoletti, R.)
Elsevier, Amsterdam

Weyand, T. G., and Swadlow, H.A. (1980) :
Interhemispheric projections in the prosimian primate galago senegalensis.
Brain Beh. Evol., **17** : pp. 473-477

Weyand, T.G., Malpeli, J., Choongkil,L., Schwark, H. (1986) :
Cat Area 17: III. Response properties and orientation anisotropies of corticotectal cells.
J. Neurophysiol., **56** : pp. 1088-1108

White, E.L. (1978) :
Identified neurons in mouse Sm I cortex which are postsynaptic to thalamo-cortical axon terminals: a combined Golgi-electronmicroscopic and degeneration study
J. Comp. Neurol., **181** : pp.627-662

Wiesendanger, R., and Wiesendanger, M. (1982) :
The corticopontine system in the rat .I. Mapping of corticopontine neurons
J. Comp. Neurol., **208** : pp. 215-226

Winfield, D.A., Gatter, K.C., and Powell. T.P.S. (1980) :
An electron microscopic study of the types and proportions of neurons in the cortex of the motor and visual areas of the cat and rat
Brain, **103** : pp. 245-258

Wise, S.P., and Jones, E.G. (1976) :
The organization and postnatal development of the commisural projection of the rat somatosensory cortex
J. Comp. Neurol., **175** : pp. 129-158

Wise, S.P., Fleshman, J.W., and Jones, E.G. (1979) :
Maturation of pyramidal cell form in relation to developing afferent and efferent connections of rat somatic sensory cortex
Neurosci., **4** : pp.1275-1297

Wong, D., and Kelly, J.P. (1981) :
The corticothalamic and callosal projections of layer VI in the cats auditory cortex arise from different population of cells
Anat. Rec., **199** : pp. 280A

Wong, R.K.S., and Prince, D.A. (1978) :
Participation of calcium spikes during intrinsic burst firing in hippocampal neurons
Brain Res., **159** : pp.385-390

Wright, L.D., Cresson, E.L., Liebert, K.V., and Sheggs, H.R. (1952) :
Biological studies of biocytin.
J. Am. Chem. Soc., **74** : pp.2004-2006

Y

Yoshii, K., Moore, L.E., and Christensen, B.N. (1988) :
Effects of subthreshold voltage-dependent conductances on the transfer function of branched excitable cells and the condution of synaptic potentials
J. Neurophysiol., **59** : pp.706-716

Z

Zhang, L., Spigelman, I., and Carlen, P.L. (1990) :
Whole cell patch study of GABAergic inhibition in CA1 neurons of immature rat hippocampal slice
Dev. Brain Res., **56** : pp. 127-130

Zilles, K. (1985) :
The Cortex of the Rat, A Stereotaxic Atlas
Springer-Verlag, Berlin, Heidelberg, Tokyo

Zilles, K. (1990) :
Anatomy of the neocortex: Cytoarchitechture and Myeloarchitecture
Chapter 4 in : the Cerebral Cortex of the Rat, pp. 275-307
(Eds. Kolb, B., and Tees, R.C.)
The MIT Press, Cambridge MA

Zilles, K., Wree, A., and Dausch, N.-D. (1990) :
Anatomy of the neocortex: Neurochemical Organisation
Chapter 5 in : The Cerebral Cortex of the Rat : pp. 113-150
(Eds. Kolb, B., and Tees, R.C.)
The MIT Press, Cambridge MA

Zona, C., Pirrone, G., Avoli, M., and Dichter, M. (1988) :
Delayed and fast transient potassium currents in rat neocortical neurons in cell culture
Neurosci. Lett., **94** : pp. 285-290

Appendices :

Appendix 1

Protocol for cresyl violet stain for Nissl substance

Appendix 1

Protocol for cresyl violet stain for Nissl substance :

A) defatting of frozen sections :

1. 100% alcohol for 2 min.
2. Xylene 1 for 2-3 min.
3. Xylene 2 for 20 min.

B) re-hydration :

1. 100% alcohol 1 for 2-3 min.
2. 100% alcohol 2 for 2-3 min.
3. 96% alcohol for 2-3 min.
4. 70% alcohol for 2-3 min.
5. 50% alcohol for 2-3 min.
6. dH_2O for 2-3 min.

C) Staining period with cresyl violet

The protocol for making up and using the cresyl violet solution was as follows :

1. Dissolve 500 mg cresyl violet acetate in 1000ml dH_2O
2. Place solution on heater for 15min. at around 65°C to assist in dissolving crystals
3. Add 3ml glacial acetic acid when solution is cooled down
4. Filter solution and stain the tissue for 10-15min.

D) Differentiation

1. distilled H2O
2. 70% alcohol
3. 70% acid alcohol
4. 96% alcohol for 1-2 min.
5. 100% alcohol 1 for 1-2 min.
6. 100% alcohol 2 for 1-2 min.
7. Xylene 1 for 2 min.
8. Xylene 2 for 2 min.

Sections were subsequently coverslipped with DPX

Appendix 2

Epifuorescence microscopy in combination with a *in vitro* recording technique for studies of back-labelled neurons in brain slices

A) Sketch of the experimental set-up
B) Absorption/Emission curves for the fluoroprobes and respective filter blocks used

Continuous Spectrum; Visible Region about 380-780nm

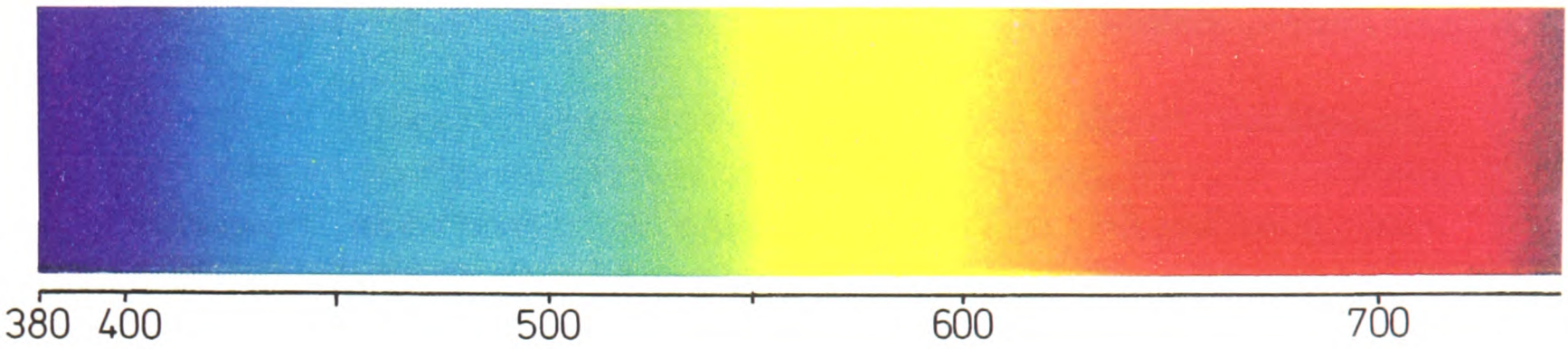

Spectrum Absorption and Emittance of Fluorescent Dyes

B (Blue) Excitation
Main wavelength: 480nm
Sample filter block: *B-2A*

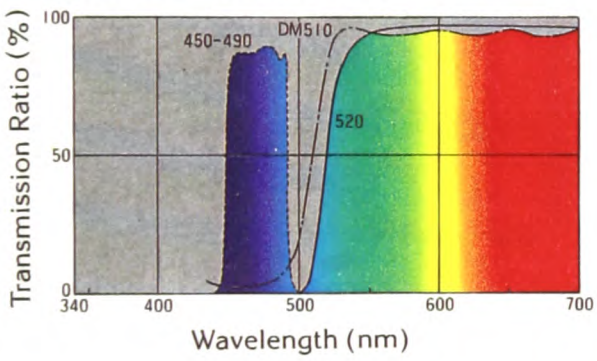

G (Green) Excitation
Main wavelength: 546nm
Sample filter block: *G-2A*

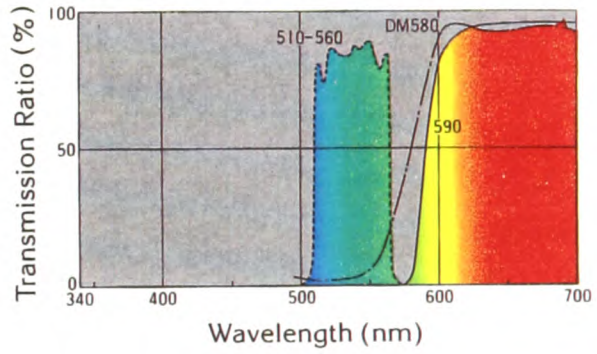

Spectrum Transmission Curves of Nikon Filter Blocks

Fluorescein

Because of the wide excitation range in the short wavelength side below 500 nm. V or B filters can be used (the B range is more efficient)

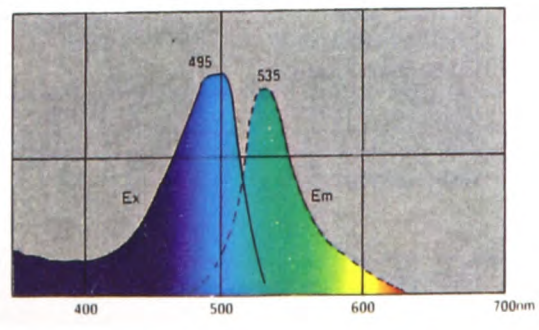

Rhodamine

Most efficiently used in the G excitation range

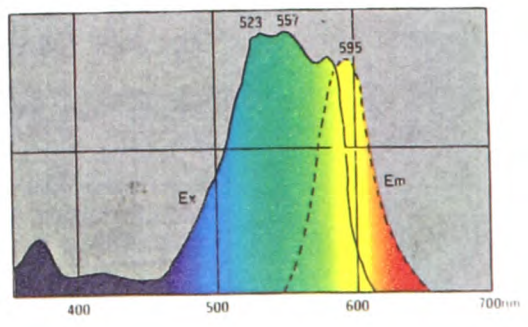

The Optical System of the Epifluorescence Microscope

Fluorescence microscopes comprise two microcopic types –episcopic and diascopic– which differ in features and applications. The recent preference for epifluorecscence microscopy is due to improvements in high-performance objectives, interference filters, mechanical accuracy and operational ease.

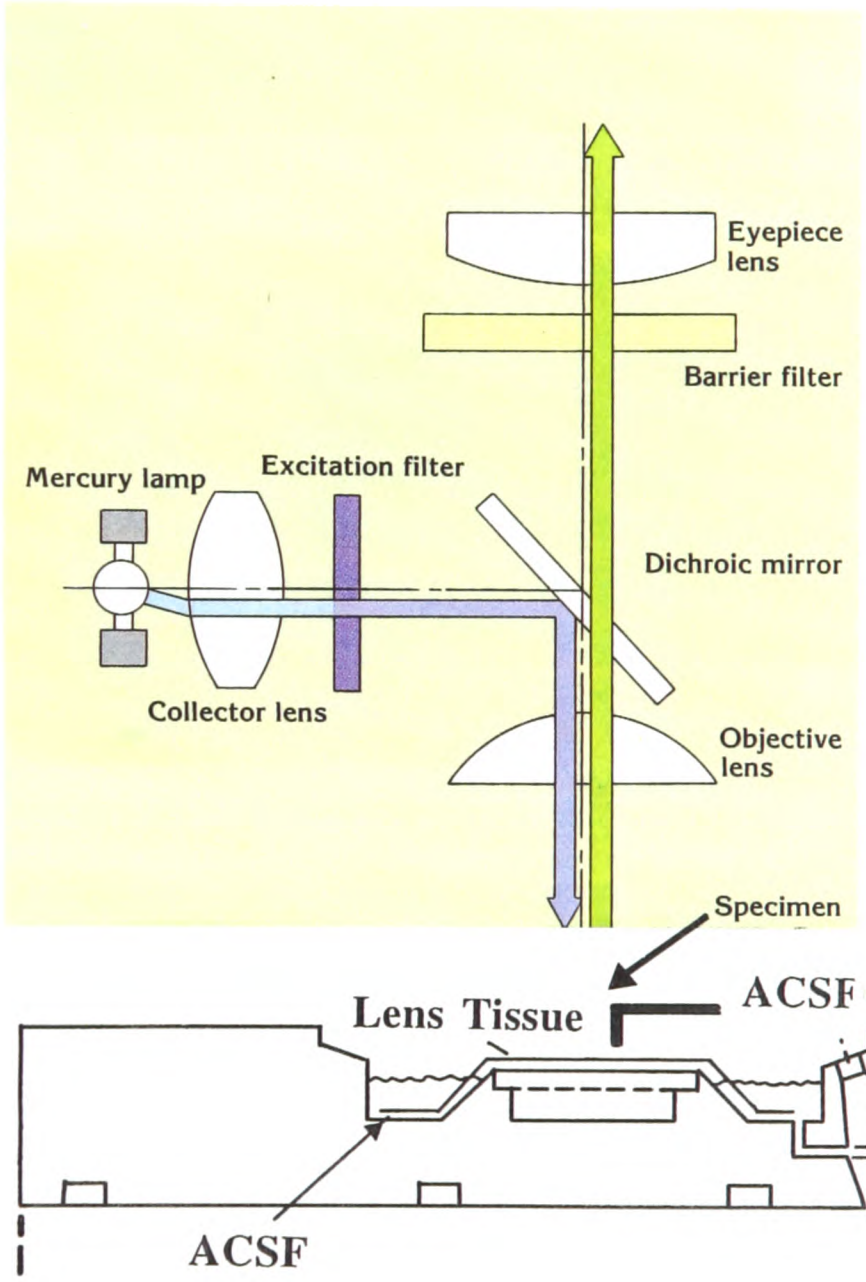

Features of the epi-fluorescence microscope:

Objectives double as condensers, so that focusing on the specimen provides optimum illumination (spot illumination), thus mini-mizing the colour fading area of the specimen.

Appendix 3

Details of an electrode bending technique to produce bent electrodes suitable for precise impalements of back-labelled cells under visual control

Electrode Bending Technique

1) A conventional glass electrode is positioned on the slide-apparatus so that its tip is in a water drop. It is held in this position with a lump of modelling clay.

2) The apparatus is placed under a dissecting microscope and the tip of a platinum wire brought close to the electrode (see Fig. A) with the aid of a micromanpulator.

3) Electrodes are bent with a white hot filament; in this case a 0.127mm platinum wire (Sigma)was used, heated by passing about 1.3A current through it.

4) As the hot filament approaches the point where the electrode is to be bent, the glass softens focally and the terminal region is pulled perpendicular to the water interface by surface tension (see Fig. B).

5) This method allows to bend electrodes in a controlled way, where the angle of the bent is determined by the placement of the filament and the angle at which the electrode enters the drop initially.

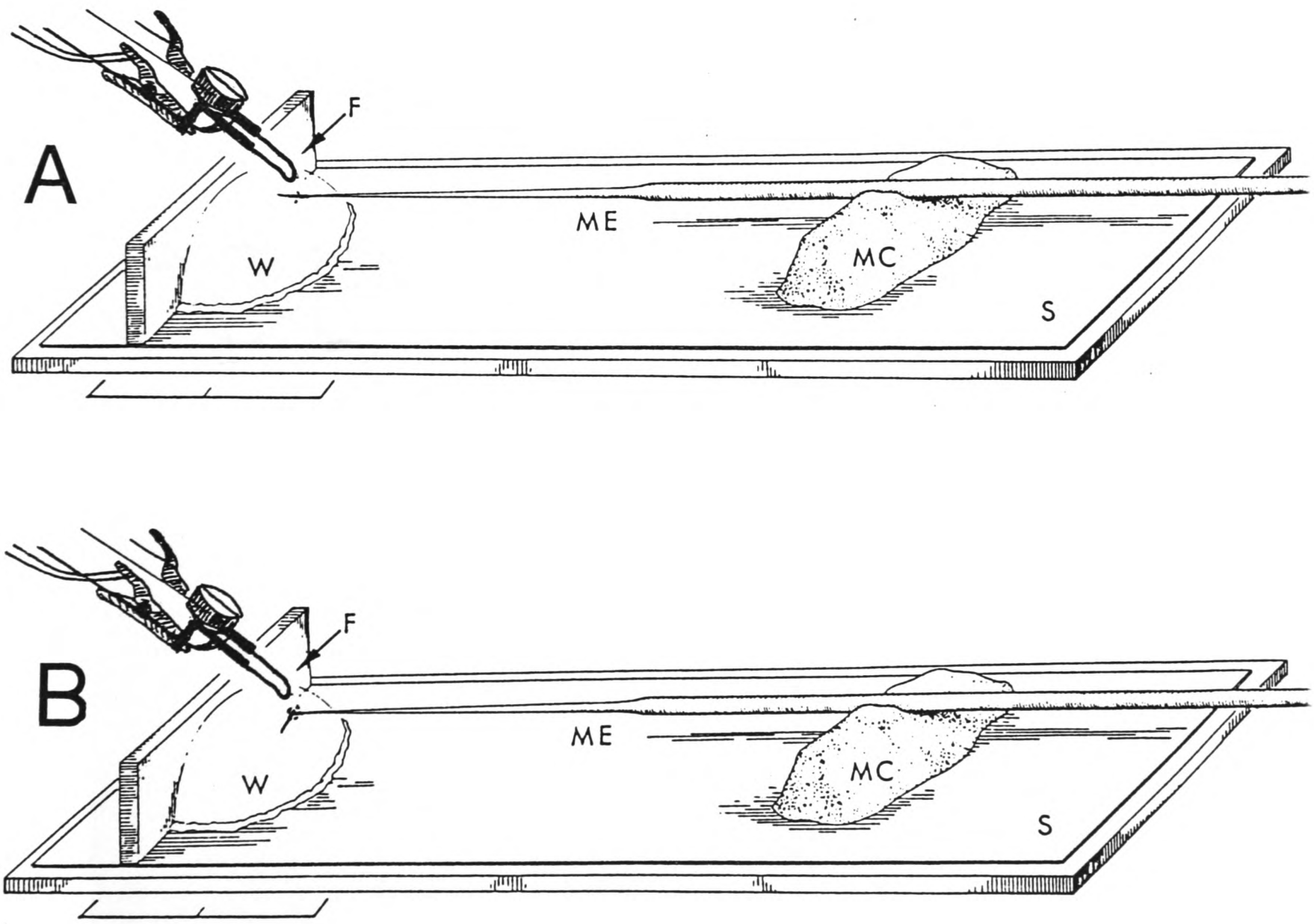

Figure legend:

ME = Microelectrode
S = Microscopic slide
MC = Modelling clay
W = Water drop
F = Platinum filament

Equipment for electrode bending

1) Narashige
   Micromanipulator

2) Zeiss Dissection
   Microscope

3) Homebuilt
   Wire Holder

4) Electrode
   Positioner

5) Platinum wire

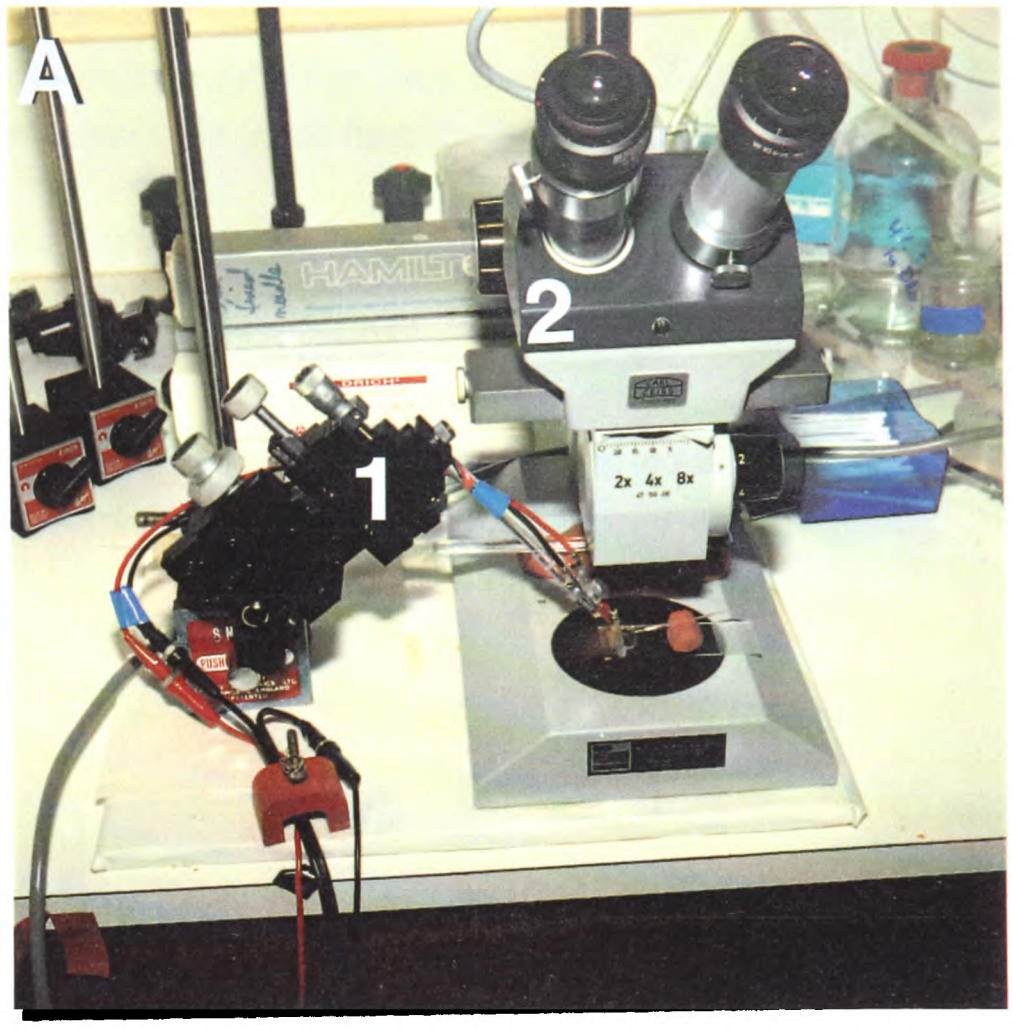

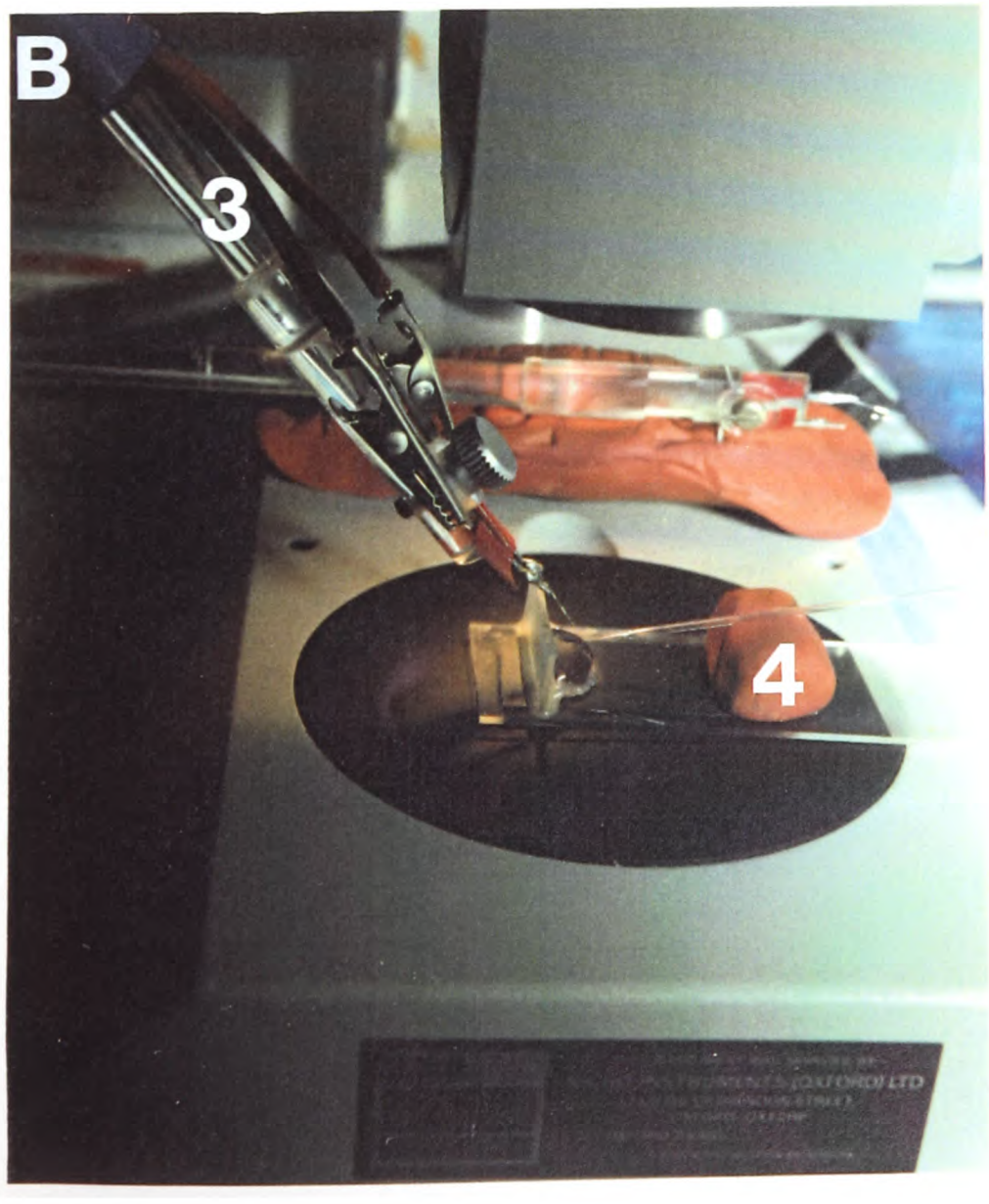

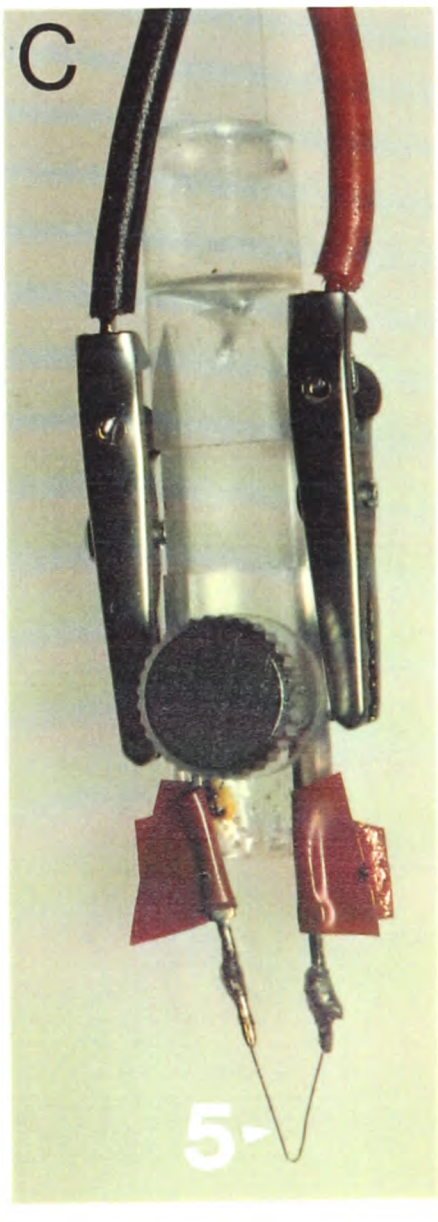

Appendix 4

Injection of fluorescent microspheres into the superior colliculus or the contralateral hemisphere

A) Injection sites and coordinates for tracer injections into adult animals, including line drawings of two representative injection sites for each injected area

B) Plates illustrating the non-stereotactic procedure in immature animals in which the midbrain can be exposed dorsally

Stereotactic Coordinates for Tracer Injections in Adult Rats

① SUPERIOR COLLCULUS

bregma	interaural	lateral	depth
-5.8	+3.2	1.0	4.0
-6.8	+2.2	1.5	3.5
-7.8	+1.2	1.0	3.5

② CONTRALATERAL HEMISPHERE

bregma	interaural	lateral	depth
-5.8	+3.2	4.0	2.0
-6.8	+2.2	3.5	1.75
-7.8	+1.2	3.5	1.5

all values in mm

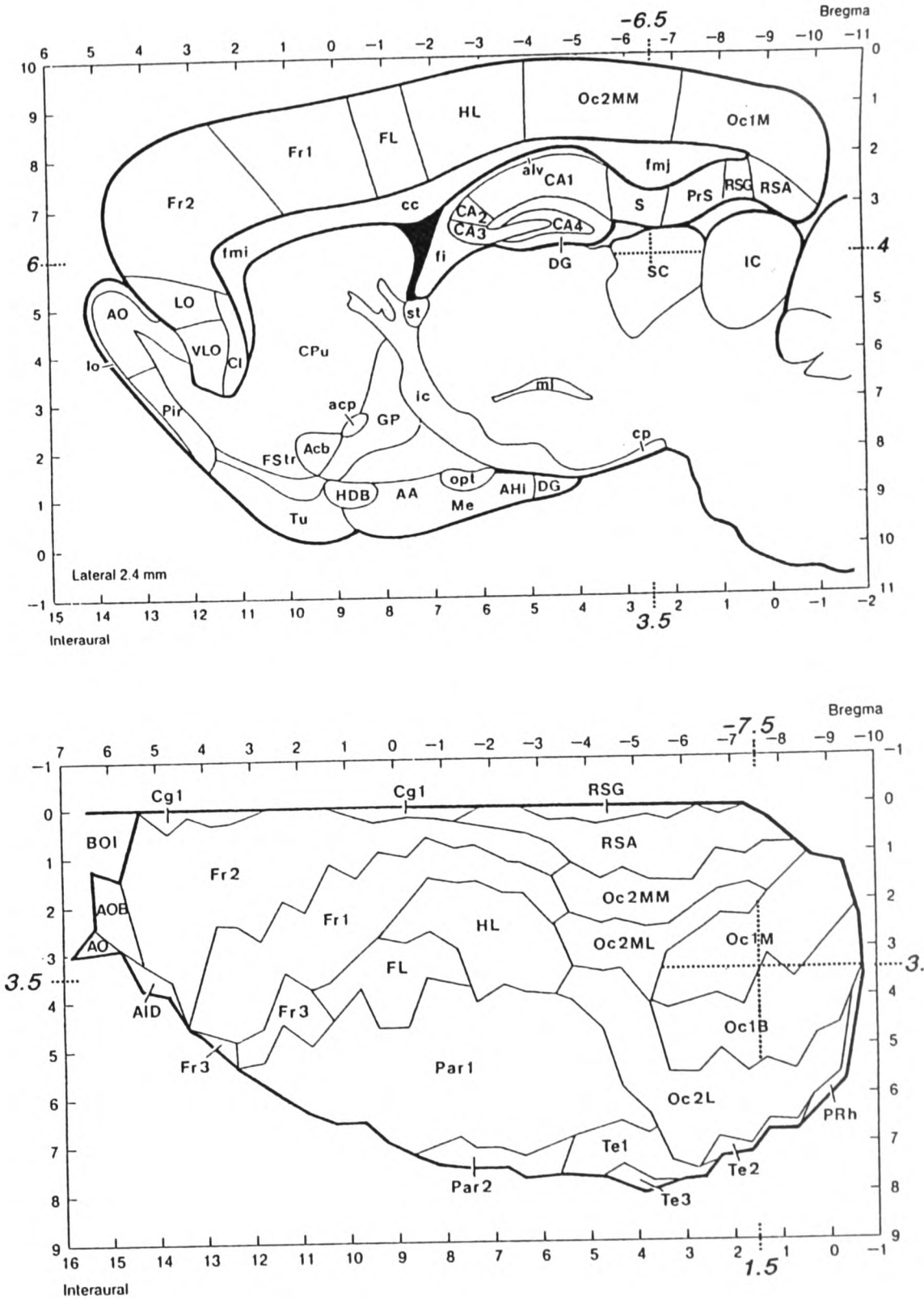

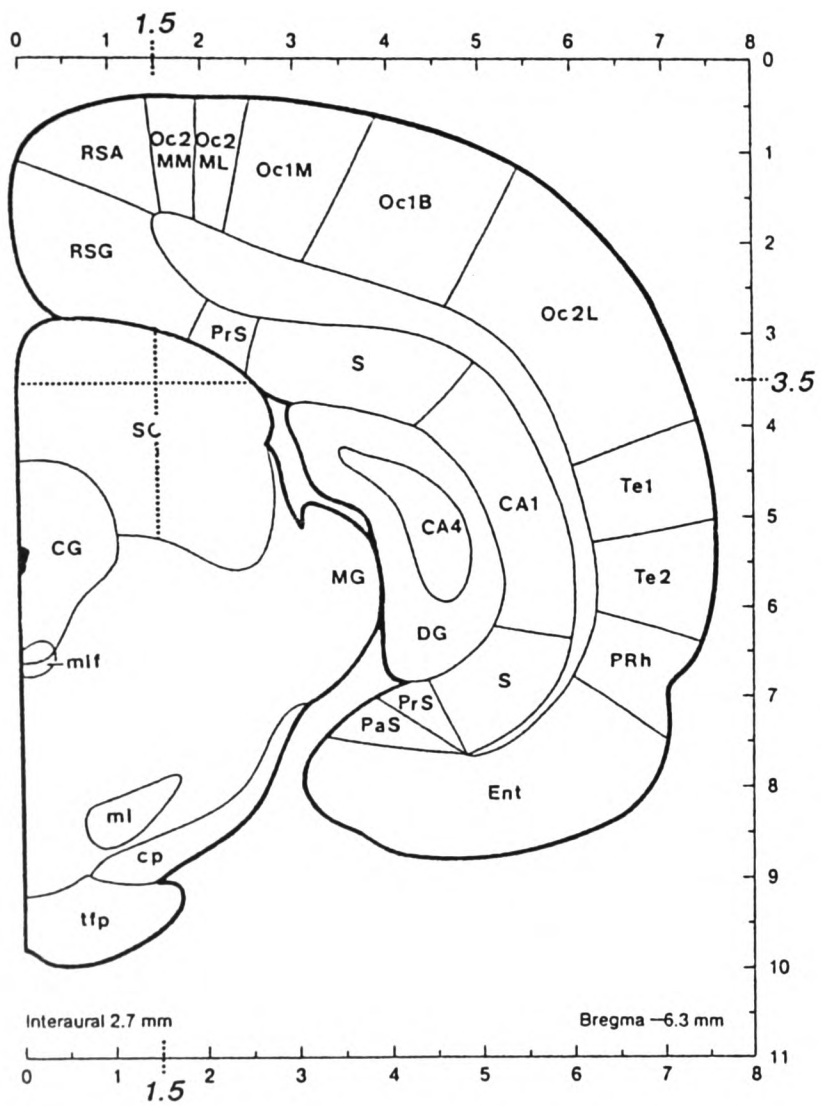
RSA
Oc2 MM
Oc2 ML
Oc1M
Oc1B
Oc2L
RSG
PrS
S
SC
CG
MG
CA4
CA1
Te1
Te2
DG
PRh
PrS
PaS
Ent
mlf
ml
cp
tfp
Interaural 2.7 mm
Bregma −6.3 mm
1.5
3.5

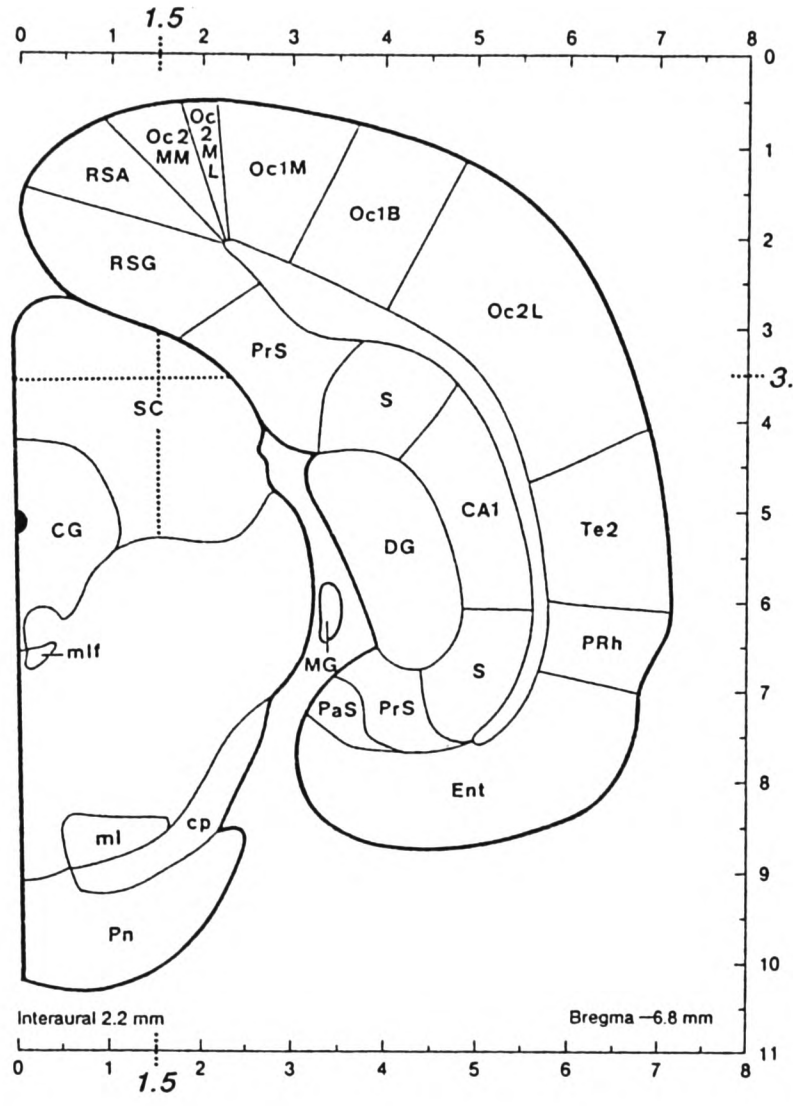
RSA
Oc2 MM
Oc 2 M L
Oc1M
Oc1B
Oc2L
RSG
PrS
S
SC
CG
DG
CA1
Te2
PRh
MG
PaS
PrS
Ent
mlf
ml
cp
Pn
Interaural 2.2 mm
Bregma −6.8 mm
1.5
3.5

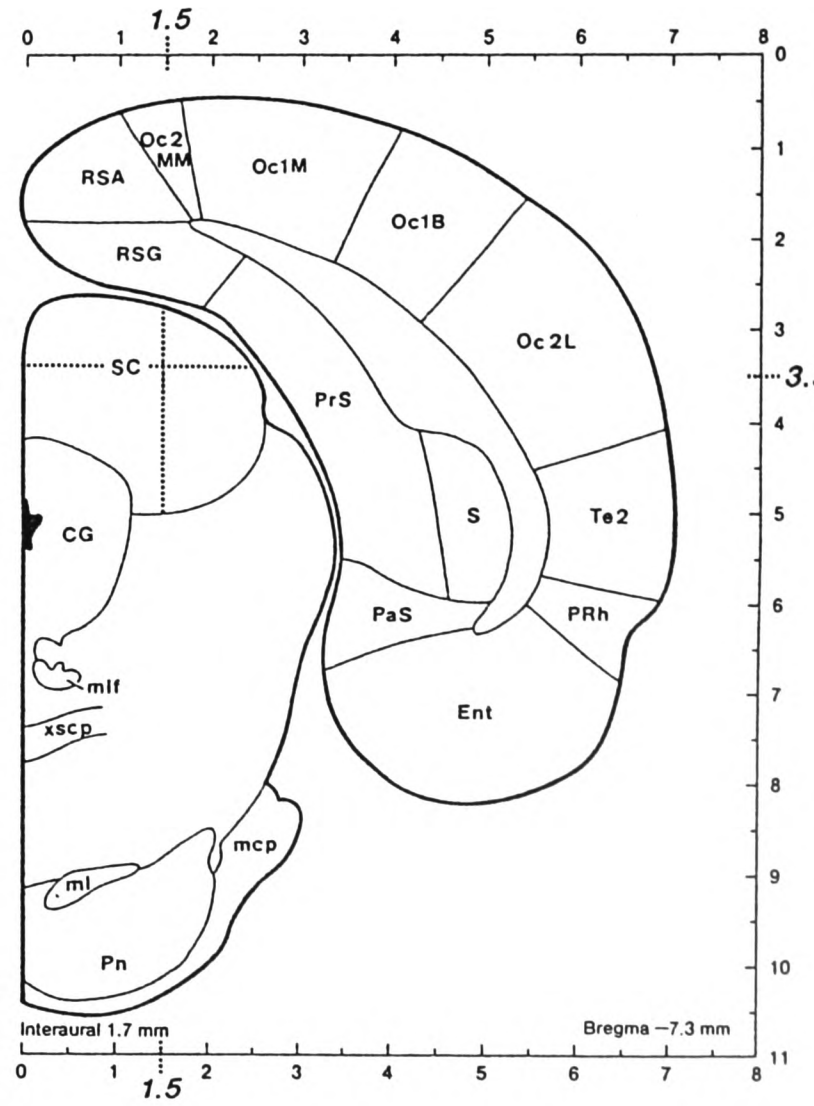
RSA
Oc2 MM
Oc1M
Oc1B
Oc2L
RSG
SC
PrS
S
CG
PaS
PRh
Ent
mlf
xscp
mcp
ml
Pn
Interaural 1.7 mm
Bregma −7.3 mm
1.5
3.5

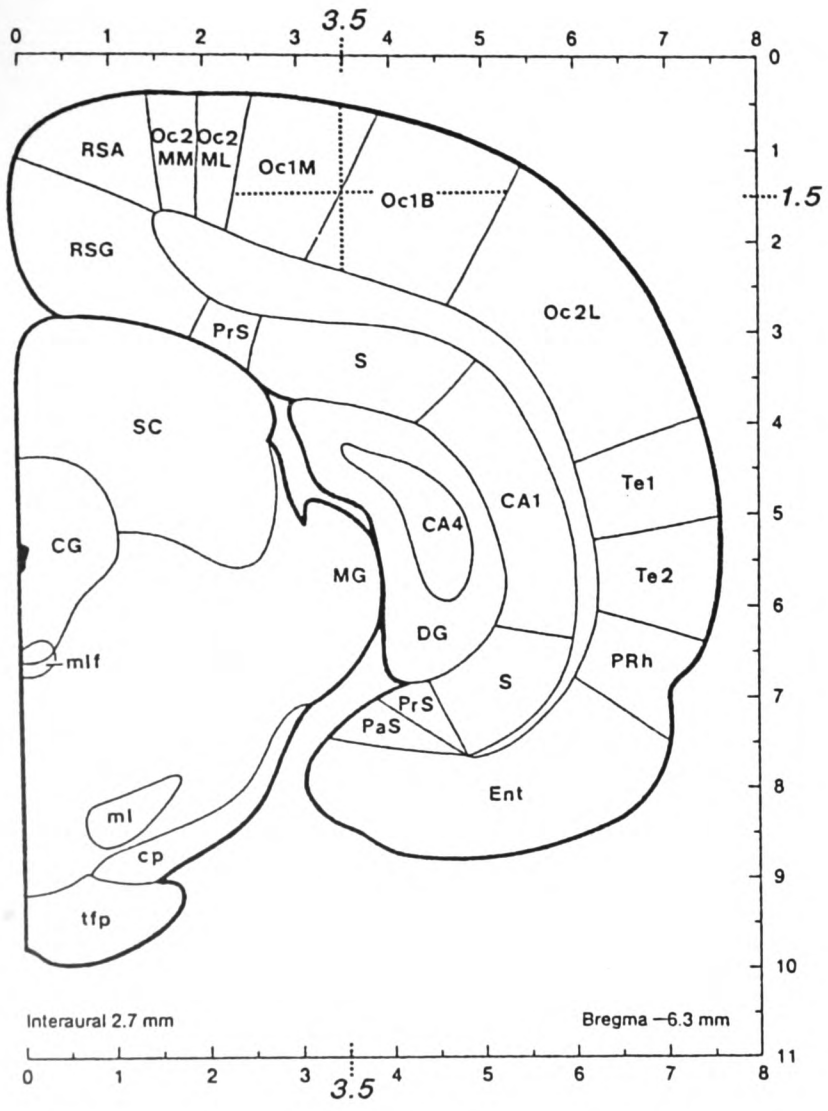
RSA
Oc2 MM
Oc2 ML
Oc1M
Oc1B
RSG
PrS
S
Oc2L
SC
CA1
Te1
CA4
CG
MG
Te2
DG
PRh
mlf
PrS
S
PaS
Ent
ml
cp
tfp
Interaural 2.7 mm
Bregma −6.3 mm
3.5
1.5

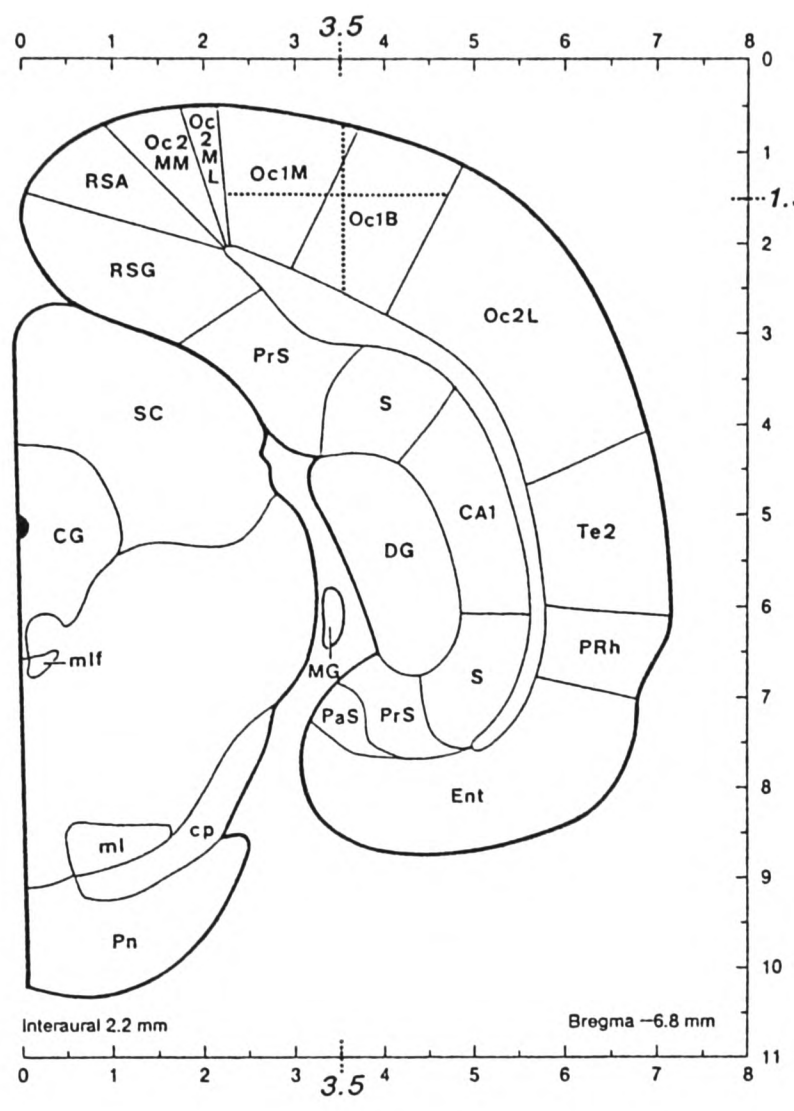
RSA
Oc2 MM
Oc 2 M L
Oc1M
Oc1B
RSG
Oc2L
PrS
S
SC
CA1
Te2
CG
DG
PRh
mlf
MG
S
PaS
PrS
Ent
ml
cp
Pn
Interaural 2.2 mm
Bregma −6.8 mm
3.5
1.5

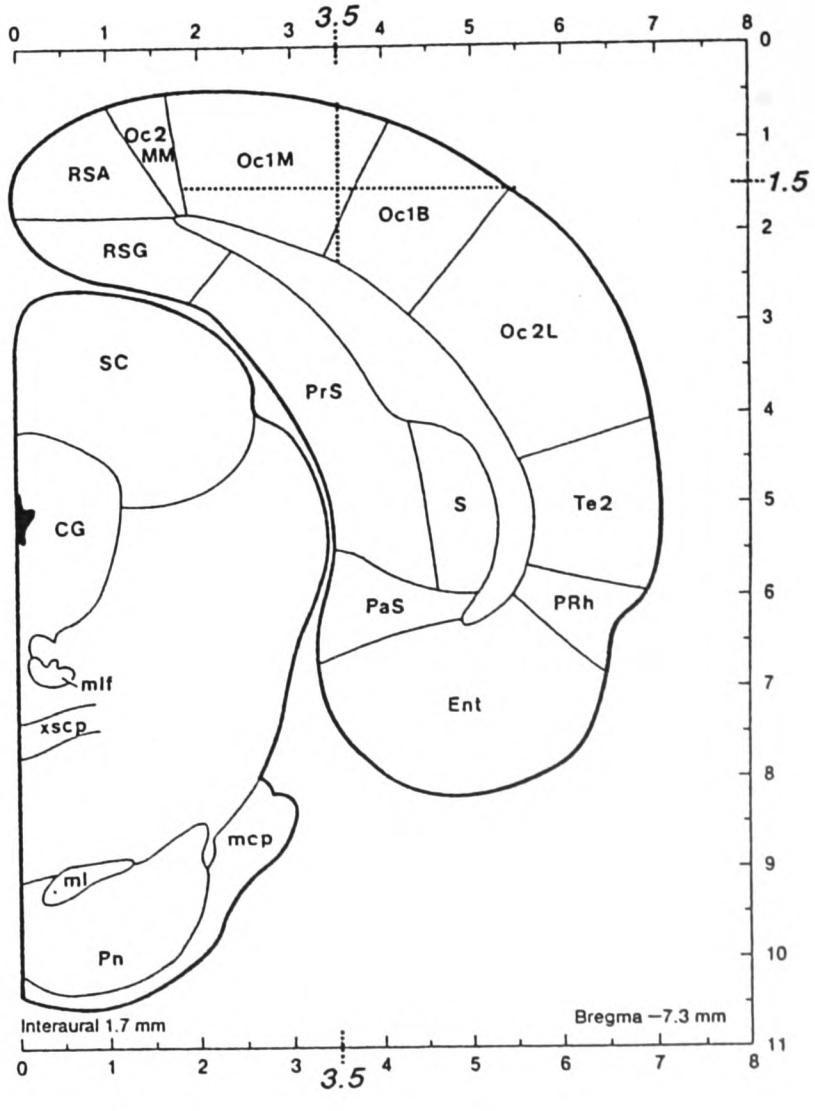
Oc2 MM
Oc1M
RSA
Oc1B
RSG
Oc2L
SC
PrS
S
Te2
CG
PaS
PRh
mlf
Ent
xscp
mcp
ml
Pn
Interaural 1.7 mm
Bregma −7.3 mm
3.5
1.5

Coronal sections A:
Injection site Superior Colliculus

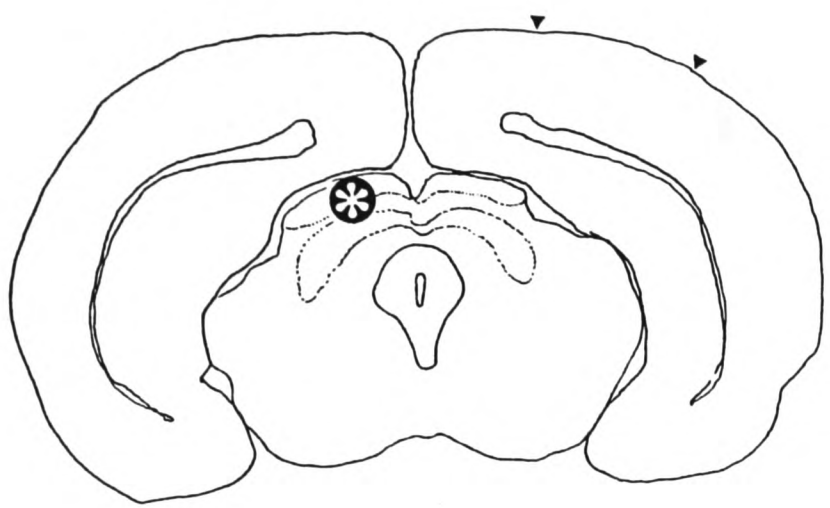

Coronal sections B:
Injection site Contralateral Hemisphere

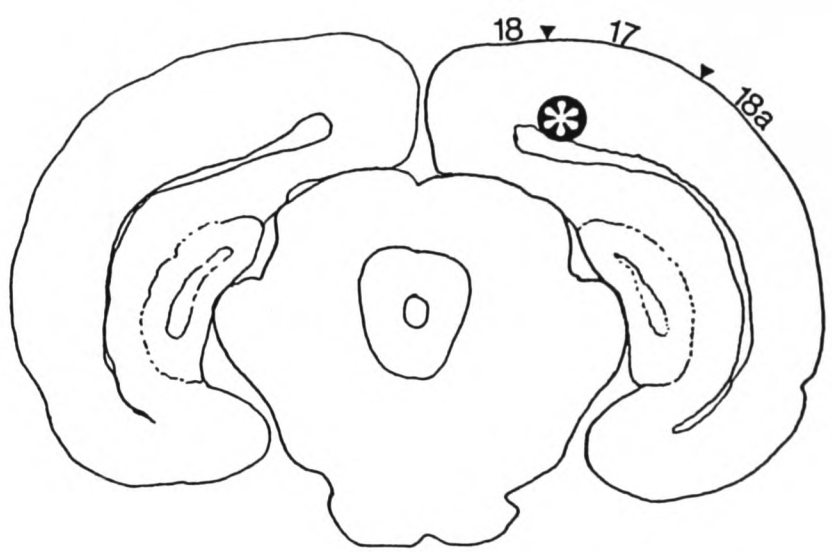

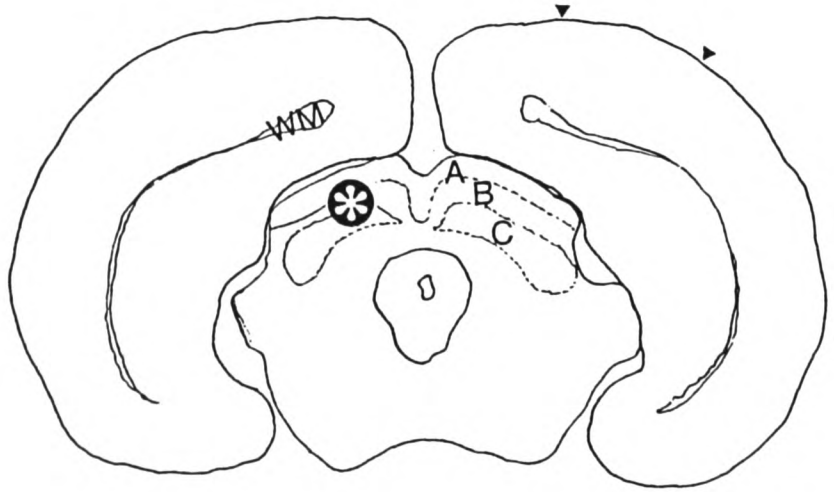

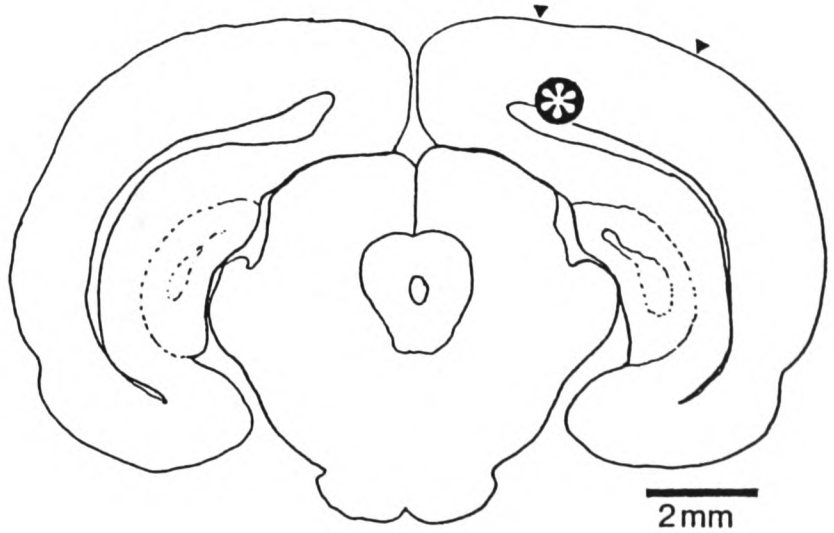

A = stratum griseum superficiale

B = stratum opticum

C = stratum griseum intermediale

⊛ = visible site of tracer injection

WM = White Matter

Cortical areas are approximately delineated

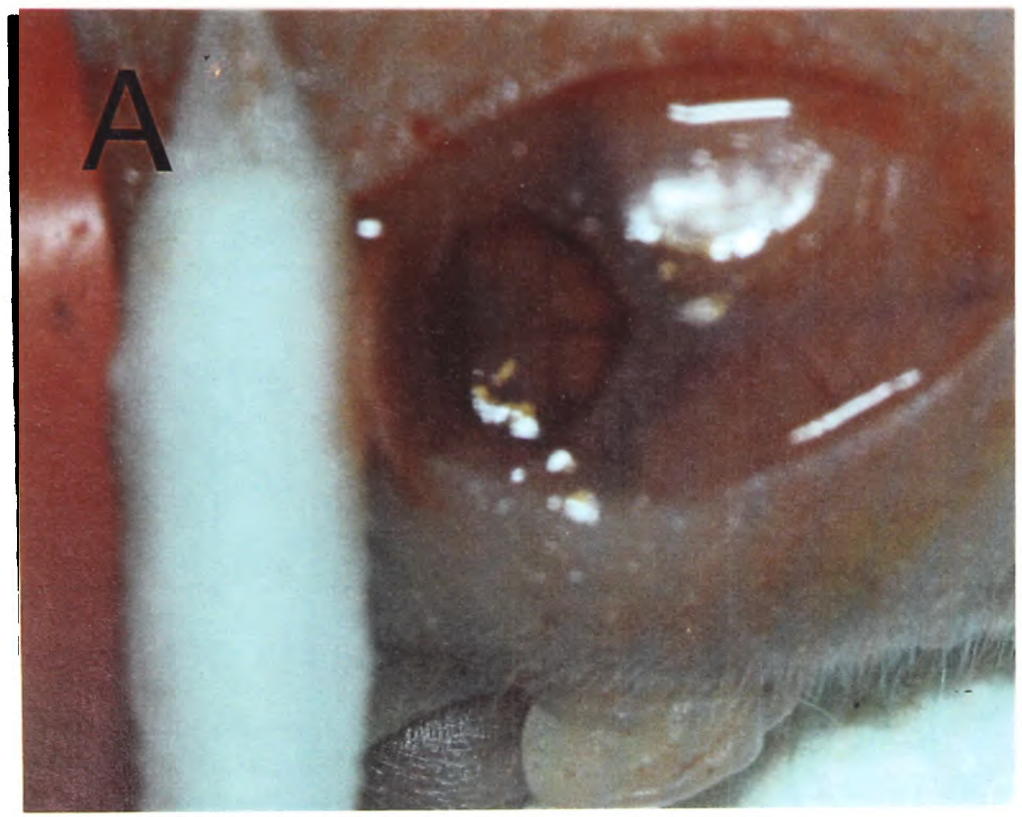
A

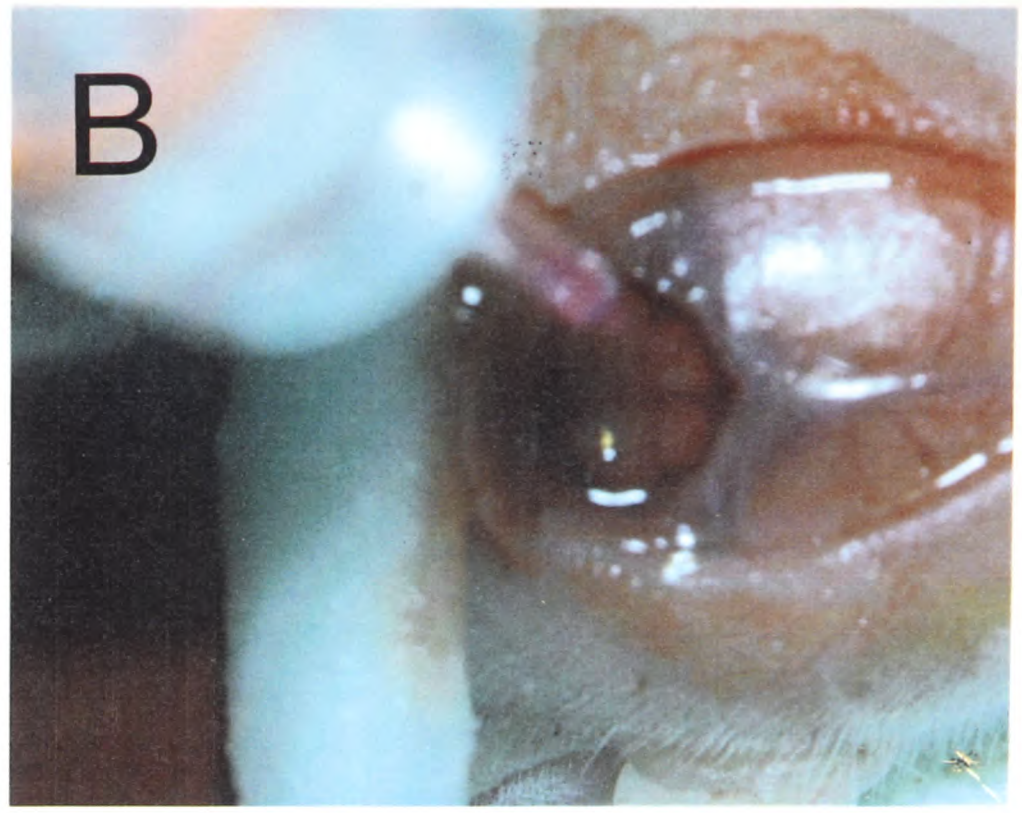
B

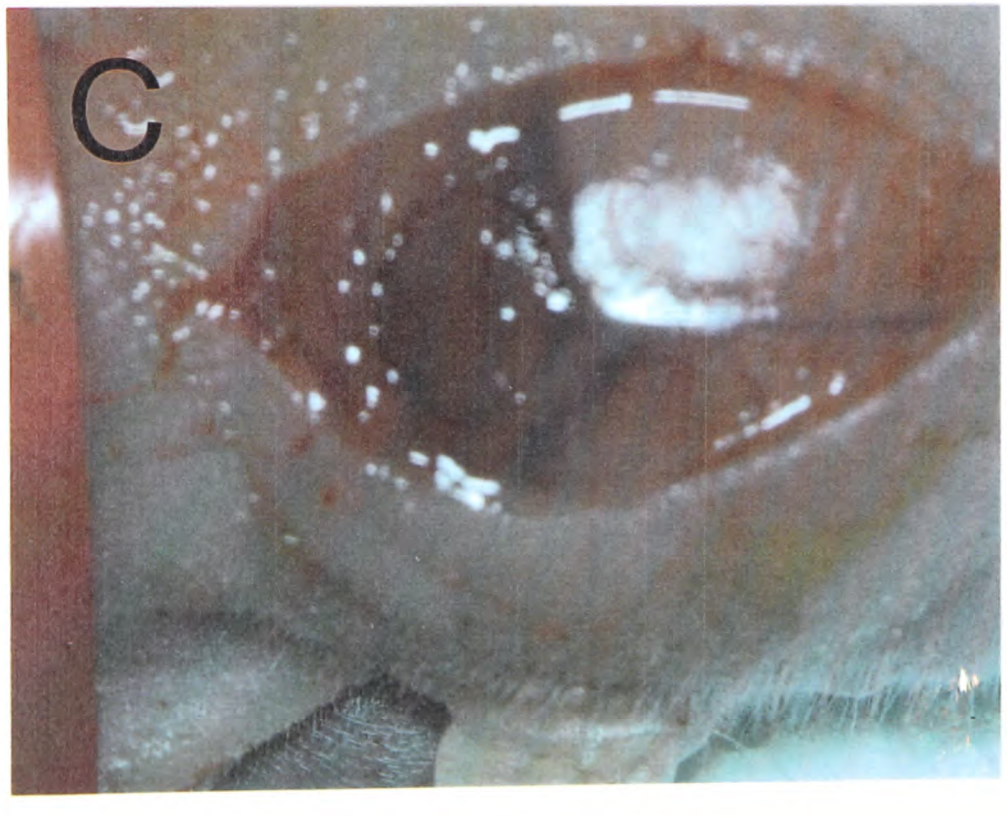
C


D

Errata

A) Text

Page	original version	corrected version
p4	(Wise and Jones, 1976 Dürsteler et al., 1979)	(for rat *see* : Wise and Jones, 1976; for hamster see : Dürsteler et al.,1979).
p5	lgn	the thalamus (e.g. the lateral geniculate nucleus)
p6	interdisciplinary	the word interdisciplinary *refers to* studies employing anatomical and physiological techniques simultaneously
p9	(Price and Thurlow, 1988; Luskin et al., 1988)	*add paragraph:* Other studies have demonstrated the multipotentiality of precursor cells generating both neuronal and glial cells (see Cepko et al., 1989).
p16	approriate	appropriate
p17	...brain kept cold. ...pial surface to finally obtain...	*add:* ...brain kept cold (2°C). *change to* ...pial surface to obtain finally...
p18	standart-wall gratilule The **distance** of layer 5... immresion	standard-wall gratitule *replace:* The **depth** of layer 5... immersion
p19	... into several sections of ...	*add:*...into several **coronal** sections...
p21	... (Katz et al., 1984; 1987).	*add:* ...which were injected into the respective axonal projection target.
p22	...impalements of the **in** cells ...	*omit:* in
p24	This way layer 5 neurons ...	*add:* **In** this way layer 5 neurons...
p27	The breathing **performance** of...	*omit:* performance
p28	... solution a **homebuilt** pressurized ...injection device...	*omit*: homebuilt *add:* (built in the department)...
p29	...lateral **from**...	*change to*...lateral **to**...
p30	...were anaesthesized... ... in appendix **5**).	*change to* ...were anaesthetized... *change to* ... in appendix **4B**).
p37	... of a different **appaerance**...	appearance
p40	... (see Table 4.1).	*add:* ... Table 4.1; **before p.41**).
p49	...lebelled neurons **neurons**...	*omit:* neurons
p47	... woud...	*change to* ... would...
p50	... if present they **are** also...	*omit:* are
p54	... All cells showed a **decrease** in ...	...All cells showed a **change** in...
p59	... deos...	does
p80	... the expected i.p.s.p. active ...	*omit :* active
p82	... populations, **thereby being** of...	*change to* ...populations which were of...
p89	... which also occurs ...	*change to* ... occur ...
p101	... was insignificant. The ...	*add:* ...insignificant (Student's t-test).
p103	... extent...	extend
p104	...(see drawing Figure **6.15**).	*change to* ...(see drawing Figure **6.16**).

p109	... preparations from **the** the ...	*omit:* the
p110	... did **also** not allow a ...	*omit:* also
p112	... demonstrated in **tyoical** ...	typical
p118	It could be...potential waveform.	*omit:* ... action potential waveform.
p120	...**as well as** interhemispheric...	*change to* ... **and** interhemispheric...
p122	Such a influence has...	*change to:* ... Such **an** influence...

B) Figures

Fig. 3.1 b) c-f)	.... represetnig ... ...be recognized as layer of **a**...	representing *change to:* ...as **a** layer of...
Fig. 5.13	...the i.p.s.p. recorded **art**...	recorded **at**
Fig. 6.2/6.3	... developing visual cortex...	*add:* ...cortex **(p5)**...
Fig. 6.4 A)	...markes...	marks
Fig 7.2 to 7.7	The term **juvenile** refers to animals which were sacrificed at postnatal day15 or16 to prepare brain slices for all the experiments described in chapter 7.	

C) Appendices

Appendix 3) Electrode bending technique : Paragraph 5)

This method allows to bend...	*Add:* This method allows **one** to...
..where the angle of the **bent**...	*Change to:* ...angle of the bend...

D) Insertion:

In **Chapter 3** (Materials and Methods) is a section missing which should be placed as a paragraph on page 31 as:

Statistical Methods:

The student's t-test was used to compare data obtained from two or more cell groups of various animals (e.g. cells binned in groups at different ages; see Chapter 5). The difference in terms of statistical significance was tested for the following levels: $p \leq 0.1$, $p \leq 0.05$, $p \leq 0.01$, and $p \leq 0.001$. Differences in parameters were interpreted as statistically significant in cases where the t-test result fulfilled the $p \leq 0{,}05$ level requirements.